

Electroporation ablation:
a new ablation modality for the ablation
of arrhythmogenic cardiac substrate

Vincent van Driel

Colofon

copyright 2016 Vincent van Driel

The copyright of the articles that have been published or accepted for publication has been transferred to the respective journals. Remaining parts of this thesis may not be reproduced, stored or transmitted, in any form or by any means, without prior permission from the author.

Electroporation ablation:

A new ablation modality for the ablation of arrhythmogenic substrate

PhD thesis, Utrecht University, the Netherlands

The generously provided financial support by the Hartcentrum HagaZiekenhuis for the publication of this thesis is gratefully acknowledged.

Cover design: Ferdinand van Nispen tot Pannerden,
Citroenvlinder DTP&Vormgeving, *my-thesis.nl*

Lay out: Ferdinand van Nispen tot Pannerden,
Citroenvlinder DTP&Vormgeving, *my-thesis.nl*

Printed by: GVO drukkers & vormgevers B.V., Ede, the Netherlands

ISBN: 978-94-6332-037-5

Electroporation ablation: A new energy modality for ablation of arrhythmogenic cardiac substrate

Electroporatie-ablatie: Een nieuwe energiemodaliteit voor
de behandeling van het aritmogene cardiale substraat
(met een samenvatting in het Nederlands)

Proefschrift

ter verkrijging van de graad van doctor aan de Universiteit Utrecht

op gezag van de rector magnificus, prof. dr. G.J. van der Zwaan,

ingevolge het besluit van het college van promoties
in het openbaar te verdedigen

op maandag 20 juni 2016 des avonds te 6.00 uur

door

Vincent Jean Hendrik Michel van Driel

geboren op 28 augustus 1967
te Middelburg

promotor: Prof. dr. P.A.F.M. Doevendans

co-promotor: Dr. F.H.M. Wittkampf
Dr. R.J. Hassink

Table of contents

Chapter 1	General introduction and outline of this thesis	9
Chapter 2	Feasibility of Electroporation for the Creation of Pulmonary Vein Ostial Lesions <i>Journal of Cardiovascular Electrophysiology</i> 2011;22(3):302-309	29
Chapter 3	Myocardial Lesion Depth with Circular Electroporation Ablation <i>Circulation: Arrhythmia & Electrophysiology</i> 2012;5(3):581-586	49
Chapter 4	Minimal Coronary Artery Damage by Myocardial Electroporation Ablation <i>Europace</i> 2013;15(1):144-149	65
Chapter 5	Myocardial Lesion Size after Epicardial Electroporation Catheter Ablation after Subxiphoid Puncture <i>Circulation: Arrhythmia & Electrophysiology</i> 2014;7(4):728-733	81
Chapter 6	Safety and Feasibility of Closed Chest Epicardial Catheter Ablation using Electroporation <i>Circulation: Arrhythmia & Electrophysiology</i> 2014;7(5):913-919	99
Chapter 7	Epicardial Linear Electroporation Ablation and Lesion Size <i>Heart Rhythm</i> 2014;11(8):1465-1470	117

Chapter 8	Pulmonary Vein Stenosis after Catheter Ablation: Electroporation versus Radiofrequency <i>Circulation: Arrhythmia & Electrophysiology</i> 2014;7(4):734-738	133
Chapter 9	Low Vulnerability of the Right Phrenic Nerve for Electroporation Ablation <i>Heart Rhythm</i> 2015;12(8):1838-1844	149
Chapter 10	Time Course of Myocardial Electroporation Lesion Development <i>submitted</i>	167
Chapter 11	General discussion	185
Chapter 12	Summary	207
Chapter 13	Samenvatting	213
Chapter 14	Curriculum Vitae	219
Chapter 15	Dankwoord	223
Chapter 16	List of publications	231



CHAPTER 1

General introduction and outline of this thesis

Introduction

1 Exposition

High-energy Direct Current (DC) ablation was introduced in the 1980s to ablate cardiac arrhythmias. Unfortunately, the use of high-energy shocks was associated with complications due to a predictable cascade of physical occurrences comprising arcing, gas formation and shockwave generation. After various needed adjustments in energy supply, low-energy DC ablation demonstrably lacked these adverse events, while still allowing sufficient creation of myocardial lesions solely achieved by permanent (or irreversible) formation of pores (electroporation) in the cell membrane.

Before low-energy DC ablation could be further developed, DC ablation was rendered obsolete altogether by the much more refined and controlled radiofrequency (RF) ablation technique. However, inherent to its mode of operation and potential side-effects, RF energy is associated with a high recurrence rate of arrhythmias due to insufficient creation of myocardial lesions, particularly when transmural lesions are requested, for instance in pulmonary vein antrum isolation (PVAI) for atrial fibrillation (AF). In addition, catheter-ablation with RF energy is associated with an unremitting risk on serious complications such as cardiac perforation, thromboembolism and collateral injury to nerves and esophagus. The use of alternative thermal energy modalities such as cryo-ablation did not result in major improvement yet.

This thesis explores and re-examines the low-energy DC ablation technique in a modified setting in a porcine model, in order to evaluate safety and efficacy for the prospect of human catheter ablation.

2 The High-Energy DC Ablation Era

In 1979 the occurrence of atrio-ventricular conduction (AVC) block, accidentally caused by external cardioversion during an electrophysiological study, was reported.¹ The energy was assumed to have crossed the catheter located over the His bundle. From that moment a surge of interest in high-energy DC energy emerged for the aim of cardiac tissue ablation. One should realize that the potential of DC ablation was investigated as an alternative for surgical ablation, which at that time was associated with a high perioperative mortality. With high-energy DC ablation, electrical energy is delivered from a defibrillator through a catheter to destroy the targeted myocardial tissue. This technique employs delivery of high-

energy applications in a range of 100 to 400 Joules (J) per shock. Most commonly a peak voltage (V) between 1 and 3 kV, related to a peak current flow of 40-60 Ampere (A) is achieved in 1 to 3 msec.

In several animal studies, AVC could be successfully interrupted with high-energy pulses to the His bundle.^{2,3} Encouraged by these promising initial results, closed-chest ablation of AVC developed rapidly as an alternative for drug-resistant supraventricular tachycardias.⁴⁻⁹ Right after, this new technique was explored for the ablation of accessory pathways, atrial tachycardias and life-threatening ventricular tachycardias (VT).¹⁰⁻¹⁴

At that time, complete AVC block could only be realized with high energy levels up to 500 J per shock.^{4,6,9} Despite the use of extreme high energies success rate was still limited in the longer-term (65%-75%).^{5,8,9} Afterwards, proper catheter positioning was found a much more important issue in predicting permanent AVC block than the energy amount.¹⁵⁻¹⁷ Likewise, DC ablation with extreme high energies (300-400 J) was initially not very successful for left-sided accessory pathway ablation from the coronary sinus.^{10,18} Actually, the catheter was far away from the endocardial accessory pathway. Success rate increased tremendously with an endocardial approach and improved mapping techniques.¹³⁻¹⁶

In conclusion, in the early DC days very high energies, up to 500 J per shock over a single electrode were used, considered necessary to achieve durable success. Lack of familiarity with anatomical landmarks and appropriate mapping techniques elicited the use of unduly high energies and its associated complications.

Complications and technical concerns regarding high-energy DC ablation

DC pioneers were confronted with serious drawbacks in an early stage of development. Closed-chest ablation of the AVC was associated with adverse side-effects and even sudden death.^{19,20} Whether these complications were exclusively related to DC ablation or (aggravation of) the underlying heart disease remained obviously an issue. For instance, a new onset of congestive heart failure following interruption of AVC may have also been partly due to chronic right ventricular pacing. Moreover, DC shocks may also cause reversibly impaired left ventricular function due to electrophysiological effects on myocardial tissue bordering the lesion.²¹ Cardiac tamponade due to coronary sinus rupture was reported in patients who underwent a left-sided accessory pathway DC ablation from the coronary sinus. This barotraumatic complication is undeniably and caused by the high-energy DC shocks.^{10,11,22} In addition, in several animal studies sustained and lethal ventricular arrhythmias were frequently observed the first day after DC

ablation using energies > 100 J.^{23, 24} To make things even worse, DC ablation of infarct-related VTs was associated with a high mortality rate, most likely caused by extensive myocardial damage due to excessive energy applications.^{12, 25} In the international registry on VT ablation four procedure-related deaths were noted whereas follow-up mortality was 25 %.²⁰ As a result, DC ablation has an infamous reputation to this day.

Electrical energy was delivered synchronously using a damped sinusoidal waveform, via standard defibrillator and catheters. However, diagnostic catheters are designed for low current and/or voltage pacing and not to withstand high-energy discharges, millions of times greater than pacing stimuli. Several mishaps with high-energy DC ablation were reported, such as disruption of the connector, perforation of the insulating sheath, separation of the tip electrode, failure of the internal conductor.^{26, 27} In addition, severe reduction of dielectric strength of the insulating material was frequently observed after DC ablation, allowing only one ablation pulse per catheter.²⁸

Arcing, gas formation and shockwave in high-energy DC ablation

From the first experiments with high-energy DC ablation physical phenomena as arcing, gas formation and shockwave-generation have been observed. Initially, arcing was considered a beneficial phenomenon and erroneously used to verify adequate energy discharge.¹⁰ (In fact, the pioneer Fontaine named DC ablation *fulguration* meaning *generating a flash*.) During DC ablation initially a small amount of gas formation occurs, caused by electrolysis of water, forming tiny bubbles on the electrode surface. The quantities of gas generated by electrolysis are generally very small: only 17 μl of O_2 (anodal) μr 41 of μl H_2 (cathodal) is produced as result of a 200 J energy application.²⁹

Yet, as enough gas is generated to create a vapor bubble insulating the electrode, current flow to the surrounding medium is interrupted because electrical impedance rises. The inertia inherent in inductor driven defibrillators causes the current flow to continue to the electrode despite a further rise in impedance, reinforcing the increase of the electric field strength between bubble-insulated electrode and medium. At a certain voltage an electron "avalanche" from electrode to bubble surface will occur (voltage breakdown), causing arcs in the plasma. Sufficient current arcing may cause an enormous temperature rise in the bubble, allowing for a very rapid gas expansion in the bubble and subsequently shock-wave generation. By extrusion of dissolved air in the surrounding medium shock-waves will cause further gas generation.^{29, 30}

In transparent liquid mediums, arcing and bubble formation during subsequent phases in DC energy delivery have been made visible on high speed cine films while voltage and current waveforms were monitored on oscilloscopes.^{27, 29, 31-34} The close relationship between bubble formation and barotrauma by shock-wave generation became increasingly clear over time.^{22, 28-30, 35} During an underwater DC shock, pressure waves were recorded in proximity of the electrode causing dramatic changes in the cardiac shape.³⁶

Obviously, there was a need to modify the high-energy DC ablation technique because of the adverse physical side-effects. Therefore, physics of DC shocks were thoroughly studied by the DC pioneers Cunningham, Bardy, Holt and Boyd: (1) Distortion in current and voltage waveform during a high-energy DC application was strongly correlated with bubbles, arcing and shock-waves.^{29, 37} However, when voltage breakdown did not occur, the relation between voltage and current during energy delivery is strict linear.^{30, 38} (2) With non-arcing DC shocks there is no bubble formation and consequently no shock-wave.³³ (3) The maximum current and voltage amplitudes of DC pulses that did not result in voltage breakdown were inversely related to pulse width in single pulses.^{30, 38} (4) In bubbles resulting from arcing DC shocks, a variety of gases was detected, predominantly nitrogen due to dissolved air. So, formation of bubbles in high-energy DC shocks went beyond a simple electrolytic gas production.^{29, 30, 37} In addition, bubble formation is proportional to the amount of applied energy and inversely related to the electrode surface area.²⁹ (5) For similar energy, voltage and current settings, anodal discharges in blood produce much more bubbles (factor 15-30 more) than cathodal.^{29, 37} The shock wave is larger with anodal shocks, both in blood as saline.^{33, 37}

Low energy DC applications were thought to minimize initiatory generation of electrolysis gas, hence preventing substantial bubble formation, arcing and shock-wave generation. However, would low-energy applications be just as effective?

3 Current Thermal Catheter Ablation Techniques

3.1 Radiofrequency (RF) ablation

Thermal injury by RF ablation is caused by a small resistive heating zone (thermal effect caused by electrical current through tissues) and thermal conduction from this zone into the tissue. A myocardial lesion is formed as the tissue temperature raises to levels exceeding protein denaturalisation threshold (> 50 °C).³⁹ A significant raise of the intracellular calcium content results in an irreversible contracture

whereas fibrillar components of the myocardial cell are injured by hyperthermia. RF ablation also denatures the extracellular tissue matrix. So, RF ablation causes loss of cellular and vascular architecture.

RF energy has limited efficacy in areas of high blood flow (heat sink), whereas oppositely electrode temperatures quickly rises and coagulates blood in areas of low blood flow. When temperatures reach 100 °C, steam formation occurs which may cause cardiac perforation and tamponade. Lesions by RF ablation are in general inhomogeneous that can cause other arrhythmias. A variety of factors contribute to the size of a myocardial lesion. Some of them are under our control, such as electrode geometry, irrigation, and energy delivery. Tissue properties (fibrosis) and local blood flow are less controllable factors.^{40,41} In addition, edema evolving during RF ablation hampers subsequent lesion formation; next attempts at the same site are usually of inferior quality.

Due to insufficient creation of myocardial lesions, PV-reconnections occur often after initial successful pulmonary vein antrum isolation (PVAI), whereas recurrence of AF can be mainly attributed to incomplete ablation lines.⁴²⁻⁴⁴ More importantly, elimination of PV-reconnections improves clinical outcome, also in longstanding persistent AF.⁴⁵⁻⁴⁹ Electrophysiological effects (such as reduction of action potential duration, maximal action potential amplitude and the conduction time) have been noticed in the surrounding of RF ablative lesions. On the outside of these lesion margin abnormalities of mitochondria, plasma membrane, sarcomeres were found. In addition, in RF ablative lesions reversible loss of excitability was observed as tissue temperature reached only 40-50°C. These reversible electrophysiological changes may conceal residual PV-conduction despite deceptive observation of PV isolation. Recovery of these PV-sleeves is perceived to account for remaining or renewed PV-conduction after PV ablation.⁵⁰

Lesion size increases significantly and linearly with increasing contact force.⁵¹⁻⁵³ Insufficient contact between mapping electrode and myocardium may lead to non-contiguous and non-transmural lesions. PVAI guided by contact force measurement enabled significant reduction of the number of PV-reconnections and improved the clinical success rate in patients with AF.⁵⁴⁻⁵⁷ General anaesthesia may also improve electrode-tissue contact. Compared to deep sedation general anesthesia provides small respiratory changes and great immobility of the patient.⁵⁸ In patients with paroxysmal AF subjected to their first PVAI under general anesthesia, the initial clinical outcome was better; also the number of PV-reconnections in those selected for repeat ablation was significantly reduced.⁵⁹

We cannot increase energy delivery into myocardial tissue unrestrictedly without compromising the safety aspects of the procedure: an excessive increase of power, duration of ablation and/or contact between electrode and myocardium may lead to steam pops, perforation and collateral damage to adjacent extra-cardiac tissues. Ideally, the optimal myocardial lesion resulting from RF catheter-ablation should be discrete, circumscribed and confined to the myocardial target tissue. In pursuit of creating transmural lesions energy delivery cannot be precisely confined to the pericardium. Consequently, demarcation between insufficient and excessive energy delivery with a risk of collateral damage is rather on the margin. Major complications due to excessive RF ablation for PVAI include cardiac perforation (tamponade), damage to extra-cardiac nerves (in particular phrenic nerve (PN)) and injury of the esophagus (left-atrio-esophageal fistula), PV stenosis and cerebrovascular accidents (CVA).⁶⁰⁻⁶² The incidence of procedure-related complications in AF ablation averages 5 % in most surveys and meta-analysis.^{63, 64}

3.2 Cryo-ablation as alternative energy source for catheter-ablation

Cryo-balloon (CB) ablation is worldwide the most widely used alternative energy source to circumvent the limitations of RF ablation in AF. CBs are designed to isolate a PV with a single energy application. Liquid nitrous oxide is delivered to a balloon under pressure via a hollow tube. A liquid to gas phase change takes place with heat extraction from the electrode-to-tissue interface.⁶⁵ The impact of cryothermal energy on myocardial tissue depends on the lowest temperature reached and application duration. Cooling to -20 °C causes reversible cell damage, due to reversible damage to the cell membrane. Cooling below -40 °C causes irreversible cell injury due to intracellular ice-formation resulting in irreversible disruption of cell organelles and cell membranes.⁶⁵

The acute technical success rate of CB ablation of the PVs approximates 100 %, although repeat freezing and focal touch-ups were sometimes needed.⁶⁶⁻⁶⁸ In a meta-analysis the longer-term clinical success rate following a single CB ablation for paroxysmal AF was 60-70 %.^{66, 69} Several studies report on an increase of acute technical success rate with a new generation CB ablation. However, clinical success rate following a single CB procedure for paroxysmal AF was not improved⁷⁰⁻⁷³ Three studies report on CB ablation for longstanding persistent AF. Clinical success rate was less than 45 %.^{69, 73, 74}

In several small studies the incidence of procedure-related complications due to CB ablation seemed low.^{66, 75, 76} However, incidence of adverse events was significantly

higher in the large STOP-AF trial, even exceeding the rate of complications in AF ablation with RF.⁷⁷ PN palsy (PNP) is particularly associated with CB ablation.⁷⁶ In the STOP-AF trial transient PNP occurred in 11 %, whereas persistent PNP occurred in 2,5 %.⁷⁷ Esophageal injury has also been observed, although it seems that incidence is less than in with RF energy.^{70, 78, 79} Unfortunately, left atrio-esophageal fistulae case reports due to CB ablation have been published recently.^{80, 81}

4 Low-Energy DC Ablation

For the purpose of avoiding arcing and subsequent equipment damage with high-energy DC shocks, catheter configuration, electrode design, configuration of energy shock delivery and power source were modified.

Energy levels lowered to 50 J combined with an active fixation catheter resulted in 70% permanent AVC block. However, arcs were still present.³¹ In dogs, durable AVC block could be accomplished with energy levels of 20 J, but absence of arcing and pressure waves was not reported.⁸² On the other hand, the use of lower energy shocks (< 60 J) was not accompanied anymore with ventricular arrhythmias.^{34, 83}

Also trains of electrical pulses were used to achieve higher DC energy delivery than safely possible with a single electrical pulse. A 200 J train of pulses using 5-20 A amplitudes could be delivered in 100 msec, without demonstration of voltage-breakdown.³⁰

A newly designed capacitive power source was able to deliver less energy in a very short time (60-100 μ sec), and thus preserving high peak current and high peak voltage.^{33, 34, 84} A significant reduction in arcing and gas formation was observed. In addition, both current and voltage could even be increased without arcing, especially when using cathodal applications.^{33, 34}

Finally, permanent AVC block could be achieved with DC shocks of only 2 J, without familiar side-effects.⁸⁵ Other studies compared favourably with high-energy DC too.⁸⁶⁻⁸⁹ Meanwhile RF energy had firmly taken its place in the ablation field, due to its favorable outcome, safe profile and lack of need for general anesthesia.

Creation of myocardial lesions by high-energy and low-energy DC-ablation

Based on physical phenomena linked to DC ablation, four mechanisms of cell death have been postulated: cell membrane disruption (by electroporation), thermal effect (protein denaturation due to heating), electrochemical interactions (free radical formation) and barotrauma (shock-wave generation). Data regarding development of myocardial lesions caused by DC energy are mainly obtained from animal studies. Only a few valuable observations on myocardial lesion formation

by low-energy DC ablation were made. The extent of myocardial necrosis in lesions created with multiple 15 J non-arcing applications was similar as lesions created with the same number of 40 J arcing shocks. In addition, multiple non-arcing DC shocks caused more myocardial necrosis than a single arcing shock, whereas a lesion created with a single non-arcing DC shock was not significantly smaller than the lesion that was created with a single arcing DC shock.³⁴ So, arcing and/or barotrauma were considered merely as pure adverse side-effects as they do not contribute to lesion creation. Therefore, in low-energy DC ablation myocardial cell death was thought to be achieved solely by cell membrane disruption. As it turned out later, irreversible electroporation is the underlying principle of cell membrane injury in low-energy DC ablation. In conclusion, creation of myocardial lesions with low-energy DC energy predominantly reflects a voltage (and current) dependent process injuring the cell membrane (electroporation), poorly related to the amount of energy used.

5 Reversible and Irreversible Electroporation Ablation

By exposing a biological cell or tissue to a strong electrical field (> 200 V/cm), cell membrane permeabilization will occur due to formation of pores in the cell membrane, from which the term *electroporation* derives.^{90,91} These pores have been clearly demonstrated with electron microscopy.^{92,93} (**Figure 1**) The mechanism by which electroporation is established by a strong electric field is not yet completely clarified.

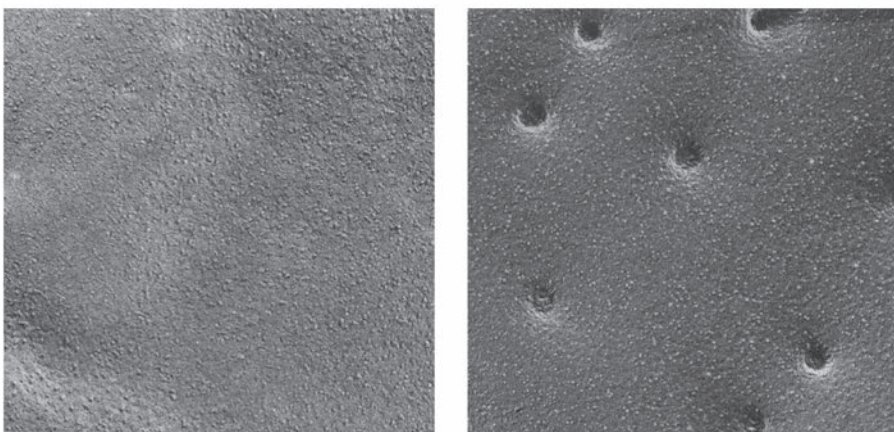


Figure 1. micrographs showing the intact cell membrane of a red cell before (a) and the pore-like red cell membrane 40 ms after applying the electrical pulse (b)

As function of electrical parameters and tissue properties, electrical pulses can exert different effects on the cell membrane, such as no effect at all, reversible electroporation (RE) or irreversible electroporation (IRE).

In RE the cell membrane reseals after delivery of electrical pulses; the cell will be completely repaired in time and survive. RE has been used for gene transport and delivery of macromolecular drugs which are normally too large to enter the cell to facilitate cell ablation and improve the effectiveness of cancer treatment (electrochemotherapy).⁹⁴⁻⁹⁹ By enabling incorporation of drugs in the cell, effectiveness of cancer treatment could be improved, as was summarized in many publications.⁹⁴⁻⁹⁸

In IRE the cell membrane does not reseal, insufficiently or untimely, resulting in disruption of the cellular homeostasis and ultimately leading to cell death.^{100,101} Cell death due to electroporation is caused by *necrosis* (permanent disruption of the cell membrane) or *apoptosis* (disruption of DNA without permanent disruption of the cell membrane, with lower energy levels). (**Figure 2**) Because cells are required to survive in electrochemotherapy, IRE was considered an undesirable side-effect of RE procedures. Precisely, the upper limits of electrical field parameters were studied intensively to avoid IRE.

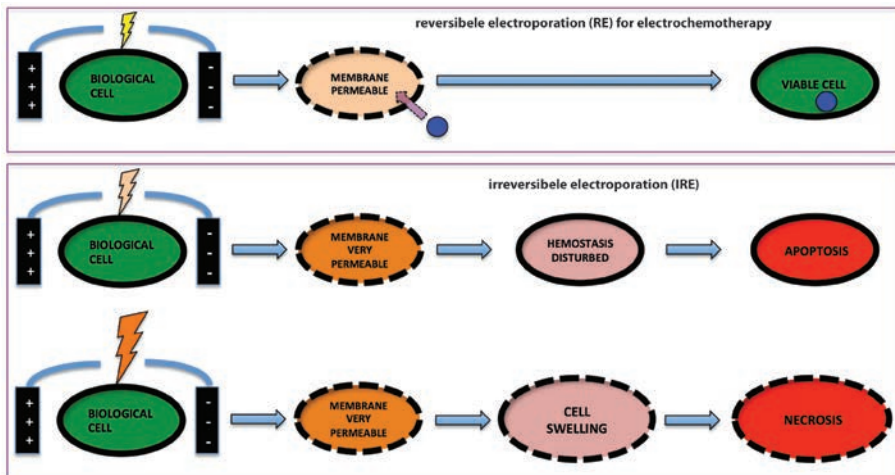


Figure 2. the effects of an electrical pulse on a cell with increasing energy delivery: reversible electroporation for the use of electro-chemotherapy (a), irreversible electroporation resulting in apoptosis (b) and irreversible electroporation resulting in necrosis

IRE as a stand-alone clinical ablation treatment (without adjuvant drugs), was first investigated by Davalos et al.¹⁰⁰ Because electrical pulses generating IRE instead

of RE require a longer duration and larger amplitude, there was serious concern about potential thermal tissue damage due to resistive heating.³⁹ Likewise previous RE studies, thermal effects of any importance were ruled out in IRE.^{100, 102} Presently, the concept IRE applies to the application of electrical pulses producing tissue ablation, without thermal effects. Actually, IRE can be considered as a (series of) low-energy non-arcing DC shock(s) in which heat and barotrauma are no elements in tissue ablation.

With regard to this thesis the terms *IRE* and *electroporation ablation* have been used interchangeably. However, forced by prospective one-sided approach (endocardial or epicardial) we use (single) unipolar electrical pulses in our studies. For reasons of clarity, in our recent studies we did name our technique *electroporation ablation* whereas *IRE* in studies by others generally refers to (non-cardiac) tissue ablation due to electroporation using multiple pulses per energy application.

By its non-thermal nature IRE only affects living cells by change of cell membrane integrity and spares the non-cellular tissue scaffold. Consequently, IRE does not cause denaturation of proteins and is not affected by local blood flow. IRE has already been widely used for tumor ablation (prostate^{103, 104}, kidney^{105, 106}, liver^{107, 108}, breast^{109, 110}, brain¹¹¹⁻¹¹⁴ cancer). The beneficial hallmarks of IRE with regard to lesion creation were clearly illustrated in all these studies. A well defined region of tissue ablation was observed, without transitional areas from ablated to healthy tissue. Large blood vessels, urethra and bile ducts, incorporated in lesions, were not damaged at all. Also the architecture of nerves was preserved.^{103, 105, 115} Therefore, IRE has become increasingly popular in the medical field to ablate specific areas of undesired tissue without destroying surrounding tissues.

6 Aim and Outline of this thesis

Catheter-ablation in patients with AF or VT related to structural heart diseases, requires the creation of transmural or deep myocardial lesions, accomplished safely and at once. Above all, thermal catheter-ablation for these arrhythmias is associated with an unremitting high risk on procedure-related complications. Last decade, IRE has been increasingly used as a non-thermal emerging ablation modality in the non-cardiac field. Due to certain characteristics distinctive from thermal ablation techniques, electroporation ablation might resolve shortcomings in the cardiac field as well.

We hypothesized:

- 1) Sufficient myocardial lesions can be created in a controlled and complete manner because energy delivery with non-thermal electroporation ablation is not effected by local blood flow. In addition, there is a strong dose-response-relationship between lesion size and energy amount.
- 2) Because electroporation ablation destroys cells by irreversible disruption of the cell membrane without heat, collateral damage of coronary arteries, pulmonary veins and the phrenic nerve can be ruled out.

7 References

1. Vedel J, Frank R, Fontaine G, Fournial JF, Grosogoeat Y. [permanent intra-hisian atrioventricular block induced during right intraventricular exploration]. *Archives des maladies du coeur et des vaisseaux*. 1979;72:107-112
2. Gonzalez R, Scheinman M, Margaretten W, Rubinstein M. Closed-chest electrode-catheter technique for his bundle ablation in dogs. *The American journal of physiology*. 1981;241:H283-287
3. Bardy GH, Ideker RE, Kasell J, Worley SJ, Smith WM, German LD, Gallagher JJ. Transvenous ablation of the atrioventricular conduction system in dogs: Electrophysiologic and histologic observations. *The American journal of cardiology*. 1983;51:1775-1782
4. Gallagher JJ, Svenson RH, Kasell JH, German LD, Bardy GH, Broughton A, Critelli G. Catheter technique for closed-chest ablation of the atrioventricular conduction system. *The New England journal of medicine*. 1982;306:194-200
5. Trantham JL, Gallagher JJ, German LD, Broughton A, Guarnieri T, Kasell J. Effects of energy delivery via a his bundle catheter during closed chest ablation of the atrioventricular conduction system. *The Journal of clinical investigation*. 1983;72:1563-1574
6. Scheinman MM, Morady F, Hess DS, Gonzalez R. Catheter-induced ablation of the atrioventricular junction to control refractory supraventricular arrhythmias. *JAMA : the journal of the American Medical Association*. 1982;248:851-855
7. Wood DL, Hammill SC, Holmes DR, Jr, Osborn MJ, Gersh BJ. Catheter ablation of the atrioventricular conduction system in patients with supraventricular tachycardia. *Mayo Clinic proceedings*. 1983;58:791-796
8. Scheinman MM, Evans-Bell T. Catheter ablation of the atrioventricular junction: A report of the percutaneous mapping and ablation registry. *Circulation*. 1984;70:1024-1029
9. Nathan AW, Bennett DH, Ward DE, Bexton RS, Camm AJ. Catheter ablation of atrioventricular conduction. *Lancet*. 1984;1:1280-1284
10. Brodman R, Fisher JD. Evaluation of a catheter technique for ablation of accessory pathways near the coronary sinus using a canine model. *Circulation*. 1983;67:923-929
11. Fisher JD, Brodman R, Kim SG, Matos JA, Brodman LE, Wallerson D, Waspe LE. Attempted nonsurgical electrical ablation of accessory pathways via the coronary sinus in the wolff-parkinson-white syndrome. *Journal of the American College of Cardiology*. 1984;4:685-694
12. Fontaine G, Tonet JL, Frank R, Lacroix H, Farenq G, Gallais Y, Drobinski G, Grosogoeat Y. [emergency treatment of chronic ventricular tachycardia after myocardial infarction by endocavitary fulguration]. *Archives des maladies du coeur et des vaisseaux*. 1985;78:1037-1043
13. Hartzler GO. Electrode catheter ablation of refractory focal ventricular tachycardia. *Journal of the American College of Cardiology*. 1983;2:1107-1113
14. Gillette PC, Wampler DG, Garson A, Jr, Zinner A, Ott D, Cooley D. Treatment of atrial automatic tachycardia by ablation procedures. *Journal of the American College of Cardiology*. 1985;6:405-409
15. Iwa T, Tonet J, Evans S, Frank R, Lascault G, Brito M, Adragao P, Rougier I, Fontaine G, Grosogoeat Y. Better predictors of successful his-bundle ablation analysis of first shocks. *Pacing and clinical electrophysiology : PACE*. 1990;13:2008-2013
16. Haissaguerre M, Warin JF, D'Ivernois C, Le Metayer PH, Montserrat P. Fulguration for av nodal tachycardia: Results in 42 patients with a mean follow-up of 23 months. *Pacing and clinical electrophysiology : PACE*. 1990;13:2000-2007
17. Jordaens L, Van Wassenhove E, Clement L. Electrocardiographic determinants of efficacy of 8-joule shocks for ablation of the atrioventricular node. *European heart journal*. 1991;12:608-611
18. Morady F, Scheinman MM, Winston SA, DiCarlo LA, Jr, Davis JC, Griffin JC, Ruder M, Abbott JA, Eldar M. Efficacy and safety of transcatheter ablation of posteroseptal accessory pathways. *Circulation*. 1985;72:170-177
19. Rosenqvist M, Lee MA, Moulinier L, Springer MJ, Abbott JA, Wu J, Langberg JJ, Griffin JC, Scheinman MM. Long-term follow-up of patients after transcatheter direct current ablation of the atrioventricular junction. *Journal of the American College of Cardiology*. 1990;16:1467-1474

20. Evans GT, Jr., Scheinman MM, Zipes DP, Benditt D, Camm AJ, el-Sherif N, Fisher J, Fontaine G, German L, Hartzler G, et al. Catheter ablation for control of ventricular tachycardia: A report of the percutaneous cardiac mapping and ablation registry. *Pacing and clinical electrophysiology : PACE*. 1986;9:1391-1395
21. Auricchio A, Klein H, Trappe HJ, Salo R. Effect on ventricular performance of direct current electrical shock for catheter ablation of the atrioventricular junction. *Pacing and clinical electrophysiology : PACE*. 1992;15:344-356
22. Bardy GH, Ivey TD, Coltorti F, Stewart RB, Johnson G, Greene HL. Developments, complications and limitations of catheter-mediated electrical ablation of posterior accessory atrioventricular pathways. *The American journal of cardiology*. 1988;61:309-316
23. Lerman BB, Weiss JL, Bulkley BH, Becker LC, Weisfeldt ML. Myocardial injury and induction of arrhythmia by direct current shock delivered via endocardial catheters in dogs. *Circulation*. 1984;69:1006-1012
24. Moak JP, Friedman RA, Garson A, Jr. Electrical ablation of atrial muscle. II. Early and late electrophysiologic observations in canine atria. *American heart journal*. 1987;113:1404-1413
25. Fontaine G, Tonet JL, Frank R, Rougier I. Clinical experience with fulguration and antiarrhythmic therapy for the treatment of ventricular tachycardia. Long-term follow-up of 43 patients. *Chest*. 1989;95:785-797
26. Ward DE, Camm AJ. The current status of ablation of cardiac conduction tissue and ectopic myocardial foci by transvenous electrical discharges. *Clinical cardiology*. 1986;9:237-244
27. Fisher JD, Brodman R, Johnston DR, Waspe LE, Kim SG, Matos JA, Scavin G. Nonsurgical electrical ablation of tachycardias: Importance of prior in vitro testing of catheter leads. *Pacing and clinical electrophysiology : PACE*. 1984;7:74-81
28. Bardy GH, Coltorti F, Ivey TD, Yerkovich D, Greene HL. Effect of damped sine-wave shocks on catheter dielectric strength. *The American journal of cardiology*. 1985;56:769-772
29. Bardy GH, Coltorti F, Ivey TD, Alferness C, Rackson M, Hansen K, Stewart R, Greene HL. Some factors affecting bubble formation with catheter-mediated defibrillator pulses. *Circulation*. 1986;73:525-538
30. Bardy GH, Coltorti F, Stewart RB, Greene HL, Ivey TD. Catheter-mediated electrical ablation: The relation between current and pulse width on voltage breakdown and shock-wave generation. *Pacing and clinical electrophysiology : PACE*. 1986;9:1381-1383
31. Holt PM, Boyd EG, Crick JC, Sowton E. Low energies and helifix electrodes in the successful ablation of atrioventricular conduction. *Pacing and clinical electrophysiology : PACE*. 1985;8:639-645
32. Boyd EG, Holt PM. An investigation into the electrical ablation technique and a method of electrode assessment. *Pacing and clinical electrophysiology : PACE*. 1985;8:815-824
33. Lemery R, Lavallee E, Girard A, Montpetit M. Physical and dynamic characteristics of dc ablation in relation to the type of energy delivery and catheter design. *Pacing and clinical electrophysiology : PACE*. 1991;14:1158-1168
34. Lemery R, Leung TK, Lavallee E, Girard A, Talajic M, Roy D, Montpetit M. In vitro and in vivo effects within the coronary sinus of nonarcing and arcing shocks using a new system of low-energy dc ablation. *Circulation*. 1991;83:279-293
35. Coltorti F, Bardy GH, Reichenbach D, Greene HL, Thomas R, Breazeale DG, Alferness C, Ivey TD. Catheter-mediated electrical ablation of the posterior septum via the coronary sinus: Electrophysiologic and histologic observations in dogs. *Circulation*. 1985;72:612-622
36. Tidd MJ, Webster J, Wright HC, Harrison IR. Mode of action of a surgical electronic lithoclast—high speed pressure, cinematographic and schlieren recordings following an ultrashort underwater electronic discharge. *Biomedical engineering*. 1976;11:5-11,24
37. Holt PM, Boyd EG. Hematologic effects of the high-energy endocardial ablation technique. *Circulation*. 1986;73:1029-1036
38. Cunningham D, Ahsan AJ, Rowland E, Rickards AF. Impedance changes during catheter ablation and their relationship to electrical arcing and clinical efficacy. *Pacing and clinical electrophysiology : PACE*. 1989;12:144-149
39. Wittkampf FH, Nakagawa H. Rf catheter ablation: Lessons on lesions. *Pacing and clinical electrophysiology : PACE*. 2006;29:1285-1297
40. Badger TJ, Adjei-Poku YA, Marrouche NF. Mri in cardiac electrophysiology: The emerging role of delayed-enhancement mri in atrial fibrillation ablation. *Future cardiology*. 2009;5:63-70

41. d'Avila A, Houghtaling C, Gutierrez P, Vragovic O, Ruskin JN, Josephson ME, Reddy VY. Catheter ablation of ventricular epicardial tissue: A comparison of standard and cooled-tip radiofrequency energy. *Circulation*. 2004;109:2363-2369
42. Gerstenfeld EP, Callans DJ, Dixit S, Zado E, Marchlinski FE. Incidence and location of focal atrial fibrillation triggers in patients undergoing repeat pulmonary vein isolation: Implications for ablation strategies. *Journal of cardiovascular electrophysiology*. 2003;14:685-690
43. Callans DJ, Gerstenfeld EP, Dixit S, Zado E, Vanderhoff M, Ren JF, Marchlinski FE. Efficacy of repeat pulmonary vein isolation procedures in patients with recurrent atrial fibrillation. *Journal of cardiovascular electrophysiology*. 2004;15:1050-1055
44. Seow SC, Lim TW, Koay CH, Ross DL, Thomas SP. Efficacy and late recurrences with wide electrical pulmonary vein isolation for persistent and permanent atrial fibrillation. *Europace : European pacing, arrhythmias, and cardiac electrophysiology : journal of the working groups on cardiac pacing, arrhythmias, and cardiac cellular electrophysiology of the European Society of Cardiology*. 2007;9:1129-1133
45. Ouyang F, Antz M, Ernst S, Hachiya H, Mavrakis H, Deger FT, Schaumann A, Chun J, Falk P, Hennig D, Liu X, Bansch D, Kuck KH. Recovered pulmonary vein conduction as a dominant factor for recurrent atrial tachyarrhythmias after complete circular isolation of the pulmonary veins: Lessons from double lasso technique. *Circulation*. 2005;111:127-135
46. Chun KR, Bansch D, Ernst S, Ujeyl A, Huang H, Chu H, Satomi K, Schmidt B, Antz M, Kuck KH, Ouyang F. Pulmonary vein conduction is the major finding in patients with atrial tachyarrhythmias after intraoperative maze ablation. *Journal of cardiovascular electrophysiology*. 2007;18:358-363
47. Bhargava M, Di Biase L, Mohanty P, Prasad S, Martin DO, Williams-Andrews M, Wazni OM, Burkhardt JD, Cummings JE, Khaykin Y, Verma A, Hao S, Beheiry S, Hongo R, Rossillo A, Raviela A, Bonso A, Themistoclakis S, Stewart K, Saliba WJ, Schweikert RA, Natale A. Impact of type of atrial fibrillation and repeat catheter ablation on long-term freedom from atrial fibrillation: Results from a multicenter study. *Heart rhythm : the official journal of the Heart Rhythm Society*. 2009;6:1403-1412
48. Verma A, Kilicaslan F, Pisano E, Marrouche NF, Fanelli R, Brachmann J, Geunther J, Potenza D, Martin DO, Cummings J, Burkhardt JD, Saliba W, Schweikert RA, Natale A. Response of atrial fibrillation to pulmonary vein antrum isolation is directly related to resumption and delay of pulmonary vein conduction. *Circulation*. 2005;112:627-635
49. Cappato R, Negroni S, Pecora D, Bentivegna S, Lupo PP, Carolei A, Esposito C, Furlanello F, De Ambroggi L. Prospective assessment of late conduction recurrence across radiofrequency lesions producing electrical disconnection at the pulmonary vein ostium in patients with atrial fibrillation. *Circulation*. 2003;108:1599-1604
50. Arentz T, Macle L, Kalusche D, Hocini M, Jais P, Shah D, Haissaguerre M. "Dormant" pulmonary vein conduction revealed by adenosine after ostial radiofrequency catheter ablation. *Journal of cardiovascular electrophysiology*. 2004;15:1041-1047
51. Yokoyama K, Nakagawa H, Shah DC, Lambert H, Leo G, Aebly N, Ikeda A, Pitha JV, Sharma T, Lazzara R, Jackman WM. Novel contact force sensor incorporated in irrigated radiofrequency ablation catheter predicts lesion size and incidence of steam pop and thrombus. *Circulation. Arrhythmia and electrophysiology*. 2008;1:354-362
52. Thiagalingam A, D'Avila A, Foley L, Guerrero JL, Lambert H, Leo G, Ruskin JN, Reddy VY. Importance of catheter contact force during irrigated radiofrequency ablation: Evaluation in a porcine ex vivo model using a force-sensing catheter. *Journal of cardiovascular electrophysiology*. 2010;21:806-811
53. Wong MC, Edwards G, Spence SJ, Kalman JM, Kumar S, Joseph SA, Morton JB. Characterization of catheter-tissue contact force during epicardial radiofrequency ablation in an ovine model. *Circulation. Arrhythmia and electrophysiology*. 2013;6:1222-1228
54. Kuck KH, Reddy VY, Schmidt B, Natale A, Neuzil P, Saoudi N, Kautzner J, Herrera C, Hindricks G, Jais P, Nakagawa H, Lambert H, Shah DC. A novel radiofrequency ablation catheter using contact force sensing: Toccata study. *Heart rhythm : the official journal of the Heart Rhythm Society*. 2012;9:18-23
55. Neuzil P, Reddy VY, Kautzner J, Petru J, Wichterle D, Shah D, Lambert H, Yulzari A, Wissner E, Kuck KH. Electrical reconnection after pulmonary vein isolation is contingent on contact force during initial treatment: Results from the efficacy study. *Circulation. Arrhythmia and electrophysiology*. 2013;6:327-333

56. Reddy VY, Shah D, Kautzner J, Schmidt B, Saoudi N, Herrera C, Jais P, Hindricks G, Peichl P, Yulzari A, Lambert H, Neuzil P, Natale A, Kuck KH. The relationship between contact force and clinical outcome during radiofrequency catheter ablation of atrial fibrillation in the toccata study. *Heart rhythm : the official journal of the Heart Rhythm Society*. 2012;9:1789-1795
57. Wakili R, Clauss S, Schmidt V, Ulbrich M, Hahnefeld A, Schussler F, Siebermair J, Kaab S, Estner HL. Impact of real-time contact force and impedance measurement in pulmonary vein isolation procedures for treatment of atrial fibrillation. *Clinical research in cardiology : official journal of the German Cardiac Society*. 2014;103:97-106
58. Firme EB, Cavalcanti IL, Barrucand L, Assad AR, Figueiredo NV. Curative ablation of atrial fibrillation: Comparison between deep sedation and general anesthesia. *Revista do Colegio Brasileiro de Cirurgioes*. 2012;39:462-468
59. Di Biase L, Conti S, Mohanty P, Bai R, Sanchez J, Walton D, John A, Santangeli P, Elayi CS, Beheiry S, Gallinghouse GJ, Mohanty S, Horton R, Bailey S, Burkhardt JD, Natale A. General anesthesia reduces the prevalence of pulmonary vein reconnection during repeat ablation when compared with conscious sedation: Results from a randomized study. *Heart rhythm : the official journal of the Heart Rhythm Society*. 2011;8:368-372
60. Cappato R, Calkins H, Chen SA, Davies W, Iesaka Y, Kalman J, Kim YH, Klein G, Natale A, Packer D, Skanes A, Ambrogi F, Biganzoli E. Updated worldwide survey on the methods, efficacy, and safety of catheter ablation for human atrial fibrillation. *Circulation. Arrhythmia and electrophysiology*. 2010;3:32-38
61. Cappato R, Calkins H, Chen SA, Davies W, Iesaka Y, Kalman J, Kim YH, Klein G, Packer D, Skanes A. Worldwide survey on the methods, efficacy, and safety of catheter ablation for human atrial fibrillation. *Circulation*. 2005;111:1100-1105
62. Calkins H, Kuck KH, Cappato R, Brugada J, Camm AJ, Chen SA, Crijns HJ, Damiano RJ, Jr., Davies DW, DiMarco J, Edgerton J, Ellenbogen K, Ezekowitz MD, Haines DE, Haissaguerre M, Hindricks G, Iesaka Y, Jackman W, Jalife J, Jais P, Kalman J, Keane D, Kim YH, Kirchhof P, Klein G, Kottkamp H, Kumagai K, Lindsay BD, Mansour M, Marchlinski FE, McCarthy PM, Mont JL, Morady F, Nademanee K, Nakagawa H, Natale A, Nattel S, Packer DL, Pappone C, Prystowsky E, Raviele A, Reddy V, Ruskin JN, Shemin RJ, Tsao HM, Wilber D, Heart Rhythm Society Task Force on C, Surgical Ablation of Atrial F. 2012 hrs/ehra/ecas expert consensus statement on catheter and surgical ablation of atrial fibrillation: Recommendations for patient selection, procedural techniques, patient management and follow-up, definitions, endpoints, and research trial design: A report of the heart rhythm society (hrs) task force on catheter and surgical ablation of atrial fibrillation. Developed in partnership with the european heart rhythm association (ehra), a registered branch of the european society of cardiology (esc) and the european cardiac arrhythmia society (ecas); and in collaboration with the american college of cardiology (acc), american heart association (aha), the asia pacific heart rhythm society (aphrs), and the society of thoracic surgeons (sts). Endorsed by the governing bodies of the american college of cardiology foundation, the american heart association, the european cardiac arrhythmia society, the european heart rhythm association, the society of thoracic surgeons, the asia pacific heart rhythm society, and the heart rhythm society. *Heart rhythm : the official journal of the Heart Rhythm Society*. 2012;9:632-696 e621
63. Dagres N, Hindricks G, Kottkamp H, Sommer P, Gaspar T, Bode K, Arya A, Husser D, Rallidis LS, Kremastinos DT, Piorowski C. Complications of atrial fibrillation ablation in a high-volume center in 1,000 procedures: Still cause for concern? *Journal of cardiovascular electrophysiology*. 2009;20:1014-1019
64. Bohnen M, Stevenson WG, Tedrow UB, Michaud GF, John RM, Epstein LM, Albert CM, Koplan BA. Incidence and predictors of major complications from contemporary catheter ablation to treat cardiac arrhythmias. *Heart rhythm : the official journal of the Heart Rhythm Society*. 2011;8:1661-1666
65. De Ponti R. Cryothermal energy ablation of cardiac arrhythmias 2005: State of the art. *Indian pacing and electrophysiology journal*. 2005;5:12-24
66. Andrade JG, Khairy P, Guerra PG, Deyell MW, Rivard L, Macle L, Thibault B, Talajic M, Roy D, Dubuc M. Efficacy and safety of cryoballoon ablation for atrial fibrillation: A systematic review of published studies. *Heart rhythm : the official journal of the Heart Rhythm Society*. 2011;8:1444-1451
67. Dorwarth U, Schmidt M, Wankel M, Krieg J, Straube F, Hoffmann E. Pulmonary vein electrophysiology during cryoballoon ablation as a predictor for procedural success. *Journal of interventional cardiac electrophysiology : an international journal of arrhythmias and pacing*. 2011;32:205-211
68. Tse HF, Lau CP. Impact of duration of cryothermal application on clinical efficacy of pulmonary vein isolation using transvenous cryoablation. *Pacing and clinical electrophysiology : PACE*. 2005;28:839-843

69. Kojodjojo P, O'Neill MD, Lim PB, Malcolm-Lawes L, Whinnett ZI, Salukhe TV, Linton NW, Lefroy D, Mason A, Wright I, Peters NS, Kanagaratnam P, Davies DW. Pulmonary venous isolation by antral ablation with a large cryoballoon for treatment of paroxysmal and persistent atrial fibrillation: Medium-term outcomes and non-randomised comparison with pulmonary venous isolation by radiofrequency ablation. *Heart*. 2010;96:1379-1384
70. Furnkranz A, Bordignon S, Schmidt B, Gunawardene M, Schulte-Hahn B, Urban V, Bode F, Nowak B, Chun JK. Improved procedural efficacy of pulmonary vein isolation using the novel second-generation cryoballoon. *Journal of cardiovascular electrophysiology*. 2013;24:492-497
71. Andrade JG, Dubuc M, Guerra PG, Landry E, Coulombe N, Leduc H, Rivard L, Macle L, Thibault B, Talajic M, Roy D, Khairy P. Pulmonary vein isolation using a second-generation cryoballoon catheter: A randomized comparison of ablation duration and method of deflation. *Journal of cardiovascular electrophysiology*. 2013;24:692-698
72. Coulombe N, Paulin J, Su W. Improved in vivo performance of second-generation cryoballoon for pulmonary vein isolation. *Journal of cardiovascular electrophysiology*. 2013;24:919-925
73. Neumann T, Vogt J, Schumacher B, Dorszewski A, Kuniss M, Neuser H, Kurzidim K, Berkowitsch A, Koller M, Heintze J, Scholz U, Wetzel U, Schneider MA, Horstkotte D, Hamm CW, Pitschner HF. Circumferential pulmonary vein isolation with the cryoballoon technique results from a prospective 3-center study. *Journal of the American College of Cardiology*. 2008;52:273-278
74. Mansour M, Forleo GB, Pappalardo A, Barrett C, Heist EK, Avella A, Bencardino G, Dello Russo A, Casella M, Ruskin JN, Tondo C. Combined use of cryoballoon and focal open-irrigation radiofrequency ablation for treatment of persistent atrial fibrillation: Results from a pilot study. *Heart rhythm : the official journal of the Heart Rhythm Society*. 2010;7:452-458
75. Tse HF, Reek S, Timmermans C, Lee KL, Geller JC, Rodriguez LM, Ghaye B, Ayers GM, Crijns HJ, Klein HU, Lau CP. Pulmonary vein isolation using transvenous catheter cryoablation for treatment of atrial fibrillation without risk of pulmonary vein stenosis. *Journal of the American College of Cardiology*. 2003;42:752-758
76. Chun KR, Schmidt B, Metzner A, Tilz R, Zerm T, Koster I, Furnkranz A, Koekuer B, Konstantinidou M, Antz M, Ouyang F, Kuck KH. The 'single big cryoballoon' technique for acute pulmonary vein isolation in patients with paroxysmal atrial fibrillation: A prospective observational single centre study. *European heart journal*. 2009;30:699-709
77. Packer DL, Kowal RC, Whealan KR, Irwin JM, Champagne J, Guerra PG, Dubuc M, Reddy V, Nelson L, Holcomb RG, Lehmann JW, Ruskin JN, Investigators SAC. Cryoballoon ablation of pulmonary veins for paroxysmal atrial fibrillation: First results of the north american arctic front (stop af) pivotal trial. *Journal of the American College of Cardiology*. 2013;61:1713-1723
78. Ahmed H, Neuzil P, d'Avila A, Cha YM, Laragy M, Mares K, Brugge WR, Forcione DG, Ruskin JN, Packer DL, Reddy VY. The esophageal effects of cryoenergy during cryoablation for atrial fibrillation. *Heart rhythm : the official journal of the Heart Rhythm Society*. 2009;6:962-969
79. Ripley KL, Gage AA, Olsen DB, Van Vleet JF, Lau CP, Tse HF. Time course of esophageal lesions after catheter ablation with cryothermal and radiofrequency ablation: Implication for atrio-esophageal fistula formation after catheter ablation for atrial fibrillation. *Journal of cardiovascular electrophysiology*. 2007;18:642-646
80. Vilades Medel D, Marti-Almor J, Montiel Serrano J, Sionis A, Leta Petracca R. Atrioesophageal fistula secondary to pulmonary vein cryo-ablation. *European heart journal cardiovascular Imaging*. 2014;15:116
81. Stockigt F, Schrickel JW, Andrie R, Lickfett L. Atrioesophageal fistula after cryoballoon pulmonary vein isolation. *Journal of cardiovascular electrophysiology*. 2012;23:1254-1257
82. Tarjan P, Boveja B, Cohen D, Joubert T, Zalewski E. An experimental device for low-energy, precise ablation of av conduction. *Pacing and clinical electrophysiology : PACE*. 1986;9:1396-1402
83. Moroe K, Hiroki T, Okabe M, Sasaki Y, Fukuda K, Arakawa K. A transarterial approach of electrical ablation of atrioventricular junction in a dog model: Comparison of the effects between high and low energy shocks. *Pacing and clinical electrophysiology : PACE*. 1989;12:1474-1484
84. Ahsan AJ, Cunningham D, Rowland E, Rickards AF. Catheter ablation without fulguration: Design and performance of a new system. *Pacing and clinical electrophysiology : PACE*. 1989;12:1557-1561
85. Cunningham D, Rowland E, Rickards AF. A new low energy power source for catheter ablation. *Pacing and clinical electrophysiology : PACE*. 1986;9:1384-1390

86. Ahsan AJ, Cunningham D, Rowland E. Low energy catheter ablation of right ventricular outflow tract tachycardia. *British heart journal*. 1991;65:231-233
87. Connelly DT, Rowland E, Ahsan AJ, Cunningham D. Low energy catheter ablation of a posteroseptal accessory pathway associated with a diverticulum of the coronary sinus. *Pacing and clinical electrophysiology : PACE*. 1991;14:1217-1221
88. Lemery R, Talajic M, Roy D, Coutu B, Lavoie L, Lavallee E, Cartier R. Low energy direct current ablation in patients with the wolff-parkinson-white syndrome: Clinical outcome according to accessory pathway location. *Pacing and clinical electrophysiology : PACE*. 1991;14:1951-1955
89. Rowland E, Cunningham D, Ahsan A, Rickards A. Transvenous ablation of atrioventricular conduction with a low energy power source. *British heart journal*. 1989;62:361-366
90. Weaver JC. Electroporation theory. Concepts and mechanisms. *Methods in molecular biology*. 1995;47:1-26
91. Freeman SA, Wang MA, Weaver JC. Theory of electroporation of planar bilayer membranes: Predictions of the aqueous area, change in capacitance, and pore-pore separation. *Biophysical journal*. 1994;67:42-56
92. Chang DC, Reese TS. Changes in membrane structure induced by electroporation as revealed by rapid-freezing electron microscopy. *Biophysical journal*. 1990;58:1-12
93. Lee EW, Wong D, Prikhodko SV, Perez A, Tran C, Loh CT, Kee ST. Electron microscopic demonstration and evaluation of irreversible electroporation-induced nanopores on hepatocyte membranes. *Journal of vascular and interventional radiology : JVIR*. 2012;23:107-113
94. Okino M, Mohri H. Effects of a high-voltage electrical impulse and an anticancer drug on in vivo growing tumors. *Japanese journal of cancer research : Gann*. 1987;78:1319-1321
95. Mir LM, Orłowski S, Belehradek J, Jr., Paoletti C. Electrochemotherapy potentiation of antitumor effect of bleomycin by local electric pulses. *European journal of cancer*. 1991;27:68-72
96. Mir LM, Morsli N, Garbay JR, Billard V, Robert C, Marty M. Electrochemotherapy: A new treatment of solid tumors. *Journal of experimental & clinical cancer research : CR*. 2003;22:145-148
97. Mir LM, Glass LF, Sersa G, Teissie J, Domenge C, Miklavcic D, Jaroszeski MJ, Orłowski S, Reintgen DS, Rudolf Z, Belehradek M, Gilbert R, Rols MP, Belehradek J, Jr., Bachaud JM, DeConti R, Stabuc B, Cemazar M, Coninx P, Heller R. Effective treatment of cutaneous and subcutaneous malignant tumours by electrochemotherapy. *British journal of cancer*. 1998;77:2336-2342
98. Heller R, Gilbert R, Jaroszeski MJ. Clinical applications of electrochemotherapy. *Advanced drug delivery reviews*. 1999;35:119-129
99. Neumann E, Schaefer-Ridder M, Wang Y, Hofschneider PH. Gene transfer into mouse lyoma cells by electroporation in high electric fields. *The EMBO journal*. 1982;1:841-845
100. Davalos RV, Mir LM, Rubinsky B. Tissue ablation with irreversible electroporation. *Annals of Biomedical Engineering*. 2005;33:223-231
101. Tovar O, Tung L. Electroporation of cardiac cell membranes with monophasic or biphasic rectangular pulses. *Pacing and clinical electrophysiology : PACE*. 1991;14:1887-1892
102. Davalos RV, Rubinsky B, Mir LM. Theoretical analysis of the thermal effects during in vivo tissue electroporation. *Bioelectrochemistry*. 2003;61:99-107
103. Onik G, Mikus P, Rubinsky B. Irreversible electroporation: Implications for prostate ablation. *Technology in cancer research & treatment*. 2007;6:295-300
104. Rubinsky J, Onik G, Mikus P, Rubinsky B. Optimal parameters for the destruction of prostate cancer using irreversible electroporation. *The Journal of urology*. 2008;180:2668-2674
105. Pech M, Janitzky A, Wendler JJ, Strang C, Blaschke S, Dudeck O, Ricke J, Liehr UB. Irreversible electroporation of renal cell carcinoma: A first-in-man phase I clinical study. *Cardiovascular and interventional radiology*. 2011;34:132-138
106. Deodhar A, Monette S, Single GW, Jr., Hamilton WC, Jr., Thornton R, Maybody M, Coleman JA, Solomon SB. Renal tissue ablation with irreversible electroporation: Preliminary results in a porcine model. *Urology*. 2011;77:754-760
107. Guo Y, Zhang Y, Klein R, Nijm GM, Sahakian AV, Omary RA, Yang GY, Larson AC. Irreversible electroporation therapy in the liver: Longitudinal efficacy studies in a rat model of hepatocellular carcinoma. *Cancer research*. 2010;70:1555-1563

108. Xiao D, Yao C, Liu H, Li C, Cheng J, Guo F, Tang L. Irreversible electroporation and apoptosis in human liver cancer cells induced by nanosecond electric pulses. *Bioelectromagnetics*. 2013;34:512-520
109. Neal RE, 2nd, Davalos RV. The feasibility of irreversible electroporation for the treatment of breast cancer and other heterogeneous systems. *Ann Biomed Eng*. 2009;37:2615-2625
110. Neal RE, 2nd, Singh R, Hatcher HC, Kock ND, Torti SV, Davalos RV. Treatment of breast cancer through the application of irreversible electroporation using a novel minimally invasive single needle electrode. *Breast cancer research and treatment*. 2010;123:295-301
111. Garcia PA, Pancotto T, Rossmeis JH, Jr., Henao-Guerrero N, Gustafson NR, Daniel GB, Robertson JL, Ellis TL, Davalos RV. Non-thermal irreversible electroporation (n-tire) and adjuvant fractionated radiotherapeutic multimodal therapy for intracranial malignant glioma in a canine patient. *Technology in cancer research & treatment*. 2011;10:73-83
112. Rossmeis JH, Jr., Garcia PA, Robertson JL, Ellis TL, Davalos RV. Pathology of non-thermal irreversible electroporation (n-tire)-induced ablation of the canine brain. *Journal of veterinary science*. 2013;14:433-440
113. Ellis TL, Garcia PA, Rossmeis JH, Jr., Henao-Guerrero N, Robertson J, Davalos RV. Nonthermal irreversible electroporation for intracranial surgical applications. Laboratory investigation. *Journal of neurosurgery*. 2011;114:681-688
114. Garcia PA, Rossmeis JH, Jr., Neal RE, 2nd, Ellis TL, Olson JD, Henao-Guerrero N, Robertson J, Davalos RV. Intracranial nonthermal irreversible electroporation: In vivo analysis. *The Journal of membrane biology*. 2010;236:127-136
115. Maor E, Ivorra A, Leor J, Rubinsky B. The effect of irreversible electroporation on blood vessels. *Technology in cancer research & treatment*. 2007;6:307-312



CHAPTER 2

Feasibility of Electroporation for the Creation of Pulmonary Vein Ostial Lesions

Vincent van Driel*
Fred Wittkampf*
Harry van Wessel
Aryan Vink
Irene Hof
Paul Gründeman
Richard Hauer
Peter Loh

* Both authors contributed equally to the study and manuscript

Abstract

Introduction There is an obvious need for a better energy source for pulmonary vein (PV) antrum isolation.

Objective We investigated the feasibility and safety of electroporation for the creation of PV ostial lesions. **Methods:**After transseptal puncture, a custom 7F decapolar 20 mm circular ablation catheter was placed in the PV ostia of 10 pigs. Ablation was performed with a nonarcing, 200 J application delivered between the catheter and an indifferent patch electrode on the lower back. A single pulse was applied for each catheter position, with a maximum of 4 per ostium. Local PV electrogram amplitude and stimulation threshold were measured at multiple locations in both ostia before and directly after ablation, and after 3 weeks survival, using a regular 4 mm mapping catheter. All PV ostia were sectioned, stained, and histologically investigated.

Results The 3-week survival period was uneventful. PV ostial electrogram amplitude decreased and stimulation threshold increased significantly in most ostia. PV angiograms did not show any stenosis during this short follow-up. Histologically, up to 3.5-mm-deep lesions were found.

Conclusion Data suggest that electroporation can safely be used to create lesions in a sensitive environment like PV ostia. (J Cardiovasc Electrophysiol, Vol. pp. 1-8)

Introduction

Various techniques and different energy sources have been developed for electrical isolation of pulmonary vein (PV) ostia, with encircling by sequential radiofrequency (RF) applications as the most commonly applied ablation method.^{1,2} This method has been proven to be effective, but is often limited by long procedure times and a relatively high re-currence rate. In addition, excessive tissue heating, masked by saline cooling, may lead to serious complications, while ablation too far inside a PV ostium may lead to PV stenosis.^{3,4} Due to convective cooling by intracavitary blood, RF lesions have a relatively small diameter at the tissue surface and only reach maximal diameter a few mm deeper. This may easily lead to gaps in the ablation line. Finally, RF heating without open irrigation may cause blood clots by protein aggregation.^{5,6}

In 2007, Wijffels *et al.* described electrogram attenuation and the presence of lesions around the electrodes after internal cardioversion shocks in goats.⁷ This reminded us of the abandoned direct current (DC) catheter ablation technique that was routinely applied between 1980 and 1990.⁸⁻¹⁰ The method was most frequently used for ablation of the bundle of His and ventricular tachycardia. Despite high success rates, DC ablation was quickly replaced by the more elegant RF ablation technique when that became available around 1990. The main disadvantages of DC ablation were the required complete anesthesia, serious complications supposedly related to barotrauma, termination of the arrhythmia by the shock itself independent of lesion formation, and proarrhythmia in the first few days after ablation.¹¹⁻¹³ Barotrauma can be the result of a high-pressure shock-wave that is caused by arcing through an electrically isolating gas bubble around the ablation electrode.¹¹ At the end of the DC ablation era, Ashan *et al.* developed low-energy DC ablation without arcing and the clinical results demonstrated that a sufficiently high current density alone suffices to create myocardial lesions.¹⁴⁻¹⁸ Later studies revealed that lesions are created by the formation of pores in cell membranes and then the term "irreversible electroporation" (IRE) was introduced.¹⁹⁻²¹

In this animal study, we investigated the hypothesis that IRE ablation at an energy level below arcing threshold may be a feasible, safe, and potentially fast technique for the creation of lesions in PV ostia.

Methods

All animal studies were performed with approval from the animal experimental ethical committee of the University Medical Center Utrecht.

Pilot Safety Study

Five Response CV catheters (St. Jude Medical Inc, Minnetonka, MN, USA) were thermally shaped similar to a standard 20 mm circular mapping catheter using heating to 135°C and cooling down in a custom mould. The circular section included the 10 electrodes; the most distal 4 electrodes were 1 mm long, while the proximal 6 electrodes were 2 mm long. Interelectrode spacing was 2–7–2 mm. The proximal coil electrode of the modified catheter was not used. A pilot safety study was performed in 5 pigs of 60–75 kg. Calcium carbasalate (80 mg a day) and clopidogrel (75 mg a day, first dose 300 mg) were started 3 days before the procedure and continued until euthanasia. An intravenous bolus of 2,500 i.u. heparine was administered every 2 hours. An indifferent patch electrode (7506, Valley Lab Inc, Boulder, CO, USA) was placed on a shaven area under the lower back. The modified response CV catheter that was too short to reach the left atrium was transvenously inserted into the ostium of the superior vena cava. In all animals, the diameter of the superior vena cava was smaller than the diameter of the circular catheter section and the catheter had to be pushed into the SVC ostium. A standard response CV catheter was placed in the great cardiac vein. An external defibrillator (Lifepak 9, Physio-Control Inc, Redmond, WA, USA) was used for energy delivery. Connections between Lifepak, skin patch, and the ablation catheters were made using modified paddle cables and a modified catheter connection cable that connected all 10 electrodes together. Five 200 J shocks were delivered via each catheter, using different positions of the indifferent back patch electrode to determine arcing threshold. All pulses were delivered with the endocardial electrodes as anode because of a higher arcing threshold than with cathodal applications when tested in saline.^{14,16,18} Arcing was determined by monitoring current and voltage waveforms on a storage oscilloscope.²² After 2 weeks survival, the pigs were euthanized by exsanguinations and the heart, and circumjacent tissue were thoroughly inspected for damage.

Feasibility and Safety of PV Ostial Ablation

This second study was performed to investigate the feasibility and safety of PV ostial ablations. The custom built nondeflectable 7F circular ablation catheters (St. Jude Medical Inc.) had a 115 cm shaft length and a circular distal section with a diameter of 20 mm containing 10 2 mm-long ring electrodes with 5 mm spacing (**Figure 1**). Experiments were performed in 10 pigs of 60–75 kg. Calcium carbasalate (80 mg a day) and clopidogrel (75 mg a day, first dose 300 mg) were started 3 days before the procedure and continued until euthanasia. The animals were anesthetized and intubated. An indifferent patch electrode (7506, Valley Lab) was placed on the lower back. A quadripolar catheter was inserted via the left femoral vein into the right ventricular apex for back-up pacing. A tiny screw-in wire (6416, Medtronic Inc, Minneapolis, MN, USA) was also inserted via the left femoral vein and fixated in the interatrial septum to serve as positional reference for the NavX system (St. Jude Medical). Transseptal puncture was performed via the right femoral vein for access to the left atrial cavity. Intravenous heparin was administered to maintain an activated clotting time of 250–300 seconds.



Figure 1. The circular IRE catheter that was used for the feasibility and safety study. The distal circular, 20 mm diameter, segment of the nondeflectable 7F catheter contains 10 electrodes of 2 mm in length.

Because of difficulties reaching the PVs, the sheath initially used for transseptal puncture (SR0, St. Jude Medical, Minnetonka, MN, USA) was replaced by a deflectable sheath (Agilis, St. Jude Medical, Minnetonka, MN, USA) after 3 animals. At first, the left atrial geometry was reconstructed using the NavX system (St. Jude Medical) and a standard deflectable quadripolar-mapping catheter (Biosense Webster Inc,

Diamond Bar, CA, USA). Then, a high density left atrial voltage map was created using the distal bipolar electrogram of the mapping catheter. The NavX system was set to interpolate over 10 mm and we attempted to collect enough data points to fill the left atrial geometry completely. In the last 6 animals 2 steps were added to the protocol: (1) PV angiography (AP direction only) before ablation and after 3 weeks, and (2) measurement of bipolar 2 ms pacing threshold at multiple sites in and around the PV ostia before and directly after ablation and after 3 weeks. All stimulation sites were tagged on the NavX geometry. Initially, we tried to place the circular ablation catheter at the PV antrum to deliver a single application at that location. Catheter positioning, however, was complicated by nondeflectability of the prototype catheter, the small porcine left atrial cavity and the location of both ostia very close to the interatrial septum and transeptal puncture site. We never succeeded in placing the circular part of the catheter at the PV antrum. Therefore, and to increase the likelihood of complications, we decided to insert the circular catheter section into the PV ostia and to deliver 1 synchronized 200 J shock for each position that could be obtained inside the ostium with a maximum of 4 applications per ostium. The energy level of 200 J was chosen because it was the highest level that could be delivered via this catheter without arcing. The orientation of the circular catheter section in the PV ostia usually was very slanted and often the circular section was more spiraling than circular. In all PV's, parts of the ostium never came in contact with the ablation electrodes. Directly after each application, the catheter was reconnected to the NavX and electrophysiological recording system (Cardiolab, General Electric Healthcare, Waukesha, WI, USA) to check for electrode integrity by monitoring unipolar electrograms and visualizing electrode positions on the NavX system. In case of electrode failure, the catheter was replaced. Directly after ablations in both ostia, a second left atrial voltage map was created using the distal bipole of a mapping catheter with a 4 mm distal electrode and 2–5–2 interelectrode spacing. Again, enough electrograms sites were collected to cover the complete left atrial geometry using an interpolation of 10 mm, but these sites were not intended to be identical to those of the preablation map. In the last 6 animals, bipolar stimulation threshold was measured again at multiple sites in and around both PV ostia and these sites were also tagged on the NavX geometry. As with the voltage maps, we did not attempt to perform these measurements at sites identical to those where stimulation threshold had been measured before ablation. Then, all catheters were removed and the animals were allowed to recover and kept under daily surveillance. After 3 weeks, a second

catheterization was performed to create a third voltage map. In the last 6 animals PV angiography was performed to check for PV stenosis and stimulation threshold was determined in and around the PV ostia, as had been done during the first catheterization. Thereafter, the animals were euthanized by exsanguination and the heart was removed for gross inspection, and histological investigation of the PV ostia.

Histological Investigation

After fixation in formalin, consecutive circular 4 mm thick segments of the ablated ostia were dissected from the hearts of pig 1–5. From the hearts of pig 6–10, longitudinal PV ostial wall sections of each of the 2 ablated ostia evenly distributed around the ostial perimeter (4–6 sections per ostium) were collected. Circular segments of pig 3 in which the ostia could not be reached with the ablation catheter and longitudinal sections of the ostia of 2 other pigs of another unrelated study in which the left atrium had never been entered served as controls. Sections were embedded in paraffin, sectioned, and stained with hematoxylin–eosin and with elastic–Van Gieson, and evaluated by light microscopy. In addition, a selection of slides was immunohistochemically stained for desmin, which stains cardiomyocytes and smooth muscle cells. A monoclonal mouse antidesmin antibody (dilution 1:100; Biogenesis, Poole, UK) was used as primary antibody, followed by Powervision poly HRP-antimouse IgG (Immunologic, Duiven, The Netherlands). The signal was visualized using diaminobenzidine. Sections were counter-stained with hematoxylin.

Electrogram Amplitude and Stimulation Threshold Analysis

Electrogram amplitude and stimulation threshold data before ablation was compared to the measurements directly postablation and at 3 weeks to investigate the presence of lesions at those locations. In this analysis, we included all measurements obtained within the complete tubular segment of each PV ostium where IRE pulses had been delivered, irrespective of the fact that parts of those segments had not been in contact with the IRE catheter during ablation.

PV Angiograms

PV angiograms obtained before ablation, and after 3 weeks, were visually compared by 2 independent cardiologists who were not informed about when each angiogram was taken.

Statistical Analysis

Data are expressed in mean \pm SD. Differences between the 3 groups of electrogram amplitude data were compared with ANOVA using the Scheffe method for multiple comparisons. Stimulation threshold data were compared by calculating the proportion of sites within each ostial segment with a stimulation threshold ≤ 10 mA. The proportion of such sites directly after ablation and at 3 weeks were compared with the proportion before ablation within the same segment using the 2-tailed exact test. A P-value of 0.05 was used as the level of statistical significance.

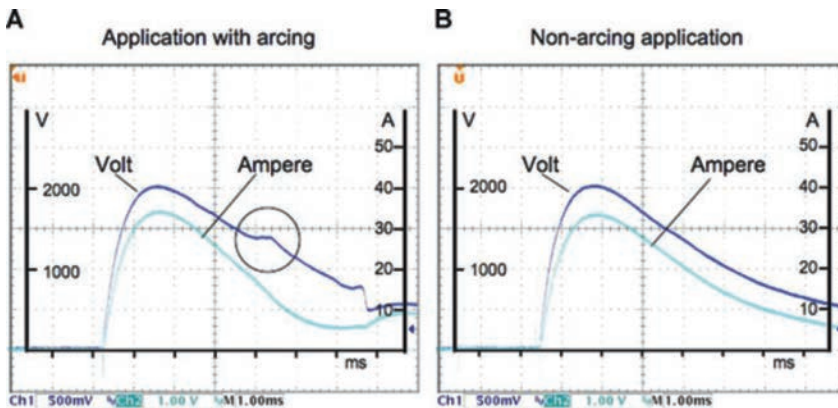


Figure 2. A–B: Examples of voltage and current waveforms with (panel A) and without (panel B) arcing. With too high current, electrolysis causes a large enough gas bubble to electrically isolate the ablation electrodes. This results in a rise in resistance and voltage during the shock (panel A) followed by arcing that causes an explosion, pressure wave, and possibly barotrauma. In panel B, the indifferent patch electrode on the back has been moved further away from the heart. This increases impedance and eliminates arcing.

Results

Pilot Safety Study

The position of the patch electrode affected total impedance and thus also the magnitude of the current delivered by the shock. In the 5 pilot pigs, the voltage waveforms started to show minor waveform discontinuities when total peak current during the shock reached values above 30 A (**Figure 2**).²² With the indifferent patch electrode on the lower back, total impedance was high enough to prevent arcing. The 2-week survival of these animals was uneventful. After euthanasia, the hearts and circumjacent tissue were visually inspected, especially the great cardiac vein and ostium of the superior vena cava, but no abnormalities

were found despite the fact that we had produced some arcing in all animals while testing for arcing threshold.

Feasibility of PV Ostial Ablation with IRE

The porcine left atrium usually has 2 PV ostia of 15–20 mm in diameter; 1 on the right side, dorsal to the right atrium and oriented to the right and 1 in the inferior left atrium and caudally posteriorly oriented. We sometimes also found a small (approximately 5 mm wide) left-sided PV, too small for our circular ablation catheter to enter. The voltage maps that were created before and directly after ablation, and at 3 weeks consisted of 159 ± 77 , 148 ± 78 , and 189 ± 72 (n.s.) mapping sites, respectively. In **Tables 1** and **2**, we list all animals and PV's with the number of applications that had been delivered per ostium. In the first 2 pigs, we could only obtain a single position of the ablation catheter in each ostium and then only a single application was delivered. In pig 3, we did not succeed to place the nondeflectable catheter in any of the 2 PV ostia and no applications were delivered. Adding the Agilis deflectable sheath (St. Jude Medical Inc.) to our armamentarium facilitated positioning of the ablation catheter inside the ostia in the remaining 6 animals.

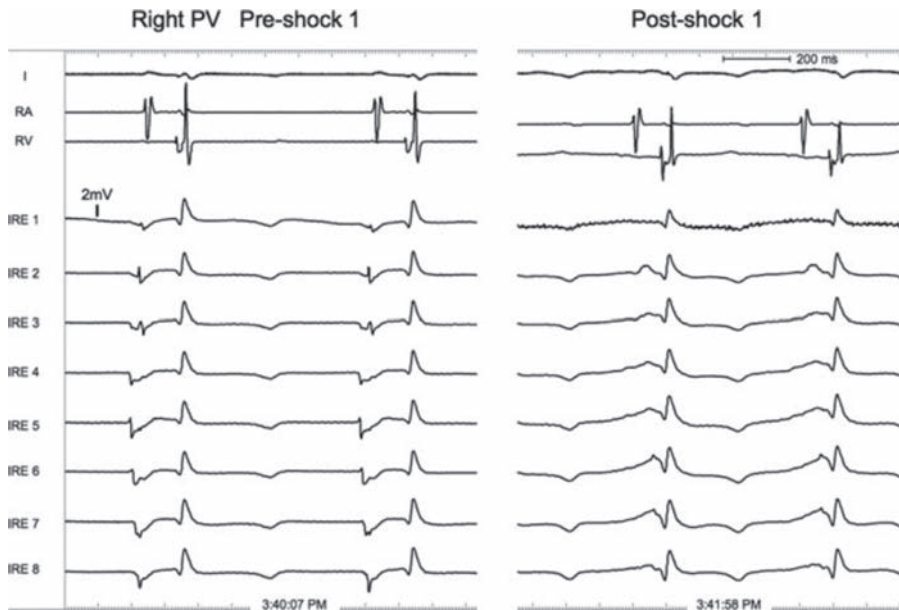


Figure 3. Unipolar pulmonary vein (PV) ostial potentials recorded with the irreversible electroporation (IRE) catheter before and after a first 200 J shock in the right PV ostium of 1 of the animals. Due to limitations of the electrogram recording system, only 8 unipolar electrograms could be recorded simultaneously.

Table 1. Electrogram Amplitudes Inside PV Ostia

Pig no.	PV	Ablations	Pre		Post		3 weeks	
			Sites (n)	Mean EGM (mV)	Sites (n)	Mean EGM (mV)	Sites (n)	Mean EGM (mV)
1	Right	1	9	2.2	7	0.1 s	9	0.9 n.s.
2	Right	1	7	3.1	5	0.3 s	8	0.8 s
	Inferior	1	8	3.1	4	0.5 n.s.	6	1.8 n.s.
4	Right	3	23	2.8	12	0.0 s	10	0.2 s
	Inferior	4	20	2.4	10	0.0 s	8	0.1 s
5	Right	4	16	4.8	13	0.1 s	8	0.3 s
	Inferior	4	14	2.9	20	0.2 s	11	0.1 s
6	Right	3	8	1.8	10	0.3 s	12	0.4 s
	Inferior	3	10	3.1	6	0.0 s	13	0.6 s
7	Right	3	9	2.9	5	0.2 s	16	0.6 s
	Inferior	3	5	3.4	7	0.1 s	7	0.7 s
8	Right	3	17	2.5	13	0.0 s	23	0.4 s
	Inferior	4	18	0.9	13	0.0 n.s.	9	0.2 n.s.
9	Right	2	13	3.7	20	0.0 s	13	0.3 s
	Inferior	3	16	1.2	20	0.0 s	14	0.6 s
10	Right	4	13	2.9	15	0.0 s	11	1.0 n.s.
	Inferior	3	10	0.8	21	0.0 s	21	0.3 n.s.
Pooled mean	2.9		2.6 ±2.1		0.1 ±0.2		0.5 ±0.5	

Electrogram amplitudes measured in the right and inferior pulmonary vein ostium postablation and at 3 weeks. Pooled data are shown in the bottom line.

Differences between the 3 groups were compared with ANOVA using Scheffe's method for multiple comparisons. Electrogram amplitudes postablation and at 3 weeks were both significantly different from preablation amplitudes, but the difference between postablation and 3 weeks data did not reach statistical significance. PV=pulmonary vein; EGM=electrogram; s=significant; n.s.=nonsignificant.

An example of unipolar electrogram reduction by a first circular 200 J shock delivered in a right PV ostium of 1 of the animals is shown in **Figure 3**. Despite very slanted catheter positions and absence of electrode contact with parts of the ostia during most ablations, there is a significant reduction in electrogram amplitudes after 1 to 4 applications in the 15 of the 17 treated PV ostial segments (**Table 1**). At 3 weeks, significant electrogram attenuation persists in 12 of the 17 ostia. The NavX reconstruction of the right PV ostium of animal 8 and shadows of the 3 catheter positions where shocks were delivered is shown in **Figure 4A**. The voltage maps obtained before ablation, directly after ablation, and after 3 weeks are shown in panels B, C, and D, respectively (**Figure 4**). Remarkably, the 3 ablations inside the ostium also affected the electrograms proximal to the ostium. At 3 weeks, most of this area had recovered, indicating a transient effect of electroporation around a permanently affected area. In agreement with the observed electrogram reduction,

the percentage of sites with a stimulation threshold ≤ 10 mA (4 mm distal electrode) decreased significantly from before to directly after ablation in 9 of 12 PV ostia (**Table 2**). After 3 weeks, the proportion of stimulation sites with a threshold ≤ 10 mA in the treated ostial segments remained significantly lower in 7 of 12 ostia.

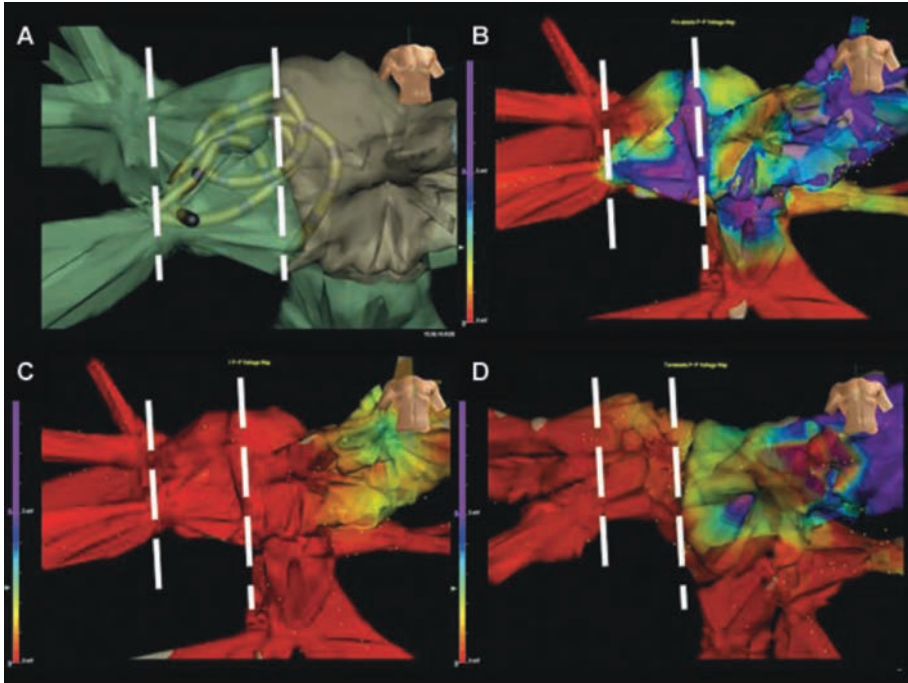


Figure 4. A–D: A: Anterior view of the NavX reconstruction of part of the left atrial geometry of animal 8 with shadows of the 3 catheter positions inside the ostium of the right pulmonary vein where 200 J shocks were delivered. The ostial segment where electrogram amplitudes and stimulation threshold data were compared is indicated with the dotted lines. B–D: Using the distal bipole of a deflectable mapping catheter with a 4 mm distal electrode and 2–5–2 mm interelectrode spacing, electrogram amplitude maps were created with a 0–5 mV scale and an interpolation of 10 mm. Voltage map before ablation (panel A), directly after ablations (panel B) and after 3 weeks survival (panel C). Directly after 3 ostial ablations, electrograms have completely been eliminated inside the ostium. An area proximal to the ablation ostium apparently also is affected. After 3 weeks survival, this latter area has partly recovered and inside the ostium small amplitude electrograms have reappeared at the roof of ostium.

PV Angiography

PV ostial angiography of both ostia was attempted in the last 6 animals, before ablation and after 3 weeks. Of 10 of these 12 PV ostia, both angiograms were of sufficient quality to allow visual comparison. The consensus of both independent cardiologists was no change in diameter of any of the 10 PV ostia, 3 weeks after ablation.

Table 2 Stimulation Thresholds Inside PV Ostia

Pigno.	PV	Ablations n	Pre		Post		3 weeks	
			Sites n	≤10 mA n	Sites n	≤10 mA n	Sites n	≤10 mA n(%)
5	Right	4	5	4	6	0 s	8	2 s
	Inferior	4	4	2	3	0 n.s.	5	2 n.s.
6	Right	3	10	8	6	0 s	5	1 s
	Inferior	3	5	1	5	0 n.s.	7	2 n.s.
7	Right	3	6	5	3	0 s	8	0 s
	Inferior	3	5	5	5	0 s	8	0 s
8	Right	3	6	6	3	0 s	8	2 s
	Inferior	4	5	5	3	0 s	8	2 s
9	Right	2	5	4	6	0 s	7	4 n.s.
	Inferior	3	6	4	4	2 n.s.	6	3 n.s.
10	Right	4	13	13	6	1 s	10	2 s
	Inferior	3	6	5	6	0 s	8	5 n.s.
Pooled			76	62	56	3 s	88	25 s

The proportion of stimulation sites with stimulation threshold ≤ 10 mA directly after ablation and after 3 weeks were compared with the corresponding value before ablation using the 2-tailed exact test, with $P=0.05$ as the level of statistical significance. Pooled data are shown in the bottom line. PV=pulmonary vein; s=significant; n.s.=nonsignificant.

Histological Investigation

Histological sections from the control pigs revealed the transition from the atrial wall into the wall of the PV, where cardiomyocytes from the atrial sleeve pass into smooth muscle cells of the vein (**Figure 5**). In the ablated veins, a uniform scar consisting of loose connective tissue with fibroblasts was observed at the site of the transition. In addition, granulation tissue was observed. The elastic lamina was disrupted and in some cases a giant cell reaction was found in areas where the elastic fibers were fragmented. Remnants of degenerated cardiomyocytes were observed at the borders of the scar tissue. At the luminal side, intimal fibrosis was present in some of the veins. Lesion depth could only be measured at a few sites where atrial myocardium was larger than lesion depth, and the maximum depth was 3.5 mm.

Discussion

In this feasibility and safety study, we used circular low power DC applications to create PV ostial lesions. IRE is an attractive technology: it lacks the risk of thermal blood clot formation, does not require a complex catheter design because

thermocouples and irrigation are not required, and the application only takes a few milliseconds. The preliminary data of this study suggest that this form of energy can safely be applied to PV ostia. IRE also has some disadvantages: It cannot be titrated as easily as RF and the necessity to use anesthesia, is a drawback especially in Europe. These disadvantages may have to be balanced against an expected much shorter procedure duration.

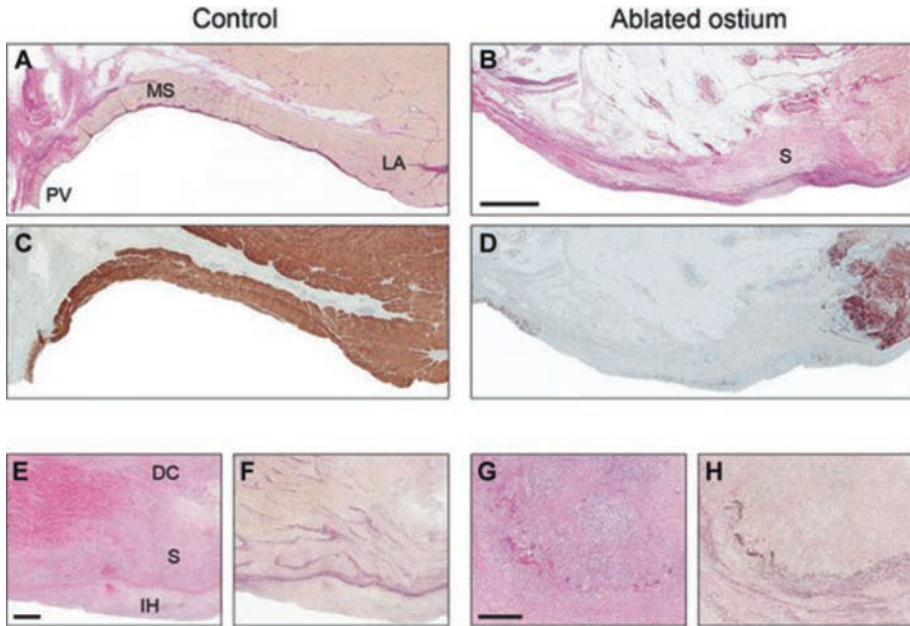


Figure 5. A–H: Histology of pulmonary vein ostial tissue. A and C: Control showing the transition of the myocardium of the left atrium (LA) to a pulmonary vein (PV) with a myocardial sleeve (MS) in the proximal part of the vein. A: Elastic–Van Gieson stain (EvG) showing cardiomyocytes and smooth muscle cells (yellow), connective tissue (red), and elastica fibers (black). C: Desmin immunostain showing a continuum of cardiomyocytes in the left atrium and the myocardial sleeve and smooth muscle cells in the pulmonary vein. B and D: Ablated vein showing a scar (S) in the transition from the left atrium to the myocardial sleeve. B: EvG stain showing replacement of the cardiomyocytes (yellow) by loose connective tissue (red). Bar =2 mm. D: Desmin immunostain showing remnants of the cardiomyocytes of the left atrium and smooth muscle cells in the pulmonary vein (brown staining). The scar induces a disruption of the cardiomyocytes in the atrium and myocardial sleeve. E: Intimal hyperplasia (IH) at the luminal site of the scar (S). At the border of the scar, degenerated cardiomyocytes (DC) with vacuolization are present. Hematoxylin and eosin (H&E) staining; bar =500 μ m. F: EvG staining of the same area as panel E. G: Granulation tissue with giant cells around fragments of the disrupted elastic lamina of the pulmonary vein. H&E staining; bar =500 μ m. H: EvG staining of the same area as panel G showing the fragmented elastic lamina in black.

In the past, high energy was delivered via a 2 mm distal ablation electrode in patients. In a saline tank there is an impressive difference between 360 J delivered via a single electrode and 20 J delivered via each of the 10 electrodes of the

prototype catheter. The former causes a frightening explosion, arcing with a melted footprint on the platinum electrode, and multiple (>10) 2–4 mm diameter gas bubbles. Remarkably, permanent neurological damage by the latter has never been reported. The 200 J via 10 electrodes only leads to a soft tick and grayish discoloration of the electrodes by microscopically small gas bubbles that adhere to the metal surface and dissolve within a few seconds.

Energies higher than 200 J may be required for PV antrum isolation in humans. With the prototype catheter having a total electrode surface area of 150 mm², arcing threshold with anodal applications can be reached at 200 J by using an indifferent skin patch electrode close to the heart. However, a circular all metal 6-7F catheter with a 20 mm diameter circular segment will have a surface area >400 mm² and will undoubtedly allow for higher energy applications and larger lesions. Separate electrodes, however, remain preferable because they allow mapping and nonfluoroscopic catheter localization, but there still is room for increasing electrode size to 200–300 mm² and thus for delivery of higher current without arcing.

The objective of catheter ablation in patients with AF is complete electrical isolation of all PV's. The gold standard for determination of PV isolation is the abolishment of all PV potentials. In this study, our main goal was to investigate the feasibility and acute safety of IRE for the creation of lesions inside PV ostia. Complete electrical PV isolation would have been an unrealistic goal with the prototype catheters. We therefore did not study PV isolation, but only the presence of lesions in the area that was targeted.

Despite slanted catheter positions that left great parts of the ostia untouched by the ablation electrodes, we often observed a major electrogram amplitude reduction and stimulation threshold increase throughout almost the complete PV ostial segments where ablations had been performed. One may speculate that with current density as the ablative mechanism, the lesions may be broader than with RF where the lesion diameter at the tissue surface remains relatively small due to blood cooling. Like with other ablation techniques, the design of a circular catheter that can be placed at the PV antrum remains a major challenge.

Limitations

This study does not pretend to demonstrate an instant solution for circular PV isolation. It only is a first attempt to investigate whether IRE can be used safely

to create lesions in a sensitive environment like a PV ostium. Obviously, further studies will be required to determine the relationship between applied energy and lesion size for such circular application. In addition, lesions will probably have to become larger to isolate PV ostia in humans. We used a standard external monophasic defibrillator that only allowed for a limited number of discrete energy levels. A different generator will also have to be developed with better adjustability of shock magnitude and monitoring of the application.

In this study, only anodal shocks were delivered based on our own saline tank experiments and other *in vitro* saline studies that demonstrated higher arcing threshold for anodal than for cathodal pulses.^{13,15} Studies that used a blood environment, however, report that cathodal applications have a higher threshold for arcing.^{14,21} For the formation of lesions, it is unlikely that polarity will play a role because the direction of the electrical current through the cell membrane at 1 side of the cell will be opposite to the direction at the other side.

During PV ostial ablations, the indifferent skin patch was placed at the lower back, a site that eliminated arcing during the pilot study at the same energy setting of 200 J. However, current and voltage waveforms were not monitored during PV ostial ablations. We therefore cannot exclude that small sparks had occurred during these latter ablations. If so, then they did not cause any complications.

The ablation energy was delivered via all 10 electrodes connected together, and we did not monitor the electrical current delivered via each individual electrode. According to Ohm's law, electrode impedance determines the amount of current that will flow through each electrode when all electrodes are connected to the same power source. During catheter mapping, electrode impedance is only minimally affected by the degree of tissue contact.²³ Therefore, there is little reason to suspect significant differences in current delivery via individual electrodes.

Comparison of ostial electrogram and stimulation data within the same ostial segment is hindered by some differences between left atrial geometries as reconstructed with the NavX system during the 2 procedures. In addition, electrograms and stimulation threshold data were not obtained at identical locations pre- and postablation and at 3 weeks.

For the interpretation of stimulation threshold data we used a value of 10 mA to discriminate between viable and nonviable tissue under the (4 mm) stimulation electrode. On healthy atrial myocardium in patients, stimulation threshold with a 7F, 4 mm long distal electrode usually is between 2 and 5 mA. With a radial spread

of stimulation current, the magnitude of a stimulus (current density) decreases with the square root of distance from the center of the electrode, and with bipolar stimulation this decay is even faster. The reach of a 10 mA stimulus will therefore be in the order of 1–2 mm from the electrode surface. However, 10 mA remains an arbitrary criterion. We therefore also analyzed our data with a 20 mA limit and the only difference was the directly postablation data in the right PV ostium in Fig 7 that became nonsignificantly different from the situation before ablation (**Table 2**).

Lesion size, depth, and continuity could not properly be analyzed in the present study. The delivery of multiple IRE shocks in most veins, the complex anatomy of PV ostia, the often very thin myocardial sleeves, and the uncertainty where exactly ablations had been performed complicates histological analysis of the lesions. A following study, in a different animal model, focusing on the relationship between tissue contact, delivered current, number of applications, and lesion depth created with a circular arrangement of the ablation electrodes, is required for further development of this technique.

Lesion borders appeared to be sharp, as far as we could observe given the often very thin myocardial sleeves.

In this study, lesions were created inside PV ostia. Angiograms did not show a reduction in size of the PV ostia after ablation, at least not in the coronal plane, approximately perpendicular to the PV longitudinal axis, but the follow-up after the procedure was too short to exclude this potential complication. A study with canine PV ostal RF ablations however, has reported PV stenoses already after 2 weeks. The absence of any change in diameter of the 10 PV ostia that were followed for 3 weeks may suggest a difference in reaction of PV ostial tissue between thermal and electroporation injury.²⁴ This important issue should also be addressed in future studies.

Conclusions

Data of this study suggest that low energy IRE can create lesions in PV ostia and in this limited experience it appears surprisingly safe in this sensitive environment. Further study is necessary to determine the required ablation current, mode of delivery, safety limits, and optimal catheter design for the creation of transmural circular lesions.

References

1. Cappato R, Calkins H, Chen SA, Davies W, Iesaka Y, Kalman J, Kim YH, Klein G, Packer D, Skanes A: Worldwide survey on the methods, efficacy, and safety of catheter ablation for human atrial fibrillation. *Circulation* 2005;111:1100-1105.
2. Calkins H, Brugada J, Packer DL, Cappato R, Chen SA, Crijns HJ, Damiano RJ Jr, Davies DW, Haines DE, Haissaguerre M, Iesaka Y, Jackman W, Jais P, Kottkamp H, Kuck KH, Lindsay BD, Marchlinski FE, McCarthy PM, Mont JL, Morady F, Nademanee K, Natale A, Pappone C, Prystowsky E, Raviele A, Ruskin JN, Shemin RJ: HRS/EHRA/ECAS Expert consensus statement on catheter and surgical ablation of atrial fibrillation: Recommendations for personnel, policy, procedures and follow-up. A report of the Heart Rhythm Society (HRS) task force on catheter and surgical ablation of atrial fibrillation. *Heart Rhythm* 2007;4:816-861.
3. Scanavacca MI, D'Avila A, Parga J, Sosa E: Left atrial-esophageal fistula following radiofrequency catheter ablation of atrial fibrillation. *J Cardiovasc Electrophysiol* 2004;15:960-962.
4. Robbins IM, Colvin EV, Doyle TP, Kemp WE, Loyd JE, McMahon WS, Kay GN: Pulmonary vein stenosis after catheter ablation of atrial fibrillation. *Circulation* 1998;98:1769-1775.
5. Yokoyama K, Nakagawa H, Wittkamp FHM, Pitha JV, Lazzara R, Jackman WM: Comparison of electrode cooling between internal and open irrigation in radiofrequency ablation lesion depth and incidence of thrombus and steam pop. *Circulation* 2006;113:11-19.
6. Sauren LD, van Belle Y, de Roy L, Pison L, LA Meir M, Van Der Veen FH, Crijns HJ, Jordaens L, Mess WH, Maessen JG: Transcranial measurement of cerebral microembolic signals during endocardial pulmonary vein isolation: Comparison of three different ablation techniques. *J Cardiovasc Electrophysiol* 2009;20:1102-1107.
7. Wijffels MCEF, Timmermans CCMM, van Suylen RJ, Rodriguez LM: Internal atrial shock delivery by standard diagnostic electrophysiology catheters in goats: Effects on atrial electrogram amplitude and tissue architecture. *Europace* 2007;9:203-207.
8. Scheinman MM, Morady F, Hess DS, Gonzalez R: Catheter-induced ablation of the atrioventricular junction to control refractory supraventricular arrhythmias. *JAMA* 1982;248:851-855.
9. Gallagher JJ, Svenson RH, Kasell JH, German LD, Bardy GH, Broughton A, Critelli G: Catheter technique for closed-chest ablation of the atrioventricular conduction system. *N Engl J Med* 1982;306:194-200.
10. Gonzalez R., Scheinman MM, Margaretten W, Rubinstein M: Closed-chest electrode-catheter technique for His bundle ablation in dogs. *Am J Physiol* 1981;241:H283-H287.
11. Bardy GH, Coltorti F, Stewart RB, Greene HL, Ivey TD: Catheter-mediated electrical ablation: The relation between current and pulse width on voltage breakdown and shock-wave generation. *Circ Res* 1988;63:409-414.
12. Haissaguerre M, Montserrat P, Warin JF, Donzeau JP, Le Metayer P, Massiere JP: Catheter ablation of left posteroseptal accessory pathways and of long RP' tachycardias with a right endocardial approach. *Eur Heart J* 1991;12:845-859.
13. Hauer RN, Robles de Medina EQ, Borst C: Proarrhythmic effects of ventricular electrical catheter ablation in dogs. *J Am Coll Cardiol* 1987;10:1350-1356.
14. Ahsan AJ, Cunningham D, Rowland E, Rickards AF: Catheter ablation without fulguration: Design and performance of a new system. *Pacing Clin Electrophysiol* 1989;12:1557-1561.
15. Rowland E, Cunningham D, Ahsan A: Transvenous ablation of atrioventricular conduction with a low energy power source. *Br Heart J* 1989;62:361-366.
16. Lemery R, Leung TK, Lavallee E, Girard A, Talajic M, Roy D, Montpetit M: In vitro and in vivo effects within the coronary sinus of nonarc and arcing shocks using a new system of low-energy DC ablation. *Circulation* 1991;83:279-293.
17. Ahsan AJ, Cunningham D, Rowland E: Low energy catheter ablation of right ventricular outflow tract tachycardia. *Br Heart J* 1991;65:231-233.
18. Lemery R, Talajic M, Roy D, Coutu B, Lavoie L, Lavallee E, Cartier R: Success, safety, and late electrophysiological outcome of low-energy direct-current ablation in patients with the Wolff-Parkinson-White syndrome. *Circulation* 1992;85:957-962.

Chapter 2

19. Jones JL, Jones RE, Balasky G: Microlesion formation in myocardial cells by high-intensity electric field stimulation. *Am J Physiol* 1987;253:H480-H486.
20. Tovar O, Tung L: Electroporation of cardiac cell membranes with monophasic or biphasic rectangular pulses. *Pacing Clin Electrophysiol* 1991;14:1887-1892.
21. Lee RC, Zhang D, Hannig J: Biophysical injury mechanisms in electrical shock trauma. *Annu Rev Biomed Eng* 2000;02:477-509.
22. Bardy GH, Coltorti F, Ivey TD, Alferness C, Rackson M, Hansen K, Stewart R: Some factors affecting bubble formation with catheter-mediated defibrillator pulses. *Circulation* 1986;73:525-538.
23. Nakagawa H, Kautzner J, Natale A, Peichl P, Ikeda A, Jackman WM: Electrogram amplitude and impedance are poor predictors of electrode-tissue contact force in ablation of atrial fibrillation. *Heart Rhythm* 2010;5S:S65 (abstract).
24. Taylor GW, Kay GN, Zheng X, Sanford Bishop S, Ideker RE: Pathological effects of extensive radiofrequency energy applications in the pulmonary veins in dogs. *Circulation* 2000;101:1736-1742.



CHAPTER 3

Myocardial Lesion Depth with Circular Electroporation Ablation

Fred Wittkamp
Vincent van Driel
Harry van Wessel
Kars Neven
Paul Gründeman
Aryan Vink
Peter Loh
Pieter Doevendans

Abstract

Background Recently, we demonstrated the feasibility and safety of circular electroporation ablation in porcine pulmonary vein ostia, but the relationship between the magnitude of the application and lesion dimensions is still unknown.

Methods and Results An in vivo porcine study was performed on left ventricular epicardium submerged under 10 mm of blood, using devices that mimic a 20-mm-diameter 7F circular ablation catheter. Model D contained 10 separate electrodes, whereas model M consisted of 1 circular electrode. Ablations were performed at 50, 100, and 200 J with model D and at 100 J with model M. Lesion dimensions were measured after 3-week survival. All applications resulted in smooth voltage waveforms demonstrating the absence of vapor globe formation, arcing, and a pressure wave. Applications up to 100 J with model D resulted in separate lesions under the electrodes. At 200 J, continuous deep circular lesions were created despite the use of separate electrodes. There was a significant relationship between applied current and median lesion depth, with a slope of 0.17 mm/A. At 100 J, there was no difference in lesion depth or width between models D and M. The electrodes and ablation site directly after ablation showed no signs of thermal damage.

Conclusions In an epicardial porcine model with blood around the application site, continuous circular lesions, deep enough for electric pulmonary vein isolation, were created with a single circular 200-J application. Lesions were continuous despite the use of separate electrodes. Lesion depth increased with the magnitude of the application. (Circ Arrhythm Electrophysiol. 2012;5:581-586.)

Introduction

A strong electric field can permanently permeabilize a cell membrane, and this may lead to exhaustion of metabolic energy and tissue necrosis.¹ This was part of the ablative effect of direct current (DC) catheter ablation used between 1980 and 1990.² Typically, 300 to 400 J was applied via the 2-mm distal electrode of a nondeflectable catheter. However, these shocks caused electroporation and a cascade of events initiated by sufficient electrolysis at the electrode surface to create an electrically isolating vapor globe. This led to a spark (arcing), an explosion, and a pressure wave. The spark even left a melted footprint on the platinum electrode surface.

At the end of the 1980s, low-energy DC ablation was developed.³ Several studies^{3,4} demonstrated that an energy level lower than the arcing threshold could successfully create myocardial lesions without the previously mentioned hazardous adverse effects.

Recently, Lavee et al⁵ demonstrated epicardial nonthermal electroporation ablation of myocardial tissue. We recently presented the first results of a feasibility study using irreversible electroporation (IRE) ablation inside pulmonary vein (PV) ostia.⁶ To pave the way for clinical electric PV isolation using electroporation technology, the relationship between delivered energy and lesion size in this setting needs to be known, but the fairly thin myocardium of PV ostia precludes assessment of this relationship.

The purpose of our porcine study was to investigate the relationship between the magnitude of the IRE application and the dimensions of the lesion using a circular arrangement of ablation electrodes in a tissue-blood environment.

Methods

All studies were performed with approval from the Animal Experimentation Committee of the University Medical Center Utrecht, Utrecht, the Netherlands.

Study Protocol

The study was performed in 5 pigs (weight, 60–75 kg). Calcium carbasalate (80 mg/d) and clopidogrel (75 mg/d; first dose, 300 mg) therapy was started 3 days before the procedure and continued until euthanasia. Amiodarone therapy was

started 1 week before the procedure (600 mg/d) and continued in a 400-mg/d schedule to prevent procedure-related arrhythmias. The animals were intubated and anesthetized according to standard procedures. The thorax was opened via a medial sternotomy. A 10-cm-long incision was made in the pericardial sack, and its edges were lifted and attached to surrounding instrumentation to create a pericardial cradle. A Starfish Heart Positioner (Medtronic Inc; Minneapolis, MN) was used to raise the apex and to expose the basal left ventricular area.

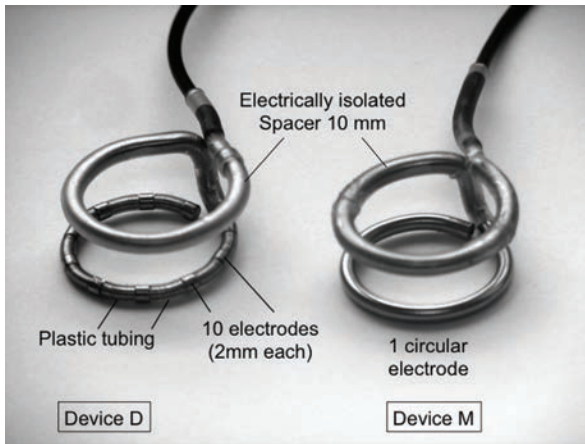


Figure 1. The 2 custom devices used for ablation. Type D has 10 metal 2-mm-long and 7F-diameter contacts mimicking a decapolar circular ablation catheter with all electrodes interconnected. Type M has one 7F circular electrode. Both devices are 20 mm in diameter and have a spacer to ensure at least 10 mm of blood above the ablation area within the pericardial space.

Circular epicardial ablations were performed with 2 different 7F 20-mm-diameter circular devices (**Figure 1**). Decapolar device D contained 2-mm-long electrodes, whereas monopolar device M consisted of 1 metal hoop. Both devices had a second electrically isolated hoop to keep the pericardium at least 10-mm free from the ablation site. Before ablation, one of the devices was fixated to the basal left ventricular epicardium with 3 sutures (**Figure 2**). No additional contact pressure was applied. The energy was delivered using a monophasic external defibrillator (Lifepak 9, Physio-Control, Inc; Redmond, WA). A large skin patch (7506, Valleylab Inc; Boulder, CO) was used as an indifferent electrode. A cathodal shock polarity was chosen because that has the highest threshold for arcing in a blood environment.⁷ With device D, applications were performed at 50, 100, or 200 J, corresponding to 5, 10, and 20 J per electrode, respectively. With Device M, only a 100-J application was delivered. All 4 applications were delivered around the left ventricular base

in random sequence while avoiding lesion overlap. During ablation, voltage and current waveforms were stored on a digital oscilloscope for measurement of maximal ablation current and detection of discontinuities in the voltage waveform that coincide with vapor globe development and arcing.⁷

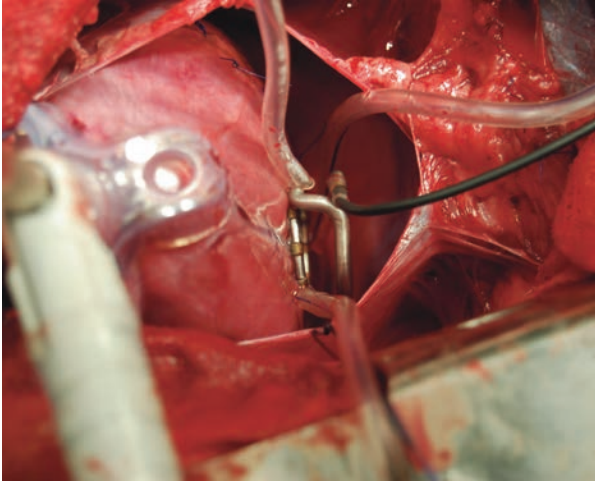


Figure 2. Decapolar device D is temporarily fixated to the porcine basal left ventricular epicardium with 3 sutures. Thereafter, the pericardial space is filled with heparinized blood and the application is delivered.

After each ablation, the blood was removed from the pericardial sac and the lesion area and electrodes were inspected for abnormalities. Then, the ablation device was detached from the heart while the 3 sutures remained in place to mark the ablation site. After 4 ablations, the thorax was closed and the animal was allowed to recover. After 3-week survival, the thorax was opened and the animal was euthanized by exsanguination. The lungs and surrounding structures were visually inspected for damage, and the heart was removed. The pericardium was peeled off, and the area with ablation lesions was excised, pinned to a flat support, and fixated in formalin.

Histological Evaluation

After fixation, multiple (range, 3–10) 3- to 4-mm-thick segments were dissected from each circular lesion. All sections were taken perpendicular to the epicardial surface. As many radial segments as possible were taken to facilitate measurement of lesion width and depth. Of each circular lesion, we also collected at least one tangential section to study lesion continuity. Paraffin-embedded segments were

sectioned and stained with hematoxylin-eosin and with elastic–van Gieson. Slides were digitized, and lesion depth and width were measured.

Measurement of Lesion Size

Large lesions often showed tissue thinning, as is also common after myocardial infarction.⁸ When sufficient undamaged myocardium was present in the histological section, the estimated original epicardial contour was used to measure lesion depth. Lesion depth and width were measured in each histological section. Some sections included multiple lesions; in those sections, lesion depth and width were measured for each lesion separately. At a few sites, 2 neighboring tangential sections were available; from those sections, maximal lesion depth was taken. Along each circular ablation line, median lesion depth and width were calculated.

Statistical Analysis

Differences in applied peak currents and median lesion depths and widths between the 100-J applications via devices D and M were investigated with a paired *t* test. Continuous variables were expressed as mean \pm SD. The relation between delivered peak current and median lesion depths obtained with device D was investigated by randomized block regression analysis. Statistical significance was defined as $P \leq 0.05$.

Results

The applications ranged between 950 and 2150 V, with a peak current between 15 and 37 A and a pulse duration of <10 ms. All applications resulted in smooth voltage wave-forms, demonstrating the absence of electrically isolating gas bubbles around electrodes and arcing.⁷ The only noticeable response to the applications was cardiac and peripheral muscle contraction.

Visual inspection of the ablation area and electrodes, directly after the application, never revealed any blood clots or charring. There was never a white imprint of the electrode contact on the tissue, as is common with tissue electrocoagulation. After 200-J applications, a light purplish circular epicardial colorization was visible.

The 3-week survival period was uneventful, except in 1 animal that experienced a period of sickness and fever, pre-sumably due to pericarditis. At removal of the

hearts, the pericardium was adhered to the epicardium in most animals. Visual inspection of tissue surrounding the heart did not reveal any lesions. The 3 sutures that had held the ablation devices and whitish colorization of the lesion(s) allowed identification of the 4 circular application areas, even when superficial epicardial damage due to pericardial adhesion obscured the epicardial aspect of the lesions. Except for some 50-J ablation sites, the original position of the 10 electrodes of device D could not be identified, because those ablations had resulted in 1 continuous whitish ablation ring on the epicardial surface.

Lesion Characteristics

Tangential sections of lesions obtained with device D at 50 J always showed separate lesions under the presumed electrode contact sites (**Figure 3**). Tangential sections of decapolar 100-J applications showed separate lesions at 2 of 5 ablation sites, a mixed pattern with deeper lesions under the electrodes and shallower lesions between electrodes at 2 ablation sites, and 1 continuous lesion at 1 ablation site. Tangential sections of lesions obtained at 100 J with device M always showed continuous lesions. Tangential sections of lesions obtained after a single 200-J application via decapolar device D were also continuous. In 3 of 5 lesions obtained at 200 J, a surviving central island was present in at least 1 of the histological sections (**Figure 4**).

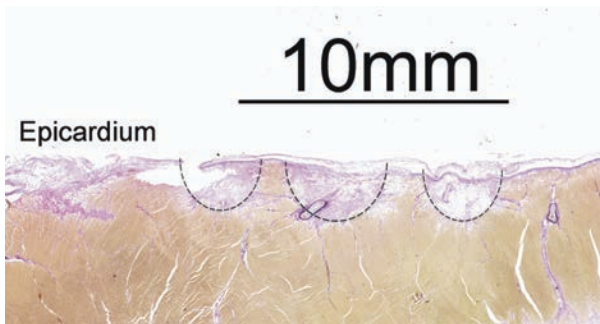


Figure 3. A tangential elastic–van Gieson–stained section of a lesion obtained with a circular 50-J application via decapolar device D showing separate small lesions under each of the presumed electrode contact sites. Lesion borders are marked with a dashed line.

In all sections along each circular ablation line, a lesion was found, except at 4 sites (1 at 50 J, D; 2 at 100 J, M; and 1 at 200 J, D) where epicardial fat, thicker than the median lesion depth of those particular lesions, was present.

The relationship between delivered peak current and median lesion depth along each circular lesion is shown in **Figure 5** and **Table**. This relationship is significant, with a slope of 0.17 mm/A ($P=0.001$; 95% CI, 0.09–0.25). When all sections of 200-J (D) lesions are combined, the 5th and 95th percentiles of all observed lesion depths are 2.9 and 8.7 mm, respectively (**Figure 6**). The corresponding values for 50- and 100-J applications via device D are 0.8 to 4.6 and 1.2 to 5.5 mm, respectively.

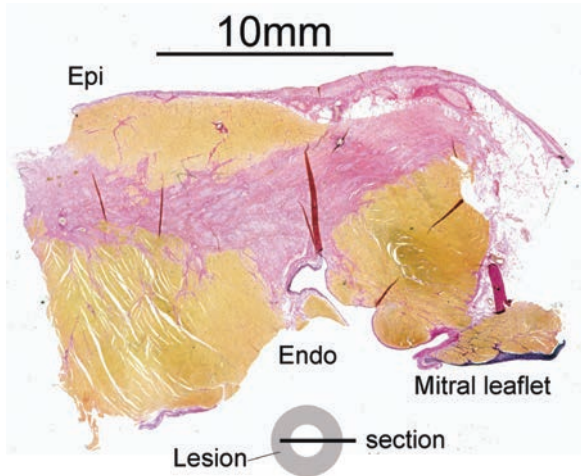


Figure 4. Histological elastic–van Gieson–stained section through the center of a circular lesion created at 200 J with the decapolar device D. The section was taken perpendicular to the epicardial surface and approximately through the middle of the lesion. Left, The lesion apparently continues beyond the end of the section. The lesion extends under a central surviving area. Bottom, The location of the section relative to the circular lesion is sketched.

Ablations at 100 J via devices D and M resulted in average peak currents of 24.3 ± 1.3 and 25.7 ± 1.6 A, respectively ($P=0.14$). Median lesion depths and widths were not significantly different between these 2 types of ablation ($P=0.49$ and $P=0.27$, respectively). The 5th and 95th percentile range of all lesion depths observed in sections of 100-J applications via device M was 0.5 to 5.3 mm.

Of 102 histological sections, 3 showed an exceptionally narrow and deep lesion, as if the ablation current had followed a specific path through the myocardium (**Figure 7**). This path was always perpendicular through the myocardial wall and not directed toward the indifferent skin electrode. Such lesions were observed at each energy level. The depth/ width ratio of these 3 lesions was 11 ± 1 , whereas it was 1.0 ± 0.6 for all other lesions. Rootlike extensions that were usually observed at the border of the lesions (**Figures 3** and **4**) were not included in lesion depth and width.

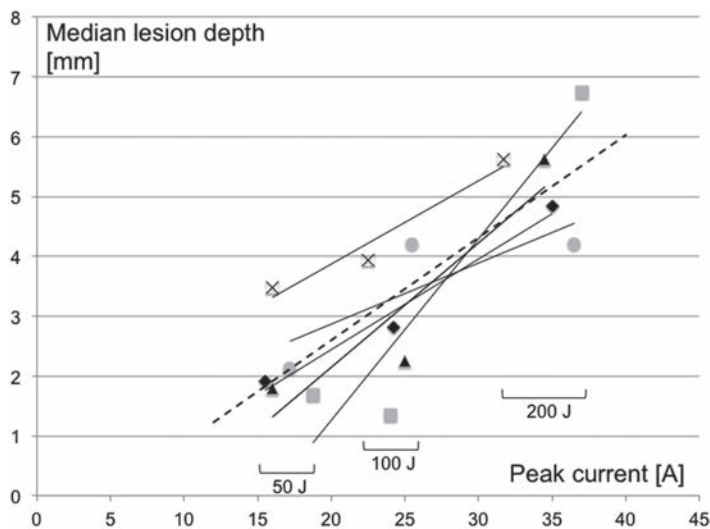


Figure 5. Relationship between magnitude of the application, expressed in peak ablation current, and median lesion depth for device D only. Values of ≈ 17 , ≈ 24 , and ≈ 34 A were reached at 50, 100, and 200 J, respectively. Symbols indicate the median lesion depths observed in 5 animals at 3 energy levels. The relationship between delivered peak current and median lesion depth (dashed line) was investigated with randomized block regression analysis and was significant, with a slope of 0.17 mm/A ($P=0.001$; 95% CI, 0.09–0.25 mm/A).

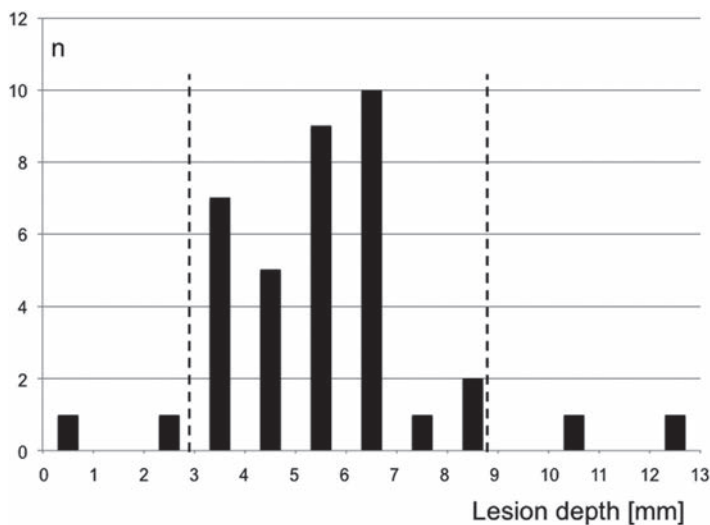


Figure 6. Histogram of all lesion depths observed after 200-J applications via decapolar device D. The 5th and 95th percentiles (dashed lines) are 2.9 and 8.7 mm, respectively.

Lesion Histological Features

All lesions showed complete replacement of cardiomyocytes by granulation tissue consisting of fibroblasts with loose collagen fibers and capillaries. Lesions have irregular outer margins, with tiny extensions at their borders (**Figure 4**).

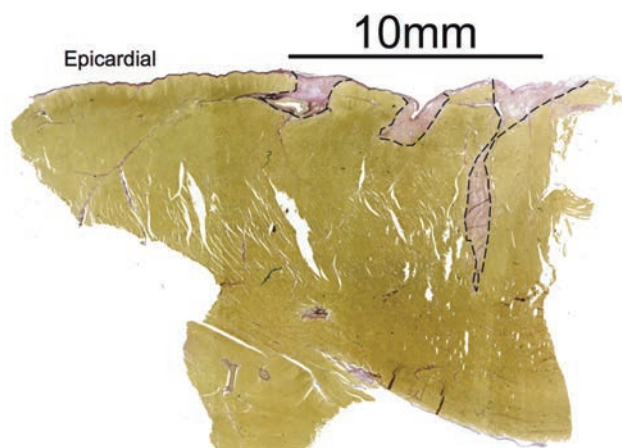


Figure 7. Histological elastic–van Gieson–stained tangential section of a 50-J application via decapolar device D. Three separate lesions, of which the lesion at the right is exceptionally deep and narrow, can be appreciated. Lesion borders are marked with a dashed line. In total, 3 of such lesions were found. The cause of this phenomenon is unknown, but apparently the ablative current has followed a narrow path through the myocardium.

Discussion

This study demonstrates a significant relationship between the magnitude of the application and median lesion depth. In addition, it demonstrates the possibility of creating continuous 20-mm circular lesions with a single ultrashort 200-J DC application via 10 electrodes (7F and 2-mm diameter). At that energy level, voltage waveforms were smooth, demonstrating the absence of vapor globe development and of hazardous adverse effects associated with DC ablation.⁷

Lesion Depth

In this study, 200-J applications delivered via device D resulted in continuous lesions with a median depth of 5.2 ± 1.2 mm. The 0.05 to 0.95 percentile range of lesion depths is 2.9 to 8.7 mm, suggesting that electric PV isolation is a realistic goal for this development.

Myocardial cells do not sense total applied energy, only local current density and impulse duration. Local current density is directly proportional to delivered current at any moment, independent of electrode interface impedance, polarization, and position of the indifferent electrode. Therefore, delivered current (and duration) is the most direct measure of the magnitude of the application (**Figure 5**). Total peak current delivered with a 200-J application is only twice that of a 50-J application, which was the standard energy level for endocardial cardioversion before the arrival of biphasic defibrillators (**Table**).

Table. Data of the 4 Types of Circular Epicardial Applications and Resulting Lesions

Device	Energy, J	Peak Current, A	Median Depth, mm	Median Width, mm	Lesion Continuity
D	50	16.1±1.3	2.1±0.0.6	2.6±0.7	0/5
D	100	24.3±1.3	2.9±1.2	4.5±1.2	1/5
<i>P</i> value		0.136	0.492	0.270	
M	100	25.7±1.6	2.8±1.1	3.7±1.2	5/5
D	200	34.9±2.1	5.2±1.2	5.3±3.0	5/5

Ablations were performed with a 7F 20-mm-diameter decapolar device (D) at 50, 100, and 200 J and with a 20-mm-diameter 7F ring electrode (M) at 100 J. Lesion depth and width were measured in all histological sections, and their median values were calculated per circular lesion. Data are given as the average±SD of the 5 peak ablation currents and of the 5 median lesion depths and widths obtained per type of application. Lesion continuity, determined in tangential sections, is scored in the last column. Values obtained at 100 J with devices D and M were compared using paired t tests.

Unanticipated Lesion Formation

Three histological sections showed an exceptionally deep and narrow lesion with an ≈10 times larger depth/width ratio than of the other lesions (**Figure 7**). Further studies might reveal why the ablative current sometimes finds such an abnormal path through myocardial tissue.

Thermal Effects

Blood clots and/or carbonization were never observed on the electrodes or application site. Energetically, 20 J per electrode is <0.7 seconds of radiofrequency (RF) delivery at 30 W. Thermally, this energy level cannot explain a 7-mm lesion depth. At the application sites, a whitish tissue colorization, as is common with thermal RF ablation, was never observed acutely. In addition, RF lesions have a fairly sharp demarcation between damaged and healthy myocardium, whereas lesions in the present study have a more irregular border with tiny fibrous extensions.⁹ The exact local temperature increase near the electrodes still needs to be investigated, but our data suggest that tissue heating is not the ablative mechanism.¹⁰

Tissue Contact

Given the better conductivity of blood than of tissue, electrode-tissue contact will definitely affect lesion depth. Final catheter design and perhaps electric means to measure tissue contact may determine the success of this technique for PV antrum isolation.

Lesion Width

The main purpose of our study was to investigate lesion depth and continuity at various energy levels. Lesion width is important too, because we expect that circular IRE ablations must be placed just inside PV ostia to achieve sufficient electrode-tissue contact. Lesion width will then determine how much of the antrum will be ablated, and this may affect clinical success (**Table**).¹⁰⁻¹²

Catheter Configuration

For 3D localization, mapping, and PV isolation, a circular catheter with multiple electrodes may be more attractive than one with a single circular electrode. The ultimate catheter design will also depend on whether mapping of PV potentials remains important for PV isolation with IRE, but the results of our study suggest that electrode design is not a critical issue as long as electrode size is large enough to prevent arcing.

Limitations

The design of the decapolar device did not allow for measurement of individual electrode impedances. Theoretically, impedance differences may cause differences in delivered current between electrodes. However, except for a wedged situation, measurement of electrode impedance with a roving endocardial catheter usually shows little variation. We presumed that the same would be true for the electrodes of device D.

Measurement of lesion size from radial segments could have missed the center and presumably greatest lesion depth and width of separate 50- or 100-J lesions. Tangential sections may also have missed greatest lesion depth. This could have led to an underestimation of lesion depth. Despite this, lesions were always found in all sections along each circular ablation line, except at 4 locations with relatively thick epicardial fat.

Lesion size with IRE will depend on electrode-tissue contact and, thus, on the ultimate catheter design and measures to ensure electrode-tissue contact.

Given the major differences between the present model and circular catheter ablation of PV ostia, extrapolation of the results of this study to PV isolation should be performed with great caution. Data of this study, however, suggest that electroporation technology definitely has the potential to facilitate extremely fast PV isolation.^{13,14} Further studies must address potential complications, such as PV and coronary stenosis, nerve damage, esophageal fistula, and other unwanted adverse effects.^{15,16}

Side Contact

The plane of the circular ablation device was positioned parallel to the tissue (**Figure 2**). The plane of a circular ablation catheter positioned against a PV antrum may also be parallel to the tissue. With a circular arrangement of electrodes, the ablation current will preferentially be directed outward. With the catheter hoop positioned inside a PV ostium, an even deeper lesion than what was obtained in the present study may be expected.

Clinical Implications

IRE ablation might not be the optimal approach for all other cardiac arrhythmias. RF and cryoablation are much more controllable because they allow monitoring the electrophysiological response during energy application. However, for electric PV isolation and in cases in which deep transmural lesions are desired, a fast technique that does not require tissue heating may be preferable.

The design used in the present study had a 7F 20-mm-diameter hoop. In clinical use, a different hoop diameter may be required. With identical electrode size and spacing, total applied current should be scaled proportional to the diameter of the ablation hoop to maintain the same lesion depth and safety margin below arcing threshold.

Conclusions

The data of this study demonstrate a significant relationship between the magnitude of the application and myocardial lesion depth. In a blood-myocardial tissue environment, continuous 20-mm circular lesions, deep enough for electric PV isolation, can be created with a single 200-J application of a few milliseconds in duration. Tissue heating does not appear to play a role in lesion formation.

Acknowledgments

We thank Mrs. Ingeborg van der Tweel, PhD, for performing statistical analysis; and the staff of the Department of Experimental Cardiology, University Medical Center Utrecht, for technical assistance during the experiments.

Sources of Funding

Dr Doevendans received a research grant from the Bekalis Foundation.

Disclosures

Dr Wittkamp is a consultant for St Jude Medical, Atrial Fibrillation division.

Clinical perspective

This article presents data of lesions created with a novel energy source that induces irreversible myocyte membrane electroporation, leading to apoptosis. The study demonstrates that a single 6-ms high current application, delivered via a circular arrangement of electrodes in a blood-tissue environment, can create a continuous circular lesion sufficiently deep for pulmonary vein antrum isolation. The data of this study suggest that the application does not cause enough temperature elevation to induce blood or tissue coagulation. The technology would allow for ultrafast nonthermal electric pulmonary vein isolation as an alternative for multiple sequential radiofrequency applications. The ablation technology still relies on electrode-tissue contact. Clinical application will, therefore, require the means to determine electrode-tissue contact to ensure sufficient lesion depth.

References

1. Lee RC, Zhang D, Hannig J. Biophysical injury mechanisms in electrical shock trauma. *Annu Rev Biomed Eng.* 2000;2:477–509.
2. Gallagher JJ, Svenson RH, Kasell JH, German LD, Bardy GH, Broughton A, Critelli G. Catheter technique for closed chest ablation of the atrio-ventricular conduction system: a therapeutic alternative for the treatment of refractory supraventricular tachycardia. *N Engl J Med.* 1982;306:194–200.
3. Rowland E, Cunningham D, Ahsan AJ, Rickards AF. Transvenous ablation of atrioventricular conduction with a low energy power source. *Br Heart J.* 1989;62:361–366.
4. Lemery R, Talajic M, Roy D, Coutu B, Lavoie L, Lavallee E, Cartier R. Success, safety, and late electrophysiological outcome of low-energy direct-current ablation in patients with the Wolff-Parkinson-White syndrome. *Circulation.* 1992;85:957–962.
5. Lavee J, Onik G, Mikus P, Rubinsky B. A novel nonthermal energy source for surgical epicardial atrial ablation: irreversible electroporation. *Heart Surg Forum.* 2007;10:E162–E167.
6. Wittkampf FH, van Driel V, van Wessel H, Vink A, Hof IE, Grundeman PF, Hauer RNW, Loh P. Feasibility of electroporation for the creation of pulmonary vein ostial lesions. *J Cardiovasc Electrophysiol.* 2011;22:302–309.
7. Bardy GH, Coltorti F, Ivey TD, Alferness C, Rackson M, Hansen K, Stewart R. Some factors affecting bubble formation with catheter-mediated defibrillator pulses. *Circulation.* 1986;73:525–538.
8. Ganame J, Messalli G, Masci PG, Dymarkowski S, Abbasi K, Van de Werf F, Janssens S, Bogaert J. Time course of infarct healing and left ventricular remodelling in patients with reperfused ST segment elevation myocardial infarction using comprehensive magnetic resonance imaging. *Eur Radiol.* 2011;21:693–701.
9. Huang SKS, Graham AR, Lee MA, Ring ME, Gorman GD, Schiffman R. Comparison of catheter ablation using radiofrequency versus direct current energy: biophysical, electrophysiologic and pathologic observations. *J Am Coll Cardiol.* 1991;18:1091–1097.
10. Arentz T, Weber R, Burkle G, Herrera C, Blum T, Stockinger J, Minners J, Neumann FJ, Kalusche D. Small or large isolation areas around the pulmonary veins for the treatment of atrial fibrillation? Results from a prospective randomized study. *Circulation.* 2007;115:3057–3063.
11. Oral H, Scharf C, Chugh A, Hall B, Cheung P, Good E, Veerareddy S, Pelosi F, Morady F. Catheter ablation for paroxysmal atrial fibrillation segmental pulmonary vein ostial ablation versus left atrial ablation. *Circulation.* 2003;108:2355–2360.
12. Liu X, Dong J, Mavrakis HE, Hu F, Long D, Fang D, Yu R, Tang R, Hao P, Lu C, He X, Liu X, Vardas PE, Ma C. Achievement of pulmonary vein isolation in patients undergoing circumferential pulmonary vein ablation: a randomized comparison between two different isolation approaches. *J Cardiovasc Electrophysiol.* 2006;17:1263–1270.
13. Cabrera JA, Ho SY, Climent V, Sanchez-Quintana D. The architecture of the left lateral atrial wall: a particular anatomic region with implications for ablation of atrial fibrillation. *Eur Heart J.* 2008;29:356–362.
14. Beinart R, Abbara S, Blum A, Ferencik M, Heist K, Ruskin J. Left atrial wall thickness variability measured by CT scans in patients undergoing pulmonary vein isolation. *J Cardiovasc Electrophysiol.* 2011;22:1232–1236.
15. Wittkampf FHM, van Driel VJ, van Wessel H, Loh P, Doevendans PA. Pulmonary vein stenosis after catheter ablation: comparison between radiofrequency and irreversible electroporation. *Heart Rhythm.* 2011;8:S248–S249.
16. Wittkampf FHM, du Pré BC, van Driel VJ, van Wessel H, Loh P, Doevendans PA, Vink A. Effect of irreversible electroporation ablation on coronary arteries. *Heart Rhythm.* 2011;8:S342.



CHAPTER 4

Minimal Coronary Artery Damage by Myocardial Electroporation Ablation

Bastiaan du Pré
Vincent van Driel
Harry van Wessel
Peter Loh
Pieter Doevendans
Roel Goldschmeding
Fred Wittkamp
Aryan Vink

Abstract

Aims Radiofrequency catheter ablation is a successful treatment for cardiac arrhythmias, but may lead to major complications such as permanent coronary damage. Irreversible electroporation (IRE) is a new non-thermal ablation modality, but its effect on coronary arteries is still unknown.

Methods and results In a porcine model, epicardial IRE lesions were created at the base of the left ventricle in four hearts (group A) and directly on the left anterior descending artery (LAD) in five hearts (group B). After 3 weeks, coronary arteries inside IRE lesions and in apparently undamaged myocardium next to the lesions were (immuno-)histologically studied. Two untreated hearts served as controls. Coronary damage was defined as intimal hyperplasia. Left anterior descending artery angiograms were obtained before ablation, directly after ablation, and before termination in group B. In group A, 103 arterial branches were studied. Of these, 5 of 56 arterial branches inside lesions and 1 of 47 outside lesions showed intimal hyperplasia, but all had, <50% area stenosis. Targeted LADs (group B) did not reveal intimal hyperplasia and angiograms showed no signs of stenosis. Expression of connective tissue growth factor was observed in the scar tissue, but not in the fibrotic tissue directly around the arteries, confirming that the arteries are indeed spared from tissue damage and remodelling.

Conclusion Coronary arteries remain free of clinically relevant damage 3 weeks after epicardial IRE ablation, even amid very large myocardial lesions. This suggests that IRE ablation can be applied safely near or even on coronary arteries. With IRE ablation, arterial blood flow does not appear to affect lesion formation.

Introduction

Radiofrequency (RF) catheter ablation is a technique that was introduced in cardiac electrophysiology in 1987 and evolved from a highly experimental procedure to a standard treatment option for cardiac arrhythmias.¹

Radiofrequency induces heat damage to all tissue types near the ablation site. Ablation near coronary arteries therefore has serious risks.^{2,3} Radiofrequency heating may not only coagulate blood inside the vessel, but also causes intimal hyperplasia and shrinkage of the collagen fibres in the arterial wall. This may lead to vessel stenosis and subsequent infarction of the perfused territory.⁴ Conversely, tissue cooling by arterial flow may limit lesion formation and lead to unsuccessful ablations.^{5,6} Both thermal side effects are relevant not only for endocardial catheter ablation, but also for epicardial catheter ablation inside the pericardial space.^{7,8}

Recently, circular irreversible electroporation (IRE) ablation has been proposed as a new catheter ablation modality.⁹ Irreversible electroporation uses direct current (DC) to create myocardial lesions. It is based on low-energy DC catheter ablation, a technology that avoids the cascade of potentially harmful side effects, such as the generation of vapour globe, sparking, explosion, and pressure waves associated with standard DC catheter ablation.¹⁰⁻¹³ Low-energy DC ablation, however, was abandoned shortly after its introduction when RF ablation became available.

Irreversible electroporation was tested and the first results demonstrated that it is capable of creating huge myocardial lesions within a few milliseconds, apparently without thermal side effects.⁹ With such large lesions, the effect of the application on coronary arteries certainly has to be investigated before further development to a clinically applicable technology.

Tissue damage by IRE is the result of an electrical field-driven re-organization of the lipid structure of the cell membrane.¹⁴ This causes formation of permanent microlesions in the membrane that increase cellular permeability. This disrupts cellular homeostasis and initiates apoptosis of the cell. Other parts of the cell, such as DNA, collagen, or other proteins are not directly affected by IRE. The amount of damage caused by IRE depends on the presence of cell membranes, the applied electrical field, and the electrical resistivity of the target tissue.^{15,16} Therefore, some tissues may be more vulnerable for IRE than others. In oncological IRE application, it has been demonstrated that vital structures such as vessels remain relatively spared.^{17,18}

The aim of the present study was to analyse the effect of IRE on coronary arteries to pave the way for development of IRE catheter ablation in the pericardial space.

Methods

Animal experiments

All animal experiments were performed with approval from the Animal Experimental Ethical Committee of the University Medical Center Utrecht. In nine 60–75 kg pigs, median sternotomy was performed and the pericardium was opened. Its edges were lifted and sutured to surrounding instrumentation. A Starfish Heart Positioner (Medtronic Inc., Minneapolis, MN, USA) was used to raise the apex and expose the basal left ventricular (LV) area. Three custom devices (types A–C) were used for circular or linear IRE ablations on LV epicardium (**Figure 1**).

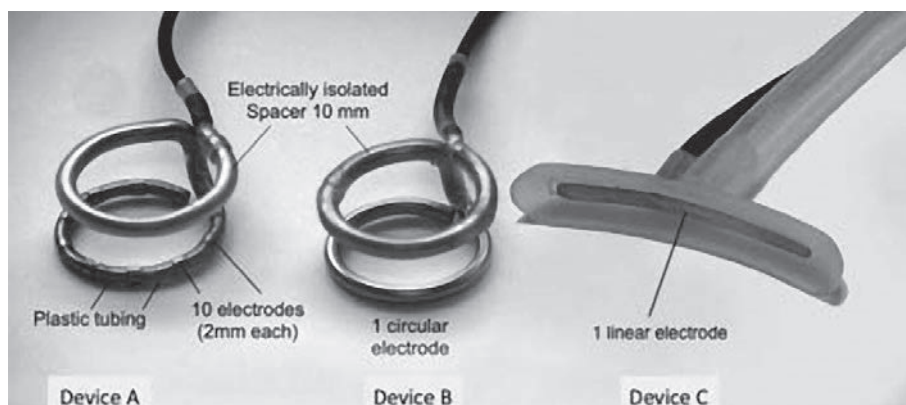


Figure 1. Three custom devices used for circular or linear irreversible electroporation ablations on left ventricular epicardium. Type A consists of a 20 mm circular 7F ablation hoop with 10 electrodes. Type B is a single 20 mm circular 7F electrode. Types A and B include a circular spacer above the ablation electrodes to keep the pericardium at 10 mm distance from the ablation area. Type C was a linear suction device with a single 35 mm long and 3 mm broad linear electrode inside a 42 mm long and 7 mm broad plastic suction cup.

In a first series of four pigs, circular IRE was performed with device type A or B. The device was sutured around the LV base, the heart was lowered into the pericardial sac, and the pericardium was filled with heparinized blood. Energy was applied between the device and a remote indifferent electrode using a monophasic external defibrillator (Lifepak 9, Physio-Control, Inc., Redmond, WA, USA). The applied energy ranged between 50 and 360 J. This procedure was repeated at

three other sites around the LV base, without overlap between lesions. In a second series of five pigs, on the antero-septal part of the heart circular IRE applications were purposely delivered directly on the left anterior descending artery (LAD) by positioning the ablation hoop over the LAD using devices A and B at an energy level between 50 and 200 J. In four of five animals, one or two additional single linear applications were delivered more distally on the LAD using device C at a lower setting of 30 J, because the suction prevented energy leakage to the surrounding blood pool.

After these ablations, the thorax was closed and the animal was allowed to recover. After 3 weeks the animals were terminated and the hearts were collected. Two hearts from untreated pigs served as controls.

In the second series of five animals, where ablations were performed directly on the LAD, coronary angiography was performed shortly before the ablation, within 60 min after ablation and before termination 3 weeks later. These angiograms were analysed for arterial stenosis.

Histological investigation

The hearts of the nine pigs treated with IRE and the two control hearts were fixated in formalin. From each heart, between one and nine consecutive 4 mm thick segments were dissected from each lesion. In the control hearts, an area similar to the treated hearts was used for histological analysis. The segments were embedded in paraffin, sectioned, and stained with haematoxylin–eosin and elastic–Van Gieson.

All histological sections were scanned with a ScanScope XT scanner (Aperio Technologies, Inc., CA, USA) and analysed using Imagescope (Aperio Technologies). Lesion depths were measured in the nine ablated hearts. Of all coronary arteries and branches found in sections of the first series of four hearts where ablation was performed at the base of the LV, the luminal area, the area encompassed by the internal elastic lamina (IEL area), and the area encompassed by the external elastic lamina (EEL area) were measured. The intimal area was calculated by subtracting the luminal area from the IEL area. All arteries with an EEL area $>0.15 \text{ mm}^2$ were considered clinically relevant and included in the study. Of the five hearts of the second series, where ablations had been performed directly on the LAD, only sections containing the LAD were analysed. Coronary damage was defined as intimal hyperplasia and the percentage stenosis due to the intimal hyperplasia was calculated as follows: $(\text{IEL area} - \text{luminal area}) / \text{IEL area} \times 100\%$.

In a subset of LV basal sections obtained from lesions and control hearts, connective tissue growth factor (CTGF) expression was determined using immunohistochemistry with a mouse anti-human CTGF monoclonal antibody (SC-14939; Santa Cruz Biotechnologies, Inc., CA, USA). Connective tissue growth factor is a pro-fibrotic growth factor that can be used as a biomarker for active tissue remodelling.¹⁹

Statistical analysis

Difference in coronary artery size and lesion depth between affected and unaffected arteries was analysed with an unpaired *t*-test. The statistical significance was defined as a *P* value ≤ 0.05 .

Results

All animals survived the procedure and the 3 weeks follow-up period. One animal suffered from an episode of fever, presumably due to pericarditis. No other complications were reported.

In the first series of five animals, 81 sections from 16 IRE lesions were analysed. The lesion depth was 6.5 ± 2.7 mm (range 1.7–13.5 mm). In 26 of 81 lesion sections, the lesion was transmural. The transmural lesions were mainly found in ablations with relative high-energy levels. As expected, arterial branches were predominantly located epicardially, sometimes very close to the application site. A total of 103 arterial branches with an EEL area >0.15 mm² were found. These arteries were subdivided into 56 arteries that were located within a lesion and 47 that were located outside a lesion. None of the arteries inside the lesion were surrounded by intact myocardial tissue. In 15 control sections of untreated hearts, 30 arteries with an EEL area >0.15 mm² were found. Major coronary branches (EEL area >1 mm²) were present inside lesions ($n = 6$), outside lesions ($n = 12$), and in control sections ($n = 6$) (**Figure 2A** and **B**).

Intimal hyperplasia was observed in 5 of 56 arteries inside lesions, in 1 of 47 arteries outside the lesions, and in 0 of 30 arteries from control sections (**Figure 2E**). The single affected artery outside a lesion had an EEL area of 0.16 mm². This artery was located 11 mm outside the lesion border and was surrounded by several small and large unaffected arteries. In all affected arteries, stenosis was $<50\%$, with an average of $22 \pm 15\%$. Lesions depth did not differ significantly between lesions

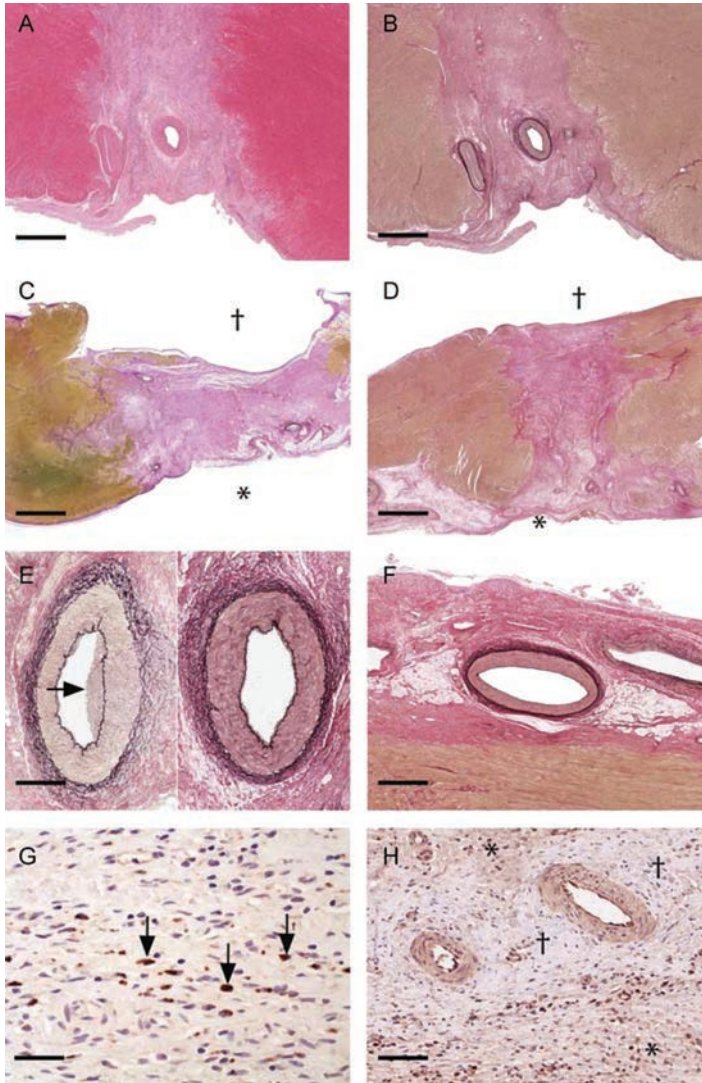


Figure 2. Histological analysis of myocardial tissue after electroporation ablation. (A) Haematoxylin–eosin stain of an epicardial lesion. The area in the middle is the electroporation lesion, the pink area on both sides is undamaged myocardium. Bar = 1.25 mm. (B) Elastic-Van Gieson stain of the same lesion as in (A). Inside the lesion are several small arterial braches and two large undamaged coronary branches present. Bar = 1.0 mm. (C and D) Elastic-Van Gieson stain of transmural lesions. * Indicates the epicardial side of the heart and # the endocardial side of the heart. C, Bar = 2.8 mm; D, Bar = 2.3 mm. (E) Elastic-Van Gieson stain of two examples of large coronary arteries in an electroporation lesion; one with intimal hyperplasia on the left and one without intimal hyperplasia on the right. Bar = 0.25 mm. (F) Elastic-Van Gieson stain of an undamaged left anterior descending artery surrounded by electroporation lesion. The pink area is the ablation lesion, the brown area at the bottom of the figure is intact myocardium. Bar = 0.7 mm. (G) Electroporation lesion. The brown areas designated by the arrows indicate connective tissue growth factor expression in fibroblasts. Bar = 0.035 mm. (H) Connective tissue growth factor expression around coronary artery branches, * shows connective tissue growth factor expression in electroporation lesion, † indicates the area around vessels where CTGF is absent. Bar = 0.070 mm.

with and without affected arteries (7.4 ± 3.3 vs. 7.2 ± 2.7 mm, respectively, $P = 0.7$). Affected arteries were significantly smaller than unaffected arteries inside the lesion (average EEL area of 0.35 ± 0.13 vs. 0.69 ± 0.85 mm², respectively, $P < 0.001$). None of the large coronaries (EEL area >1 mm²) was affected.

In the second series of four animals, 29 histological sections of five LAD lesions were analysed. All LADs were fully surrounded by the electroporation lesion. Lesions were 2.9 ± 1.2 mm deep (range 0.2–6.3 mm). In none of these LAD sections, intimal hyper-plasia was found (**Figure 2F**). Left anterior descending artery coronary angiograms showed no signs of stenosis directly after ablation or before termination (**Figure 3** and **Table 1**).

In sections stained for CTGF, the expression was observed in fibroblasts of scar tissue, confirming the existence of a remodelling process in the lesion. Strikingly, in the areas directly around coronary branches, CTGF expression was not detected (**Figure 2G** and **H**). The medial and intimal arterial layers of lesion and control sections showed a diffuse expression of CTGF.

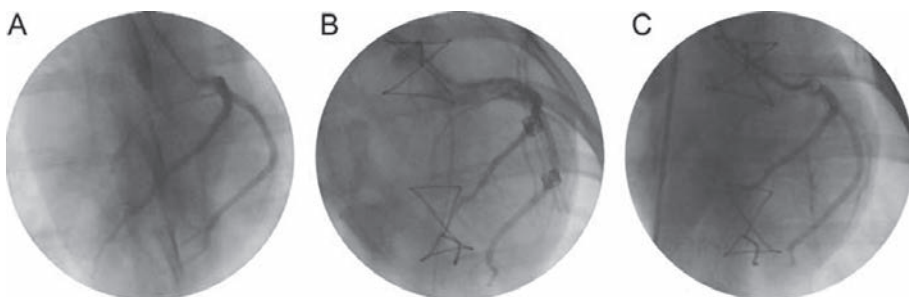


Figure 3. Coronary angiograms of the left anterior descending artery. (A) Before electroporation ablation. (B) Directly after ablation. (C) Before termination, 3 weeks after ablation.

Table 1. Results summary

	Ablation at base of LV	Ablation on the LAD	Controls
Number of hearts	4	5	2
1. Number of coronary artery segments >0.15 mm ²	103	5	30
Intimal hyperplasia inside lesion	5/56 (9%)	0/5 (0%)	–
Intimal hyperplasia outside lesion	1/47 (2%)	–	0/30 (0%)
2. Angiographic LAD stenosis	–	0/5 (0%)	–

Discussion

In this study, we investigated the effect of various types of epicardial IRE ablation on coronary arteries. Electroporation energy was delivered epicardially with blood around the electrode–tissue contact site to simulate the situation during endocardial catheter ablation.

The data suggest that coronary arteries do not develop significant stenosis within 3 weeks after epicardial IRE, even not amid large LV lesions and despite their epicardial location near the ablation electrode(s).

In RF and cryo-energy ablation, coronary damage is a rare, but well-recognized complication in epicardial ablation procedures.² Acute coronary damage as well as damage several weeks after an RF ablation procedure requiring interventions such as coronary stenting have been described.² Several mechanisms explain the occurrence of coronary damage after RF. First, RF heat induces mechanical damage to all tissue types near the ablation site.²⁰ If ablation is applied in the proximity of a coronary artery, the artery will also be damaged. Secondly, animal models demonstrate that heat from RF can induce clot formation in the coronary vessels which may lead to an acute coronary artery occlusion. Clots are caused by protein aggregation, which is initiated by blood temperatures $>50^{\circ}\text{C}$.^{21,22} Thirdly, heat of RF denatures collagen in coronary artery walls, which accounts for induced vessel constriction and subsequent coronary damage.²³ During RF ablation, coronary angiography is routinely performed to exclude the presence of major arteries near the target site. During endocardial catheter ablation, the risk of ablating in close proximity to a coronary artery is smaller, but even then coronary artery damage has been reported.^{24,25} Irreversible electroporation is a new ablation modality that creates large myocardial lesions within a few milliseconds. Formation of large lesions involves a significant risk of coronary artery presence in the ablation area. Our observations suggest that IRE may be a relatively safe ablation modality for epicardial ablation near coronary arteries and that coronary angiography before epicardial ablation may no longer be required when using this ablation technique. Connective tissue growth factor [also known as CCN2 (Cyr61/CTGF/NOV)] is a profibrotic growth factor that induces accumulation of extracellular matrix by inducing collagen production and inhibiting matrix breakdown.²⁶ It is a protein that is involved in numerous physiological processes in several organs. In the heart, CTGF is expressed in remodelling processes involving myocardial fibrosis, such as heart failure, myocardial infarction, and myocardial damage due to chronic

hypertension.^{27,28} *In vivo*, there is a strong association between cardiac fibrosis and CTGF expression.¹⁹ In the current study we therefore considered CTGF a biomarker for active remodelling of scar tissue and used it to compare remodelling in different parts of the IRE lesion. Indeed, CTGF expression was found in the fibroblasts of the lesions caused by IRE. In the areas that directly surround coronary arteries (the adventitia), however, no CTGF expression was found. This suggests the absence of remodelling and scar tissue formation in these parts of the lesion. A diffuse expression of CTGF was observed in the medial and intimal layers of the arteries inside lesions and in controls. From previous studies it is known that a basal CTGF expression without an underlying pathological process is present in these artery layers.^{29,30} This was confirmed by the fact that we also observed this expression pattern in control arteries. The observed CTGF expression pattern suggests that not only the arteries, but also connective tissue around coronary arteries remains unaffected by IRE.

Lesion formation in RF and cryoablation is a thermal process and logically affected by arterial and venous blood flow cooling, the so-called cold/heat sink effect.^{5,31,32} Blood flow protects the artery from thermal damage, but also cools or warms myocardial tissue in its direct vicinity. This may lead to incomplete lesion formation, gaps in ablation lines, and arrhythmia recurrences necessitating multiple ablation sessions.^{5,6} Theoretically, lesion formation in IRE is not temperature related and indeed inside lesions we did not find intact myocardial tissue around blood vessels. Data of the present study therefore suggest that with IRE ablation, coronary arteries are not or only minimally affected by the application and conversely that myocardial lesion formation does not appear to be affected by the presence of major arteries. These are two reasons why IRE may be a much better ablation method than RF for targeting an arrhythmogenic substrate near coronary arteries. There are two possible explanations for the preservation of coronary arteries. Connective tissue around coronary arteries has an extensive extracellular network and exhibits a relative reduction in large cell membranes, which may make them relatively invulnerable to IRE.^{33,34} An alternative explanation may be that connective tissue around coronary arteries has a relatively high electrical resistivity.¹⁶ This may protect the medial and intimal arterial layer against high electrical fields.³⁵

Limitations

Analysis of coronary arteries was limited to arteries with an EEL area ≥ 0.15 mm². This limit was arbitrarily chosen before the analysis because of the abundance of

very small coronary artery branches within the myocardium. Another limit may have yielded different results, especially since the affected arteries found in the current study were relatively small. However, stenosis of tiny arteries and arterioles is clinically less relevant and might be secondary to the lesion formation as part of a remodelling process.^{36,37}

Lesions that resulted from IRE applications directly on the LAD were relatively small. In part this may be due to the presence of epicardial fat with a higher electrical resistivity resulting in reduced local current density and thus limited lesion extension. This latter aspect requires further study. The LADs were completely surrounded by electroporation lesion and other transmural lesions show large intact coronary artery branches near the ablation electrode. Nevertheless, higher energy applications that cause transmural lesion directly on the LAD may be required to strengthen the evidence that IRE application directly on major arteries is safe.

The follow-up period was limited to 3 weeks. The long-term effects of IRE on coronary arteries and the role of remodelling therefore remain unknown. However, the absence of CTGF expression in arterial layers and surrounding connective tissue suggests that these arteries are not affected by IRE ablation. Longer follow-up periods may be required to analyse the long-term effect of IRE on coronary arteries, but the absence of CTGF expression suggests that a late response is unlikely.

Coronary damage was defined as intimal hyperplasia because this is the clinically most appropriate marker of coronary damage. Others have shown that the vascular smooth muscle cells in the medial layer of the artery may be affected by IRE.³⁸ Although we did not systematically score medial thickness and the number of vascular smooth muscle cells in the medial layer, we did not observe evident pathological changes in the media. The data of our study therefore suggest that the medial layer is not affected at the settings used in the present protocol.

Different custom devices and different energy levels were applied to create myocardial lesions. In the current study, we filled the pericardial sac with blood to simulate the situation during endocardial catheter ablation where blood also surrounds the electrode–tissue contact sites. The relatively high conductivity of blood shunts most of the ablation current. With catheter ablations in the pericardial space in the absence of electrically shunting blood, a much lower energy level will be required to create similar lesions. However, the range of lesion sizes investigated in the present study is sufficiently broad for pericardial ablation and data of the present study are therefore believed to be relevant for such application.

Conclusions

Coronary arteries remain free of significant damage amid huge transmural myocardial lesions, 3 weeks after epicardial IRE ablation very near to these arteries. This suggests that IRE ablation has a low risk of coronary damage and that epicardial IRE ablation near or even on large coronary arteries is relatively safe. With IRE, myocardial lesion extension does not appear to be affected by the presence of arterial blood flow. This ablation modality may therefore be an appropriate solution for epicardial target sites near coronary arteries.

Acknowledgements

The authors thank Petra van der Kraak – Homoet and Dionne van der Giezen for technical assistance.

Conflict of interest: F.H.W. and H.v.W. work for St. Jude Medical AF Division and are inventors of circular electroporation ablation. The other authors have no conflicts of interest to declare.

References

1. Borggreve M, Budde T, Podczeczek A, Breithardt G. High frequency alternating current ablation of an accessory pathway in humans. *J Am Coll Cardiol* 1987;**10**:576–82.
2. Roberts-Thomson KC, Steven D, Seiler J, Inada K, Koplan BA, Tedrow UB *et al*. Coronary artery injury due to catheter ablation in adults: presentations and out-comes. *Circulation* 2009;**120**:1465–73.
3. Aoyama H, Nakagawa H, Pitha JV, Khammar GS, Chandrasekaran K, Matsudaira K *et al*. Comparison of cryothermia and radiofrequency current in safety and efficacy of catheter ablation within the canine coronary sinus close to the left circumflex coronary artery. *J Cardiovasc Electrophysiol* 2005;**16**:1218–26.
4. Paul T, Bokenkamp R, Mahnert B, Trappe HJ. Coronary artery involvement early and late after radiofrequency current application in young pigs. *Am Heart J* 1997;**133**:436–40.
5. Pardo Meo J, Scanavacca M, Sosa E, Correia A, Hachul D, Darrieux F *et al*. Atrial coronary arteries in areas involved in atrial fibrillation catheter ablation. *Circ Arrhythm Electrophysiol* 2010;**3**:600–5.
6. Jones DL, Guiraudon GM, Skanes AC, Guiraudon CM. Anatomical pitfalls during encircling cryoablation of the left atrium for atrial fibrillation therapy in the pig. *J Interv Card Electrophysiol* 2008;**21**:187–93.
7. Viles-Gonzalez JF, de Castro Miranda R, Scanavacca M, Sosa E, d'Avila A. Acute and chronic effects of epicardial radiofrequency applications delivered on epicardial coronary arteries. *Circ Arrhythm Electrophysiol* 2011;**4**:526–31.
8. Sacher F, Roberts-Thomson K, Maury P, Tedrow U, Nault I, Steven D *et al*. Epicardial ventricular tachycardia ablation a multicenter safety study. *J Am Coll Cardiol* 2010;**55**:2366–72.
9. Wittkamp FH, van Driel VJ, van Wessel H, Vink A, Hof IE, Grundeman PF *et al*. Feasibility of electroporation for the creation of pulmonary vein ostial lesions. *J Cardiovasc Electrophysiol* 2011;**22**:302–9.
10. Gallagher JJ, Svenson RH, Kasell JH, German LD, Bardy GH, Broughton A *et al*. Catheter technique for closed-chest ablation of the atrioventricular conduction system. *N Engl J Med* 1982;**306**:194–200.
11. Bardy GH, Coltorti F, Stewart RB, Greene HL, Ivey TD. Catheter-mediated electrical ablation: the relation between current and pulse width on voltage break-down and shock-wave generation. *Circ Res* 1988;**63**:409–14.
12. Ahsan AJ, Cunningham D, Rowland E, Rickards AF. Catheter ablation without ful-guration: design and performance of a new system. *Pacing Clin Electrophysiol* 1989;**12**:1557–61.
13. Lemery R, Talajic M, Roy D, Coutu B, Lavoie L, Lavallee E *et al*. Success, safety, and late electrophysiological outcome of low-energy direct-current ablation in patients with the Wolff–Parkinson–White syndrome. *Circulation* 1992;**85**:957–62.
14. Teissie J, Golzio M, Rols MP. Mechanisms of cell membrane electroporation: a minireview of our present (lack of ?) knowledge. *Biochim Biophys Acta* 2005;**1724**:270–80.
15. Lee RC, Zhang D, Hannig J. Biophysical injury mechanisms in electrical shock trauma. *Annu Rev Biomed Eng* 2000;**2**:477–509.
16. Sances A Jr, Myklebust JB, Larson SJ, Darin JC, Swiontek T, Prieto T *et al*. Experimental electrical injury studies. *J Trauma* 1981;**21**:589–97.
17. Onik G, Mikus P, Rubinsky B. Irreversible electroporation: implications for prostate ablation. *Technol Cancer Res Treat* 2007;**6**:295–300.
18. Lee EW, Thai S, Kee ST. Irreversible electroporation: a novel image-guided cancer therapy. *Gut Liver* 2010;**4**(Suppl 1):S99–104.
19. Daniels A, van Bilsen M, Goldschmeding R, van der Vusse GJ, van Nieuwenhoven FA. Connective tissue growth factor and cardiac fibrosis. *Acta Physiol (Oxf)* 2009;**195**:321–38.
20. Calkins H, Brugada J, Packer DL, Cappato R, Chen SA, Crijns HJ *et al*. HRS/EHRA/ ECAS expert consensus statement on catheter and surgical ablation of atrial fibrillation. *Europace* 2007;**9**:335–79.
21. Matsudaira K, Nakagawa H, Wittkamp FH, Yamanashi WS, Imai S, Pitha JV *et al*. High incidence of thrombus formation without impedance rise during radiofrequency ablation using electrode temperature control. *Pacing Clin Electrophysiol* 2003;**26**:1227–37.
22. Demolin JM, Eick OJ, Munch K, Koullick E, Nakagawa H, Wittkamp FH. Soft thrombus formation in radiofrequency catheter ablation. *Pacing Clin Electrophysiol* 2002;**25**:1219–22.

23. Gorisch W, Boergen KP. Heat-induced contraction of blood vessels. *Lasers Surg Med* 1982;**2**:1–13.
24. Takahashi Y, Jais P, Hocini M, Sanders P, Rotter M, Rostock T *et al*. Acute occlusion of the left circumflex coronary artery during mitral isthmus linear ablation. *J Cardiovasc Electrophysiol* 2005;**16**:1104–7.
25. Mykitysey A, Kehoe R, Bharati S, Maheshwari P, Halleran S, Krishnan K *et al*. Right coronary artery occlusion during RF ablation of typical atrial flutter. *J Cardiovasc Electrophysiol* 2010;**21**:818–21.
26. Blom IE, Goldschmeding R, Leask A. Gene regulation of connective tissue growth factor: new targets for antifibrotic therapy? *Matrix Biol* 2002;**21**:473–82.
27. Koitabashi N, Arai M, Kogure S, Niwano K, Watanabe A, Aoki Y *et al*. Increased connective tissue growth factor relative to brain natriuretic peptide as a determinant of myocardial fibrosis. *Hypertension* 2007;**49**:1120–7.
28. Dean RG, Balding LC, Candido R, Burns WC, Cao Z, Twigg SM *et al*. Connective tissue growth factor and cardiac fibrosis after myocardial infarction. *J Histochem Cytochem* 2005;**53**:1245–56.
29. Friedrichsen S, Heuer H, Christ S, Cuthill D, Bauer K, Raivich G. Gene expression of connective tissue growth factor in adult mouse. *Growth Factors* 2005;**23**:43–53.
30. Chuva de Sousa Lopes SM, Feijen A, Korving J, Korchynskiy O, Larsson J, Karlsson S *et al*. Connective tissue growth factor expression and Smad signaling during mouse heart development and myocardial infarction. *Dev Dyn* 2004;**231**:542–50.
31. D'Avila A, Thiagalingam A, Foley L, Fox M, Ruskin JN, Reddy VY. Temporary occlusion of the great cardiac vein and coronary sinus to facilitate radiofrequency catheter ablation of the mitral isthmus. *J Cardiovasc Electrophysiol* 2008;**19**:645–50.
32. Fuller IA, Wood MA. Intramural coronary vasculature prevents transmural radio-frequency lesion formation: implications for linear ablation. *Circulation* 2003;**107**:1797–803.
33. Rubinsky J, Onik G, Mikus P, Rubinsky B. Optimal parameters for the destruction of prostate cancer using irreversible electroporation. *J Urol* 2008;**180**:2668–74.
34. Deodhar A, Monette S, Single GW Jr, Hamilton WC Jr, Thornton R, Maybody M *et al*. Renal tissue ablation with irreversible electroporation: preliminary results in a porcine model. *Urology* 2011;**77**:754–60.
35. Grodzinsky AJ. Electromechanical and physicochemical properties of connective tissue. *Crit Rev Biomed Eng* 1983;**9**:133–99.
36. de Boer RA, Pinto YM, Suurmeijer AJ, Pokharel S, Scholtens E, Humler M *et al*. Increased expression of cardiac angiotensin II type 1 (AT(1)) receptors decreases myocardial microvessel density after experimental myocardial infarction. *Cardiovasc Res* 2003;**57**:434–42.
37. Wang B, Ansari R, Sun Y, Postlethwaite AE, Weber KT, Kiani MF. The scar neo-vasculature after myocardial infarction in rats. *Am J Physiol Heart Circ Physiol* 2005;**289**:H108–13.
38. Maor E, Ivorra A, Leor J, Rubinsky B. The effect of irreversible electroporation on blood vessels. *Technol Cancer Res Treat* 2007;**6**:307–12.



CHAPTER 5

Myocardial Lesion Size after Epicardial Electroporation Catheter Ablation after Subxiphoid Puncture

Kars Neven
Vincent van Driel
Harry van Wessel
René van Es
Pieter Doevendans
Fred Wittkampf

Abstract

Background Irreversible electroporation is a promising nonthermal ablation modality able to create deep myocardial lesions. We investigated lesion size after epicardial electroporation catheter ablation with various energy levels after subxiphoid pericardial puncture.

Methods and Results In six 6-month-old pigs (60–75 kg), a custom deflectable octopolar 12-mm circular catheter with 2-mm ring electrodes was introduced via a deflectable sheath after pericardial access by subxiphoid puncture. Nonarcing, nonbarotraumatic, cathodal 50, 100, and 200 J electroporation applications were delivered randomly on the basal, mid and lateral left ventricle. After 3-month survival, myocardial lesion size and degree of intimal hyperplasia of the coronary arteries were analyzed histologically. Five animals survived the follow-up without complications and 1 animal died of shock after the subxiphoid puncture. At autopsy, whitish circular scars with indentation of the epicardium could be identified. Average lesion depths of the 50-, 100-, and 200-J lesions were 5.0 ± 2.1 , 7.0 ± 2.0 , and 11.9 ± 1.5 mm, respectively. Average lesion widths of the 50-, 100-, and 200-J lesions were 16.6 ± 1.1 , 16.2 ± 4.3 , and 19.8 ± 1.8 mm, respectively. In the 100- and 200-J cross sections, transmural left ventricular lesions and significant tissue shrinkage were observed. No intimal hyperplasia of the coronary arteries was observed.

Conclusions Epicardial electroporation ablation after subxiphoid pericardial puncture can create deep, wide, and transmural ventricular myocardial lesions. There is a significant relationship between the amounts of electroporation energy delivered epicardially and lesion size in the absence of major adverse events. (Circ Arrhythm Electrophysiol. 2014;7:728-733.)

Introduction

Radiofrequency catheter ablation has become the standard ablation technique for the treatment of cardiac arrhythmias after direct current catheter ablation was abandoned, this was because of the high complication rate attributable to the generation of vapor globe, sparking, explosion, and pressure waves.¹⁻⁴ Since its introduction, epicardial radiofrequency ablation is increasingly being performed for the treatment of ventricular arrhythmias because of ischemic and especially nonischemic cardiomyopathies.⁵ Radiofrequency causes heat damage to all tissue near the ablation site. Ablation near coronary arteries can therefore have hazardous adverse effects, such as coagulation of blood inside the vessel and vessel stenosis with subsequent myocardial infarction.⁶⁻⁸ In addition, the cooling effect of arterial and endocardial blood flow may limit lesion formation and success of the procedure.^{9,10}

In recent years, irreversible electroporation has been proposed as a new ablation modality for cardiac arrhythmias.¹¹⁻¹⁴ du Pré et al¹⁵ showed that epicardial electroporation ablation over coronary arteries, with a follow-up of 3 weeks, has a low risk of coronary damage and that the use of this technique near or even on large coronary arteries is relatively safe. In addition, lesion formation by electroporation did not seem to be affected by the presence of arterial blood flow. We recently demonstrated that epicardial catheter ablation using 200 J electroporation applications can create extensive and deep myocardial lesions without significant damage to the coronary arteries after a 3-month follow-up period.¹⁶

The purpose of the present study is to investigate the relationship between the magnitude of an epicardial electroporation application and lesion size.

Methods

All studies were performed after prior approval from the Animal Experiments Committee of the University Medical Center Utrecht, Utrecht, The Netherlands and were performed in compliance with the Guide for the Care and Use of Laboratory Animals.¹⁷

Study Protocol

The study was performed in 6 pigs (weight, 60–75 kg). Amiodarone was started 1 week before the procedure (400 mg QD) to prevent procedure-related arrhythmias. Carbasalate calcium (80 mg QD) and clopidogrel (75 mg QD) were started 3 days before the procedure and continued until euthanasia. The animals were sedated, intubated, and anesthetized according to the standard procedures. Using a subxiphoid pericardial puncture, a custom deflectable octopolar 12-mm circular catheter with 2-mm ring electrodes was introduced in the pericardial space via a 40-cm long 8.5 French deflectable sheath (Agilis EPI Steerable Introducer, St. Jude Medical, St. Paul, MN; **Figure 1**). After left anterior descending coronary artery and circumflex coronary artery angiography, 3 single, QRS-wave triggered, cathodal 50, 100 or 200 J applications were delivered on 3 nonoverlapping left ventricular (LV) locations: the midanterior LV, the anteriorapical LV, and the midlateral LV. In each animal, 50, 100, and 200 J were delivered in random sequence. The energy was generated by a monophasic external defibrillator (Lifepak 9, Physio-Control, Inc, Redmond, WA). A large skin patch (7506, Valleylab Inc, Boulder, CO) on the lower back served as indifferent electrode.^{13,14} A cathodal polarity was chosen because that has the highest threshold for arcing in a blood environment.¹⁸ The impulse waveform was similar to that applied in our earlier studies.^{13,14} Coronary arteries were not specifically targeted, but coronary angiography was repeated after the last application.



Figure 1. Subxiphoid pericardial puncture and ablation catheter. **Left**, The black guidewire after subxiphoid pericardial puncture and the distal end of the steerable pericardial sheath with the dilator inside. **Right**, The custom circular electroporation ablation catheter that was used for this study. The distal circular, 12-mm diameter segment of the deflectable 7-French catheter contains 8 electrodes of 2 mm in length.

After 3-month survival, coronary angiography of the left anterior descending coronary and circumflex coronary arteries was repeated, the thorax was opened by sternotomy, and the animal was euthanized by exsanguination. After the heart was removed, the pericardium was peeled off and the areas with ablation lesions were excised and fixated in formalin.

Histological Evaluation

After fixation, three 4.0-mm wide segments were dissected from each lesion perpendicular to the epicardial surface to facilitate measurement of lesion width and depth. The first segment (A) was taken through the middle of what visibly appeared to be the center of the circular lesion; 2 other segments (B and C) were dissected perpendicular to that first segment, again through the apparent center of the lesion. (**Figure 2**) After embedding in paraffin, these segments were sectioned and stained with hematoxylin–eosin and with elastic van Gieson. All histological sections were digitally scanned and analyzed using Imagescope (Aperio Technologies). Lesion size was measured in each section.

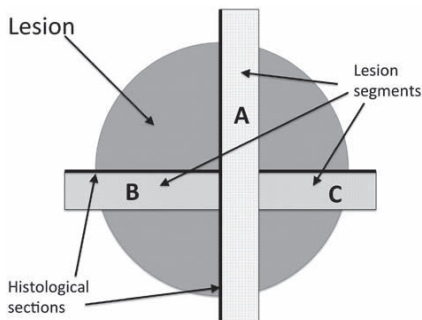


Figure 2. Schematic drawing of a lesion and the positions of the 3 segments. The first 4.0-mm wide lesion segment (A) was taken aside from the middle of what visibly appeared to be the center of the circular lesion (gray circle); 2 other lesion segments (B and C) were dissected perpendicular to that first segment, again aside from the apparent center of the lesion. The histological sections were taken from the side of the segment, which went through the center of the lesion. Maximal lesion depth was measured in lesion segment A, lesion width was calculated as the average value of lesion width in lesion segment A and the sum of lesion widths in lesions segments B and C plus 4.0 mm.

Measurement of Lesion Size

Two investigators, blinded for the energy settings used, independently measured lesion depth and width: maximal lesion depth was measured in segment A. Lesion width was calculated as the average value of lesion width in segment A and the sum of lesion widths in segments B and C plus 4.0 mm. Values obtained by the 2

blinded investigators were averaged. Large lesions often showed tissue shrinkage, as also seen after myocardial infarction.¹⁹ When sufficient undamaged myocardium was present in the histological section, the estimated original epicardial contour was used to measure lesion depth.¹⁴ With relatively deep lesions, tissue shrinkage apparently also affected the endocardial contour and then also the estimated original endocardial contour was used to measure lesion depth.

Evaluation of the Coronary Arteries

All pre- and postablation angiograms were qualitatively analyzed by 2 experienced investigators. Consensus had to be reached on the degree of luminal narrowing. All histological cross sections were analyzed for the degree of intimal hyperplasia of the coronary arteries.

Statistical Analysis

The relationship between delivered peak current and mean lesion depth and width was calculated by randomized block regression analysis using Tukey's multiple comparison post hoc test. Continuous variables were expressed as mean±SD. Statistical significance was defined as $P\leq 0.05$.

Results

Five animals survived the procedure and the 3-month follow-up period without complications. One animal had to be euthanized acutely before electroporation applications had been delivered because of complications caused by failed subxiphoid puncture. The novel ablation catheter had never been deployed in this animal.

Pericardial Ablation

All recorded voltage and current waveforms were smooth, suggesting the absence of arcing.¹³ Average peak currents of the 50, 100, and 200 J applications were 11.6 ± 1.4 , 19.0 ± 1.5 , and 27.1 ± 0.7 A, respectively (**Table**).

Macroscopic Findings

Careful inspection of the organs adjacent to the pericardium showed no abnormalities in any animal. No macroscopic signs of bleeding, scarring, or excessive fibrotic tissue proliferation were found

Table. Relationship Between Magnitude of Application, Output, and Lesion Size

Energy, J	Peak Power, V	Peak Current, A	Peak Resistance, Ω	Lesion Depth, mm	Lesion Width, mm	Transmural Lesion, %
50	1220±46	11.6±1.4	107±14	5.0±2.1	16.6±1.1	0
100	1670±74	19.0±1.5	91±14	7.0±2.0	18.1±1.0	20
200	2305±54	27.1±0.7	85±4	11.9±1.5	19.8±1.8	80

Ablations were performed with 50, 100, and 200 J. Lesion depth and width were measured in all histological cross sections. Lesion transmuralty was determined per lesion. Data are given as the mean±SD.

Lesion Size

In 5 animals, 43 cross sections from 15 electroporation lesions were analyzed. In total, we obtained 15 cross sections from five 50-J lesions, 13 cross sections from five 100-J lesions, and 15 cross sections from five 200-J lesions (**Figure 3**).

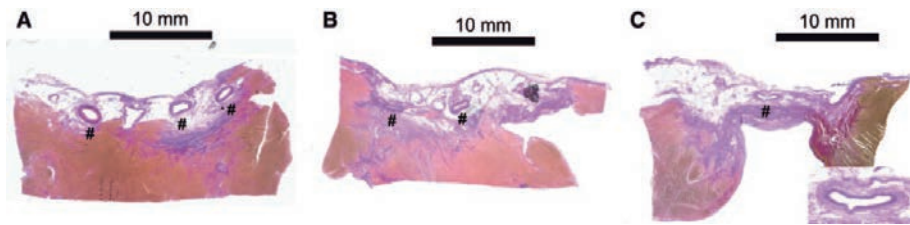


Figure 3. Histological sections of epicardial lesions. Histological elastic van Gieson–stained sections through the center of epicardial lesions created with 50 J (**A**), 100 J (**B**), and 200 J (**C**). Each section was taken perpendicular to the epicardial surface and over the course of the diameter of the lesion. The endocardial side is at the **bottom** and the epicardial side is at the **top** of the picture. Note that there is no heat sink effect of the coronary arteries: the lesion includes the coronary artery completely and continues on the endocardial side of the coronary artery. Also, note the shrinkage caused by scar contracture in **C**. The **inset** in the lower right corner of **C** shows a magnification of the coronary artery shown in **C**. #Coronary artery.

At visual inspection after euthanization, the lesions had a circular, whitish aspect on the epicardial surface with denting in the center of the lesion, because of tissue shrinkage. All but one of the lesions showed continuous lesions, with a sharp demarcation between the ablation lesion and the surrounding tissue. Because of vital myocardium in the center of the lesion, one 50-J lesion did not show 1 continuous lesion, but 2 separate lesions in segment A (**Figure 4**). For this lesion we averaged lesion depths observed in the 3 histological sections; because of the absence of a continuous lesion we could not calculate a lesion width in this lesion.

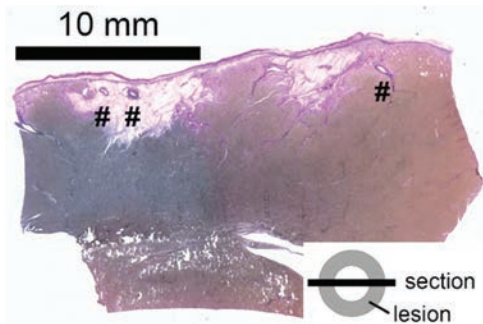


Figure 4. Histological section of epicardial lesion after 50 J electroporation application. Histological elastic van Gieson–stained section through the center of an epicardial lesion created with 50 J. The section was taken perpendicular to the epicardial surface and over the course of the diameter of the lesion. The endocardial side is at the **bottom** and the epicardial side is at the **top** of the picture. There are 2 separate, whitish lesions visible beneath the epicardial surface with vital myocardium in-between. The location of the cross section relative to the circular lesion is sketched in the **inset** in the **lower right corner**. #Coronary artery.

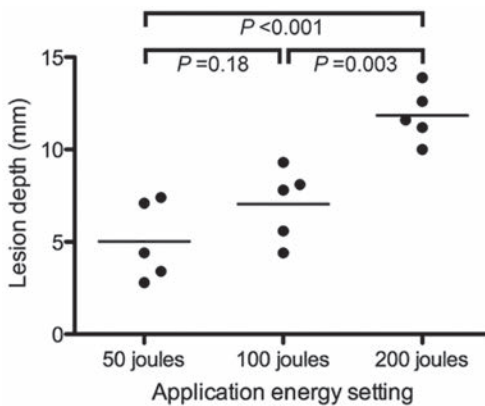


Figure 5. Magnitude of electroporation application and maximal lesion depth. Relationship between magnitude of electroporation application and maximal lesion depth per lesion. The horizontal bar shows the mean value of the lesion depths per energy setting. The differences in depth between the 50- vs 200-J lesions and the 100- vs 200-J lesions are statistically significant.

Lesion Depth

Mean depth (range) of the 50-, 100-, and the 200-J lesions was 5.0 ± 2.1 (range, 2.8–7.4) mm, 7.0 ± 2.0 (range, 4.4–9.3) mm, and 11.9 ± 1.5 (range, 10.0–13.9) mm, respectively (**Figure 5**). Mean depth of all lesions combined was 8.0 ± 3.4 mm. In the 100-J, and especially in the 200-J lesions, significant shrinkage caused by scar contracture was obvious. The difference in depth between the respective lesions was statistically highly significant ($P < 0.001$). In more detail, the differences in

depth between the 50- versus 200-J lesions and the 100- versus 200-J lesions were statistically significant ($P<0.001$ and $P=0.003$, respectively). The difference in depth between the 50- and 100-J lesions was not statistically significant ($P=0.18$). Transmurality of the lesion was seen in 20% of the 100-J lesions and in 80% of the 200-J lesions.

Lesion Width

Mean maximal width (range) of the 50-, 100-, and the 200-J lesions was 16.6 ± 1.1 (range, 15.2–17.7) mm, 18.1 ± 1.0 (range, 16.6–18.9) mm, and 19.8 ± 1.8 (range, 17.4–21.3) mm, respectively. Mean maximal width of all lesions combined was 18.2 ± 1.9 mm. The differences in width between the 50- and 200-J lesions were statistically significant ($P=0.007$; **Figure 6**).

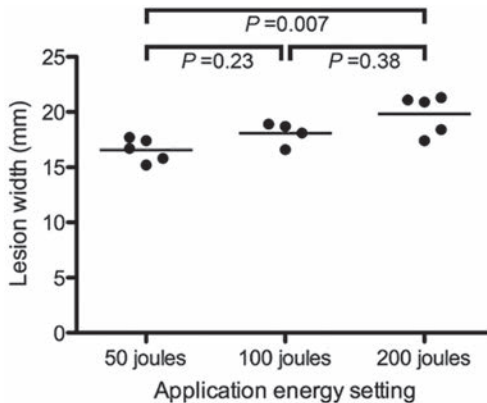


Figure 6. Magnitude of electroporation application and mean maximal lesion width. Relationship between magnitude of electroporation application and mean maximal width per lesion. The horizontal bar shows the mean value of the lesion widths per energy setting. The differences in width between the 50- vs 200-J lesions are statistically significant.

Coronary Angiography

All preablation coronary angiograms were normal. Postablation coronary angiography demonstrated short-lasting (<30 minutes) luminal narrowing with subsequent normalization in the targeted area, suggestive of coronary spasm. After 3-month survival, there was no significant narrowing of any coronary artery. Visually, all coronary angiograms resembled the preablation coronary angiograms. No significant intimal hyperplasia of coronary arteries was seen in any histological section.

Discussion

Epicardial radiofrequency ablation has a long history. From the first publication by Sosa et al,²⁰ percutaneous epicardial radiofrequency ablation is nowadays being performed in many electrophysiological centers and for a variety of indications, mainly ablation of ventricular tachycardia.²¹ However, severe complications, such as damage to the coronary arteries and the phrenic nerve, were described soon after the introduction of epicardial radiofrequency ablation.^{22,23} Since then, many techniques have been introduced with varying success to prevent severe complications, such as coronary angiography,²¹ endocardial ablation with an ablation catheter equipped with a retractable needle,²⁴ endocardial ablation to reduce or obviate epicardial ablation,²⁵ and injection of air or saline into the pericardium.²⁶

Recently, Wittkamp et al¹⁴ and du Pré et al¹⁵ have demonstrated that epicardial ablation using electroporation in pigs is feasible, safe, and causes only minimal damage to the coronary arteries. These ablations were performed in an open-chest model, where the epicardium was surgically exposed. This is not the regular, clinical approach when performing epicardial ablation in humans. Therefore, we recently demonstrated that closed-chest epicardial catheter ablation using electroporation is feasible, safe, and able to create deep myocardial lesions.¹⁶ Ablation with 200 J electroporation applications on top of main coronary arteries only caused temporary spasm and a median of $4\pm 10\%$ luminal stenosis.

Electroporation Pulse and Catheter Model

Between 1980 and 1990, direct current catheter ablation was the only energy source available for catheter ablation. At the end of that era, low-energy direct current ablation was developed, but soon thereafter it was replaced by the more elegant radiofrequency ablation technique. In the present and earlier studies, we used a readily available monophasic defibrillator to deliver the electroporation pulse.^{13–15} However, instead of using a single electrode, a circular arrangement of 8 electrically connected electrodes was used in the present study for application of electroporation energy.

In general, a circular electrode catheter has an important advantage over a single ablation electrode for the application of electric current. Although the latter creates an exponential decay in current density with increasing distance from the ablation electrode, a circular arrangement of electrically connected electrodes creates a

thorus-shaped electric field near to and around the ablation hoop, at least in a first approximation. The surface area of a torus relates linearly to the thickness of the torus. Therefore, current density will initially decrease linearly with increasing distance from the ablation hoop and not exponentially. Penetration depth of an electroporation pulse will therefore be greater with such an ablation hoop than with a single ablation electrode. In addition, a circular multi-electrode arrangement will allow for faster electrophysiological mapping than a linear electrode catheter because it can be used to determine not only the timing but also the direction of the activation wavefront. Finally, the 8-ring electrodes of 2-mm length have a total surface area of 115 mm², which definitively allows for a higher arcing threshold than a single electrode; even an 8-mm 7F electrode only has a total surface area of 58 mm² and such a large electrode has poor mapping characteristics.

Lesion Size

In this study, we were able to create deep, wide, and continuous lesions. There was a significant relationship between magnitude of the electroporation application and lesion depth and width, with a larger magnitude of the application a larger myocardial lesion could be created. Where a single 50 J application was able to create myocardial lesions ≤ 7.4 -mm deep and 17.7-mm wide, single 200 J applications created myocardial lesions ≤ 13.9 -mm deep and 21.3-mm wide. These 200 J electroporation applications are sufficiently powerful to create transmural ventricular lesions. There were no adverse effects associated with these applications.^{27,28}

Mean width of all lesions was 18.2 ± 1.9 mm. The widest 200-J lesion was 21.3 mm; this is $\approx 2\times$ the width of the diameter of the ablation catheter itself. Although ≤ 21 -mm-wide lesions might be undesirable for the ablation of a focal epicardial source of arrhythmia, lesions of this width might be useful and effective when homogenization of a large area of epicardial scar tissue is required. With future catheter design and further titration of energy settings, it should be possible to find the optimal energy settings for clinical applications.

Effect on Coronary Arteries

The coronary arteries were not specifically targeted in this study, but they were also not purposely avoided. Apart from short-lasting (< 30 minutes) coronary spasm, no long-term luminal narrowing was seen. After 3-month follow-up, the luminal diameters of the main coronary arteries were similar to the baseline

luminal diameters. These data support the findings of du Pré et al¹⁵ and our previous findings;¹⁶ similar results were found after a follow-up period of 3 weeks and 3 months, respectively.

Clinical Implications

Data from this study and previous studies suggest that epicardial electroporation ablation is a safe and effective ablation modality.^{15,16} It is able to create large and deep myocardial lesions while sparing the coronary arteries; electroporation ablation is the first and only ablation modality capable of doing so. Using this new technology, safe and effective epicardial ablation on or near coronary arteries can become a real possibility for the treatment of ventricular tachycardias, which would otherwise not be treatable with catheter ablation.

Also, deep intramural foci of ventricular arrhythmia will become within reach of catheter ablation using electroporation because a single 200 J electroporation application is able to safely create deep, continuous, and transmural myocardial lesions. This desirable feature is also unique for electroporation ablation.

The clinical introduction of epicardial electroporation ablation could possibly significantly change the way epicardial ablation is being performed.

Limitations

We investigated only 3 energy settings: 50, 100, and 200 J. We have no information on lesion size or adverse effects when using other energy settings.

Significant shrinkage caused by scar contracture of the 100-J and especially the 200-J lesions definitively caused underestimation of lesion size. Also, transmuralities of the lesion could have caused underestimation of lesion depth.

Although we did not record any arrhythmia after the ablation nor experienced sudden death in the animals during follow-up, we cannot exclude the occurrence of proarrhythmic effects after electroporation ablation.

We did not investigate the possible negative influence of (the amount of) epicardial fat or preexisting myocardial fibrosis on lesion size.

In this study, the electroporation ablation catheter was placed on the LV epicardium to investigate the effects of certain energy settings on lesion size. Although we might expect a similar outcome, we do not have information about lesion size created by epicardial electroporation ablation in atrial tissue.

Lesion size and form with electroporation ablation will depend on the ultimate catheter/device design and measures to ensure electrode–tissue contact. Given

the experimental character of this study, extrapolation of the results of this study to final catheter/device design should be performed with great caution.

Conclusions

Epicardial electroporation ablation after subxiphoid pericardial puncture can create deep, wide, and transmural ventricular myocardial lesions. There is a significant relationship between the amounts of electroporation energy delivered epicardially and lesion size in the absence of major adverse events.

Acknowledgments

We wish to thank the staff of the Department of Experimental Cardiology of the University Medical Center Utrecht for technical assistance during the experiments.

Disclosures

Fred Wittkampf is a consultant for St. Jude Medical, Atrial Fibrillation division. Both Fred Wittkampf and Harry van Wessel are coinventors of circular electroporation. The other authors report no conflicts.

Clinical perspective

Despite the use of advanced 3-dimensional mapping systems and coronary angiography, coronary artery damage remains one of the potential complications of epicardial ablation using radiofrequency ablation. Not seldom, the close proximity of the targeted ablation site to a coronary artery forces the investigator to refrain from epicardial ablation. Electroporation ablation is a novel ablation technique. It has been proven that one 6-ms, 200 J electroporation application can create deep and wide myocardial lesions and can isolate a pulmonary vein. However, the safety and efficacy of epicardial electroporation ablation still are unknown. In this porcine model, after subxiphoid puncture, epicardial electroporation ablation was performed using different energy settings. We demonstrated that epicardial electroporation ablation is able to create deep and wide myocardial lesions, and

that there is a clear dose–response relationship. We also demonstrated that the coronary arteries are spared from electroporation ablation directly on the coronary arteries. The clinical implementation of subxiphoid epicardial electroporation ablation as a novel, safe, effective, and fast ablation technique could therefore be performed safely, without the risk of damage to the coronary arteries.

References

1. Bor ggreffe M, Budde T, Podczeczek A, Breithardt G. High frequency alternating current ablation of an accessory pathway in humans. *J Am Coll Cardiol*. 1987;10:576–582.
2. Ahsan AJ, Cunningham D, Rowland E, Rickards AF. Catheter ablation without fulguration: design and performance of a new system. *Pacing Clin Electrophysiol*. 1989;12:1557–1561.
3. Bardy GH, Coltorti F, Stewart RB, Greene HL, Ivey TD. Catheter-mediated electrical ablation: the relation between current and pulse width on voltage breakdown and shock-wave generation. *Circ Res*. 1988;63:409–414.
4. Gallagher JJ, Svenson RH, Kasell JH, German LD, Bardy GH, Broughton A, Critelli G. Catheter technique for closed-chest ablation of the atrioventricular conduction system. *N Engl J Med*. 1982;306:194–200.
5. Aliot EM, Stevenson WG, Almendral-Garrote JM, Bogun F, Calkins CH, Delacretaz E, Della Bella P, Hindricks G, Jaïs P, Josephson ME, Kautzner J, Kay GN, Kuck KH, Lerman BB, Marchlinski F, Reddy V, Schalij MJ, Schilling R, Soejima K, Wilber D; European Heart Rhythm Association (EHRA); Registered Branch of the European Society of Cardiology (ESC); Heart Rhythm Society (HRS); American College of Cardiology (ACC); American Heart Association (AHA). EHRA/HRS Expert Consensus on Catheter Ablation of Ventricular Arrhythmias: developed in a partnership with the European Heart Rhythm Association (EHRA), a Registered Branch of the European Society of Cardiology (ESC), and the Heart Rhythm Society (HRS); in collaboration with the American College of Cardiology (ACC) and the American Heart Association (AHA). *Heart Rhythm*. 2009;6:886–933.
6. Aoyama H, Nakagawa H, Pitha JV, Khammar GS, Chandrasekaran K, Matsudaira K, Yagi T, Yokoyama K, Lazzara R, Jackman WM. Comparison of cryothermia and radiofrequency current in safety and efficacy of catheter ablation within the canine coronary sinus close to the left circumflex coronary artery. *J Cardiovasc Electrophysiol*. 2005;16:1218–1226.
7. Paul T, Bökenkamp R, Mahnert B, Trappe HJ. Coronary artery involvement early and late after radiofrequency current application in young pigs. *Am Heart J*. 1997;133:436–440.
8. Roberts-Thomson KC, Steven D, Seiler J, Inada K, Koplan BA, Tedrow UB, Epstein LM, Stevenson WG. Coronary artery injury due to catheter ablation in adults: presentations and outcomes. *Circulation*. 2009;120:1465–1473.
9. Jones DL, Guiraudon GM, Skanes AC, Guiraudon CM. Anatomical pitfalls during encircling cryoablation of the left atrium for atrial fibrillation therapy in the pig. *J Interv Card Electrophysiol*. 2008;21:187–193.
10. Pardo Meo J, Scanavacca M, Sosa E, Correia A, Hachul D, Darrieux F, Lara S, Hardy C, Jatene F, Jatene M. Atrial coronary arteries in areas involved in atrial fibrillation catheter ablation. *Circ Arrhythm Electrophysiol*. 2010;3:600–605.
11. Lavee J, Onik G, Mikus P, Rubinsky B. A novel nonthermal energy source for surgical epicardial atrial ablation: irreversible electroporation. *Heart Surg Forum*. 2007;10:E162–E167.
12. Hong J, Stewart MT, Cheek DS, Francischelli DE, Kirchhof N. Cardiac ablation via electroporation. *Conf Proc IEEE Eng Med Biol Soc*. 2009;2009:3381–3384.
13. Wittkamp FH, van Driel VJ, van Wessel H, Vink A, Hof IE, Gründeman PF, Hauer RN, Loh P. Feasibility of electroporation for the creation of pulmonary vein ostial lesions. *J Cardiovasc Electrophysiol*. 2011;22:302–309.
14. Wittkamp FH, van Driel VJ, van Wessel H, Neven KG, Gründeman PF, Vink A, Loh P, Doevendans PA. Myocardial lesion depth with circular electroporation ablation. *Circ Arrhythm Electrophysiol*. 2012;5:581–586.
15. du Pré BC, van Driel VJ, van Wessel H, Loh P, Doevendans PA, Goldschmeding R, Wittkamp FH, Vink A. Minimal coronary artery damage by myocardial electroporation ablation. *Europace*. 2013;15:144–149.
16. Neven K, van Driel VJ, van Wessel H, van Es R, Du Pre BC, Doevendans PA, Wittkamp FH. Epicardial electroporation ablation after surgical sub-xiphoid access. *Heart Rhythm*. 2014;11:1465–1470.
17. Institute for Laboratory Animal Research. *Guide for the Care and Use of Laboratory Animals*. 8th ed. Washington DC: National Academies Press; 2011.
18. Bardy GH, Coltorti F, Ivey TD, Alferness C, Rackson M, Hansen K, Stewart R, Greene HL. Some factors affecting bubble formation with catheter-mediated defibrillator pulses. *Circulation*. 1986;73:525–538.

19. Ganame J, Messalli G, Masci PG, Dymarkowski S, Abbasi K, Van de Werf F, Janssens S, Bogaert J. Time course of infarct healing and left ventricular remodelling in patients with reperfused ST segment elevation myocardial infarction using comprehensive magnetic resonance imaging. *Eur Radiol*. 2011;21:693–701.
20. Sosa E, Scanavacca M, d'Avila A, Pileggi F. A new technique to perform epicardial mapping in the electrophysiology laboratory. *J Cardiovasc Electrophysiol*. 1996;7:531–536.
21. Pisani CF, Lara S, Scanavacca M. Epicardial ablation for cardiac arrhythmias: techniques, indications and results. *Curr Opin Cardiol*. 2014;29:59–67.
22. Sosa E, Scanavacca M, d'Avila A. Transthoracic epicardial catheter ablation to treat recurrent ventricular tachycardia. *Curr Cardiol Rep*. 2001;3:451–458.
23. Rumbak MJ, Chokshi SK, Abel N, Abel W, Kittusamy PK, McCormack J, Patel MM, Fontanet H. Left phrenic nerve paresis complicating catheter radiofrequency ablation for Wolff-Parkinson-White syndrome. *Am Heart J*. 1996;132:1281–1285.
24. Sapp JL, Beeckler C, Pike R, Parkash R, Gray CJ, Zeppenfeld K, Kuriachan V, Stevenson WG. Initial human feasibility of infusion needle catheter ablation for refractory ventricular tachycardia. *Circulation*. 2013;128:2289–2295.
25. Komatsu Y, Daly M, Sacher F, Cochet H, Denis A, Derval N, Jesel L, Zellerhoff S, Lim HS, Jadidi A, Nault I, Shah A, Roten L, Pascale P, Scherr D, Aurillac-Lavignolle V, Hocini M, Haïssaguerre M, Jaïs P. Endocardial ablation to eliminate epicardial arrhythmia substrate in scar-related ventricular tachycardia. *J Am Coll Cardiol*. 2014;63:1416–1426.
26. Di Biase L, Burkhardt JD, Pelargonio G, Dello Russo A, Casella M, Santarelli P, Horton R, Sanchez J, Gallinghouse JG, Al-Ahmad A, Wang P, Cummings JE, Schweikert RA, Natale A. Prevention of phrenic nerve injury during epicardial ablation: comparison of methods for separating the phrenic nerve from the epicardial surface. *Heart Rhythm*. 2009;6:957–961.
27. Evans GT Jr, Scheinman MM, Scheinman MM, Zipes DP, Benditt D, Breithardt G, Camm AJ, el-Sherif N, Fisher J, Fontaine G. The Percutaneous Cardiac Mapping and Ablation Registry: final summary of results. *Pacing Clin Electrophysiol*. 1988;11(11 Pt 1):1621–1626.
28. Rosenqvist M, Lee MA, Moulinier L, Springer MJ, Abbott JA, Wu J, Langberg JJ, Griffin JC, Scheinman MM. Long-term follow-up of patients after transcatheter direct current ablation of the atrioventricular junction. *J Am Coll Cardiol*. 1990;16:1467–1474.



CHAPTER 6

Safety and Feasibility of Closed Chest Epicardial Catheter Ablation using Electroporation

Kars Neven
Vincent van Driel
Harry van Wessel
René van Es
Pieter Doevendans
Fred Wittkampf

Abstract

Background Permanent coronary artery damage is a hazardous complication of epicardial radiofrequency ablation. Irreversible electroporation (IRE) is a promising nonthermal ablation modality able to create deep myocardial lesions. We investigated the effects of epicardial IRE on luminal coronary artery diameter and lesion depth.

Methods and Results In 5 pigs (60–75 kg), the pericardium was exposed using surgical subxiphoidal epicardial access. A custom deflectable octopolar 12-mm circular catheter with 2-mm ring electrodes was introduced in the pericardium via a steerable sheath. After coronary angiography (CAG), the proximal, mid, and distal left anterior descending, and circumflex coronary arteries were targeted with a single, cathodal 200 J application. CAG was repeated after IRE and after 3 months follow-up. Using quantitative CAG, the minimal luminal diameter at the lesion site was compared with the average of the diameters just proximal and distal to that lesion. Intimal hyperplasia and lesion size were measured histologically. CAG directly postablation demonstrated short-lasting luminal narrowing with normalization in the targeted area, suggestive of coronary spasm. After 3 months, all CAGs were identical to preablation CAGs: mean reference luminal diameter was 2.2 ± 0.3 mm, mean luminal diameter at the lesion site was 2.1 ± 0.3 mm ($P=0.35$). Average intimal hyperplasia in all arteries was $2\pm 4\%$. Median lesion depth was 6.4 ± 2.6 mm.

Conclusions Luminal coronary artery diameter remained unaffected 3 months after epicardial IRE, purposely targeting the coronary arteries. IRE can create deep lesions and is a safe modality for catheter ablation on or near coronary arteries. (Circ Arrhythm Electrophysiol. 2014;7:913-919.)

Introduction

Before radiofrequency catheter ablation was introduced in cardiac electrophysiology in the late 1980s, direct current catheter ablation was used to treat cardiac arrhythmias. This method caused severe and hazardous adverse effects by creation of an electrically isolating vapor globe. This led to a spark (arcing), an explosion, and a pressure wave.¹ During the past 20 years, radiofrequency catheter ablation has become the standard ablation technique for the treatment of cardiac arrhythmias.² Radiofrequency causes heat damage to all tissue near the ablation site. Ablation near coronary arteries can, therefore, have hazardous adverse effects such as coagulation of blood inside the vessel and vessel stenosis with subsequent myocardial infarction.³⁻⁵ In addition, the cooling effect of arterial and endocardial blood flow may limit lesion formation and success of the procedure.^{6,7}

Recently, Lavee et al,⁸ Hong et al,⁹ and Wittkamp et al¹⁰ published feasibility of epicardial nonthermal electroporation ablation of myocardial tissue, demonstrating that an energy level lower than the arcing threshold could successfully create large myocardial lesions without hazardous adverse effects. du Pré et al¹¹ showed that epicardial electroporation ablation over coronary arteries, with a follow-up of 3 weeks, has a low risk of coronary damage and that the use of this technique near or even on large coronary arteries is relatively safe. In addition, electroporation ablation did not seem to be affected by the presence of arterial blood flow.

The purpose of the present study was to investigate the safety and feasibility of catheter ablation using electroporation in the pericardial space. More specifically, the long-term (3 months) effects of electroporation ablation on the coronary arteries (safety) and the ability to create myocardial lesions by electroporation ablation from the pericardium (feasibility) were subject to investigation.

Methods

All studies were performed after prior approval from the Animal Experimentation Committee of the University Medical Center Utrecht, Utrecht, The Netherlands, and were performed in compliance with the Guide for the Care and Use of Laboratory Animals.¹²

Study Protocol

The study was performed in 6 pigs (weight 60–75 kg). Amiodarone therapy was started 1 week before the index procedure (400 mg once daily) to prevent procedure-related arrhythmias. Carbasalate calcium (80 mg once daily) and clopidogrel (75 mg once daily) therapy was started 3 days before the index procedure and continued until euthanasia. The animals were sedated, intubated, and anesthetized according to standard procedures. Using a surgical subxiphoidal pericardial approach, a custom deflectable octopolar 12-mm circular catheter with 2-mm ring electrodes was introduced in the pericardial space via a 40-cm 8.5F deflectable sheath (Agilis EPI Steerable Introducer; St Jude Medical, St Paul, MN; **Figure 1**). After left anterior descending artery (LAD) and circumflex coronary artery (RCx) angiography, the mid and distal LAD and RCx were targeted with electroporation catheter ablation (**Figure 2**). A single, cathodal 200 J application was delivered. This was repeated at 2 or 3 different locations over the LAD and RCx while avoiding overlap. The energy was generated by a monophasic external defibrillator (Lifepak 9; Physio-Control, Inc, Redmond, WA). A large skin patch (7506; Valleylab Inc, Boulder, CO) on the lower back served as indifferent electrode. A cathodal polarity was chosen because that has the highest threshold for arcing in a blood environment.¹³ Coronary angiography (CAG) was repeated after the last application.



Figure 1. Circular electroporation ablation catheter. The custom circular electroporation ablation catheter that was used for this safety and feasibility study. The distal circular, 12-mm diameter segment of the deflectable 7F catheter contains 8 electrodes 2 mm in length.

After 3-month survival, CAG of the LAD and RCx was repeated, the thorax was opened by sternotomy, and the animal was euthanized by exsanguination. After the heart was removed, the pericardium was peeled off and the areas with ablation lesions were excised and fixated in formalin.

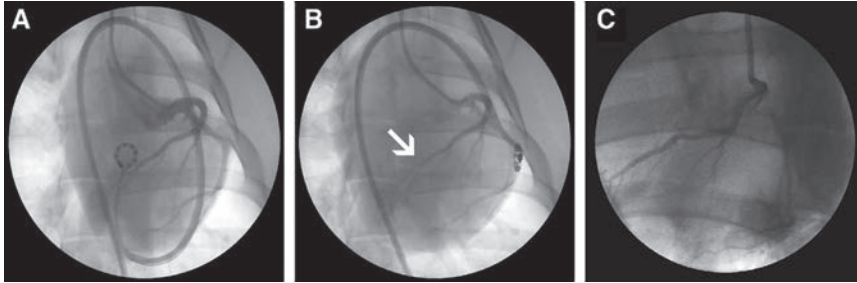


Figure 2. Coronary angiography (CAG) before and after catheter ablation. CAG before (A), directly after (B), and 3 mo after (C) electroporation catheter ablation using a steerable sheath. Note the coronary spasm of the left anterior descending artery (LAD) after electroporation ablation over the LAD (arrow in B) and complete normalization after 3 mo (C).

Measurement of Coronary Diameters

Luminal diameters of the coronary artery, proximal and distal to the application site, and the minimal diameter at the application site were measured using quantitative CAG. The latter value was then compared with the average value of the diameters proximal and distal to the application site.

Histological Evaluation

After fixation, multiple 3- to 4-mm-thick segments were dissected from each lesion to facilitate measurement of lesion width and depth. All sections were taken perpendicular to the epicardial surface and to the main course of the targeted coronary artery. Paraffin-embedded segments were sectioned and stained with H&E and elastic–van Gieson. All histological sections were scanned with a ScanScope XT scanner (Aperio Technologies, Inc, Vista, CA) and analyzed using Imagescope (Aperio Technologies). Lesion depth was measured in each section. Of all coronary arteries and branches, the luminal area, the area encompassed by the internal elastic lamina (IEL area), and the area encompassed by the external elastic lamina (EEL area) were measured. The intimal area was calculated by subtracting the luminal area from the IEL area. All arteries with an EEL area $>0.15 \text{ mm}^2$ were considered clinically relevant and were included in the study. Coronary damage was defined as intimal hyperplasia, and percentage stenosis because of intimal

hyperplasia was calculated as follows: $([\text{IEL area} - \text{luminal area}] / \text{IEL area}) \times 100$.¹¹ From these data, the median values of each lesion were calculated. Subsequently, the mean value of all medians was calculated.

Measurement of Lesion Depth

Lesion depth was measured in each histological section. Large lesions often showed tissue shrinkage as also seen after myocardial infarction.¹⁴ When sufficient undamaged myocardium was present in the histological section, the estimated original epicardial contour was used to measure lesion depth.¹⁵ In case the lesion was transmural also, the estimated original endocardial contour was used to measure lesion depth. From these data, the median depth of each lesion was calculated. Subsequently, the mean value of all median lesion depths was calculated. An ablation lesion was considered to be transmural when transmuralities were observed in at least 2 consecutive histological sections.

Statistical Analysis

Differences in lesion depth and coronary artery luminal diameters were examined with a Wilcoxon signed rank test. These analyses are lesion-based and not pig-based. Continuous variables were expressed as mean \pm SD. Statistical significance was defined as $P \leq 0.05$ (2-sided).

Results

Five animals survived the index procedure and the 3-month follow-up without complications.

Acute Death

One animal suddenly developed cyanosis with prolonged, untreatable hemodynamical instability after the end of the index procedure, ≈ 7 hours after the last ablation. This animal was euthanized acutely.

The procedure of the animal that died was complicated by multiple episodes of catheter-induced, hemodynamically unstable ventricular tachycardia requiring acute electrocardioversion. This already happened before the first electroporation application, despite the pretreatment with amiodarone to prevent occurrence of tachyarrhythmias as much as possible. After each electrocardioversion, the animal

was allowed to recover for 20 to 30 minutes. This was uneventful. After the 3 planned electroporation applications (following protocol), the animal was hemodynamically stable. There were no signs of upcoming complications. Seven hours after the last application, after the end of the procedure, the animal suddenly developed cyanosis and severe dyspnoea. Despite basic emergency medical care, the clinical situation did not stabilize. Therefore, the animal was euthanized following protocol. Although there was no ECG monitoring anymore at the time the adverse event happened, we suspect that the animal had again developed a sustained, hemodynamically unstable ventricular tachycardia. At autopsy, no pericardial effusion or trauma other than the ablation lesions was found. Gross inspection of other organs also showed no abnormalities.

Pericardial Ablation

In the 5 surviving animals, a total of 13 (median, 3; range, 2–3) 200 J electroporation applications were delivered over the LAD and RCx arteries. No arcing or barotrauma was seen during any of the applications. Frequently, noise on 1 or several local bipolar electrograms suggested the presence of air in the pericardial space between the pericardium and the epicardium, possibly because of the pericardial incision and the supine position of the animal (**Figure 3**).

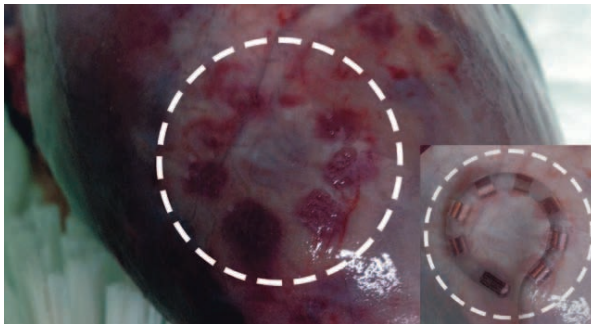


Figure 3. Acute electroporation ablation lesion. Macroscopic picture of a 7-hour-old circular electroporation catheter ablation lesion on the epicardial side of the left ventricle. The markings from the 8 individual electrodes of the 12-mm circular ablation catheter can be seen. A \approx 22-mm-wide whitish coloration of the surrounding epicardium can be identified; the dashed circle marks its outer border. The inset in the lower right corner shows the circular ablation catheter from Figure 1 projected over the markings.

Coronary Angiography

All preablation coronary angiograms were normal. CAG postablation demonstrated short-lasting (<30 minutes) luminal narrowing with subsequent normalization

in the targeted area, suggestive of coronary spasm. After 3-month survival, all coronary angiograms were identical to the preablation coronary angiograms: mean reference luminal diameter was 2.2 ± 0.3 mm, mean luminal diameter at the lesion site was 2.1 ± 0.3 mm ($P=0.35$; **Figure 2** and **Table**).

Table. Lesion Depth, Coronary Artery Diameter, and Patency

Pig #	Median Lesion Depth, mm	Transmurality of Lesion	Coronary artery	Proximal Reference Diameter, mm	Distal Reference Diameter, mm	Minimal Diameter in Lesion, mm	Median Stenosis, %	Maximal Stenosis, %
1	0.0	No	LAD proximal	2.4	2.7	2.4	0	9
1	6.9	Yes	LAD mid	2.8	2.6	2.9	0	4
2	6.5	No	LAD proximal	2.4	2.1	2.2	2	61
2	8.4	No	LAD mid	2.1	1.6	1.8	2	61
2	4.8	No	LAD distal	NA	NA	NA	NA	NA
3	5.5	No	LAD proximal	2.2	2.2	2.2	0	23
3	5.9	No	LAD mid	2.2	1.4	1.8	0	11
4	7.2	No	LAD proximal	2.3	2.3	2.2	0	29
4	7.5	No	LAD mid	2.3	1.9	2.0	5	26
4	6.8	Yes	RCx	2.0	2.1	2.2	9	36
5	3.8	No	LAD proximal	2.4	2.1	2.2	0	4
5	10.4	Yes	LAD mid	2.1	1.7	1.8	0	33
5	9.5	Yes	RCx	2.1	1.8	1.9	10	20
Mean	6.4			2.3	2.0	2.1	2	26
SD	2.6			0.2	0.4	0.3	4	19

Results per lesion after 3 mo follow-up. Median stenosis (%) is median value of luminal stenosis in all sections of the respective lesion. Maximal stenosis (%) is the absolute value of the maximal luminal stenosis in all sections of the respective lesion. In the cross-sections of pig 2, lesion 3, no arteries were visible. The angiographic caliber of the coronary artery was too small to analyze for the third electroporation application of pig 2. Therefore, no information about coronary diameters was available for this application. LAD indicates left anterior descending artery; NA, not available; and RCx, circumflex coronary artery.

Acute Epicardial Lesions

Although 1 animal died shortly after the end of the procedure, already the four 7-hour-old lesions on the epicardium could clearly be identified. Next to the imprint of the separate electrodes of the 12-mm circular ablation catheter, a ≈ 22 -mm-wide whitish coloration of the surrounding epicardium could be identified (**Figure 4**).

Macroscopic Findings

Careful inspection of the organs adjacent to the pericardium showed no abnormalities in any animal. No macroscopic signs of bleeding, scarring, or excessive fibrotic tissue proliferation were found.

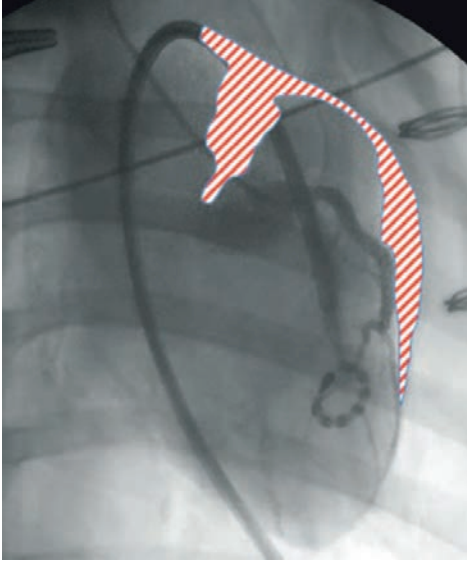


Figure 4. Anteroposterior fluoroscopic image of the heart showing air in the pericardium (red/white striped area).

Lesion Depth and Coronary Arteries

In 5 animals, 104 cross-sections from 13 electroporation lesions, with a median of 9 (range 2–10) cross-sections per lesion, were analyzed. Using 200 J electroporation applications, there was no central surviving area of myocardial tissue visible in any lesion. Transmurality of the ablation lesion was seen in 4 of 13 (31%) lesions and significant shrinkage because of scar contracture was obvious. Mean value of the median lesion depths was 6.4 ± 2.6 mm (range, 0.0–10.4 mm; **Table**). Arterial branches were predominantly located epicardially, very close to the application site. A total of 167 arterial branches with an EEL area >0.15 mm² were found. These arteries were divided into 154 arterial sections that were surrounded by a lesion and 13 that were located outside a lesion. None of the arteries inside the lesion was surrounded by intact myocardial tissue.

Intimal hyperplasia was observed in 66 of 154 arteries inside lesions and in 1 of 13 arteries outside lesions (**Figure 5**). The single affected artery outside a lesion had an EEL area of 0.99 mm². This artery was located 1.6 mm from the lesion border and was surrounded by several smaller and larger unaffected arteries. Mean value of median luminal stenosis in all arteries was $2 \pm 4\%$ (range, 0–61%), whereas mean value of median luminal stenosis of affected arteries was $8 \pm 5\%$ (range, 1–61%; **Table**). Arteries with intimal hyperplasia located inside a lesion were similar in size

to arteries inside a lesion without intimal hyperplasia (mean EEL area of 1.04 ± 0.73 versus 1.01 ± 0.81 mm², respectively; $P=0.86$). Lesion depth measured in cross-sections with arteries showing intimal hyperplasia was greater than lesion depth in cross-sections with arteries showing no intimal hyperplasia (6.9 ± 2.7 versus 4.4 ± 3.3 mm, respectively; $P < 0.0001$).

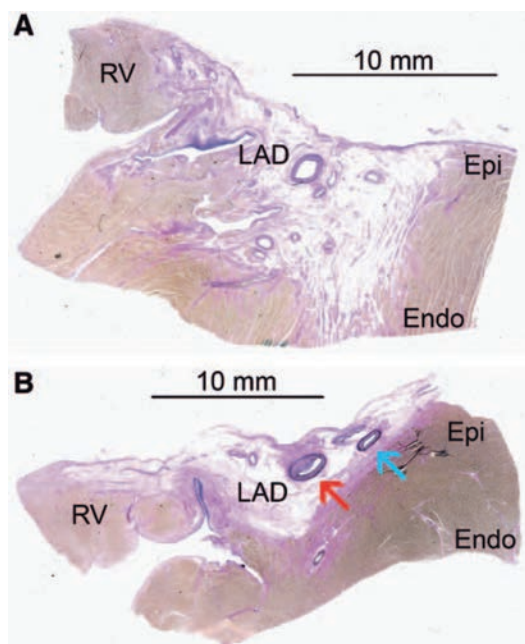


Figure 5. Histological analysis of myocardial tissue after electroporation catheter ablation. Histological sections showing transmural lesion with unaffected left anterior descending artery (LAD; **A**), and lesion with LAD showing intimal hyperplasia and 10% to 25% stenosis (red arrow) and unaffected coronary artery (blue arrow; **B**). Note no heat sink effect. Endo indicates endocardium; Epi, epicardium; and RV, right ventricle.

Discussion

This is the first study investigating the effect of epicardial irreversible electroporation by an ablation catheter placed in the pericardial space.

In recent years, the possibilities and number of catheter ablation procedures of cardiac arrhythmias have skyrocketed.¹⁶⁻¹⁸ Endocardial ablation of ventricular arrhythmias is performed in a large number of centers, but some ventricular arrhythmias can better be ablated from the epicardial side.^{19,20} An epicardial approach, however, is associated with severe complications like cardiac tamponade,

ventricular arrhythmias, phrenic nerve damage, and damage to the coronary arteries.^{21,22} Based on available data and experience, a distance of >5 mm between the ablation catheter and an epicardial artery is commonly recommended when radiofrequency ablation is considered.¹⁹

In this study, we simulated epicardial ventricular catheter ablation in humans. Because of our inexperience with porcine pericardial puncture and to minimize occurrence of periprocedural complications, such as cardiac tamponade, we made a small (<10 mm) pericardial window to obtain pericardial access.

Acute Outcome

One animal died because of unstable ventricular tachycardia \approx 7 hours after ablation. Unfortunately, pigs are susceptible to developing hemodynamically unstable ventricular arrhythmias and the success rate of resuscitation of a pig after prolonged unstable ventricular tachycardia is known to be disappointing.^{23–25} Visual inspection of the epicardium clearly revealed epicardial lesions, \approx 22 mm in diameter despite a only 12-mm circular ablation catheter. This raises the question how fast the effect of electroporation ablation takes in. In a study by Hong et al,⁹ sheep hearts were ablated with electroporation. They proved conduction block directly after ablation. With a maturation period in the animal before euthanization as short as 1 hour, the lesions were in general not visible grossly, but could be detected via histology on lesion cross-sections.

Pericardial Ablation

No complications occurred during or after pericardial access. With a deflectable sheath, the steerable ablation catheter could easily be moved toward target areas. The pericardial window resulted in a layer of air in the pericardial space in some animals. Therefore, tissue contact of the ablation catheter may sometimes have been suboptimal.

Coronary Angiography

In this study we purposely targeted the main coronary arteries. Apart from short-lasting (<30 minutes) coronary spasm, no long-term luminal narrowing was seen; after 3 months follow-up, the luminal diameters of the main coronary arteries were identical to the baseline luminal diameters. This suggests that the patency of the main coronary arteries is not affected by irreversible electroporation. These data support the findings of du Pré et al¹¹ who found similar results after a shorter follow-up period of only 3 weeks.

Lesion Size and Coronary Arteries

One of the limiting factors of conventional catheter ablation is the inability to create transmural left ventricular lesions. With epicardial electroporation ablation, transmural lesions were easily created.

These deep lesions did not come at the cost of major damage to the coronary arteries. Intimal hyperplasia was observed in 67 of 167 arteries. Mean values of median luminal stenosis in all arteries were $2\pm 4\%$; mean values of median luminal stenosis of the arteries showing any intimal hyperplasia were $8\pm 5\%$. There were no occluded main arteries. These results are again in line with the findings of du Pré et al¹¹ who found similar results after a follow-up period of only 3 weeks.

This could be a major breakthrough in the treatment of epicardial ventricular arrhythmias, because no other ablation technique can create deep myocardial lesions very close to or even on top of the coronary arteries without causing significant damage to them.

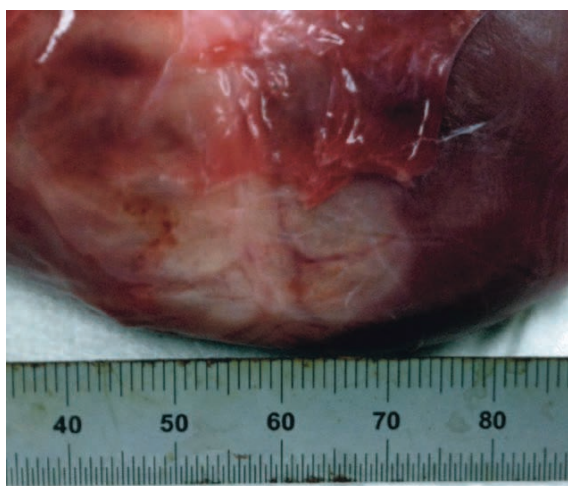


Figure 6. Chronic electroporation ablation lesion. Macroscopic picture of a 3-month-old electroporation ablation lesion over the distal left anterior descending artery (LAD) showing extensive scar formation with a width of ≈ 25 mm. In the middle of the ablation lesion, the LAD with side branches can be identified, running from the top of the picture toward the bottom.

Limitations

We used only 1 energy setting (200 J). From a previous study, we know that this energy setting is able to create wide and deep lesions.¹⁵ This was also seen in the current study: up to 22 mm wide and 11 mm deep lesions resulted from a single

ablation using a 12-mm circular ablation catheter (**Figure 6**). These large lesions may have a negative effect on total myocardial contractility and ejection fraction, especially when placed at multiple different locations. A possibly proarrhythmic effect of these lesions through creation of a substrate should also be addressed in future studies.

Significant shrinkage because of scar contracture of the 200 J lesions definitively caused underestimation of lesion size after 3 months follow-up.

Lesion size with electroporation ablation will depend on the ultimate catheter design and measures to ensure electrode–tissue contact.

Because of the pericardial window, air entered the pericardial space, and this may have caused suboptimal contact between the ablation catheter and the left ventricular epicardium. Future studies on epicardial electroporation catheter ablation should be performed after subxiphoidal puncture of the pericardium, thereby minimizing the risk of air entrapment in the pericardial space.

In the current study, we used \approx 6-week-old pigs, which did not show much epicardial fat at autopsy. In humans, there can be a thick layer of epicardial fat, especially at the basal part of the ventricles and over the interventricular groove. The influence of (the amount of) epicardial fat on myocardial lesion depth created with electroporation ablation has to be investigated in future studies.

The coronary arteries showed short-lasting (<30 minutes) spasm after electroporation catheter ablation directly on the coronary arteries. It is known that pretreatment with vasodilators can prevent or decrease the occurrence of arterial spasm after insertion of a sheath in the radial artery.²⁶ In this study, the coronary arteries were not pretreated with vasodilators. Pretreatment of the coronary arteries with vasodilators should be investigated in future studies.

Apart from damage to the coronary arteries, phrenic nerve damage is another possible complication during conventional epicardial ablation. In this study, we did not investigate the effects of electroporation catheter ablation on phrenic nerve function. Additional studies have to investigate whether or not electroporation catheter ablation affects phrenic nerve function.

In this study, the ablation catheter was placed on the left ventricular epicardium. Although we might expect a similar outcome, we do not have information about lesion size or adverse events created by epicardial electroporation ablation in atrial tissue.

Conclusions

The data of this study demonstrate that epicardial catheter ablation using electroporation can create extensive and deep myocardial lesions without significant damage to the coronary arteries after a 3-month follow-up. This effective new ablation technique could possibly solve one of the most important current limitations of epicardial catheter ablation: safe ablation on or near main coronary arteries.

Acknowledgments

We thank the staff of the Department of Experimental Cardiology of the University Medical Center Utrecht for technical assistance during the experiments; Aryan Vink, MD, PhD, of the Department of Pathology, University Medical Center Utrecht, for support during analyses of the cross-sections; and Paul Westers, PhD, of the Department of Biostatistics, University Medical Center Utrecht, for assistance with the statistical analyses.

Disclosures

Dr Wittkampf is a consultant for St Jude Medical, Atrial Fibrillation division. Both Dr Wittkampf and H. van Wessel are coinventors of circular electroporation. The other authors report no conflicts.

Clinical perspective

Despite the use of advanced 3-dimensional mapping systems and coronary angiography, coronary artery damage remains one of the potential complications of epicardial ablation using radiofrequency ablation. Not seldomly, the close proximity of the targeted ablation site to a coronary artery forces the investigator to refrain from epicardial ablation. Electroporation ablation is a novel ablation technique. It has been proven that one 6 ms, 200 J electroporation application can create deep and wide myocardial lesions and can isolate a pulmonary vein. However, the safety and efficacy of epicardial electroporation ablation still is

unknown. In this porcine model, after surgical subxiphoid access, epicardial electroporation ablation was performed purposely targeting the coronary arteries. Luminal coronary artery diameter remained unaffected 3 months after epicardial electroporation ablation. We demonstrated that epicardial electroporation ablation is able to create deep lesions. We also demonstrated that the coronary arteries are spared from electroporation ablation directly on the coronary arteries. The clinical implementation of subxiphoid epicardial electroporation ablation as a novel, safe, effective and very fast ablation technique could therefore be performed safely, without the risk of damage to the coronary arteries.

References

- Gallagher JJ, Svenson RH, Kasell JH, German LD, Bardy GH, Broughton A, Critelli G. Catheter technique for closed-chest ablation of the atrioventricular conduction system. *N Engl J Med*. 1982;306:194–200.
- Borggreve M, Budde T, Podczek A, Breithardt G. High frequency alternating current ablation of an accessory pathway in humans. *J Am Coll Cardiol*. 1987;10:576–582.
- Aoyama H, Nakagawa H, Pitha JV, Khammar GS, Chandrasekaran K, Matsudaira K, Yagi T, Yokoyama K, Lazzara R, Jackman WM. Comparison of cryothermia and radiofrequency current in safety and efficacy of catheter ablation within the canine coronary sinus close to the left circumflex coronary artery. *J Cardiovasc Electrophysiol*. 2005;16:1218–1226.
- Paul T, Bökenkamp R, Mahnert B, Trappe HJ. Coronary artery involvement early and late after radiofrequency current application in young pigs. *Am Heart J*. 1997;133:436–440.
- Roberts-Thomson KC, Steven D, Seiler J, Inada K, Koplan BA, Tedrow UB, Epstein LM, Stevenson WG. Coronary artery injury due to catheter ablation in adults: presentations and outcomes. *Circulation*. 2009;120:1465–1473.
- Jones DL, Guiraudon GM, Skanes AC, Guiraudon CM. Anatomical pitfalls during encircling cryoablation of the left atrium for atrial fibrillation therapy in the pig. *J Interv Card Electrophysiol*. 2008;21:187–193.
- Pardo Meo J, Scanavacca M, Sosa E, Correia A, Hachul D, Darrieux F, Lara S, Hardy C, Jatene F, Jatene M. Atrial coronary arteries in areas involved in atrial fibrillation catheter ablation. *Circ Arrhythm Electrophysiol*. 2010;3:600–605.
- Lavee J, Onik G, Mikus P, Rubinsky B. A novel nonthermal energy source for surgical epicardial atrial ablation: irreversible electroporation. *Heart Surg Forum*. 2007;10:E162–E167.
- Hong J, Stewart MT, Cheek DS, Francischelli DE, Kirchof N. Cardiac ablation via electroporation. *Conf Proc IEEE Eng Med Biol Soc*. 2009;2009:3381–3384.
- Wittkamp FH, van Driel VJ, van Wessel H, Vink A, Hof IE, Gründeman PF, Hauer RN, Loh P. Feasibility of electroporation for the creation of pulmonary vein ostial lesions. *J Cardiovasc Electrophysiol*. 2011;22:302–309.
- du Pré BC, van Driel VJ, van Wessel H, Loh P, Doevendans PA, Goldschmeding R, Wittkamp FH, Vink A. Minimal coronary artery damage by myocardial electroporation ablation. *Europace*. 2013;15:144–149.
- Institute for Laboratory Animal Research. *Guide for the Care and Use of Laboratory Animals*. 8th ed. Washington, DC: National Academies Press; 2011.
- Bardy GH, Coltorti F, Ivey TD, Alferness C, Rackson M, Hansen K, Stewart R, Greene HL. Some factors affecting bubble formation with catheter-mediated defibrillator pulses. *Circulation*. 1986;73:525–538.
- Ganame J, Messalli G, Masci PG, Dymarkowski S, Abbasi K, Van de Werf F, Janssens S, Bogaert J. Time course of infarct healing and left ventricular remodelling in patients with reperfused ST segment elevation myocardial infarction using comprehensive magnetic resonance imaging. *Eur Radiol*. 2011;21:693–701.
- Wittkamp FH, van Driel VJ, van Wessel H, Neven KG, Gründeman PF, Vink A, Loh P, Doevendans PA. Myocardial lesion depth with circular electroporation ablation. *Circ Arrhythm Electrophysiol*. 2012;5:581–586.
- Martin-Doyle W, Essebag V, Zimetbaum P, Reynolds MR. Trends in US hospitalization rates and rhythm control therapies following publication of the AFFIRM and RACE trials. *J Cardiovasc Electrophysiol*. 2011;22:548–553.
- Ferrero de Loma-Osorio A, Diaz-Infante E, Macias Gallego A. Spanish Catheter Ablation Registry. 12th Official Report of the Spanish Society of Cardiology Working Group on Electrophysiology and Arrhythmias (2012). *Rev Esp Cardiol (Engl Ed)*. 2013;66:983–992.
- Madeira F, Oliveira M, Ventura M, Primo J, Bonhorst D, Morais C. [National registry on cardiac electrophysiology (2010 and 2011)]. *Rev Port Cardiol*. 2013;32:95–100.

19. Aliot EM, Stevenson WG, Almendral-Garrote JM, Bogun F, Calkins CH, Delacretaz E, Bella PD, Hindricks G, Jaïs P, Josephson ME, Kautzner J, Kay GN, Kuck KH, Lerman BB, Marchlinski F, Reddy V, Schalij MJ, Schilling R, Soejima K, Wilber D; European Heart Rhythm Association; European Society of Cardiology; Heart Rhythm Society. EHRA/HRS Expert Consensus on Catheter Ablation of Ventricular Arrhythmias: developed in a partnership with the European Heart Rhythm Association (EHRA), a Registered Branch of the European Society of Cardiology (ESC), and the Heart Rhythm Society (HRS); in collaboration with the American College of Cardiology (ACC) and the American Heart Association (AHA). *Europace*. 2009;11:771–817.
20. Pisani CF, Lara S, Scanavacca M. Epicardial ablation for cardiac arrhythmias: techniques, indications and results. *Curr Opin Cardiol*. 2014;29:59–67.
21. Della Bella P, Brugada J, Zeppenfeld K, Merino J, Neuzil P, Maury P, Maccabelli G, Vergara P, Baratto F, Berruezo A, Wijnmaalen AP. Epicardial ablation for ventricular tachycardia: a European multicenter study. *Circ Arrhythm Electrophysiol*. 2011;4:653–659.
22. D'Avila A, Gutierrez P, Scanavacca M, Reddy V, Lustgarten DL, Sosa E, Ramires JA. Effects of radiofrequency pulses delivered in the vicinity of the coronary arteries: implications for nonsurgical transthoracic epicardial catheter ablation to treat ventricular tachycardia. *Pacing Clin Electrophysiol*. 2002;25:1488–1495.
23. Niemann JT, Cruz B, Garner D, Lewis RJ. Immediate countershock versus cardiopulmonary resuscitation before countershock in a 5-minute swine model of ventricular fibrillation arrest. *Ann Emerg Med*. 2000;36:543–546.
24. Achleitner U, Wenzel V, Strohmer HU, Krismer AC, Lurie KG, Lindner KH, Amann A. The effects of repeated doses of vasopressin or epinephrine on ventricular fibrillation in a porcine model of prolonged cardiopulmonary resuscitation. *Anesth Analg*. 2000;90:1067–1075.
25. Strohmer HU, Lindner KH, Pregel AW, Pfenninger EG, Bothner U, Lurie KG. Effects of epinephrine and vasopressin on median fibrillation frequency and defibrillation success in a porcine model of cardiopulmonary resuscitation. *Resuscitation*. 1996;31:65–73.
26. Varenne O, Jégou A, Cohen R, Empana JP, Salengro E, Ohanessian A, Gaultier C, Allouch P, Walspurger S, Margot O, El Hallack A, Jouven X, Weber S, Spaulding C. Prevention of arterial spasm during percutaneous coronary interventions through radial artery: the SPASM study. *Catheter Cardiovasc Interv*. 2006;68:231–235.



CHAPTER 7

Epicardial Linear Electroporation Ablation and Lesion Size

Vincent van Driel*

Kars Neven*

Harry van Wessel

René van Es

Pieter Doevendans

Fred Wittkampf

* Both authors contributed equally to the study and manuscript

Abstract

Background Electroporation can be used as a nonthermal method to ablate myocardial tissue. However, like with all electrical ablation methods, determination of the energy supplied into the myocardium enhances the clinically required controllability over lesion creation.

Objective To investigate the relationship between the magnitude of epicardial electroporation ablation and the lesion size using an electrically isolating linear suction device.

Methods In 5 pigs (60–75 kg), the pericardium was opened after medial sternotomy. A custom linear suction device with a single 35 × 6-mm electrode inside a 42-mm-long and 7-mm-wide plastic suction cup was used for electroporation ablation. Single cathodal applications of 30, 100, or 300 J were delivered randomly at 3 different epicardial left ventricular sites. Coronary angiography was performed before ablation, immediately after ablation, and after 3 months survival. Lesion size was measured histologically after euthanization.

Results The mean depth of 30, 100, and 300 J lesions was 3.2 ± 0.7 , 6.3 ± 1.8 , and 8.0 ± 1.5 mm, respectively ($P = .0003$). The mean width of 30, 100, and 300 J lesions was 10.1 ± 0.8 , 15.1 ± 1.5 , and 17.1 ± 1.3 mm, respectively ($P < .0001$). Significant tissue shrinkage was observed at the higher energy levels. No luminal arterial narrowing was observed after 3 months: 2.3 ± 0.3 mm vs 2.3 ± 0.4 mm ($P = .85$).

Conclusion The relationship between the amount of electroporation energy delivered through a linear suction device with a single linear electrode and the mean myocardial lesion size is significant in the absence of major adverse events or permanent damage to the coronary arteries.

Abbreviations **AF** = atrial fibrillation; **LAD** = left anterior descending

Heart Rhythm 2014;0:1–6

Introduction

Cell membranes can be permanently damaged by a high electric gradient. This may lead to increased permeability, loss of cellular proteins, and eventually necrosis.¹ In the 1980s, the principle of direct current catheter ablation was based on this effect.² However, direct current catheter ablation caused electrolysis at the electrode surface that led to a gas bubble, arcing, explosion, and a pressure wave.²⁻⁵ Therefore, when radiofrequency catheter ablation was introduced to cardiac electrophysiology in 1987, it soon became the standard treatment method for cardiac arrhythmias.⁶ Unfortunately, radiofrequency energy can cause severe complications such as steam pops or blood coagulation. It can also cause permanent damage to blood vessels and nerves as well as constriction of (pulmonary) veins owing to induction of heat damage to all tissue types near the ablation site.⁷⁻⁹ Recently, circular electroporation ablation was introduced as a new endocardial catheter ablation energy modality for the treatment of atrial fibrillation (AF).¹⁰ Electroporation ablation also uses a high current density to create myocardial lesions. Its main difference with the technique used in the 1980s is the lower current density at the electrode surface, which prevents the cascade of adverse events. Lavee et al¹¹ demonstrated the feasibility and safety of epicardial nonthermal electroporation ablation of myocardial tissue. du Pre et al¹² showed that linear epicardial electroporation ablation can create myocardial lesions safely and effectively.

Linear epicardial electroporation ablation could be an effective and fast ablation modality for the (video-assisted) thoracoscopic treatment of atrial arrhythmias and for the treatment of epicardial ventricular arrhythmias.

The purpose of the present porcine study was to investigate the relationship between the magnitude of a linear epicardial electroporation application and the lesion size.

Methods

All studies were approved by the Animal Experiments Committee of the University Medical Center Utrecht, Utrecht, The Netherlands, and were performed in compliance with the *Guide for the Care and Use of Laboratory Animals*.¹³

Study protocol

The study was performed in 5 pigs (weight 60–75 kg). Carbasalate calcium (80 mg daily) and clopidogrel (75 mg daily) were given 3 days before the procedure and continued until euthanasia. Amiodarone was given 1 week before the procedure (600 mg daily) to prevent procedure-related ventricular arrhythmias. The animals were sedated, intubated, and anesthetized according to standard procedures.

Linear ablation

The thorax was opened via a medial sternotomy. After angiography of the left anterior descending (LAD) and circumflex coronary arteries via a catheter in the right carotid artery, an approximately 10-cm-long incision was made in the pericardial sack. Epicardial ablation was performed with a custom linear suction device, comprising a 35-mm-long and 6-mm-wide linear electrode inside a 42-mm-long and 7-mm-wide plastic suction cup (**Figure 1**). The suction device was sucked with a constant under pressure of 50–60 cm H₂O on a position parallel to LAD coronary artery on the left ventricle, on the basal anterolateral part of the left ventricle, or on the apicolateral part of the left ventricle (**Figure 2**). The constant under pressure should ensure a good electrode-tomyocardium contact in the absence of blood.

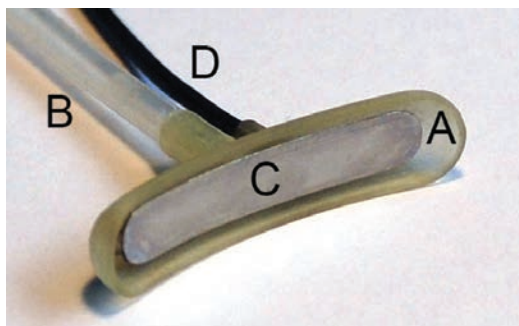


Figure 1. Linear suction device consisting of a 42-mm-long and 7-mm-wide plastic suction cup (A) connected to a vacuum system by a tube (B) and containing a single 35-mm-long and 6-mm-wide protruding linear electrode (C), which is connected by a cable (D) to the pulse generator.

A single, 6-ms cathodal application was then delivered. The energy was generated with a monophasic external defibrillator (Lifepak 9, Physio-Control, Inc, Redmond, WA). A large skin patch (7506, Valleylab Inc, Boulder, CO) on the lower back served as an indifferent electrode. The ablation procedure was repeated at 2 other left ventricular epicardial locations, as described above. In each animal, 30, 100, and

300 J were delivered in a random sequence. Voltage and current waveforms of all applications were recorded as described previously.¹⁰ With the suction device still in position after the application, both ends of the device were marked with sutures. Coronary angiography was repeated after the last application.

After a 3-month survival period, coronary angiography of the LAD and circumflex coronary arteries was repeated, the thorax was opened by sternotomy, and the animal was euthanized by exsanguination. The heart was removed; the pericardium was peeled off; and the areas with ablation lesions were excised, pinned to a flat support, and fixed in formalin.

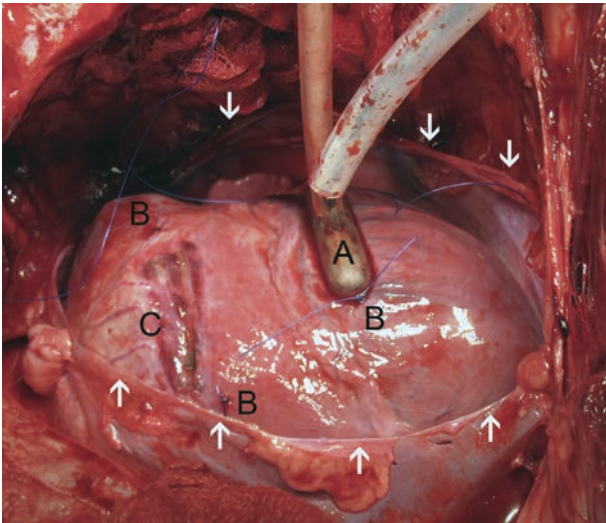


Figure 2. Linear suction device (A) is sucked on the epicardium. Around the suction device, a narrow zone of hematoma can be seen. The location of ablation is marked with stitches (B) at both far ends of the suction cup. A linear hematoma (C) from a previous ablation procedure can be identified. The arrows indicate the pericardium.

Coronary angiography

Luminal diameters of the coronary artery proximal and distal to the lesion site and the minimal luminal diameter at the lesion site were measured by using quantitative coronary angiography.

Histological evaluation

After fixation, multiple (range 10–17) 3–4-mm-thick segments of each lesion were taken perpendicular to the linear lesion and to the epicardial surface. Paraffin-embedded segments were sectioned and stained with hematoxylin and eosin

and with elastic van Gieson. All sections were scanned and digitized to measure lesion depth and width.

Measurement of lesion size

Lesion depth and width were measured in each histological section. Large lesions often showed tissue shrinkage, as was also seen after myocardial infarction.¹⁴ When sufficient undamaged myocardium was present in the histological section, the estimated original epicardial contour was used to measure lesion depth.¹⁵ From these data, the median depth and width of each lesion were calculated. Subsequently, the mean depth and width of all lesions created with the same energy setting were calculated.

Statistical analysis

Differences in coronary artery luminal diameters were calculated using a paired *t* test. The relationship between delivered peak current and mean lesion depth and width was calculated by performing randomized block regression analysis using the Tukey multiple comparison post hoc test. Continuous variables were expressed as mean \pm SD. Statistical significance was defined as $P \leq .05$.

Results

All animals survived the procedure and the 3-month follow-up period without complications. The sutures that had marked both far ends of the ablation line and the whitish colorization of the lesions allowed identification of the 3 application areas, even when superficial epicardial damage due to pericardial adhesion obscured the epicardial aspect of the lesions.

Epicardial ablation

All recorded voltage and current waveforms were smooth, demonstrating the absence of arcing.¹⁰ The average peak currents of 30, 100, and 300 J applications were 7.9 0.5, 15.8 1.2, and 28.4 1.1 A, respectively (**Table 1**).

Table 1. Relationship between magnitude of application, output, and lesion size

Energy (J)	Peak power (V)	Peak current (A)	Peak resistance (Ω)	Lesion depth (mm)	Lesion width (mm)	Transmural lesion (%)
30	960 \pm 21	7.9 \pm 0.5	118 \pm 16	3.2 \pm 0.7	10.1 \pm 0.8	25
100	1845 \pm 241	15.8 \pm 1.2	119 \pm 25	6.3 \pm 1.8	15.1 \pm 1.5	100
300	2930 \pm 67	28.4 \pm 1.1	103 \pm 4	8.0 \pm 1.5	17.1 \pm 1.3	100

Ablation procedures were performed using 30, 100, and 300 J. Lesion depth and width were measured in all histological cross sections. Lesion transmural was determined per lesion. Data are presented as mean SD.

Visual inspection of the ablation area and the electrodes directly after the energy application never revealed any blood clots or charring. Acutely, the suction device did cause some local epicardial hematoma owing to bursting of superficial small epicardial blood vessels. After every 300 J application, a light purplish circular epicardial colorization around the bruised area was visible.

Coronary angiography

As expected, all pre-ablation coronary angiograms were normal. Repeat coronary angiography at the end of the procedure showed some degree of luminal narrowing in nearby coronary arteries, suggestive of coronary spasm. After 3 months survival, however, all coronary angiograms were identical to the pre-ablation coronary angiograms: the mean reference luminal diameter was 2.3 ± 0.3 mm, and the mean luminal diameter at the lesion site was 2.3 ± 0.4 mm ($P = .85$; **Figure 3**). No significant intimal hyperplasia of coronary arteries was seen in any histological section.

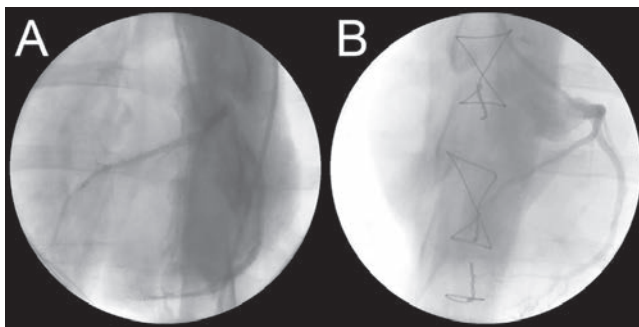


Figure 3. Coronary angiography of the left anterior descending and circumflex coronary arteries in anteroposterior projection before (A) and 3 months after (B) electroporation ablation. There is no significant narrowing of the coronary artery lumen.

Lesion size

In 5 animals, 170 cross sections from 14 electroporation lesions were analyzed. Owing to adhesion to the sternum, one 30 J lesion was severely damaged during the repeat sternotomy after 3 months survival and could not be analyzed. In total, we obtained 45 cross sections from four 30 J lesions, 62 cross sections from five 100 J lesions, and 63 cross sections from five 300 J lesions.

Lesion depth

The mean depth of 30, 100, and 300 J lesions was 3.2 ± 0.7 , 6.3 ± 1.8 , and 8.0 ± 1.5 mm, respectively (**Figure 4**). In 100 J lesions, and especially in 300 J lesions, significant shrinkage due to scar contracture was obvious. The median lesion depth and width per lesion are shown in **Figures 5A** and **5B**, respectively.

The difference in depth between the respective lesions is statistically highly significant ($P = .0003$). In more detail, the differences in depth between 30 and 100 J lesions and between 30 and 300 J lesions are statistically highly significant ($P < .01$ and $P < .001$, respectively). The difference in depth between 100 and 300 J lesions is statistically nonsignificant (**Figure 5A**).

Transmurality of the ablation lesion was seen in 25% of the 30 J lesions and in 100% of the 100 and 300 J lesions.

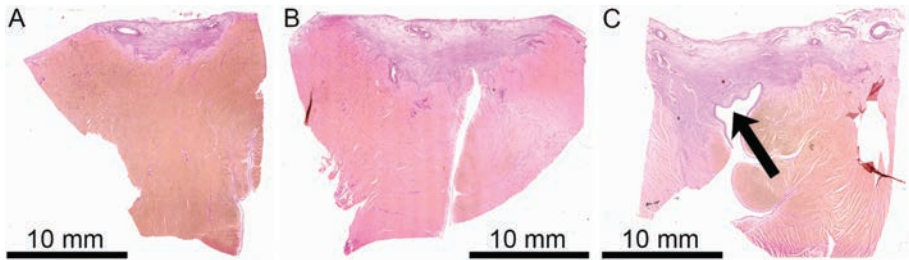


Figure 4. Histological elastic van Gieson–stained sections through the center of linear lesions created with 30 J (A), 100 J (B), and 300 J (C). Each section was taken perpendicular to the epicardial surface and approximately through the middle of the lesion. The endocardial side is at the bottom and the epicardial side is at the top of the picture. Note that there is no heat sink effect of the coronary arteries: the lesion includes the coronary artery completely and continues on the endocardial side of the coronary artery. Also note the shrinkage due to scar contracture in panel C.

Lesion width

The mean width of 30, 100, and 300 J lesions was 10.1 ± 0.8 , 15.1 ± 1.5 , and 17.1 ± 1.3 mm, respectively.

The difference in width between the respective lesions is also statistically highly significant ($P < .0001$). In more detail, the differences in depth between 30 and 100 J lesions, between 30 and 300 J, and between 100 and 300 J lesions are statistically highly significant ($P < .001$, $P < .001$, and $P < .01$, respectively; **Figure 5B**).

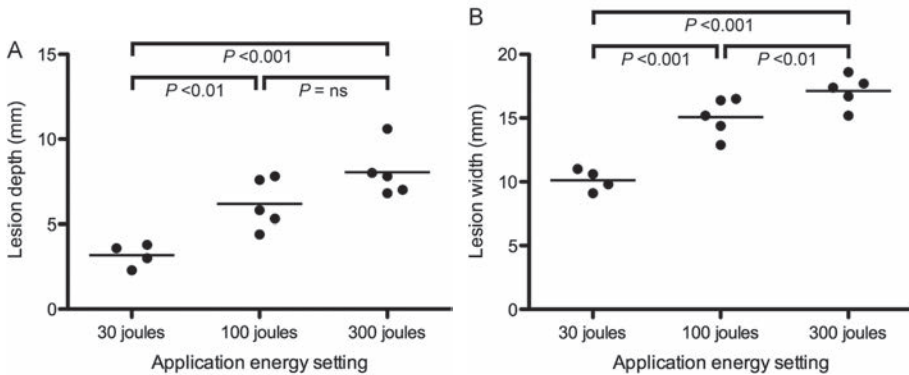


Figure 5. A: Relationship between the magnitude of electroporation application and the median lesion depth per lesion. The horizontal bar shows the mean value of the median lesion depths per energy setting. B: Relationship between the magnitude of electroporation application and the median lesion width per lesion. The horizontal bar shows the mean value of the median lesion widths per energy setting. The relationship is significant between all magnitudes.

Discussion

Electroporation is an emerging nonthermal ablation technique for tissue ablation. Electrical pulses at high local current density are applied across the cell to produce damage by the process of irreversible cell membrane permeabilization: nanopores in the cell membrane increase the permeability of cells, resulting in disruption of cellular homeostasis, ultimately leading to cell death.¹⁶

This new ablation technique, inferred from the earlier direct current ablation, has already been widely used for tumor ablation and was recently reintroduced in the cardiovascular field.¹¹ Its main difference with the technique used in the 1980s is the lower current density at the electrode surface that prevents the cascade of adverse events.

Lesion size

There is a significant relationship between the amount of energy delivered epicardially through a linear suction device containing a single linear electrode and the median myocardial lesion depth. There was absence of arcing and potential adverse effects associated with direct current ablation.^{17,18}

In this study, we were able to create deep, wide, and continuous lesions. With single 300 J applications, myocardial lesions were up to 12.1 mm deep and 24.1 mm wide. Significant shrinkage due to scar contracture of 100 J lesions and especially 300 J lesions definitively led to an underestimation of lesion size, explaining the nonsignificant difference between lesion depths created by 100 J vs 300 J applications. These 100 and 300 J electroporation applications are sufficiently powerful to create transmural ventricular lesions; for transmural atrial lesions, a lower energy setting would suffice.

The median lesion depths created with 100 J applications in this study were significantly larger than the median lesion depths created with 100 J in a previous study by Wittkamp et al:¹⁵ 6.4 mm vs 2.9 mm. This can be explained by the fact that in that study a 7-F decapolar 20-mm circular ablation catheter with 2-mm-long electrodes was stitched on the epicardium and there was a layer of at least 10 mm of blood above the ablation area within the pericardial space. This setting intended to simulate endocardial conditions, and a large part of applied energy could leak away through this blood layer. In the present study, the electrically isolated ablation electrode was actively sucked against the epicardium, ensuring electrode-tissue contact and simultaneously preventing undefined current leak to surrounding structures. Therefore, in this study, a contact between the electrode and the myocardium was appropriate and exclusive and had a larger area. Consequently, all current was delivered into the myocardial tissue, creating a larger lesion.

The mean width of 30, 100, and 300 J lesions was 10.1 ± 0.8 , 15.1 ± 1.5 , and 17.1 ± 1.3 mm, respectively. For 100 and 300 J lesions, this width is approximately 2–3 times wider than the width of the linear ablation electrode itself. To our knowledge, there are no scientific data on “minimal” lesion width required to achieve myocardial conduction block, but a 17-mm-wide lesion might be “overkill” and therefore be undesirable. With lesions this wide, far more myocardial tissue than minimally required could be destroyed. With future catheter design and further titration of energy settings, it should be possible to find the optimal energy settings for both atrial and ventricular applications. Especially for the atria, a lower energy setting, between 30 and 100 J, would be sufficient.

Effects on coronary arteries

In this study, we did not purposely target the main coronary arteries with electroporation ablation. Apart from short-lasting (<30 minutes) spasm of coronary arteries, no long-term luminal narrowing was observed. Also, no significant intimal hyperplasia of coronary arteries was seen in any histological cross section. This is in line with the findings of du Pre et al,¹² who investigated coronary arteries 3 weeks after an electroporation application. The data of the present study confirm that coronary arteries are only mildly affected by electroporation. In other studies, where radiofrequency- or high-intensity-focused ultrasound ablation on or near coronary arteries was performed, moderate to severe damage to the coronary arteries was seen.¹⁹⁻²¹

Clinical implications

Epicardial ablation can be used for the treatment of both atrial and ventricular arrhythmias. Before closed chest catheter ablation was invented, open-chest ablation was performed for the treatment of cardiac arrhythmias.^{22,23} For the treatment of AF, Cox et al²⁴ created an electrical “maze” in the atria by an extensive series of full-thickness incisions through the walls of both atria. This method was then further improved and several noncutting alternatives of the Cox-maze procedure have been developed since by using a variety of energy sources including radiofrequency energy, cryoablation, and high-intensity focused ultrasound.^{25,26} However, these thermal ablation techniques do not reach the success rate of the original cut-and-sew method, in part probably because of the presence of warm endocardial blood that limits penetration depth in off-pump procedures.^{27,28} Electroporation is a nonthermal ablation method that facilitates permanent and deep myocardial lesions even without cardiopulmonary bypass.

The length of the cross-clamp time is correlated with increased morbidity and mortality.^{29,30} Electroporation ablation can be performed within a few seconds. Therefore, when applied during concomitant cardiac surgery, this new ablation technique may reduce the cross-clamp time significantly, which is correlated with increased morbidity and mortality and improve clinical outcome. This would be a major breakthrough in the surgical treatment of AF. A similar suction device as described in this study ensures electrode-tissue contact and simultaneously prevents undefined current leak to surrounding structures. It could be developed into a safe and effective single-shot device for ablation of AF via video-assisted thoracoscopy.

Study limitations

We investigated only 3 energy settings: 30, 100, and 300 J. We have no information on lesion size or adverse effects when using other energy settings.

Significant shrinkage due to scar contracture of 100 J lesions and especially 300 J lesions definitively led to an underestimation of lesion size. Also, transmuralty of the lesion could have led to an underestimation of lesion depth. In this study, the suction device was placed on the left ventricular epicardium to investigate the effects of certain energy settings on lesion size. Although we might expect a similar outcome, we do not have information about lesion size created by epicardial electroporation ablation in atrial tissue and about possible adverse effects of placement of a suction device on atrial tissue.

We have no information about the possible effect of scar tissue or fat on lesion size created by epicardial electroporation ablation.

Although we did not record any arrhythmia after ablation, nor experienced sudden death in the animals during follow-up, we cannot exclude occurrence of proarrhythmic effects after electroporation ablation.

Lesion size with electroporation ablation will depend on the ultimate catheter/device design and measures to ensure electrode-tissue contact. Given the experimental character of this study, extrapolation of the results of this study to the final catheter/device design should be performed with great caution.

Conclusion

There is a significant relationship between the amount of electroporation energy delivered epicardially through a linear suction device with a single linear electrode and the mean myocardial lesion depth and width in the absence of major adverse events or permanent damage to the coronary arteries. These results could lead to the cardiosurgical implementation of electroporation ablation for the treatment of cardiac arrhythmias.

Acknowledgments

We thank the staff of the Department of Experimental Cardiology of the University Medical Center Utrecht for technical assistance during the experiments and Mr Paul Westers, PhD, the Department of Biostatistics, Utrecht University, for statistical analyses.

References

1. Lee RC, Zhang D, Hannig J. Biophysical injury mechanisms in electrical shock trauma. *Annu Rev Biomed Eng* 2000;2:477–509.
2. Gallagher JJ, Svenson RH, Kasell JH, German LD, Bardy GH, Broughton A, Critelli G. Catheter technique for closed-chest ablation of the atrioventricular conduction system. *New Engl J Med* 1982;306:194–200.
3. Bardy GH, Coltorti F, Stewart RB, Greene HL, Ivey TD. Catheter-mediated electrical ablation: the relation between current and pulse width on voltage breakdown and shock-wave generation. *Circ Res* 1988;63:409–414.
4. Ahsan AJ, Cunningham D, Rowland E, Rickards AF. Catheter ablation without fulguration: design and performance of a new system. *Pacing Clin Electrophysiol* 1989;12:1557–1561.
5. Lemery R, Talajic M, Roy D, Couto B, Lavoie L, Lavallee E, Cartier R. Success, safety, and late electrophysiological outcome of low-energy direct-current ablation in patients with the Wolff-Parkinson-White syndrome. *Circulation* 1992;85:957–962.
6. Borggrefe M, Budde T, Podczeczek A, Breithardt G. High frequency alternating current ablation of an accessory pathway in humans. *J Am Coll Cardiol* 1987;10:576–582.
7. Deshmukh A, Patel NJ, Pant S, et al. In-hospital complications associated with catheter ablation of atrial fibrillation in the United States between 2000 and 2010: analysis of 93801 procedures. *Circulation* 2013;128:2104–2112.
8. Kok LC, Everett THt, Akar JG, Haines DE. Effect of heating on pulmonary veins: how to avoid pulmonary vein stenosis. *J Cardiovasc Electrophysiol* 2003;14:250–254.
9. Taylor GW, Kay GN, Zheng X, Bishop S, Ideker RE. Pathological effects of extensive radiofrequency energy applications in the pulmonary veins in dogs. *Circulation* 2000;101:1736–1742.
10. Wittkamp FH, van Driel VJ, van Wessel H, Vink A, Hof IE, Grundeman PF, Hauer RN, Loh P. Feasibility of electroporation for the creation of pulmonary vein ostial lesions. *J Cardiovasc Electrophysiol* 2011;22:302–309.
11. Lavee J, Onik G, Mikus P, Rubinsky B. A novel nonthermal energy source for surgical epicardial atrial ablation: irreversible electroporation. *Heart Surg Forum* 2007;10:E162–E167.
12. du Pre BC, van Driel VJ, van Wessel H, Loh P, Doevendans PA, Goldschmeding R, Wittkamp FH, Vink A. Minimal coronary artery damage by myocardial electroporation ablation. *Europace* 2013;15:144–149.
13. Institute for Laboratory Animal Research. Guide for the Care and Use of Laboratory Animals. 8th ed. Washington, DC: National Academies Press; 2011.
14. Ganame J, Messalli G, Masci PG, Dymarkowski S, Abbasi K, Van de Werf F, Janssens S, Bogaert J. Time course of infarct healing and left ventricular remodelling in patients with reperfused ST segment elevation myocardial infarction using comprehensive magnetic resonance imaging. *Eur Radiol* 2011;21:693–701.
15. Wittkamp FH, van Driel VJ, van Wessel H, Neven KG, Grundeman PF, Vink A, Loh P, Doevendans PA. Myocardial lesion depth with circular electroporation ablation. *Circ Arrhythm Electrophysiol* 2012;5:581–586.
16. Rubinsky B, ed. *Irreversible Electroporation*. Heidelberg: Springer; 2010. Series in Biomedical Engineering.
17. Evans GT Jr, Scheinman MM, Scheinman MM, et al. The Percutaneous Cardiac Mapping and Ablation Registry: final summary of results. *Pacing Clin Electrophysiol* 1988;11:1621–1626.
18. Rosenqvist M, Lee MA, Moulinier L, Springer MJ, Abbott JA, Wu J, Langberg JJ, Griffin JC, Scheinman MM. Long-term follow-up of patients after trans-catheter direct current ablation of the atrioventricular junction. *J Am Coll Cardiol* 1990;16:1467–1474.
19. Aliot EM, Stevenson WG, Almendral-Garrote JM, et al. EHRA/HRS expert consensus on catheter ablation of ventricular arrhythmias: developed in a partnership with the European Heart Rhythm Association (EHRA), a Registered Branch of the European Society of Cardiology (ESC), and the Heart Rhythm Society (HRS); in collaboration with the American College of Cardiology (ACC) and the American Heart Association (AHA). *Europace* 2009;11:771–817.

20. Della Bella P, Brugada J, Zeppenfeld K, Merino J, Neuzil P, Maury P, Maccabelli G, Vergara P, Baratto F, Berruezo A, Wijnmaalen AP. Epicardial ablation for ventricular tachycardia: a European multicenter study. *Circ Arrhythm Electrophysiol* 2011;4:653–659.
21. Koruth JS, Dukkupati S, Carrillo RG, Coffey J, Teng J, Eby TB, Reddy VY, D'Avila A. Safety and efficacy of high-intensity focused ultrasound atop coronary arteries during epicardial catheter ablation. *J Cardiovasc Electrophysiol* 2011;22:1274–1280.
22. Burchell HB, Frye RL, Anderson MW, McGoan DC. Atrioventricular and ventriculoatrial excitation in Wolff-Parkinson-White syndrome (type B): temporary ablation at surgery. *Circulation* 1967;36:663–672.
23. Harrison L, Gallagher JJ, Kasell J, Anderson RH, Mikat E, Hackel DB, Wallace AG. Cryosurgical ablation of the A-V node-His bundle: a new method for producing A-V block. *Circulation* 1977;55:463–470.
24. Cox JL, Schuessler RB, D'Agostino HJ Jr, Stone CM, Chang BC, Cain ME, Corr PB, Boineau JP. The surgical treatment of atrial fibrillation, III: Development of a definitive surgical procedure. *J Thorac Cardiovasc Surg* 1991;101:569–583.
25. Khargi K, Hutten BA, Lemke B, Deneke T. Surgical treatment of atrial fibrillation: a systematic review. *Eur J Cardiothorac Surg* 2005;27:258–265.
26. Melby SJ, Lee AM, Damiano RJ. Advances in surgical ablation devices for atrial fibrillation. In: Wang P, Naccarelli GV, Rosen MR, eds. *New Arrhythmia Technologies*. Malden, MA: Blackwell; 2005:233–241.
27. Lustgarten DL, Bell S, Hardin N, Calame J, Spector PS. Safety and efficacy of epicardial cryoablation in a canine model. *Heart Rhythm* 2005;2:82–90.
28. Milla F, Skubas N, Briggs WM, Girardi LN, Lee LY, Ko W, Tortolani AJ, Krieger KH, Isom OW, Mack CA. Epicardial beating heart cryoablation using a novel argon-based cryoclamp and linear probe. *J Thorac Cardiovasc Surg* 2006;131:403–411.
29. Doenst T, Borger MA, Weisel RD, Yau TM, Maganti M, Rao V. Relation between aortic cross-clamp time and mortality—not as straightforward as expected. *Eur J Cardiothorac Surg* 2008;33:660–665.
30. Al-Sarraf N, Thalib L, Hughes A, Houlihan M, Tolan M, Young V, McGovern E. Cross-clamp time is an independent predictor of mortality and morbidity in low-and high-risk cardiac patients. *Int J Surg* 2011;9:104–109.



CHAPTER 8

Pulmonary Vein Stenosis after Catheter Ablation: Electroporation versus Radiofrequency

Vincent van Driel*

Kars Neven*

Harry van Wessel

Bastiaan du Pré

Aryan Vink

Pieter Doevendans

Fred Wittkampf

* Both authors contributed equally to the study and manuscript

Abstract

Background Radiofrequency ablation inside pulmonary vein (PV) ostia can cause PV stenosis. A novel alternative method of ablation is irreversible electroporation, but the long-term response of PVs to electroporation ablation is unknown.

Methods and Results In ten 6-month-old pigs (60–75 kg), the response of PVs to circular electroporation and radiofrequency ablation was compared. Ten consecutive, nonarcing, electroporation applications of 200 J were delivered 5 to 10 mm inside 1 of the 2 main PVs, using a custom-deflectable, 18-mm circular decapolar catheter. Inside the other PV, circular radiofrequency ablation was performed using 30 W radiofrequency applications via an irrigated 4-mm ablation catheter. PV angiograms were made before ablation, immediately after ablation, and after 3-month survival. PV diameters and heart size were measured. With electroporation ablation, PV ostial diameter decreased $11\pm 10\%$ directly after ablation, but had increased $19\pm 11\%$ after 3 months. With radiofrequency ablation, PV ostial diameter decreased $23\pm 15\%$ directly after ablation and remained $7\pm 17\%$ smaller after 3 months compared with preablation diameter despite a $21\pm 7\%$ increase in heart size during aging from 6 to 9 months.

Conclusions In this porcine model, multiple circumferential 200-J electroporation applications inside the PV ostia do not affect PV diameter at 3-month follow-up. Radiofrequency ablation inside PV ostia causes considerable PV stenosis directly after ablation, which persists after 3 months. (*Circ Arrhythm Electrophysiol.* 2014;7:734-738.)

Introduction

Circular electroporation ablation is a novel technique for pulmonary vein (PV) isolation. In a previous animal study, feasibility and safety of circular electroporation for the creation of PV lesions were investigated after a 3-week survival period. One to 4 sequential, nonarcing, electroporation applications of 200 J eliminated PV electrograms in most ostia.¹ However, the long-term risk of PV stenosis after electroporation ablation is still unknown.

The present animal study was performed to investigate the response of the PV to an excessive number of circular electroporation applications compared with circular radiofrequency ablation after a 3-month survival period.

Methods

All 10 porcine experiments were performed after prior approval from the Animal Experimentation Committee of the Utrecht University and in compliance with the *Guide for Care and Use of Laboratory Animals*.² Each animal (60–75 kg) was intubated and anesthetized according to standard procedures.¹

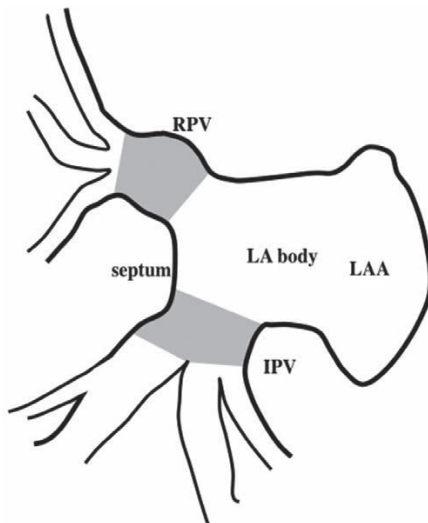


Figure 1. Simplified outline of the porcine left atrial (LA) anatomy (antero-posterior view). Because of their size, only the right pulmonary vein (RPV) and inferior PV (IPV) are eligible for catheter ablation and have been sketched. The PV tubular segments are marked in gray.

The porcine left atrium (LA) has 2 PVs suitable for circular catheter ablation: 1 right or septal PV (RPV) and 1 inferior PV (IPV; **Figure 1**). The RPV enters the LA in close proximity to the atrial septum and fossa ovalis. Before their entrance into the LA, multiple branches merge into a common RPV tubular segment of ≈ 10 to 15 mm in length. The IPV has ≈ 12 -mm-long tubular segment, and the RPV has ≈ 15 -mm-long tubular segment after the confluence of a septal and a lateral branch (**Figure 1**).

First, a coronary sinus catheter was inserted via the right jugular vein as fluoroscopic reference for transseptal access. A quadripolar catheter was inserted via the right jugular vein into the right ventricular apex for backup pacing. Transseptal puncture was performed through the right femoral vein. A deflectable 8F sheath (Agilis; St Jude Medical, Minnetonka, MN) facilitated LA catheterization. A temporary screw-in pacing wire (6416; Medtronic Inc, Minneapolis, MN) was inserted via the right femoral vein and fixated in the atrial septum to serve as positional reference for the NavX 3D Navigation system (St Jude Medical).

The LA geometry (including part of the PVs) was reconstructed using the NavX system and a standard deflectable quadripolar irrigated ablation catheter with a 4-mm distal electrode (Thermocool; Biosense Webster Inc, Diamond Bar, CA). Thereafter, angiography of both PVs was performed using the anteroposterior, 30° right anterior oblique, and 30° left anterior oblique projections for the IPV, and anteroposterior, 30° cranial, and 30° caudal projections for the RPV. After PV angiography, both PVs were alternately ablated using either electroporation or radiofrequency energy.

Electroporation Ablation

A custom-deflectable, 7F, 18 mm, circular decapolar electroporation catheter containing 2 mm ring electrodes separated by 4 mm spacing was introduced through the deflectable sheath in the right femoral vein (**Figure 2**). This catheter was deployed in the common tubular segment of 1 of the 2 PVs. Inside the PV, 10 cathodal 200-J shocks were delivered between all electrodes of the electroporation catheter and a large indifferent skin electrode (7506; Valley Laboratory Inc, Boulder, CO) on the shaven lower back. An external, monophasic defibrillator (Lifepak 9; Physio-Control Inc, Redmond, WA) was used for energy delivery.^{1,3,4} During each application, current and voltage waveforms were recorded on a dual channel oscilloscope (Tektronix TDS 2002B, Beaverton, OR). For each ablation, a different position of the electroporation catheter was chosen to cover the complete tubular segment. Ten applications of 200 J were always delivered even when

all PV electrograms had already been eliminated. All electroporation catheter positions were stored with the NavX system. After each application, the circular electroporation catheter was reconnected to the NavX and electrophysiological recording system (Cardiolab; General Electric Healthcare, Waukesha, WI) to check electrode integrity and to visualize the electrode positions on the NavX system.



Figure 2. The custom-deflectable, 7F, 18 mm, circular decapolar electroporation ablation catheter containing 2 mm ring electrodes separated by 4 mm spacing used in this study.

Radiofrequency Ablation

The other PV was circumferentially ablated approximately in the middle of the common tubular segment using sequential 30 W radiofrequency applications delivered via the 4-mm irrigated ablation catheter and a saline flow rate of 17 mL/min. Maximal electrode temperature was set at 42°C. Intentionally, maximal radiofrequency duration per vein was set at 15 minutes. PV isolation was not the objective or end point for electroporation or radiofrequency ablation.

PV angiography was performed directly after ablating both PVs using the same fluoroscopic settings as the preablation PV angiograms.

Follow-Up

All catheters were removed and the animals were allowed to recover and kept under daily surveillance. After a 3-month survival period, PV angiography was repeated in all animals using the same techniques as described above. Thereafter, the animals were euthanized by exsanguination.

Histological Investigation

After fixation, the common tubular segment of both PVs, from antrum to approximately the level of branching, was sliced in 3 circular, 4-mm-long segments and embedded in paraffin. Elastic van Gieson stained sections of the pulmonary side of each of those segments were scanned. Of each section, the percentage of the perimeter showing a myocardial sleeve was measured using ImageJ (National Institutes of Health). The ablated PVs were compared with control PVs from untreated animals.

Angiographic Analysis

Three investigators, blinded for the type of therapy, analyzed all PV angiograms. PV diameters were measured from the PV angiograms taken before ablation, directly after ablation, and at 3 months and in all 3 projections. When PV narrowing was obvious at 3 months, PV diameters were always measured at that location. When no narrowing was visible, all measurements were taken in the middle of the common tubular segment. All measurements were taken at the end-systolic phase (maximal PV filling and diameter). Diameters measured in the 3 projections were averaged to obtain 1 value for the PV diameter. The percent change in PV diameter was calculated relative to the preablation diameter.

As a measure of heart size, the largest transversal heart diameter was measured from the preablation and 3-month angiograms taken in the anteroposterior projection.

Statistical Analysis

Data are expressed in mean \pm SD or as mean (95% confidence interval). A *P* value of 0.05 was used as the level of statistical significance. Special software (SPSS Statistics 20; IBM Inc, Armonk, NY) was used for statistical analysis. A repeated-measures ANOVA of percentage change in diameter was performed to compare the radiofrequency and electroporation ablation measurements between the 3 independent and blinded investigators. The effect of ablation technology on the presence of a (part of the) myocardial sleeve in histological sections, corrected for depth of those sections, was investigated in a binary logistic mixed model. The growth in heart size between the acute and 3-month procedure was investigated with a paired *t* test.

Results

None of the electroporation applications resulted in catheter or electrode failure. All shocks resulted in smooth voltage and current waveforms, demonstrating the absence of arcing and barotrauma. The 3-month survival period was uneventful in all animals. Because of technical difficulties, IPV angiography postablation was not performed in 2 animals.

Average radiofrequency application time was 12.3 ± 5.9 minutes. In 2 IPVs (animal #2 and #4), >15 minutes of radiofrequency was necessary to complete the circle because of frequent catheter dislodgement.

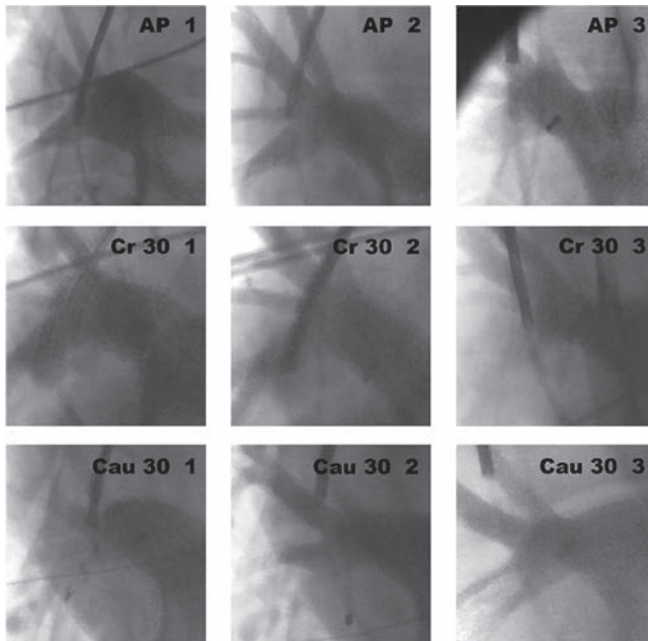


Figure 3. An example of angiograms of the right pulmonary vein (RPV) before (series 1) and after radiofrequency (RF) ablation (series 2 and 3). Angiography was performed using the antero-posterior (AP), 30° caudal (Cau 30), and 30° cranial (Cr 30) projections. Directly after RF ablation, RPV angiograms showed considerable decrease of ostial diameter in all 3 projections (series 2). After 3-mo follow-up, RPV angiography was repeated and still showed significant decrease of the ostial PV diameters (series 3).

Angiographic Analysis

Repeated-measures ANOVA showed no significant interaction between investigators and methods ($P=0.35$). With radiofrequency ablation, PV diameters decreased $23 \pm 15\%$ directly after ablation and remained $7 \pm 17\%$ smaller after

3 months, when compared with preablation diameters. An example of RPV diameter change after radiofrequency ablation is shown in **Figure 3**. Directly after electroporation ablation, PV diameters decreased $11\pm 10\%$, but had increased $19\pm 11\%$ after 3 months, when compared with preablation diameters (**Figure 4**). Repeated-measures ANOVA demonstrated a highly significant difference in long-term (3 months) response between radiofrequency and electroporation ablation (26%; $P=0.006$; 95% confidence interval, 9.54–42.01; **Table**). The acute change in PV diameter was not statistically analyzed.

During aging of animals from 6 to 9 months, the heart diameter, measured in the anterior-posterior projection, increased $21\pm 7\%$ ($P<0.001$; **Figure 4**).

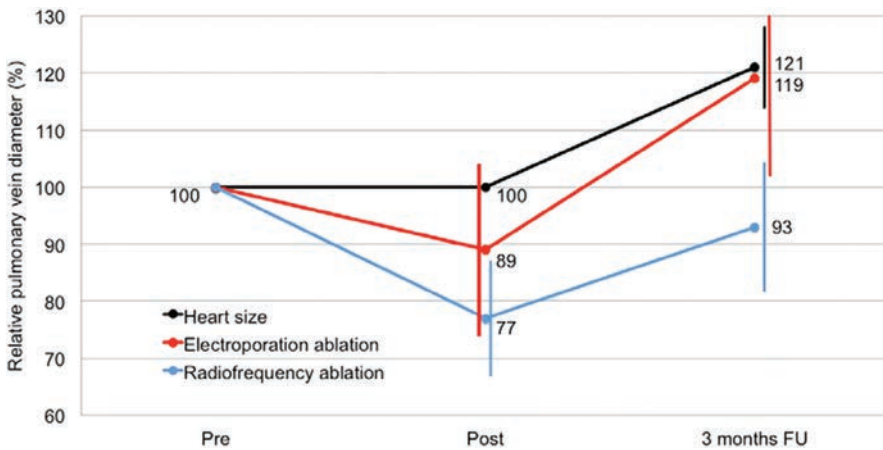


Figure 4. Graph showing the relative pulmonary vein (PV) diameter change directly after electroporation or radiofrequency ablation (post) and after 3-mo follow-up (FU). The preablation PV diameter and diameter of the heart served as baseline and were set as 100% (pre). The black line represents the mean growth in heart diameter for all 10 animals, measured in the anterior-posterior projection before ablation and at 3 mo. The vertical lines indicate the respective SDs.

Histological Analysis

Because of various reasons, unrelated to the degree of PV stenosis, 3 hearts were not available for histological analysis of PV sleeves. Of the remaining hearts, 1 IPV had accidentally been cut off during heart explantation. Consequently, only 7 RPVs and 6 IPVs could histologically be analyzed for the presence of a myocardial sleeve 3 months after ablation. In total, 37 of 39 histological sections made from these 13 PVs were eligible for analysis. Of these 13 PVs, 7 had been treated with radiofrequency and 6 with electroporation.

Table. Data of the 10 Animals

Animal	PV	Ablation Method	PV Diameter		
			Before, mm	3 mo, mm	Change, %
#1	RPV	RF	13.8	11.7	-15
	IPV	CE	24.9	33.0	+32
#2	RPV	CE	12.7	12.8	0
	IPV	RF	23.0	25.3	+10
#3	RPV	RF	16.3	11.9	-27
	IPV	CE	22.1	25.1	+13
#4	RPV	CE	13.3	16.0	+20
	IPV	RF	23.4	21.8	-7
#5	RPV	RF	16.4	10.7	-35
	IPV	CE	21.6	24.3	+13
#6	RPV	CE	15.8	20.6	+30
	IPV	RF	19.6	20.1	+3
#7	RPV	RF	16.8	17.9	+6
	IPV	CE	19.0	25.8	+36
#8	RPV	CE	16.7	18.2	+9
	IPV	RF	21.1	25.0	+19
#9	RPV	RF	17.5	13.2	-25
	IPV	CE	20.8	26.1	+26
#10	RPV	CE	13.8	14.5	+6
	IPV	RF	21.0	20.4	-3

Pulmonary vein (PV) diameters before ablation and after 3-mo survival were measured by angiography. The percentage change in diameter is listed. At 3 mo, the average change in PV diameter was $-7 \pm 17\%$ with radiofrequency (RF) ablation and $+19 \pm 11\%$ with circular electroporation (CE) ablation. IPV indicates inferior PV; and RPV, right PV.

The 3 control PVs from 2 untreated pigs revealed complete sleeve coverage and normal vessel wall of the vein (**Figure 5A** and **5B**). In the histological sections of the PVs treated with radiofrequency, scar tissue surrounded the PV (**Figure 5C**). In addition, intimal proliferation, necrotic myocardium, and proliferation of the elastic lamina were found (**Figure 5D**), comparable with previous findings of Taylor et al.⁵ Three months after ablation, the median sleeve coverage was 40%, 13%, and 0% at 4, 8, and 12 mm distance from the PV antrum, respectively.

Conversely, the PVs treated with IRE ablation are surrounded by healthy connective tissue. Apart from the ablated myocardial sleeve, only minor intimal hyperplasia was present, comparable with our findings with coronary arteries inside electroporation lesions.⁴ Median sleeve coverage in these PVs was 0% at all 3 depths. With radiofrequency, the myocardial sleeve was totally absent in 9 of 20 sections, whereas with electroporation, the myocardial sleeve was absent in 14 of 17 sections ($P=0.01$; odds ratio, 16.96; 95% confidence interval, 2.0–142.7).

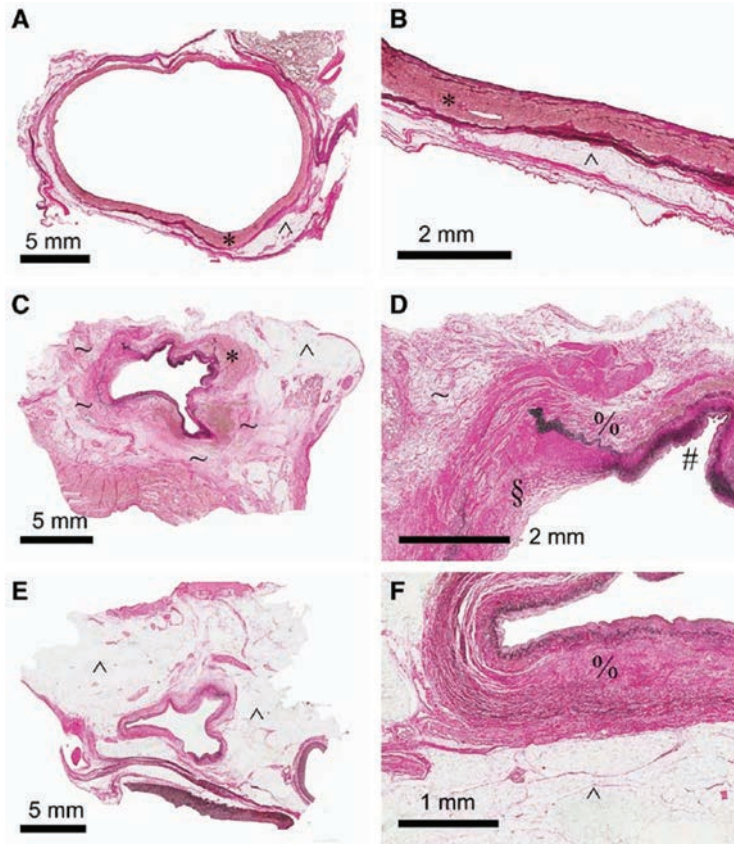


Figure 5. Elastic van Gieson stained sections of a control pulmonary vein (PV; **A** and **B**), a PV treated with radiofrequency (RF) ablation (**C** and **D**), and a PV treated with 10 circular electroporation applications (**E** and **F**). **B**, **D**, and **F**, Magnifications of **A**, **C**, and **E**, respectively. The control PV shows complete sleeve coverage and normal vessel wall. The PV treated with RF shows a partially undamaged myocardial sleeve, intimal proliferation, necrotic myocardium, and proliferation of the elastic lamina. In addition, the vein is surrounded by scar tissue. The PV treated with electroporation shows a completely ablated myocardial sleeve surrounded by healthy connective tissue. The differences in luminal area or shape of the pulmonary vein (PV) in **A** versus **C** and **E** is the result from minor differences in fixation technique. *Undamaged myocardial sleeve; ^healthy connective tissue; ≈scar tissue surrounding the PV; %ablated myocardial sleeve; §intimal hyperplasia; #proliferation of elastic lamina.

Discussion

In this porcine animal model, electroporation and radiofrequency ablation were purposely delivered inside the PVs to provoke stenosis. In the absence of previous porcine studies about PV stenosis or narrowing in response to radiofrequency ablation, we alternated circular radiofrequency and electroporation ablation

between the 2 suitable PVs, thereby using the animals as their own control. Despite a significant growth of the animals and heart size ($21\pm 7\%$) during aging from 6 to 9 months, PVs that had been ablated with radiofrequency reduced in diameter, whereas those ablated with electroporation grew in size ($-7\pm 17\%$ versus $+19\pm 11\%$; $P=0.006$).

Given the large myocardial lesions obtained with circular 200-J electroporation ablation in previous studies, histological analysis of the PVs was not part of the original study protocol.¹³ This analysis was later added to the protocol to be absolutely sure about the effectiveness of electroporation ablation. However, 3 hearts were no longer available. Data of the histological sections of 13 PVs from the remaining 7 hearts suggest that the absence of PV stenosis with electroporation ablation is not because of ineffective applications.

With focal trigger ablation and ostial PV isolation using radiofrequency energy in humans as originally described by Haïssaguerre et al,⁹ PV stenosis did occur in a relatively large number of patients ($\leq 27\%$).⁶⁻⁸ With segmental PV isolation, PV stenosis still did occur in $\approx 2\%$ of patients.¹⁰ Wide area circumferential ablation of the PV antrum has significantly reduced this incidence, but still is associated with a 0.4% risk of PV narrowing.¹¹

Results of the present study suggest that PV stenosis may not be an issue with circular electroporation ablation at the settings used in the present study, even when it is (accidentally) performed inside PVs.

Electric PV isolation was not the end point of our radiofrequency and electroporation applications. The shift from ostial to antral radiofrequency ablation has reduced the incidence of PV stenosis after PV isolation with radiofrequency energy.¹² This suggests that not PV isolation but the depth of the application inside the PV relates to the risk of PV stenosis.

PV stenosis is a well-known complication for thermal ablation.⁵⁻¹² With 10 circular 200-J applications inside the PVs, we tried hard to provoke such a response. Although difficult to compare, total energy delivered with electroporation was 2.000 J, whereas 10 minutes of radiofrequency at 30 W results in a total energy delivery of 18.000 J. With this in mind, our histological data suggest that electroporation is far more effective in ablating the myocardial sleeve.

The histological analysis of PVs treated with radiofrequency versus electroporation showed that radiofrequency-treated PV sections had more unaffected myocardial sleeve as compared with electroporation-ablated PV sections. This suggests that, at least, not more myocardial sleeve was ablated with radiofrequency than

with electroporation. Next, similar to the article of Taylor et al,⁵ we analyzed the presence of pathological changes associated with PV stenosis. We found that PVs treated with radiofrequency had intimal proliferation, necrotic myocardium, proliferation of the elastic lamina, and large amounts of scar tissue surrounding the myocardial sleeve, whereas electroporation-ablated PVs only showed minor intimal proliferation, comparable with our previous report.⁴

Despite the higher amount of successfully ablated myocardial sleeve, histological changes associated with PV stenosis seem to be less present in the electroporation-ablated PVs. These findings also correspond with our previous results,⁴ which showed that myocardial tissue is more prone to electroporation damage as compared with other structures, such as connective tissue. This demonstrates that scarring of connective tissue surrounding the PV is the explanation for PV stenosis after radiofrequency ablation.

Acute narrowing after radiofrequency application may relate to heat.¹³ Clinically, radiofrequency ablations will never or only rarely be performed inside the common tubular segment of PVs, and therefore, acute PV stenosis in humans may have only infrequently been reported.^{14,15} With electroporation ablation, holes in the cell membrane may cause acute depolarization and contraction as suggested by coronary spasm that we observed directly after epicardial applications on these arteries in other still unpublished studies. However, this resolved spontaneously <30 minutes.

Limitations

Differences in anatomy and architecture between human and porcine LAs and PVs are a serious limitation for this study. To the best of our knowledge, a porcine model has never been used to study the effects of ablation on PV diameter. Therefore, the animals were used as their own control by alternating electroporation and radiofrequency energy between the 2 PVs.

The fundamental cause of PV narrowing is still unknown, and therefore, one cannot be sure that a porcine model using young animals is valid for the elderly human population.

In this study, we used quantitative PV angiography to assess the degree of PV stenosis. Although quantitative PV angiography is a widespread and commonly used method to assess the degree of luminal stenosis, PV angiography using computed tomography may have been more accurate, but this technology was not available in our animal facility.

Conclusions

In this porcine model, multiple circular 200-J electroporation ablations inside PVs did not affect PV diameter at 3-month follow-up. Conversely, radiofrequency ablation inside PVs caused considerable PV stenosis, because of scarring of connective tissue surrounding the PV.

Acknowledgments

We thank the staff of the Department of Experimental Cardiology of the University Medical Center Utrecht for technical assistance during the experiments, and the Department of Biostatistics, Utrecht University, for statistical analyses.

Disclosures

F.H.M. Wittkampff is a consultant for St Jude Medical, Atrial Fibrillation division. Both F.H.M. Wittkampff and H. van Wessel are coinventors of circular electroporation. The other authors report no conflicts.

Clinical perspective

Despite the use of advanced 3-dimensional mapping systems, pulmonary vein (PV) stenosis remains one of the potential complications of PV isolation using radiofrequency ablation. Circular electroporation ablation is a novel technique for PV isolation. It has been proven that one 6-ms, 200-J electroporation application can isolate a PV. However, the long-term risk of PV stenosis after electroporation ablation is still unknown. In this porcine model, multiple circular 200-J electroporation ablations inside PVs did not affect PV diameter at 3-month follow-up. Conversely, radiofrequency ablation inside PVs caused considerable PV stenosis, because of scarring of connective tissue surrounding the PV. The clinical implementation of circular electroporation ablation as a novel, effective, and very fast technique for PV isolation could, therefore, be performed safely, without the risk of PV stenosis.

References

1. Wittkampfh FH, van Driel VJ, van Wessel H, Vink A, Hof IE, Gründeman PF, Hauer RN, Loh P. Feasibility of electroporation for the creation of pulmonary vein ostial lesions. *J Cardiovasc Electrophysiol*. 2011;22:302–309.
2. *Institute for Laboratory Animal Research: Guide for the Care and Use of Laboratory Animals*. 8th ed. Washington, DC: National Academies Press; 2011.
3. Wittkampfh FH, van Driel VJ, van Wessel H, Neven KG, Gründeman PF, Vink A, Loh P, Doevendans PA. Myocardial lesion depth with circular electroporation ablation. *Circ Arrhythm Electrophysiol*. 2012;5:581–586.
4. du Pré BC, van Driel VJ, van Wessel H, Loh P, Doevendans PA, Goldschmeding R, Wittkampfh FH, Vink A. Minimal coronary artery damage by myocardial electroporation ablation. *Europace*. 2013;15:144–149.
5. Taylor GW, Kay GN, Zheng X, Bishop S, Ideker RE. Pathological effects of extensive radiofrequency energy applications in the pulmonary veins in dogs. *Circulation*. 2000;101:1736–1742.
6. Arentz T, Weber R, Bürkle G, Herrera C, Blum T, Stockinger J, Minners J, Neumann FJ, Kalusche D. Small or large isolation areas around the pulmonary veins for the treatment of atrial fibrillation? Results from a prospective randomized study. *Circulation*. 2007;115:3057–3063.
7. Saad EB, Rossillo A, Saad CP, Martin DO, Bhargava M, Erciyas D, Bash D, Williams-Andrews M, Beheiry S, Marrouche NF, Adams J, Pisanò E, Fanelli R, Potenza D, Raviele A, Bonso A, Themistoclakis S, Brachmann J, Saliba WJ, Schweikert RA, Natale A. Pulmonary vein stenosis after radiofrequency ablation of atrial fibrillation: functional characterization, evolution, and influence of the ablation strategy. *Circulation*. 2003;108:3102–3107.
8. Yu WC, Hsu TL, Tai CT, Tsai CF, Hsieh MH, Lin WS, Lin YK, Tsao HM, Ding YA, Chang MS, Chen SA. Acquired pulmonary vein stenosis after radiofrequency catheter ablation of paroxysmal atrial fibrillation. *J Cardiovasc Electrophysiol*. 2001;12:887–892.
9. Haïssaguerre M, Jaïs P, Shah DC, Garrigue S, Takahashi A, Lavergne T, Hocini M, Peng JT, Roudaut R, Clémenty J. Electrophysiological end point for catheter ablation of atrial fibrillation initiated from multiple pulmonary venous foci. *Circulation*. 2000;101:1409–1417.
10. Pürerfellner H, Cihal R, Aichinger J, Martinek M, Nesser HJ. Pulmonary vein stenosis by ostial irrigated-tip ablation: incidence, time course, and prediction. *J Cardiovasc Electrophysiol*. 2003;14:158–164.
11. Gupta A, Perera T, Ganesan A, Sullivan T, Lau DH, Roberts-Thomson KC, Brooks AG, Sanders P. Complications of catheter ablation of atrial fibrillation: a systematic review. *Circ Arrhythm Electrophysiol*. 2013;6:1082–1088.
12. Holmes DR Jr, Monahan KH, Packer D. Pulmonary vein stenosis complicating ablation for atrial fibrillation: clinical spectrum and interventional considerations. *J Am Coll Cardiol Cardiovasc Interv*. 2009;2:267–276.
13. Kok LC, Everett TH IV, Akar JG, Haines DE. Effect of heating on pulmonary veins: how to avoid pulmonary vein stenosis. *J Cardiovasc Electrophysiol*. 2003;14:250–254.
14. Nilsson B, Chen X, Pehrson S, Jensen HL, Sondergaard L, Helvind M, Andersen LW, Svendsen JH. Acute fatal pulmonary vein occlusion after catheter ablation of atrial fibrillation. *J Interv Card Electrophysiol*. 2004;11:127–130.
15. Stavrakis S, Madden G, Pokharel D, Po SS, Nakagawa H, Jackman WM, Sivaram CA. Transesophageal echocardiographic assessment of pulmonary veins and left atrium in patients undergoing atrial fibrillation ablation. *Echocardiography*. 2011;28:775–781.



CHAPTER 9

Low Vulnerability of the Right Phrenic Nerve for Electroporation Ablation

Vincent van Driel
Kars Neven
Harry van Wessel
Aryan Vink
Peter Loh
Pieter Doevendans
Fred Wittkampf

* Both authors contributed equally to the study and manuscript

Abstract

Background Circular electroporation ablation is a novel ablation modality for electrical pulmonary vein isolation. With a single 200-J application, deep circular myocardial lesions can be created. However, the acute and chronic effects of this energy source on phrenic nerve (PN) function are unknown.

Objective The purpose of this study was to analyze nerve vulnerability to electroporation ablation in a porcine model.

Methods In 20 animals (60–75 kg), the course of the right PN was pace-mapped inside the superior caval vein (SCV). Thereafter, a single 200-J circular electroporation ablation was performed via a multipolar circular catheter in firm contact with the inner SCV wall.

Results In 19 of 20 animals, the PN could be captured along an estimated 6–8 cm trajectory above the right atrial contour. Directly after the application, the PN could be captured above the ablation level in 17 of 19 animals and after maximally 30 minutes in all animals. Fifteen animals were restudied after 3–13 weeks, and PN functionality was unaffected in all. Histological analysis in 5 animals in which the application had been delivered in the muscular sleeve just above the right atrium showed a transmural circular lesion. However, no lesion was found in the other animals in which the application had been delivered in the fibrous section more cranial in the SCV.

Conclusions Electroporation ablation at an energy level that may create deep myocardial lesions may spare the targeted right PN. These animal data suggest that electroporation may be a safe ablation modality near the right PN.

Abbreviations **L** = left; **PN** = phrenic nerve; **R** = right; **RA** = right atrium; **RF** = radiofrequency; **SCV** = superior caval vein

Introduction

Thermal catheter ablation may cause collateral damage to extracardiac structures. Various manifestations of phrenic nerve (PN) damage by radiofrequency (RF) energy and other energy sources have been described.¹⁻⁴

Circular electroporation ablation via a circular multi-electrode catheter is a novel, nonthermal ablation technique. A high-current density impulse of a few milliseconds creates microlesions in the cell membrane. The increased cellular permeability results in the disruption of cellular hemostasis and ultimately in cell death.^{5,6} Electroporation ablation has been shown to create sufficiently large and deep lesions for treatment of cardiac arrhythmias.⁷⁻⁹ Animal data even suggest that the application may safely be performed inside pulmonary vein ostia.¹⁰ With such applications, the risk of PN damage may be greater than that with RF or cryoablation, and this risk must be assessed before clinical implementation of electroporation ablation.

Other investigators have reported the survival of nerves in electroporation ablation.¹¹⁻¹³ We also previously found histologically intact epicardial autonomic nerves entirely surrounded by ablated myocardium in histological preparations of epicardially applied electroporation lesions (**Figure 1**).⁹ However, this is an anatomical observation and does not demonstrate nerve functionality.

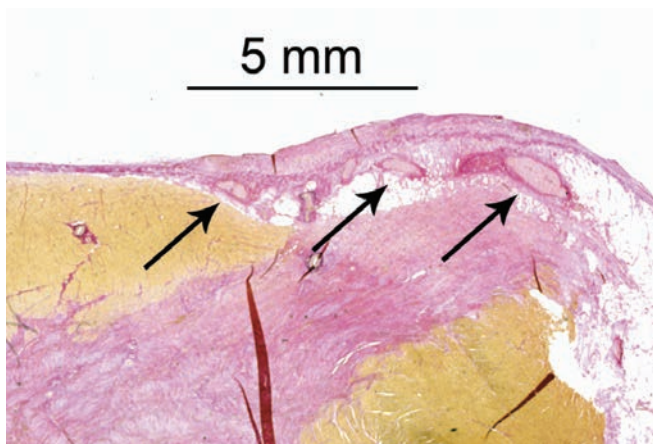


Figure 1. In a previous study of circular 200-J electroporation ablation on left ventricular epicardium, apparently intact epicardial nerves (arrows) were found in histological preparations.⁹ These nerves were totally surrounded by the electroporation lesion, which suggested that these nerves have a much lower susceptibility for electroporation ablation than that of surrounding myocardial tissue. Detail of Figure 4, reprinted with permission.⁹

In this study, the easily accessible and clinically relevant right PN was purposely targeted with electroporation ablation, using an energy level capable of creating approximately 7-mm deep lesions in myocardial tissue.⁹

Methods

This porcine study was performed in 20 animals (60–75 kg) after prior approval from the Animal Experimentation Committee of Utrecht University and is in compliance with the Guide for Care and Use of Laboratory Animals.¹⁴ All animals also participated in other acute or chronic studies. As a consequence, 4 animals underwent only the initial procedure; the remaining animals were allowed to recover and were restudied after 3–13 weeks of follow-up depending on the protocol of the major study.

Animal preparation

Each pig was intubated and anesthetized following standard procedures. According to the protocol of the main study, intravenous heparin was administered to maintain an activated clotting time of 250–300 seconds. Aspirin (loading dose 300 mg, maintenance dose 100 mg/d) and clopidogrel (loading dose 300 mg, maintenance dose 75 mg/d) were started 3 days before the first procedure and continued until euthanasia. Amiodarone was started 1 week before the first catheterization (600 mg/d) and continued on a 400 mg/d schedule for 2 weeks to prevent procedure-related arrhythmias. Where appropriate, nitroglycerin, metoprolol, or amiodarone were administered during the procedure. Arterial pressure and capnogram were continuously monitored throughout the procedure.

PN mapping and electroporation ablation

During the initial study in a first series of 10 animals, a standard deflectable mapping catheter with a 4-mm distal electrode (Biosense Webster, Diamond Bar, CA) was introduced through the right femoral vein. The course of the right PN along the SCV was pace-mapped using 5–10 mA, 1 millisecond stimuli. Successful stimulation sites were fluoroscopically documented (**Figure 2**). Thereafter, the mapping catheter was exchanged for a 20-mm diameter, octopolar, circular ablation catheter with 4-mm ring electrodes (St. Jude Medical, St. Paul, MN). The catheter was deployed approximately 4 cm superior to the upper fluoroscopic

contour of the right atrium in the anteroposterior projection, with the circular catheter section in the transversal plane, perpendicular to the longitudinal SCV axis (**Figure 3**).

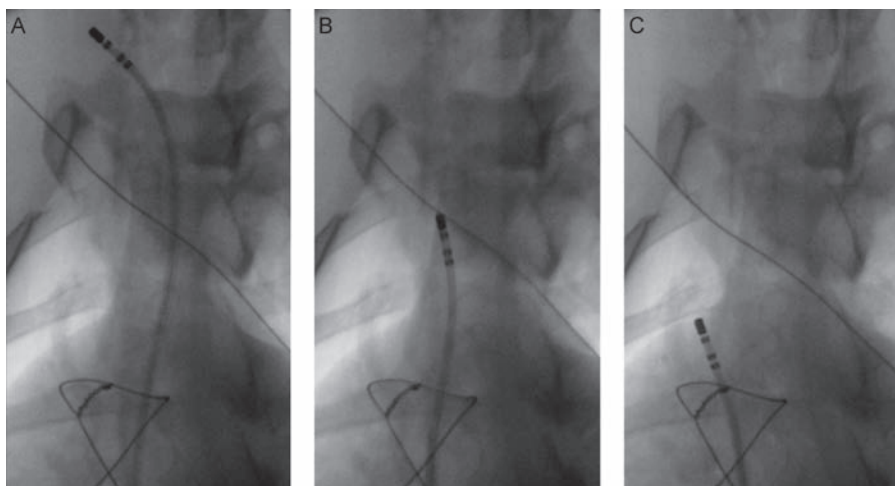


Figure 2. Phrenic nerve mapping in the superior caval vein (SCV) before euthanasia: **A:** in the superior part of the SCV, **B:** in the middle part of the SCV at the level of a 200-J circular electroporation application, 2–3 cm above the right atrium, and **C:** at the entrance of the SCV in the right atrium.

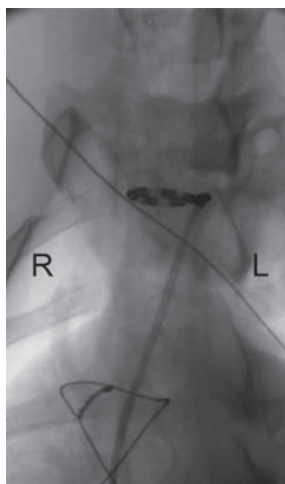


Figure 3. Fluoroscopic image of one of the circular electroporation ablation catheters inside the superior caval vein with its circular section in the transversal plane, immediately before a 200-J electroporation application. The distal 20-mm-diameter circular segment of the nondeflectable 7F catheter contains 8 electrodes, 4 mm in length and separated by 4-mm spacing. R = right; L = left.

In a second series of 5 animals that first underwent an open thorax procedure according to the original protocol in which the animals participated, a metal radiopaque clip was placed on the outside of the lateral SCV, cranial to the pericardial fold. Thereafter, the thorax was closed. After mapping the course of the right PN as in the first series, the mapping catheter was exchanged for a nondeflectable 7F, 18-mm diameter decapolar circular ablation catheter with 2-mm ring electrodes (St. Jude Medical, St. Paul, MN) that was placed as close as possible to the metal clip to facilitate histological investigation at the application site.

In a third series of 5 animals, the course of the PN was mapped using 2–5 mA, 1 millisecond bipolar stimuli via an 18-mm diameter decapolar circular ablation catheter with 2-mm ring electrodes (St. Jude Medical, St. Paul, MN). After pace-mapping, the same catheter was used for electroporation ablation at a more caudal level than in the first 2 series of animals, just above the presumed SCV entrance into the right atrium.

Electroporation ablation

Each electroporation ablation consisted of a single cathodal 200-J application via all electrodes of the circular catheter connected in parallel, using a custom connection cable. A large skin electrode (Valleylab 7506; Medtronic, Dublin, Ireland) on the shaven back served as an indifferent electrode. An external defibrillator (Lifepak 9; Physio-Control, Redmond, WA) was used for energy delivery. During the application, current and voltage waveforms of the application through all electrodes together were recorded on a dual-channel oscilloscope (Tektronix TDS 2002B, Beaverton, OR).

Directly after the application, pace-mapping of the PN, either with the standard deflectable catheter in the first 2 series of animals or via the circular ablation catheter in the third series of animals, was repeated. If the PN could not be captured cranial to the level of electroporation ablation, pace-mapping was repeated with 10 to 15 minutes intervals until the PN could be captured cranial to the level of electroporation ablation.

Follow-up

Directly after the initial study, 3 animals of the first series were euthanized according to the protocol of the original study in which the animals participated. All other animals, including those with transient block, were kept under daily surveillance for 3–13 weeks, according to the protocols of the original studies. During the final

procedure, PN integrity was reanalyzed either by pace-mapping cranial to the level of electroporation ablation or by fluoroscopic inspection of spontaneous diaphragmatic movements just before administration of general anesthesia and muscle relaxants. Thereafter, all animals were euthanized by exsanguination.

Anatomical relationships and dimensions

At autopsy, tissue around the SCV was visually inspected for damage, and the location and course of the pericardial fold was analyzed. Of all animals in long-term studies, an approximately 5-cm-long segment of the SCV including a small part of the upper right atrium was excised and fixed in formalin. For the first 2 series of animals, serial sections of the SCV were stained using hematoxylin–eosin and Elastica–van Gieson and studied histologically. In the third series of 5 animals, a circular lesion in the myocardial sleeve was macroscopically easily identifiable and the width of the lesion was measured.

Of 6 randomly selected SCVs, the thickness of the vessel wall was measured at 3–4 sites around the vessel in histological sections taken at 2–4 levels above the right atrium. The mean value of the average thicknesses in each section was taken as vessel-wall thickness and these values were averaged for the 6 vessels.

Results

Catheter mapping and electroporation ablation

In 1 animal of the second series, the PN could not be captured inside the SCV. In this animal, no ablation was performed inside the SCV, and this animal was excluded from the study. In the other 19 animals, the PN could be captured along a 4- to 6-cm trajectory inside the SCV above the right atrial contour (**Figure 1**).

While the circular ablation catheter was being positioned, it was always challenging to obtain the desired transverse position of the 18-mm or 20-mm catheter hoop inside the SCV, which suggested good tissue contact between the electrodes of the electroporation ablation catheter and the inner SCV wall (**Figure 3**).

All 19 circular electroporation applications resulted in smooth voltage and current waveforms, suggesting the absence of arcing and barotrauma.¹⁵ The average peak magnitudes of the applications were 2116 ± 152 V and 33.0 ± 3.6 A, respectively. Directly after the application, 2–5 mA stimuli cranial to the electroporation ablation level resulted in diaphragmatic contractions in 17 of 19 animals. In 2 animals (of

the first and third series of animals), stimulation directly after the application did not result in diaphragmatic contractions but within 30 minutes after the application again caused diaphragmatic contractions.

Follow-up

Follow-up was uneventful in all animals. During the second procedure, the PN was completely intact in all animals: when pace-mapping of the PN was attempted, it could always be captured successfully cranial to the electroporation ablation level with a stimulus amplitude below 6 mA (stimulus duration of 1 millisecond). Alternatively, spontaneous symmetric diaphragmatic movements just before administration of general anesthesia also proved normal PN functionality.

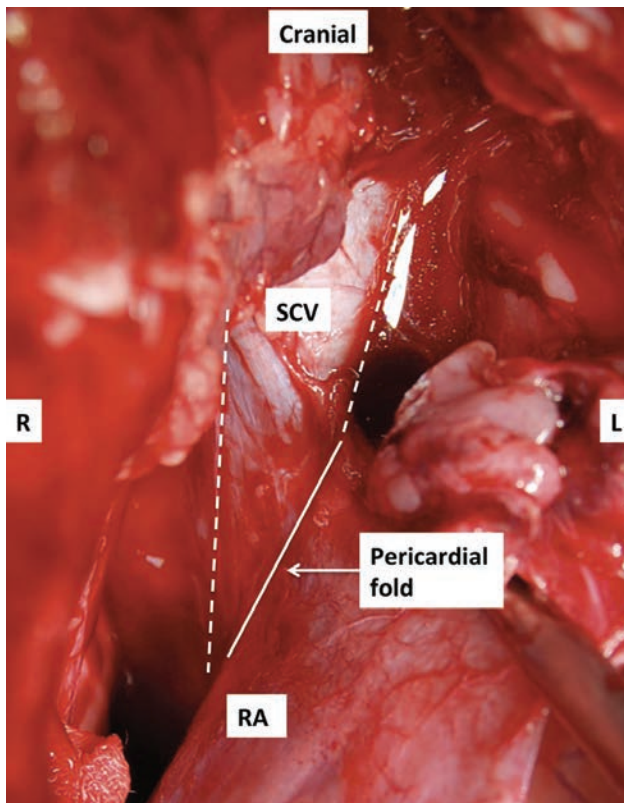


Figure 4. Photograph taken at autopsy, showing the most caudal part of the superior caval vein (SCV), above the pericardial sac, and its orientation relative to the pericardial fold and right atrium (RA). The fold runs in an oblique direction relative to the SCV from superomedial to inferolateral. The right phrenic nerve (not visible) runs down along the lateral side of the SCV until the pericardial fold, where it separates from the SCV and continues caudally over the pericardium. R = right; L = left.

Postmortem findings

Gross examination of the electroporation ablation area and circumjacent tissue after euthanasia revealed no collateral damage.

In all animals, the most cranial level of adherence between pericardium and SCV (pericardial fold) is located on the left (medial) side of the SCV. From there, the fold runs obliquely and caudally toward the right (lateral) side of the SCV (**Figure 4**). At the lateral side, where the PN had routinely been found by pace-mapping, the level of the fold ranged between 0 and 1 cm above the most cranial location of SCV entrance into the right atrium (located on the anteromedial side of the SCV, near the entrance to the right atrial appendage). Clearly, the level where the electroporation ablation hoop had intersected with the PN in the first 2 series of animals, was located several centimeters cranial to the pericardial fold, thus at a level where the PN is not separated from the outer SCV wall by pericardial tissue. Cranial to the fold, the PN was found to adhere to an extremely thin and transparent tissue membrane situated against, but not connected to the outer SCV wall.

SCV wall thickness

The average thickness of the SCV wall, measured in histological sections of 6 randomly selected vessels, was 1.4 ± 0.2 mm.

Lesion identification

In the first 2 series of animals in which the electroporation ablation had been performed relatively high above the right atrium, the atrial side of the SCV had an apparently normal 3- to 4-cm-long pink myocardial sleeve, clearly visible from the outside of the vein. Cranial to that sleeve, the SCV was white and no electroporation ablation lesion could be identified macroscopically. Also in serial histological SCV sections, no lesion could be identified, neither in the muscular sleeve, nor in the fibrous section above it. Even in the animals in which the application site had been marked with a surgical clip, no lesion could be identified in the vessel wall. Several small and apparently intact nerves were found in histological SCV sections, but none of them was thick enough to represent the right PN. Moreover, the porcine right PN is not adhered to the outer SCV wall. Inclusion of the PN in histological SCV sections was therefore unlikely.

In the third series of 5 animals, a circular transmural lesion was macroscopically easily identifiable from the outside of the vein in all animals. In 4 of 5 animals, this lesion was a whitish, semitransparent, thinner-walled circular band with an intact

myocardial sleeve cranial and caudal to this band (**Figure 5**). In 1 animal, this lesion band was located at the cranial end of the sleeve; the residual myocardial sleeve in this animal was 1–2 cm shorter than in the other 4 animals. This finding suggested that in this animal the electroporation ablation had been performed in the cranial end of the sleeve.

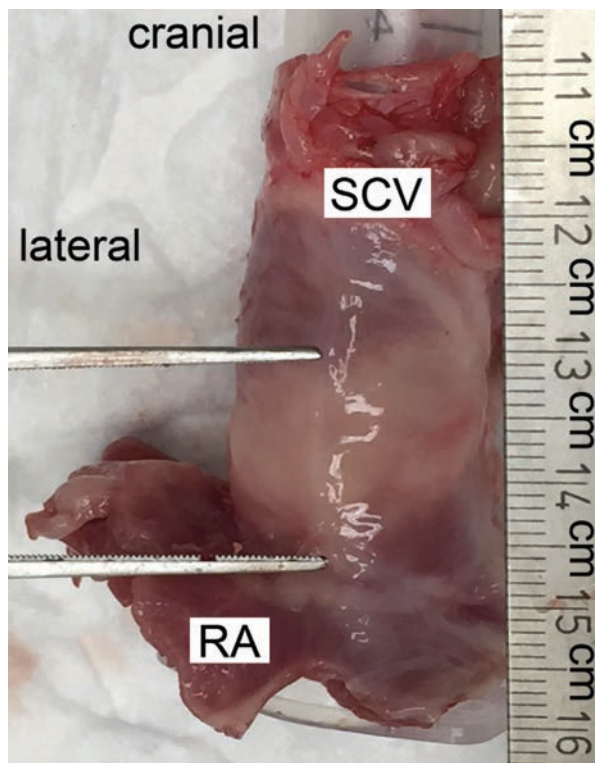


Figure 5. Image of an approximately 4-cm-long fresh section of the superior caval vein (SCV) entering into the right atrium (RA). Two months earlier, a circular 200-J application had been delivered inside the SCV just cranial to its entrance into the RA inside the myocardial sleeve. In this animal from the third series, the transmural fibrous lesion band (between the legs of a pair of tweezers) is clearly visible between intact sleeve sections cranial and caudal to the lesion. The ruler is in centimeters.

Lesion size

In the last 5 animals in the third series, the transparent and thinner-walled nature of the lesion band facilitated the macroscopic measurement of lesion width. The cranial–caudal width of the lesion was measured at 4 sides around the SCV: anterior, posterior, and at the lateral and medial side (**Table 1**).

Table 1. Lesion width within the wall of the superior caval vein

Animal	Anterior (mm)	Lateral (mm)	Posterior (mm)	Medial (mm)
1	22	6	10	22
2	21	5	12	20
3	18	4	15	20
4	10	8	10	10
5	12	7	5	16

Width of 5 lesions (from 5 animals of the third series) in the muscular section of the superior caval venous wall, just cranial to its entrance into the right atrium. Lesion width was measured in the cranial–caudal direction. Two months earlier, a single, circular 200-J application had been delivered via an 18- or 20-mm decapolar circular catheter with 2-mm electrodes. Lesions were always transmural around the circumference of the vein, with a venous wall thickness of approximately 1 mm.

Discussion

In order to examine the effects of electroporation ablation on nerves, the functional integrity of the right PN was evaluated before and after a circular 200-J cathodal application inside the SCV. The energy level of 200 J was chosen to ensure the absence of arcing and because of its capability to create approximately 7-mm-deep circular myocardial lesions in a blood-tissue environment.⁹

Circular electroporation ablation using 200-J applications inside the SCV was regarded as a worst-case scenario for human circular electroporation ablation in or near the right superior pulmonary vein. Like that in humans, the porcine right PN runs down the lateral side along the outer SCV wall until it reaches the pericardial fold, from where it separates from the SCV to continue caudally over the pericardium.

In the course of this investigation, 3 different protocols were used, for good reasons. The closest distance between the right PN and a catheter electrode inside the SCV would be expected to be found cranial to the pericardial fold. In the first series, the application was therefore delivered fairly high inside the SCV. Histologically, no lesion could be identified, and therefore a metal clip was used in the second series to mark the application site. Despite the presence of this marker, however, still no lesion could be identified in the fibrous wall of the SCV. The combination of intact PN function after electroporation ablation and the absence of identifiable lesions raised doubts about whether the application inside the SCV had any effect at all. To prove that the circular 200-J application inside the SCV indeed is sufficient for

lesion formation, the application was delivered inside the myocardial sleeve of the SCV in the last 5 animals in the third series, and lesions were found.

In all 3 studies, the course of the right PN was mapped before the application to ensure that the application was delivered as close as possible to the right PN. Mapping was performed at a fairly low pacing output of 2–5 mA to ensure close proximity to the right PN. With the plane of the circular electroporation hoop perpendicular to the cranial–caudal course of the right PN and continuous and deep circular lesions as demonstrated in previous studies, the application definitively is capable of reaching the right PN. It therefore is highly remarkable that no effect on the functionality of the right PN was observed in 17 animals and only a transient effect in 2 of 19 animals. This finding suggests that electroporation ablation in close proximity to the right PN is relatively safe.

Lesion size

Lesion width, measurable in only the last 5 animals, varied between 4 and 22 mm. The smallest width was always found at the lateral side of the SCV, in the same region where the PN was found during pace-mapping. Also, the widths at the posterior side of the SCV were smaller than the widths at the medial and anterior sides of the SCV. Possibly this consistent finding may be explained by the fact that the lateral and posterior sides of the SCV are surrounded by air-containing pulmonary tissue with a higher-than-average tissue impedance. In contrast, the medial and anterior sides of the SCV are surrounded by compact tissue that contains no air.¹⁵ As a consequence, the electroporation current may then favor the medial and anterior sides of the SCV over the lateral and posterior sides, thus creating larger (wider) electroporation ablation lesions medially and anteriorly.

With RF ablation, tissue impedance is important in only a very thin tissue layer around the ablation electrode, where resistive heating takes place. Surrounding tissue is heated only by the transfer of heat out of this central zone, and this latter process is not affected by the electrical tissue impedance. As a consequence, an RF lesion may reach and damage the right PN despite the presence of pulmonary tissue.

Previous studies have demonstrated that electroporation ablation may be performed without causing thermal lesions.^{7,16} The delivery of 20 J per electrode (200 J total) is equivalent to the energy of 7 seconds of 30-W RF ablation. It is unlikely that this energy causes tissue temperature rise to above 50°C, but even then the lesion formed would still be very shallow, much smaller than the observed lesion

depth of approximately 7 mm.⁹ Tissue cells are then affected only by the electrical current flowing through their membranes, and tissue impedance in the target area determines current density around the ablation electrode.

Nerve tissue vulnerability to electroporation ablation

A high electrical current induces a voltage gradient in the target tissue, which is mainly absorbed by the cell membranes because of their higher electrical resistance. This event may result in membrane electroporation and cell death. It is highly remarkable that the right PN was only transiently affected in 2 of 19 animals, despite an electroporation application capable of creating approximately 7-mm deep myocardial lesions. This observation is in line with the observed survival of epicardial nerves in our previous study (**Figure 1**) and with the preservation of nerve tissue in other electroporation studies.^{9,11-13} Alas, a plausible explanation for this phenomenon is not readily available. Nerve regeneration does not account for the recovery of PN functionality within 30 minutes. Electrical isolation of the nerve by a myelin sheath cannot explain this finding because such isolation would also prevent low-output electrical nerve stimulation (pace-mapping) via a catheter inside the SCV. Possibly, nerves may survive because their cell membrane is damaged over only a relatively short section compared with their total cell length, while the cell membrane of much smaller cardiac myocytes is damaged to a much larger extent or even in total. In this study, the transmural lesion in the myocardial sleeve was smallest near the right PN, presumably because of the presence of nearby pulmonary tissue. The absence of permanent right PN damage in this study may thus be related to both a relative low vulnerability of nerves and the protective effect of nearby pulmonary tissue.

In 2 of 19 animals, the right PN was transiently affected for 30 minutes. It is very well possible that the stiff circumferential ablation catheter, which was wedged in very close proximity to the PN into the SCV, could have mechanically and transiently paralyzed the PN because of the strong skeletal muscle contractions after energy delivery. This phenomenon of “bumping” is similar in mechanism to catheter-induced, transient right bundle branch block accidentally occurring during mapping of the His-bundle region. An alternative explanation could be that such a transient effect may have been caused by reversible electroporation that occurs at energy levels below the permanent ablation threshold.¹⁷ From these experiments, it is impossible to determine the safety margin between the magnitude of the circular application at 200 J and the level at which permanent

damage to the PN would have occurred. Therefore, more experimental studies will have to be conducted to estimate the risk of PN damage in a clinical situation. In addition, PN function should closely be monitored in future human application of this ablation technology.

Nerve injury with catheter ablation

PN damage due to thermal ablation is an infrequent and often transient complication.¹⁻⁴ However, PN palsy is often highly symptomatic, and recovery may take months, if it occurs at all. The observed preservation of right PN function and findings in other studies are encouraging as to the potential risk of periesophageal nerve damage after electroporation ablation in the left atrium, but the effects of electroporation ablation on esophageal tissue have to be investigated in a separate study.^{9,11-13,18,19}

Limitations

Electroporation ablations in this study were performed using 2 different circular electroporation ablation catheters: an 18-mm-diameter decapolar catheter with 2-mm electrodes (n =10) and a 20-mm-diameter octopolar catheter with 4-mm electrodes (n=9). Our previous study, in which 7- to 8-mm-deep lesions were found using 200-J electroporation ablation energy, was performed using a device that mimicked a 20-mm-diameter circular decapolar catheter with 2-mm electrodes.⁹ In that same study, lesion depth had been compared with 100-J electroporation ablations delivered via the 20-mm-diameter decapolar device with 2-mm electrodes and a 20-mm-diameter all-metal circular device. No difference in lesion depth was found between the 2 types of devices. Therefore, a significant difference in lesion depth between an octopolar and decapolar circular catheter and an effect of electrode size are highly unlikely.

Mapping of the PN in the first 2 series of animals was performed with the distal 4-mm electrode of a regular deflectable mapping/ablation catheter using 5–10 mA stimuli, whereas 2–5 mA stimuli were used for mapping with the circular electroporation catheter in the third series. This lower current magnitude in the last series was chosen because of the smaller electrode size: 2 mm vs 4 mm. Mapping per animal was used only to verify that the right PN indeed was running along the SCV. With the plane of the ablation hoop perpendicular to that course, the circular electroporation application would then always cross the right PN.

Electrical isolation of the SCV in response to the circular electroporation ablation was not investigated. In the first and second series (14/19 animals), the electroporation ablation presumably was delivered too cranially to result in electrical isolation. The third series was regarded too small to yield valuable SCV electrical isolation data.

At the end of follow-up, PN integrity was analyzed, preferably with fluoroscopic inspection of spontaneous diaphragmatic movements just before administration of general anesthesia. However, analysis by pace-mapping had to be performed when, due to various reasons, immediate application of general anesthesia after arrival of the animal in the catheterization laboratory was necessary. In these cases, fluoroscopic inspection of spontaneous diaphragmatic movements was impossible.

Conclusion

Data from this experimental study suggest that circular electroporation ablation, at an energy level that may create deep myocardial lesions, may spare the targeted right PN, even when the current is applied within a distance of 1–2 mm. The absence of any detectable lesion in the fibrous section of the SCV wall, cranial to the myocardial sleeve, suggests that connective tissue is not affected by the high electrical current density used for electroporation ablation.

Acknowledgments

The authors wish to thank Dr. Tycho van der Spoel and Dr. Steven Chamuleau for allowing participation in their animal studies, and the staff of the Department of Experimental Cardiology for technical assistance during the experiments.

Clinical perspectives

With thermal ablation using radiofrequency, laser, or cryothermal energy, the right phrenic nerve (PN) may be damaged when the application is delivered in or at the ostium of the right upper pulmonary vein or inside the SCV. High-current

density electroporation is a single-shot, nonthermal ablation technology capable of creating relatively deep myocardial lesions. Data from this study suggest that this technology may spare the PN, even when applied in good contact with the inner wall of the SCV, in close proximity to the right PN. This finding suggests that the same technology may be relatively safe when applied near to or inside the ostium of the right superior pulmonary vein and SCV. Analysis of animal data of course only is a first step in the evaluation of the response of PNs to irreversible electroporation. Whenever this technique is applied in humans, this response to the electroporation ablation should be closely monitored and compared with that of thermal ablation methods.

References

1. Sacher F, Monahan KH, Thomas SP, et al. Phrenic nerve injury after atrial fibrillation catheter ablation: characterization and outcome in a multicenter study. *J Am Coll Cardiol* 2006;47:2498–2503.
2. Sanchez-Quintana D, Cabrera JA, Climent V, Farre J, Weiglein A, Ho SY. How close are the phrenic nerves to cardiac structures? Implications for cardiac interventionalists. *J Cardiovasc Electrophysiol* 2005;16:309–313.
3. Bai R, Patel D, Di Biase L, et al. Phrenic nerve injury after catheter ablation: should we worry about this complication? *J Cardiovasc Electrophysiol* 2006;17:944–948.
4. Kuck KH, Furnkranz A. Cryoballoon ablation of atrial fibrillation. *J Cardiovasc Electrophysiol* 2010;21:1427–1431.
5. Teissie J, Golzio M, Rols MP. Mechanisms of cell membrane electroporation: a minireview of our present (lack of?) knowledge. *Biochim Biophys Acta* 2005;1724:270–280.
6. Lee RC, Zhang D, Hannig J. Biophysical injury mechanisms in electrical shock trauma. *Annu Rev Biomed Eng* 2000;2:477–509.
7. Lavee J, Onik G, Mikus P, Rubinsky B. A novel nonthermal energy source for surgical epicardial atrial ablation: irreversible electroporation. *Heart Surg Forum* 2007;10:E162–E167.
8. Wittkampf FH, van Driel VJ, van Wessel H, Vink A, Hof IE, Grundeman PF, Hauer RN, Loh P. Feasibility of electroporation for the creation of pulmonary vein ostial lesions. *J Cardiovasc Electrophysiol* 2011;22:302–309.
9. Wittkampf FH, van Driel VJ, van Wessel H, Neven KG, Grundeman PF, Vink A, Loh P, Doevendans PA. Myocardial lesion depth with circular electroporation ablation. *Circ Arrhythm Electrophysiol* 2012;5:581–586.
10. van Driel VJ, Neven KG, van Wessel H, du Pre BC, Vink A, Doevendans PA, Wittkampf FH. Pulmonary vein stenosis after catheter ablation: electroporation versus radiofrequency. *Circ Arrhythm Electrophysiol* 2014;7:734–738.
11. Onik G, Mikus P, Rubinsky B. Irreversible electroporation: implications for prostate ablation. *Technol Cancer Res Treat* 2007;6:295–300.
12. Li W, Fan Q, Ji Z, Qiu X, Li Z. The effects of irreversible electroporation (IRE) on nerves. *PLoS One* 2011;6:e18831.
13. Schoellnast H, Monette S, Ezell PC, Deodhar A, Maybody M, Erinjeri JP, Stubblefield MD, Single GW Jr, Hamilton WC Jr, Solomon SB. Acute and subacute effects of irreversible electroporation on nerves: experimental study in a pig model. *Radiology* 2011;260:421–427.
14. Institute for Laboratory Animal Research. *Guide for the Care and Use of Laboratory Animals*, In: 8th ed. Washington, DC: National Academies Press; 2011.
15. Wang D, Hulse JE, Walsh EP, Saul JP. Factors influencing impedance during radiofrequency ablation in humans. *Chin Med J (Engl)* 1995;108:450–455.
16. Hong J, Stewart MT, Cheek DS, Francischelli DE, Kirchhof N. Cardiac ablation via electroporation. *Conf Proc IEEE Eng Med Biol Soc* 2009:3381–3384.
17. Irreversible Electroporation. In: Rubinsky B, ed. *Series in Biomedical Engineering*. Heidelberg: Springer; 2010.
18. Neven K, Schmidt B, Metzner A, Otomo K, Nuyens D, De Potter T, Chun KR, Ouyang F, Kuck KH. Fatal end of a safety algorithm for pulmonary vein isolation with use of high-intensity focused ultrasound. *Circ Arrhythm Electrophysiol* 2010;3:260–265.
19. Yokoyama K, Nakagawa H, Seres KA, Jung E, Merino J, Zou Y, Ikeda A, Pitha JV, Lazzara R, Jackman WM. Canine model of esophageal injury and atriaesophageal fistula after applications of forward-firing high-intensity focused ultrasound and side-firing unfocused ultrasound in the left atrium and inside the pulmonary vein. *Circ Arrhythm Electrophysiol* 2009;2:41–49.



CHAPTER 10

Time Course of Myocardial Electroporation Lesion

Vincent van Driel
Kars Neven
Bastiaan du Pré
Aryan Vink
Harry van Wessel
Rutger Hassink
Pieter Doevendans
Fred Wittkampf

* Both authors contributed equally to the study and manuscript

submitted

Abstract

Introduction Electroporation ablation enables creation of deep and wide myocardial lesions. No data are available on time course and characteristics of lesion formation yet.

Methods For the acute phase of myocardial lesion development (< 60 minutes), 7 pigs were used. With a linear suction device a single applications of 200 joule was delivered at 4 different epicardial right ventricular sites in each pig, thus yielding a total of $4 \times 7 = 28$ lesions. The timing of the applications was designed to yield lesions at 7 time-points, i.e. 0, 10, 20, 30, 40, 50 and 60 minutes, with 4 lesions per time-point. After euthanization, lesion characteristics were histologically explored. For the chronic phase, we used tissue samples from previously conducted studies taken at 3 weeks and 3 months after electroporation ablation

Results Myocardial lesions resemble a necrosis pattern with interstitial edema and contraction band formation, immediately present after electroporation ablation. No further histological changes occurred in the next hour. Just in 3 weeks the lesion consisted of loose connective tissue. Hemorrhage and inflammatory cells were hardly present during lesion development. Although there is a clear demarcation between lesion and normal myocardium, the borderzone is characterized by connective tissue strands of which the etiology is incompletely understood.

Conclusion There were no marked histological changes in the first hour and in the period between 3 weeks and 3 months after electroporation ablation. This finding is highly relevant for potential clinical application of electroporation ablation in terms of the electrophysiological endpoint and observation period after catheter ablation.

Introduction

Electroporation ablation is a highly promising ablation modality for catheter ablation in patients with cardiac arrhythmias. In our previous animal studies large myocardial lesions could be created safely.¹⁻⁵ However, the time course and characteristics of lesion formation, highly relevant for the electrophysiological endpoint and observation period after catheter ablation, has not been studied yet. The purpose of the present study is to investigate development of myocardial lesions during the first 60 minutes after epicardial electroporation ablation, after 3 weeks and 3 months follow-up.

Methods

All pigs in the present study were used in other (main) studies, performed after prior approval from the Animal Experimentation Committee of Utrecht University, and in compliance with the *Guide for Care and Use of Laboratory Animals*. Electroporation lesions that were analyzed for the present study were either created directly before scheduled euthanasia (acute phase) or collected as part of the treatment protocol (chronic phase).

Creation and collection of lesion samples

Lesions obtained ≤ 60 minutes after ablation have been created especially for the present study 0, 10, 20, 30, 40, 50 and 60 minutes before euthanasia. After medial sternotomy, epicardial ablation was performed with a custom made linear suction device (SD) which has been used in a previous study.² After opening the chest the SD was positioned on the right ventricle (RV), perpendicularly to the left anterior descending artery (LAD). Coronary arteries were not targeted. A single cathodal application of 200 joules (J) was delivered at 4 different non-overlapping sites between the RV base and RV apex. In each of the 7 pigs, energy was delivered at 4 different time points in accordance with a predefined tight time schedule comprising fixed time intervals of 10 minutes in the 60 minutes before euthanasia. For every 10 minute time point a set of 4 epicardial lesions was obtained. For investigation of myocardial lesion development in the chronic phase, lesion samples were selected from our collection of samples taken 3 weeks and 3 months after electroporation ablation.^{1-4,6} These lesions had been created on the

left ventricle epicardially, either with a circular multi-electrode catheter under at least 1 cm blood, inside the pericardial space using a 12 mm diameter circular catheter, or using a linear SD. In total the following samples were available: 4 Lesion samples taken 0, 10, 20, 30, 40, 50 and 60 minutes after ablation (28); 30 lesion samples 3 weeks after ablation; 30 lesion samples 3 months after ablation.

Energy delivery

The ablation energy was generated with a monophasic external defibrillator (Lifepak 9, Physio-Control, Inc, Redmond, WA). A large skin patch (7506, Valleylab Inc, Boulder, CO) on the lower back of the animal served as an indifferent electrode. All lesions <60 minutes had been created using a single 200 Joule (J) application. The other lesions had been created with single applications ranging between 30 and 200 J. Voltage and current waveforms of all applications were recorded as previously described.^{4,5}

Histological evaluation

All animals were euthanized by exsanguination. The heart was removed en bloc, the area with ablation lesions was excised integrally and lesions were separated and fixated in formalin. After fixation, 3-4 mm thick segments were taken. All paraffin-embedded segments were sectioned and stained with Hematoxylin-eosin (HE) and/or Elastic-van Gieson (EvG).

Results

Inspection of all lesions

Visual inspection of the ablation area and the electrodes directly after the energy application never revealed any perforation, blood clots or charring. The SD did cause some local epicardial 'hickey like' hematoma due to bursting of superficial tiny epicardial blood vessels (**Figure 1**).

After every energy application, a light purplish colorization around the bruised area was visible. In addition, in contrast to the adjacent unaffected myocardium, the ablated area did not contract. A sharp zone between lesion and undamaged myocardium could be observed as a cross section of the lesion was taken (**Figure 2**).

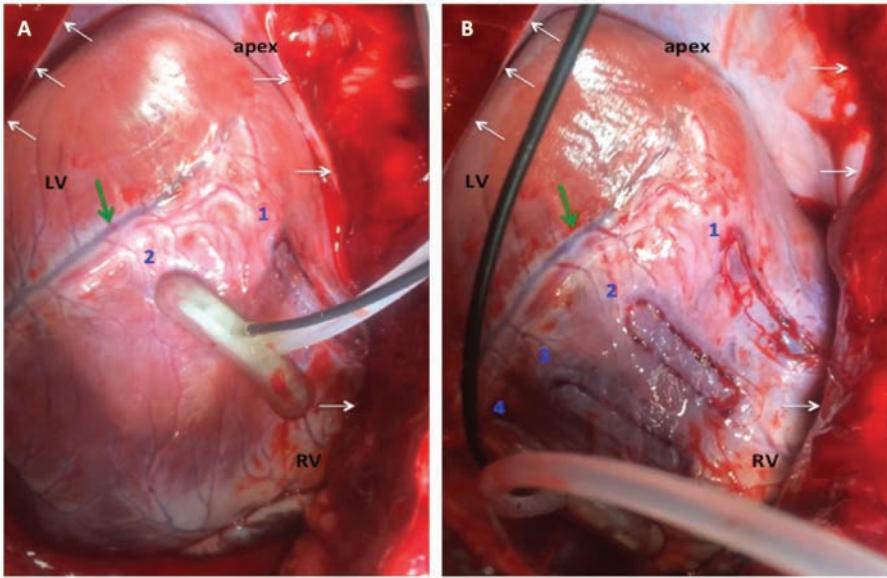


Figure 1. Electroperoration ablation of the right ventricular free wall: Using a custom made suction device (SD) a single cathodal application of 200 joules was delivered at 4 sites of the right ventricle between base and apex, perpendicularly and just aside from the left anterior descending coronary artery (green arrow). *Figure 1A* shows the suction device brought into position for the second energy application; the first energy application was delivered 10 minutes earlier, more apically. *Figure 1B* displays the situation preceding the 4th energy application from a slightly different angle; 3 energy applications were delivered 50, 40 and 20 minutes earlier respectively. The ablated myocardium is greyish colored and sunken in the fenced vital right ventricle. A linear hematoma at previous ablation sites, due to pressure of the edges of the SD, can be identified. *RV* = right ventricle; *LV* = left ventricle; *green arrow* = left anterior descending artery; *white arrows* = edges of the pericardium; 1, 2, 3, 4 (in blue) = site of the 1th, 2th, 3th and 4th application

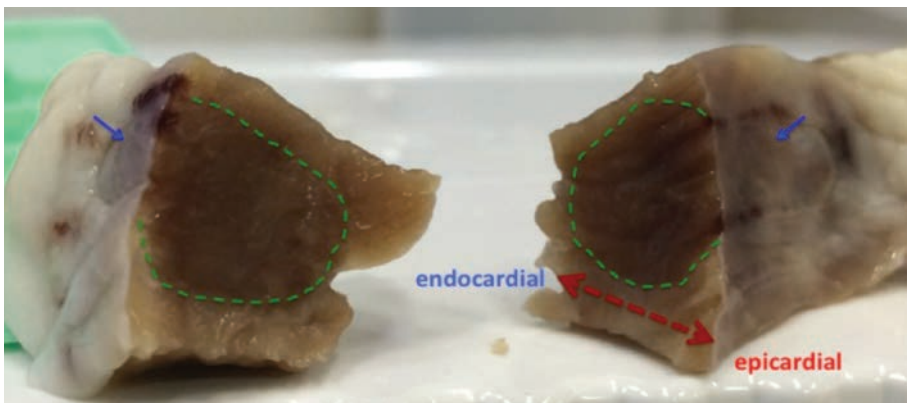


Figure 2. Cross-section of the lesion in the right ventricular free wall, created with a single application of 200 joules, using a custom made suction device (SD). A sharp borderzone between lesion and normal myocardium can be observed. *blue arrows* = lesion at the pericardial sites; *dashed green lines* = demarcation of the lesion

Acute phase lesion histology (< 60 minutes)

Lesions were readily identified from normal myocardium. In comparison with control myocardium, all sections with ablated myocardium showed interstitial edema, recognizable as empty space between cardiomyocytes and also contraction band formation (**Figure 3A-D**). Other well-known characteristics of acute myocardial necrosis, such as nuclear condensation, cardiomyocyte swelling, inflammatory cells and hemorrhage were hardly present. The histological features were present from the very beginning without change over 1 hour. Adverse mechanical side-effects, such as myocardial rupture, were not noticed.

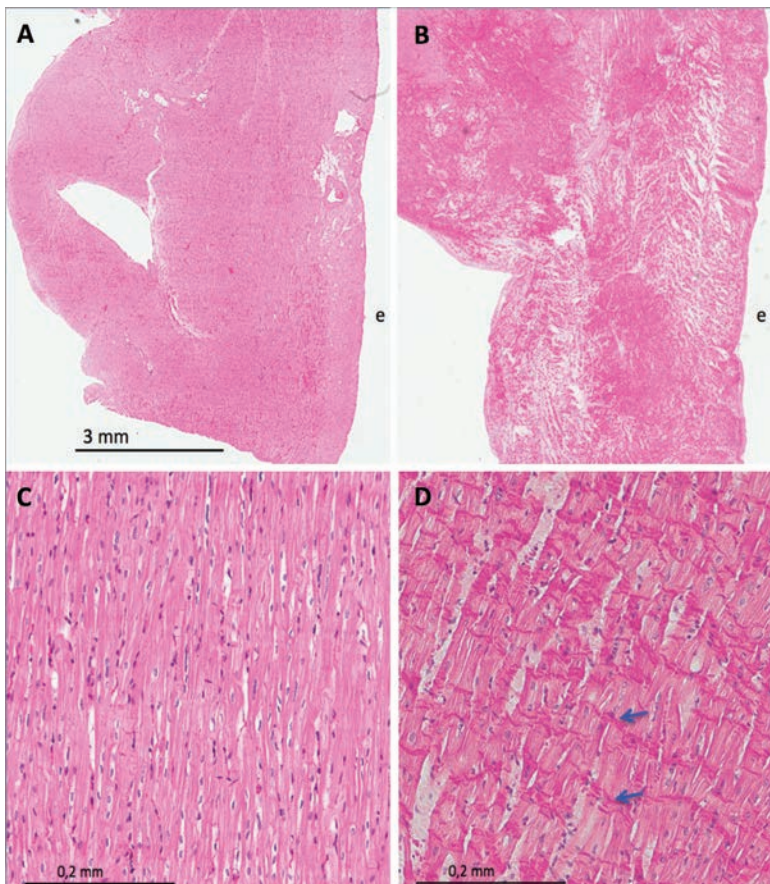


Figure 3. Hematoxylin-Eosin (HE) stain of normal myocardium of the right ventricle (A) in comparison to a section 40 minutes after a 200 J electroporation ablation using a suction device. Interstitial edema, recognizable as confluent spaces between cardiomyocytes, is present through the entire wall (B). In comparison to the unaffected myocardium (in detail) in panel C, the ablated myocardium (D) shows contraction band formation (eosinophilic staining cross bands reflecting cardiomyocyte hypercontraction). *e* = epicardial side; blue arrow in D indicate contraction bands

The ablated myocardium was well demarcated from the unaffected myocardium. However, extensions containing contraction bands (eosinophilic staining cross bands reflecting cardiomyocyte hypercontraction), envisaged an irregular borderzone between lesion and unaffected myocardium. (**Figure 4**)

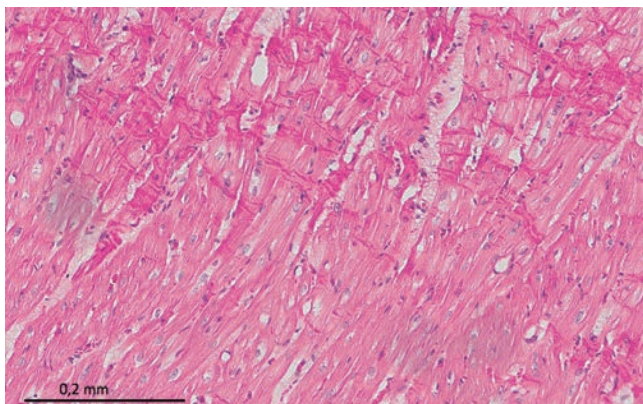


Figure 4. Hematoxylin-Eosin (HE) stain of ablated myocardium by a 200 J electroporation ablation using a suction device in detail, showing an irregular transition of the lesion (myocytes with contraction bands, above) to the undamaged myocardium (on the bottom side).

Chronic phase lesion histology

Lesions were clearly distinguishable from normal myocardium. Lesions after 3 weeks consist of loose connective tissue, in the EvG-staining pale colored red (**Figure 5**). In the lesions after 3 months, connective tissue production has increased (intensely red colored). At the borderzone irregular extensions of connective tissue penetrating the normal myocardium were frequently found. Again, hemorrhage and inflammatory cells were almost absent. As has been noted in previous electroporation studies, coronary arteries, veins and nerves were preserved.^{1, 3-5, 7, 8} (**Figure 6A-D**) Different energy settings did not affect lesion characteristics. Except for a more distinct connective tissue deposition, lesions after 3 months are similar as lesions after 3 weeks.



Figure 5. Histological analysis of myocardial tissue after electroporation ablation. Elastic–van Gieson (EvG) showing the cardiomyocytes yellow, connective tissue red, and elastica fibers black. Section of the right ventricular wall, 3 months after a 30 J electroporation ablation using a suction device. The lesion consists of loose connective tissue and is well demarcated (pink) from the undamaged myocardium (yellow). A sharp borderzone between lesion and normal myocardium (x) alternates with irregular borderzones due to connective tissue strands reaching from the lesion far into vital myocardium (black arrow). Connective tissue strands can sometimes be observed in the undamaged myocardium without connection to the lesion (white arrows). *In figure: c = coronary artery; e = epicardial site; v = vein; x = sharp demarcation zone between myocardial lesion and myocardium; black arrows = connective tissue strand in connection with the lesion; white arrows = connective tissue strand surrounded by undamaged myocardium*

Discussion

Major findings

This is the first study to investigate and compare the acute and chronic effects of epicardial electroporation ablation in a porcine model. Just as in previous studies, thermal damage was not noticed and all energy applications were delivered without arcing.^{1-5,7} Acute lesions were mainly characterized by interstitial edema and contraction band formation, whereas tissue structural integrity was preserved and myocardial lesions did not evolve histologically over the course of 1 hour. We did not find nuclear condensation, cardiomyocyte swelling, inflammatory cells and hemorrhage as previously found after high-energy DC ablation. Our findings indicate that electroporation, while providing single-shot transmural lesions, does not share the adverse barotrauma or thermal effects of high energy DC ablation.

Electrical pulses and lesion formation

Electroporation ablation provides tissue ablation without thermal damage and has been widely used for the treatment of malignant tumors.⁹⁻²² Cell death is established by injury of the cell membrane due to a high voltage gradient, consequently leading to the loss of cell hemostasis and necrosis. Protein denaturation (as in necrosis with radiofrequency (RF) energy) does not occur, connective tissue is not damaged and blood flow acting as a heat sink does not impact efficacy of lesion formation. According to current insights, cell death might also be caused by apoptosis (programmed cell death due to DNA damage), even in the absence of plasma membrane injury, with lower energies.

Histological examination of myocardial lesions caused by electrical pulses

Data regarding development of myocardial lesions due to electrical pulses are mainly obtained from animal studies from the distant past, using *high-energy* Direct Current (DC) pulses accompanied with arcing and barotrauma. Acute myocardial lesions were characterised by hemorrhage, interstitial edema and cardiomyocyte alterations such as dehiscence of intercalated disks, granulation of cytoplasm, mitochondrial swelling, pyknosis (condensation of chromatin in the nucleus) and contraction band formation.^{23,24} These characteristics resemble a necrosis pattern as in lethally injured cells undergoing reperfusion in which a massive influx of calcium into injured cells induces hypercontraction and disruption of myocytes. A few days after the high-energy DC pulse contraction bands and extensive disruption of myocardial fibers in conjunction with hemorrhage were found in lesions.^{25,26} A mix of granulation tissue and fibrosis was found after a few weeks, pure fibrosis with nearly inflammatory cell infiltration was found after a few months.²⁷⁻³²

Only two older studies report on lesion formation due to *low-energy* (non-arcing) DC ablation, however, not immediately after energy delivery but after 2-7 days.^{33,34} These authors found that *low-energy* DC and *high-energy* DC created equal amounts of necrosis and similar lesion characteristics, supporting the hypothesis that electroporation is the main lesion mechanism rather than thermal effects and barotrauma.³³

Lavee et al reported the first study in which contemporary IRE (multiple electrical pulses per energy application) was used for cardiac ablation. After 24 hours, a clear demarcation between the epicardially ablated area and unaffected atrial tissue was observed; all lesions were transmural, measuring a mean depth of 0.9 cm.⁹ In the other study, Hong et al reported on histological features of myocardial lesions

one hour after epicardial IRE: again demarcated lesions were observed, displaying contraction band formation and cardiomyocyte swelling surrounded by interstitial edema and hemorrhage.³⁵

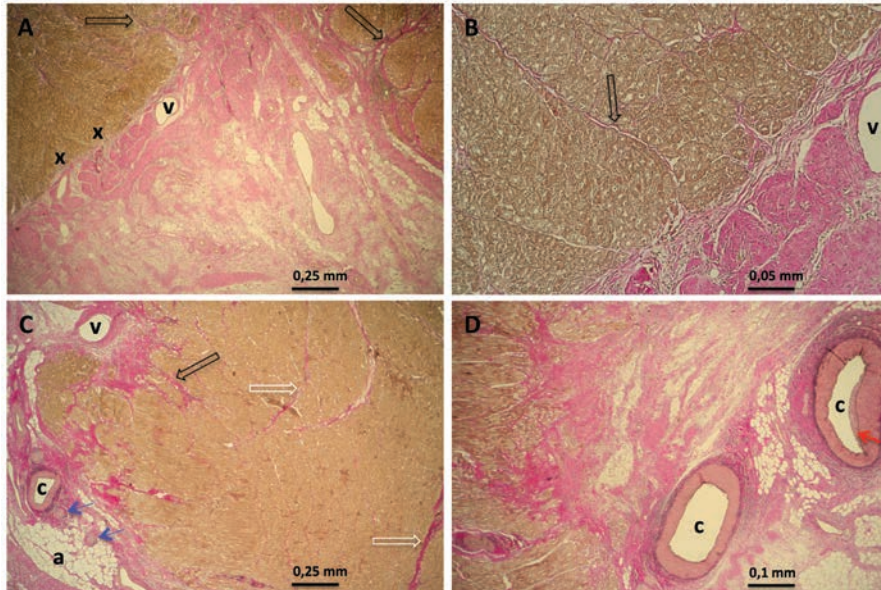


Figure 6. Elastic–van Gieson (EvG) showing in different magnifications a section of the right ventricular wall, 3 months after a 30 J electroporation ablation using a suction device. The lesion consists of loose connective tissue and is well demarcated from normal myocardium. **Panel A:** An apparently sharp borderzone between lesion and undamaged myocardium (x) alternates with irregular borderzones due to strands of connective tissue (black arrow) reaching far into the undamaged myocardium. **Panel B:** More in detail, also the apparently sharp borderzone exhibits small connective tissue strands. **Panel C:** In the lesion the architecture of fatty tissue (a), a coronary artery (c), a vein (v) and the nerves (blue arrow) is preserved. Connective tissue strands are also found in the undamaged myocardium, completely surrounded by unaffected myocardial fibers. **Panel D:** Two examples of large coronary arteries in an electroporation lesion; one with intimal hyperplasia on the right (red arrow) and one without intimal hyperplasia on the left. *In figure: a = adipose tissue, c = coronary artery; e = epicardial site; v = vein; x = sharp demarcation zone between myocardial lesion and myocardium; black arrows = connective tissue strand in connection with the lesion; white arrows = connective tissue strand in vital myocardium; blue arrows = nerve; red arrow = intima hyperplasia.*

In our study myocardial lesions were visible immediately. However, histologically a sharp border between ablated and unaffected myocardium was not always found, neither in acute nor chronic lesions. Irregular penetrating extensions disturbing the borderzone may represent pre-existing strands of connective tissue as they can also be detected in the non-ablated myocardium. **(Figure 5, 6)** On the other hand, concentration of these strands is clearly higher at the border zone and may also be caused by electroporation ablation.

Generally, smaller cell sizes require stronger electrical pulses and larger cell diameters require lower energies for successful electroporation ablation. So, the impact of an electrical pulse on myocardial cells will depend on the direction of these long and small myocardial cells with respect to the direction of the electrical field. Probably the mutable influence of an electrical pulse on myocardial cells running in variable directions in the layered myocardial wall, may account for the extensions of connective tissue at the borderzone of the lesion. Perhaps the use of an unipolar ablation technique with small electrodes in our studies instead of a bipolar approach with larger clamp electrodes directing more accurately the energy may contribute to our different finding. Whether these irregular zones with connective tissue strands are arrhythmogenic is unknown. In our earlier porcine electroporation studies we did not find proarrhythmic effects. In pursuing creation of transmural lesions the importance of this phenomenon appears questionable.

Considerations of efficacy for electroporation ablation

Understanding early myocardial lesion development might also be relevant to assess the necessity of multiple electroporation ablations and supplementary “touch up” ablations in pursuing a favorable outcome. The key questions are whether the current endpoint of abolishing of local electrical conduction is enough, or do we have to wait for potential recovery, and if so, how long? Endpoints for current thermal ablation in patients include complete pulmonary vein (PV) isolation in atrial fibrillation cases, and non-inducibility in ventricular tachycardia cases.

RF ablation causes necrosis by heating the tissue. However, hyperthermia may also induce reversible membrane depolarization and transient loss of cellular excitability. In many centers the ablation outcome is observed for at least 30 minutes in order to identify insufficiently treated sites. Administration of adenosine has become a crucial part in the evaluation of thermal PV ablation, because residual concealed PV conduction can be unmasked by hyperpolarizing the RF-induced depolarized PV cardiomyocytes.³⁶⁻⁴⁰

No further histological development of the lesion in the first hour since the electroporation ablation could imply that the electrophysiological evaluation can be performed immediately after ablation. There seems no need to wait and reconfirm electrophysiological endpoints after half an hour. Whether adenosine may unmask concealed PV-connections after electroporation ablation remains to be determined.

Apparently no further development of the lesion occurs after 3 weeks, except for a more intensive formation of connective tissue. In conjunction with the absence of hemorrhage and inflammatory cell infiltration at every stage of lesion development, the disappearance of interstitial edema after 3 weeks and the nonthermal character with regard to clot formation, subsequent redo ablation procedures might be safely scheduled already at 3 to 4 weeks.

Limitations

We investigated only the 200 J setting for acute lesions. This energy setting was commonly used in our previous studies, proven to be safe and to provide a 15-17 mm wide transmural lesion. So, we have no information on acute myocardial lesion development when using higher or lower energy settings.

In this study, the SD was placed on the right ventricular epicardium. The RV free wall is fairly regular, easy accessible and sufficiently large, allowing multiple electroporation pulses side by side, according to a strict timetable. After all, lesion size was not investigated in this study. Although we might expect a similar outcome, we do not have information about development of myocardial lesions in the thinner atrial wall.

We investigated only the first 60 minutes after electroporation ablation, considering a longer observation is not feasible in clinical practice.

Development of lesion characteristics and lesion size between 60 minutes and 3 weeks was not addressed in the present study. In our first feasibility study electrogram attenuation in the area proximal to the ablated PV ostium partly recovered in 3 weeks.⁵ In early high-energy DC studies the volume of tissue injury decreased significantly after 30 days. So, lesion size may decrease over time.

Whether decrease of lesion size was caused by recovery of reversibly electroporated tissue or shrinkage of successfully ablated tissue was unclear.⁴¹ Related to the strength of the electrical pulse across target tissue (voltage gradient) and tissue characteristics the cell membrane is either reversibly electroporated and restores in time or is irreversibly electroporated and induces cell death. In fact, areas of irreversible electroporation are always surrounded by an outer reversible electroporation zone. Other studies will be needed to explore the development of myocardial lesion size in detail.

Probably, due to the negative pressure, the SD itself contributes to myocardial lesion formation. Although we noticed small linear hematomas at ablation sites due to pressure of the edges, this is unlikely, because in our previous study using the SD, only 3 mm deep lesions were created with 30 J.

Conclusion

Immediately after electroporation ablation myocardial lesions are visible by inspection and histologically. Key features are interstitial edema and contraction band formation. Hemorrhage and inflammatory cells as abundantly seen after high energy DC, are almost absent at every stage of lesion development.

There is no histological change in the first 60 minutes after electroporation ablation. Likewise, there is only minimal histological development in the period between 3 weeks and 3 months. This may have profound implications for the upcoming clinical application of electroporation ablation, in particular with regard to the electrophysiological endpoint immediately after ablation and scheduling a repeat procedure.

References

1. du Pre BC, van Driel VJ, van Wessel H, Loh P, Doevendans PA, Goldschmeding R, Wittkamp F, Vink A. Minimal coronary artery damage by myocardial electroporation ablation. *Europace : European pacing, arrhythmias, and cardiac electrophysiology : journal of the working groups on cardiac pacing, arrhythmias, and cardiac cellular electrophysiology of the European Society of Cardiology*. 2013;15:144-149
2. Neven K, van Driel V, van Wessel H, van Es R, Doevendans PA, Wittkamp F. Epicardial linear electroporation ablation and lesion size. *Heart rhythm : the official journal of the Heart Rhythm Society*. 2014;11:1465-1470
3. Neven K, van Driel V, van Wessel H, van Es R, du Pre B, Doevendans PA, Wittkamp F. Safety and feasibility of closed chest epicardial catheter ablation using electroporation. *Circulation. Arrhythmia and electrophysiology*. 2014
4. Wittkamp F, van Driel V, van Wessel H, Neven K, Grundeman P, Vink A, Loh P, Doevendans PA. Myocardial lesion depth with circular electroporation ablation. *Circulation. Arrhythmia and electrophysiology*. 2012;5:581-586
5. Wittkamp F, van Driel V, van Wessel H, Vink A, Hof IE, Grundeman P, Hauer RN, Loh P. Feasibility of electroporation for the creation of pulmonary vein ostial lesions. *Journal of cardiovascular electrophysiology*. 2011;22:302-309
6. Neven K, van Driel V, van Wessel H, van Es R, Doevendans PA, Wittkamp F. Myocardial lesion size after epicardial electroporation catheter ablation after subxiphoid puncture. *Circulation. Arrhythmia and electrophysiology*. 2014;7:728-733
7. van Driel V, Neven K, van Wessel H, du Pre BC, Vink A, Doevendans PA, Wittkamp F. Pulmonary vein stenosis after catheter ablation: Electroporation versus radiofrequency. *Circulation. Arrhythmia and electrophysiology*. 2014;7:734-738
8. van Driel V, Neven K, van Wessel H, Vink A, Doevendans PA, Wittkamp F. Low vulnerability of the right phrenic nerve to electroporation ablation. *Heart rhythm : the official journal of the Heart Rhythm Society*. 2015;12:1838-1844
9. Lavee J, Onik G, Mikus P, Rubinsky B. A novel nonthermal energy source for surgical epicardial atrial ablation: Irreversible electroporation. *The heart surgery forum*. 2007;10:E162-167
10. Rubinsky B, Onik G, Mikus P. Irreversible electroporation: A new ablation modality--clinical implications. *Technology in cancer research & treatment*. 2007;6:37-48
11. Rubinsky J, Onik G, Mikus P, Rubinsky B. Optimal parameters for the destruction of prostate cancer using irreversible electroporation. *The Journal of urology*. 2008;180:2668-2674
12. Onik G, Mikus P, Rubinsky B. Irreversible electroporation: Implications for prostate ablation. *Technology in cancer research & treatment*. 2007;6:295-300
13. Xiao D, Yao C, Liu H, Li C, Cheng J, Guo F, Tang L. Irreversible electroporation and apoptosis in human liver cancer cells induced by nanosecond electric pulses. *Bioelectromagnetics*. 2013;34:512-520
14. Guo Y, Zhang Y, Klein R, Nijm GM, Sahakian AV, Omary RA, Yang GY, Larson AC. Irreversible electroporation therapy in the liver: Longitudinal efficacy studies in a rat model of hepatocellular carcinoma. *Cancer research*. 2010;70:1555-1563
15. Neal RE, 2nd, Davalos RV. The feasibility of irreversible electroporation for the treatment of breast cancer and other heterogeneous systems. *Ann Biomed Eng*. 2009;37:2615-2625
16. Neal RE, 2nd, Singh R, Hatcher HC, Kock ND, Torti SV, Davalos RV. Treatment of breast cancer through the application of irreversible electroporation using a novel minimally invasive single needle electrode. *Breast cancer research and treatment*. 2010;123:295-301
17. Pech M, Janitzky A, Wendler JJ, Strang C, Blaschke S, Dudeck O, Rieke J, Liehr UB. Irreversible electroporation of renal cell carcinoma: A first-in-man phase I clinical study. *Cardiovascular and interventional radiology*. 2011;34:132-138
18. Garcia PA, Pancotto T, Rossmeis JH, Jr., Henao-Guerrero N, Gustafson NR, Daniel GB, Robertson JL, Ellis TL, Davalos RV. Non-thermal irreversible electroporation (n-tire) and adjuvant fractionated radiotherapeutic multimodal therapy for intracranial malignant glioma in a canine patient. *Technology in cancer research & treatment*. 2011;10:73-83

19. Rossmeisl JH, Jr, Garcia PA, Roberston JL, Ellis TL, Davalos RV. Pathology of non-thermal irreversible electroporation (n-tire)-induced ablation of the canine brain. *Journal of veterinary science*. 2013;14:433-440
20. Ellis TL, Garcia PA, Rossmeisl JH, Jr, Henao-Guerrero N, Robertson J, Davalos RV. Nonthermal irreversible electroporation for intracranial surgical applications. Laboratory investigation. *Journal of neurosurgery*. 2011;114:681-688
21. Garcia PA, Rossmeisl JH, Jr, Neal RE, 2nd, Ellis TL, Olson JD, Henao-Guerrero N, Robertson J, Davalos RV. Intracranial nonthermal irreversible electroporation: In vivo analysis. *The Journal of membrane biology*. 2010;236:127-136
22. Davalos RV, Mir LM, Rubinsky B. Tissue ablation with irreversible electroporation. *Annals of Biomedical Engineering*. 2005;33:223-231
23. Basso C, Thiene G. The pathophysiology of myocardial reperfusion: A pathologist's perspective. *Heart*. 2006;92:1559-1562
24. Doherty PW, McLaughlin PR, Billingham M, Kernoff R, Goris ML, Harrison DC. Cardiac damage produced by direct current countershock applied to the heart. *The American journal of cardiology*. 1979;43:225-232
25. Lerman BB, Weiss JL, Bulkley BH, Becker LC, Weisfeldt ML. Myocardial injury and induction of arrhythmia by direct current shock delivered via endocardial catheters in dogs. *Circulation*. 1984;69:1006-1012
26. Lee BI, Gottdiener JS, Fletcher RD, Rodriguez ER, Ferrans VJ. Transcatheter ablation: Comparison between laser photoablation and electrode shock ablation in the dog. *Circulation*. 1985;71:579-586
27. Brodman R, Fisher JD. Evaluation of a catheter technique for ablation of accessory pathways near the coronary sinus using a canine model. *Circulation*. 1983;67:923-929
28. Gonzalez R, Scheinman M, Margaretten W, Rubinstein M. Closed-chest electrode-catheter technique for his bundle ablation in dogs. *The American journal of physiology*. 1981;241:H283-287
29. Bardy GH, Ideker RE, Kasell J, Worley SJ, Smith WM, German LD, Gallagher JJ. Transvenous ablation of the atrioventricular conduction system in dogs: Electrophysiologic and histologic observations. *The American journal of cardiology*. 1983;51:1775-1782
30. Huang SK, Graham AR, Lee MA, Ring ME, Gorman GD, Schiffman R. Comparison of catheter ablation using radiofrequency versus direct current energy: Biophysical, electrophysiologic and pathologic observations. *Journal of the American College of Cardiology*. 1991;18:1091-1097
31. Coltorti F, Bardy GH, Reichenbach D, Greene HL, Thomas R, Breazeale DG, Alferness C, Ivey TD. Catheter-mediated electrical ablation of the posterior septum via the coronary sinus: Electrophysiologic and histologic observations in dogs. *Circulation*. 1985;72:612-622
32. Ward DE, Davies M. Transvenous high energy shock for ablating atrioventricular conduction in man. Observations on the histological effects. *British heart journal*. 1984;51:175-178
33. Lemery R, Leung TK, Lavallee E, Girard A, Talajic M, Roy D, Montpetit M. In vitro and in vivo effects within the coronary sinus of nonarcing and arcing shocks using a new system of low-energy dc ablation. *Circulation*. 1991;83:279-293
34. Moroe K, Hiroki T, Okabe M, Sasaki Y, Fukuda K, Arakawa K. A transarterial approach of electrical ablation of atrioventricular junction in a dog model: Comparison of the effects between high and low energy shocks. *Pacing and clinical electrophysiology : PACE*. 1989;12:1474-1484
35. Hong J, Stewart MT, Cheek DS, Francischelli DE, Kirchhof N. Cardiac ablation via electroporation. *Conference proceedings : ... Annual International Conference of the IEEE Engineering in Medicine and Biology Society. IEEE Engineering in Medicine and Biology Society. Annual Conference*. 2009;2009:3381-3384
36. Kobori A, Shizuta S, Inoue K, Kaitani K, Morimoto T, Nakazawa Y, Ozawa T, Kurotobi T, Morishima I, Miura F, Watanabe T, Masuda M, Naito M, Fujimoto H, Nishida T, Furukawa Y, Shirayama T, Tanaka M, Okajima K, Yao T, Egami Y, Satomi K, Noda T, Miyamoto K, Haruna T, Kawaji T, Yoshizawa T, Toyota T, Yahata M, Nakai K, Sugiyama H, Higashi Y, Ito M, Horie M, Kusano KF, Shimizu W, Kamakura S, Kimura T, Investigators U-AT. Adenosine triphosphate-guided pulmonary vein isolation for atrial fibrillation: The unmasking dormant electrical reconnection by adenosine triphosphate (under-atp) trial. *European heart journal*. 2015
37. Ucer E, Fredersdorf S, Jungbauer CG, Seegers J, Debl K, Riegger G, Maier LS. Unmasking the dormant pulmonary vein conduction with adenosine administration after pulmonary vein isolation with laser energy. *Europace : European pacing, arrhythmias, and cardiac electrophysiology : journal of the working groups on cardiac pacing, arrhythmias, and cardiac cellular electrophysiology of the European Society of Cardiology*. 2015;17:1376-1382

38. Ciconte G, Chierchia GB, C DEA, Sieira J, Conte G, Julia J, G DIG, Wauters K, Baltogiannis G, Saitoh Y, Mugnai G, Catanzariti D, Tondo C, Brugada P. Spontaneous and adenosine-induced pulmonary vein reconnection after cryoballoon ablation with the second-generation device. *Journal of cardiovascular electrophysiology*. 2014;25:845-851
39. Arentz T, Macle L, Kalusche D, Hocini M, Jais P, Shah D, Haissaguerre M. "Dormant" pulmonary vein conduction revealed by adenosine after ostial radiofrequency catheter ablation. *Journal of cardiovascular electrophysiology*. 2004;15:1041-1047
40. Datino T, Macle L, Qi XY, Maguy A, Comtois P, Chartier D, Guerra PG, Arenal A, Fernandez-Aviles F, Nattel S. Mechanisms by which adenosine restores conduction in dormant canine pulmonary veins. *Circulation*. 2010;121:963-972
41. Bardy GH, Sawyer PL, Johnson GW, Ivey TD, Reichenbach DD. Effect of voltage and charge of electrical ablation pulses on canine myocardium. *The American journal of physiology*. 1989;257:H1534-1542



CHAPTER 11

General discussion of this thesis

General discussion

1 Exposition

At the end of the Direct Current (DC) era, low-energy DC ablation was demonstrated to enable sufficient myocardial lesion creation without arcing and barotrauma. In the old DC technique a single small catheter electrode was used. Current density in target tissue was high in the vicinity of the electrode and decreased rapidly, with the *square root* of distance from the center of the electrode. Consequently, control over lesion size is poor. We hypothesized that by applying a special catheter design using a circular arrangement of connected electrodes, a torus-shaped electric field could be created, in which voltage and current density decrease more *linear* from the center of the electrode(s). (**Figure 1**) This may possibly result in a better control over lesion size in relation to the energy output. In addition, by increasing the total electrode surface area, the arcing threshold is increased due to a decrease of current density at the electrode surface (8 ring-electrodes of 2 mm length represents a total surface area of 115 mm²; an 4-mm 7F electrode has only has a total surface area of 32 mm²). Summarized, with a linear (and shallower) decay of current density and a large electrode surface area, we aimed at a favorable change of distribution of current density in the tissue: a relatively low current density at the electrode site and a relatively high current density deeper in the targeted myocardial tissues. Also a linear suction device ensuring a proper electrode-tissue contact without current leak to surrounding structures, was used to improve controllability over lesion creation by directing all DC energy into the myocardium.

2 Results of the (first) feasibility and safety study

First custom built catheters with various electrode sizes and/or inter-electrode distances were tested in saline tanks by monitoring current and voltage waveforms on a storage oscilloscope (pilot safety study). (The difference between 360 Joule (J) delivered via a single 2 mm distal ablation electrode and 200 J delivered via 10 electrodes on a circular catheter (20 J per electrode) was impressive.)

In **Chapter 2** we founds that circular electroporation ablation at an energy level below the arcing threshold is a feasible and safe method for endocardial PV ablation. The use of circular catheters in the porcine left atrium (LA) was not straight forward due to non-deflectability of the prototype catheter and the small porcine left atrium. As cathodal energy applications have a higher arcing threshold in blood environment, cathodal applications were used in subsequent studies.

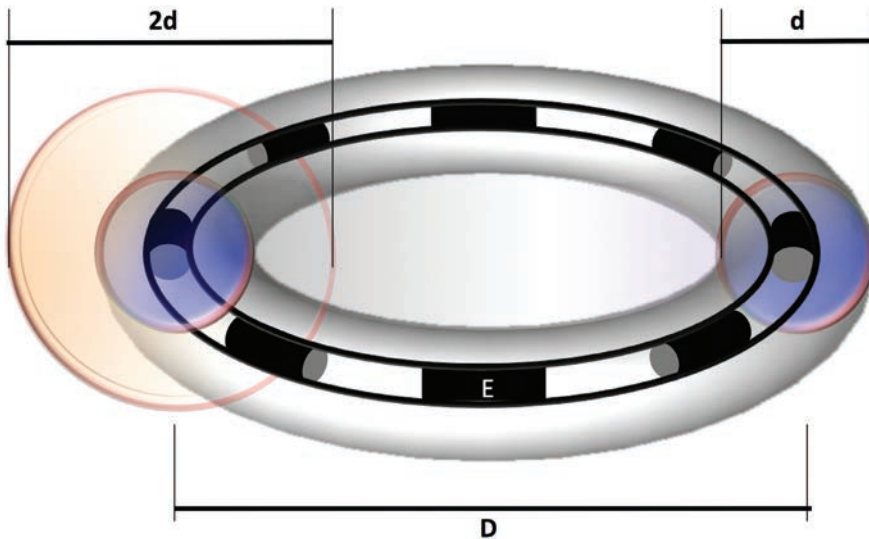


Figure 1. With a circular arrangement of (8) electroporation electrodes, the ablation current spreads off the catheter toroidally and surface areas with equal current densities will have the shape of a torus. The surface area of a torus (A) is directly proportional to the thickness of the torus (d) and the torus diameter (D) ($A = 4\pi^2 \times D \times d$). Therefore current density will decrease by half when the torus thickness doubles. (E = electrode in a circular catheter)

3 Results with respect to the creation of myocardial lesion

A. myocardial lesions created with current ablation modalities

The histological appearance of an acute myocardial lesion due to radiofrequency (RF) energy reveals a central zone (pale) of coagulation necrosis, with the loss of cellular and vascular architecture. Particularly in the outer rim of the lesion contraction bands in the sarcomeres due to calcium overload and a bordering zone of hemorrhage tissue with mononuclear cells in the (early inflammatory reaction) are found. Blood flow is reduced both in and beyond (the periphery) of the lesion. In the first few months the necrotic zone is gradually replaced with fibrosis and evolves into a fibrotic scar.

The acute cryo-lesion is caused by early irreversible changes in the subcellular organelle structure and mitochondrial destruction, however, the tissue seems macroscopically to be intact. Hemorrhage, edema, and inflammation are present within 48 hours. In the first few months the lesion is gradually replaced with fibrosis and evolves into a fibrotic scar.

In comparison to RF lesions cryo-lesions are homogeneous, extracellular tissue architecture is preserved and there are well-demarcated margins with preserved

blood flow. The extracellular collagen matrix in the lesion is preserved and endothelial disruption or thrombus formation are not often seen.

As we know from ancient animal studies, the myocardial lesion due to high-energy DC ablation starts with ecchymosis and edema in the first few hours. After a few days, hemorrhagic lesions are found with contraction bands and extensive disruption of myocardial fibers.¹ After a few months only fibrosis is found.²⁻⁴ With non-arcing low-energy DC ablation exhibiting equivalent peak voltages and currents, similar amounts of myocardial lesion could be created.⁵

In the last decade only two cardiac IRE studies have been reported. Lavee et al reported an animal study in which epicardial ablation was performed with IRE. In 5 pigs both atrial appendages were clamped and ablated between two 4-cm long parallel electrodes. Each lesion was created without local temperature rise. Durable electrical isolation was demonstrated. All lesions were transmural, with a mean depth of 0.9 cm.⁶ Hong et al also used clamp devices to isolate pulmonary veins (PV), caval veins and the right atrial auricle (RAA). Only a few PVs and RAA lesions were not transmural due to the existence of fat content on the epicardial area.⁷ In both studies a well defined region of tissue ablation was observed, without transitional areas from ablated to healthy tissue. The boundaries were very clear.^{6,7} The inflammatory reaction within acute ablation lesions was minimal. However, some collagen denaturation noted in some of the lesions suggested possible thermal effects with the use of higher settings of energy.⁷

B. myocardial lesions created with electroporation ablation (this thesis)

In **Chapters 3-7** epicardial electroporation ablation effects on myocardium were examined to evaluate the dose-response relationship between the magnitude of the electroporation application and the myocardial lesion. Several custom devices in combination with various energy levels were used. In **Chapter 3** and **4** electroporation ablation with the use of a 20 mm diameter circular device was performed in an open-chest and tissue-blood environment model, simulating an endocardial approach. In **Chapter 5** and **6** electroporation ablation was performed in a closed-chest model with a custom built 12 mm diameter device for the for the development of an effective epicardial ablation modality for (video-assisted) thoraco-surgical treatment of arrhythmias. In **Chapter 7** the dose-response relationship was investigated in an open-chest model with a linear suction device. In all studies, the impact of electroporation ablation on the coronary arteries (collateral vascular damage) and, reversely, the effect of the coronary artery blood flow on myocardial lesion formation (heat sink) was investigated.

With respect to lesion formation we came to the following findings

- 1) When the total peak current reaches values above 30 A with 200 J shocks via circular custom built catheters containing 10 electrodes of 2 mm (with a total electrode surface area of 150 mm²), the voltage waveform starts to show small waveform discontinuities due to arcing. By removing the indifferent patch electrode to the lower back causing an increase of the total impedance, arcing could be prevented. For delivery of higher peak currents without arcing, electrode size should be increased to decrease current density at the electrode surface. **(Chapter 2)**
- 2) Lesion depth increased with the magnitude of the electroporation application. **(Chapter 3-7)** This relationship is *linear* and *significant*, with a slope of 0.17 mm/A in a tissue-blood environment. **(Chapter 3)** In addition, the total peak current delivered with a 200-J application is only twice that of a 50-J application. **(Chapter 3)**
- 3) Except for the feasibility study, myocardial lesions were obtained with cathodal non-arcing low-energy DC shocks. All voltage and current waveforms were smooth, demonstrating the absence of arcing and barotrauma. **(Chapter 3, 5, 6)** As we know from previous low-energy DC studies, as long as arcing does not occur the relationship between voltage and current is strict linear and the electrode-blood impedance is constant.^{8,9}
- 4) Despite separate electrodes on the circular electroporation catheter continuous circular lesions could be created with a single 200 J application, also at the myocardial tissue surface. **(Chapter 3, 5, 6)**. As long as electrode size is large enough to prevent arcing, the electrode design seems not to be a critical issue. In contrast, due to intracavitary blood flow and saline cooling RF lesions expand relatively small diameters at the tissue surface which easily leads to gaps in the ablation line.
- 5) Lesions depth did not differ significantly between lesions containing arteries and without arteries **(Chapter 4)**. There was no impact of the coronary flow on lesion size.
- 6) Visual inspection of the ablation area and electrodes, directly after electroporation application, never revealed any blood clots, charring or carbonization. There was never a white imprint of the electrode contact on the tissue, as is commonly observed with tissue coagulation due to RF ablation. So, myocardial lesions caused by non-arcing electroporation ablation do not demonstrate signs of thermal impact.

In addition, when the total energy is divided over 10 electrodes, a 200 J circular shock delivered via 10 electrodes equals only 20 J per electrode. (Consequently, a 200 J circular shock delivered via 8 electrodes equals only 25 J per electrode.) According to Ohm's law, electrode impedance determines the amount of current that will flow through each electrode. So, a maximum total current of 40 A amounts to a maximum current of 4 A per electrode. Consequently, the thermal response can be expected to be comparable to 30 Watt of RF energy delivered during 0.7 sec per electrode, which cannot explain a 7-mm lesion depth. In conclusion, creation of myocardial lesions as result from non-arcng low-energy DC energy reflects a voltage (and current) dependent process injuring the electrical properties of the cell membrane (electroporation) and not thermal injury.

4) Potential side-effects of electroporation ablation

In **Chapter 8** and **9** the potential side-effects of electroporation ablation on the PVs, and phrenic nerve (PN) were studied in a worst-case scenarios. In the **Chapters 3-7** potential effects of electroporation ablation on coronary arteries were studied.

a) pulmonary vein stenosis (PVS)

PVS was a most common complication (21%) when RF energy inside the PV was used in AF ablation.¹⁰⁻¹³ Adaptation to segmental PV ablation clearly decreased the incidence of this complication. However, a considerable incidence of severe PVS, varying from 2 to 9 %, was still reported. The ultimate decrease to < 1 % was due to ablation outside the PV orifice (antrum level), use of less RF energy and non-fluoroscopic catheter guidance.¹⁴⁻¹⁶ PVS following PV ablation is thought to be caused by intimal thickening, thrombus formation, endocardial contraction and proliferation of the elastic lamina.¹⁷ Beneficial remodeling may explain a slight decrease of mild and moderate PV stenosis over time.

Mild PVS is generally asymptomatic and does not tend to progress. Severe PVS ($\geq 70\%$ decrease in luminal PV diameter) is associated with symptoms like dyspnea, cough or recurrent lung infection, especially when multiple PVs are affected.¹⁰⁻¹² As in congenital PV stenosis, balloon angioplasty and stenting for acquired PV stenosis is strongly associated with a high recurrence rate, particularly in occluded PVs.^{11, 15, 16, 18, 19} The incidence of PVS with cryo-balloon (CB) ablation seemed to be very low.^{20, 21} However, in the large STOP-AF trial the incidence of severe PVS was 3,1 %.²²

In this thesis PVS did not occur as result of multiple (2-4) non-arcng 200 J applications inside the PV. No change in diameter of any of the PV ostia was

observed, 3 weeks after ablation (**Chapter 2**). Much more convincing, 3 months after ablation PVS did not develop after the PVs being subjected to a worst-case scenario (10 non-arcing 200 J applications inside the PV tubulus) (**Chapter 8**).

b) phrenic nerve (PN) injury

Because of its course in close proximity to the PVs, injury of the right phrenic nerve (PN) due to *endocardial* RF ablation for AF occurs in 0,5%.²³⁻²⁵ Half of the patients is asymptomatic, the other may suffer from symptoms, such as cough, hiccup, pain and dyspnea.²⁴⁻³³ Fortunately, in 85% diaphragm contraction recovers in 12 months.^{25, 26, 33} Injury to other nerves such as the left PN and the recurrent laryngeal nerve has also been described.^{31, 34} With current cryo-balloon (CB) technique, PN palsy (PNP) occurs much more often. The incidence of persistent PNP in the STOP-AF trial was 2,5 %, whereas transient PNP occurred even in 11 %.^{21, 22}

Predictability of nerve injury during RF ablation is limited due to the variable course of nerves variable thickness of LA wall and fibrofatty tissue between heart and nerves.²⁴ PN pacing above the ablation site while monitoring diaphragm excursion fluoroscopically is a well-known method to avoid PN damage, however not completely reliable.^{25, 29} Severity of damage and rate of recovery are related to the amount of thermal energy delivery. Immediate PN function recovery after the discontinuation of RF energy delivery argues for a current mediated electromagnetic effect causing a transient PN conduction block. Spontaneous recovery after a few weeks, especially after the use of steroids, suggests edema and inflammation to account for PN injury. Recovery after a few months is thought to be caused by nerve regeneration following axonal necrosis.^{26, 27, 32, 33, 35, 36}

The left PN runs along the lateral wall of the left ventricle and may be collaterally damaged in *epicardial* ablation procedures. Several inventions moving the pericardium away have been reported. Although some were proven effective, avoidance of ablation at sites of PN capture is still recommended.³⁷

Several studies did report on a preserved architecture of nerves incorporated by large IRE-lesions.³⁸⁻⁴⁰ Nerves purposefully subjected to IRE showed transient decrease of function, normalizing after several weeks or months. Preservation of architecture of the endoneurium and proliferation of Schwann cells indicated axonal regeneration.⁴¹⁻⁴³

In this thesis the porcine PN coursing along the outside of superior caval vein (SCV) was targeted with a single circular electroporation application (200 J) from inside the SCV. The PN function was preserved, both immediately after the electroporation ablation as during 3 months follow-up (**Chapter 9**).

c) coronary artery injury

RF energy applied to coronary arteries may cause arterial wall damage due to collagen denaturation resulting in stenosis⁴⁴⁻⁴⁷, coronary spasms⁴⁸ and clot formation, caused by protein aggregation as blood temperature rises 50°C, leading to myocardial infarction.^{46, 49, 50} RF ablation via the coronary venous system in close proximity to coronary arteries (< 2 mm) was demonstrated to cause coronary artery damage (wall thickening and stenosis) too.^{46, 47, 51} Even during endocardial catheter ablation coronary artery damage has been reported.⁵² Histology did show medial necrosis with loss of intima of the coronary artery wall.⁴⁷

Particularly small coronary arteries are vulnerable to RF ablation due to limited cooling effects of local coronary blood flow (heat sink).^{49, 53} A distance > 5 mm between ablation catheter and coronary artery is commonly accepted as safe.^{49, 53, 54} In addition, the heat sink effects may also limit lesion creation, particularly myocardial tissue in contact with the coronary artery walls. So, RF ablation in close proximity to coronary arteries is both unsafe as well as ineffective, which may impede clinical outcome of epicardial ventricular arrhythmia ablation.

Cryo-ablation in vicinity of vessels was not thought to cause damage or chronic stenosis. In several animal studies coronary stenosis was not observed whereas histology showed preserved intima and media layers.^{47, 51, 55-57} However, in human studies coronary artery injury was observed after epicardial cryo-ablation.^{44, 46, 57} Besides, when coronary arteries were targeted with cryo-energy, ventricular lesions were found to be continuous but lesion depth was averaged only 2,0-2,5 mm.⁵⁷ Except for incidental mild intima hyperplasia high-energy DC ablation seemed to have rather little impact on the integrity of coronary arteries.² However, focal medial necrosis was certainly found after single or multiple arcing DC shocks and rupture and occlusion of the coronary sinus were even frequently observed.⁵ With the use of non-arcing low-energy DC energy coronary artery injury was only found after multiple DC shocks and rupture of the coronary sinus was observed to a much lesser extent.⁵

Blood vessels subjected to IRE applications are generally left intact.^{40, 58, 59} Carotid arteries were unaffected after multiple strong IRE pulses directly applied on the artery.^{40, 60}

In this thesis electroporation applications were delivered aside from (**Chapter 4, 5, 7**) and deliberately on (**Chapter 4, 6**) main coronary arteries to investigate collateral coronary damage. Using variable energy levels (50-360 J) coronary arteries did not develop a significant stenosis within 3 weeks and 3 months after

epicardial electroporation ablation, neither in a blood-tissue environment nor a closed-chest model (**Chapter 4 - 7**). Intimal hyperplasia was not found in general (**Chapter 4 - 7**). Only short-lasting coronary spasm was seen directly (<30 minutes) following electroporation ablation (**Chapter 5, 6**). In addition, intact myocardial tissue around blood vessels was not found (**Chapter 4, 6**). The implications of these observations are stretching far, because usual drawbacks of current thermal epicardial ablation methods (gaps in lesions due to the heat sink effect and collateral damage to coronary arteries) appear to have been overcome.

5. myocardial lesion development

Immediately after electroporation ablation myocardial lesions are visible by inspection (**Chapter 10**). Acute lesions were mainly characterized by interstitial edema and contraction band formation, whereas tissue structural integrity was preserved and myocardial lesions did not evolve histologically over the course of 1 hour. In view of the creation of transmural lesions not substantially affected by decreases in lesion size over time due to recovery of reversibly electroporated parts, one might assume that the electrophysiological evaluation can be performed immediately after ablation.

In addition, there is only minimal histological development in the period between 3 weeks and 3 months. Hemorrhage and inflammatory cell infiltration are almost entirely absent. Therefore, subsequent ablation procedures might be safely scheduled already at 3 to 4 weeks after the index procedure (**Chapter 10**).

6. Clinical implications of electroporation ablation

A. Endocardial catheter-ablation for AF

Pulmonary vein antrum isolation (PVAI) is considered the cornerstone for catheter ablation in all categories of AF; wide encircling lesions are applied to isolate PVs and its surrounding tissue containing triggers and substrate from the left atrium (LA).⁶¹ In patients with (longstanding) persistent AF, repeat ablation procedures, involving a 4-5 % risk of complications per procedure, are required to improve clinical success rate.⁶² Recurrence of AF following initial PVAI can be attributed to non-PV triggers inducing AF, incomplete PV ablation lines, and a prominent LA substrate caused by structural remodelling.⁶³⁻⁶⁵

Elimination of foci outside the PV initiating AF, may result in modest clinical success in paroxysmal AF.⁶³⁻⁶⁷ PV-reconnections do occur frequently after initial PVAI. Ablation of remaining PV-connections improves clinical outcome after initial successful PVAI or a surgical MAZE, also in (longstanding) persistent AF.⁶⁸⁻⁷²

Creation of linear lesions in the LA and the ablation of complex fractionated atrial electrograms (CFAE) have been investigated as adjuvant substrate modification strategies to improve the clinical outcome.⁷³⁻⁷⁵ Based on the hypothesis that AF results from randomly propagating wavelets, linear ablation lines are intended to curb circulating wavelets by reducing the critical atrial excitable mass. Due to variable LA wall thickness and fibrosis, laborious catheter manoeuvring and the heat sink effect inherent to thermal ablation, a line of block is not readily accomplished.^{76, 77} Unfortunately, incomplete lines are rather pro-arrhythmic.⁷⁸⁻⁸⁰ In only a few studies the clinical outcome was improved by addition of linear ablations.⁸¹⁻⁸³ Targeting CFAEs was also thought to improve the clinical success rate in (longstanding) persistent AF ablation. CFAEs are considered to be zones of slow conduction, related to a wide activation of the cardiac neural network, facilitating the occurrence of AF.⁸⁴⁻⁸⁷ In a few studies additional CFAE ablation was demonstrated to have better outcome in (longstanding) persistent AF.^{88, 89} Recently, the large STAR-AF2-study did not report on any value for additional LA ablation.^{90, 91} Whether additional LA ablation strategies lack convincing benefit for pathophysiological reasons or technical imperfections is unclear. However, incomplete lesion sets created with thermal energy may spare critical targets or cause arrhythmogenic areas.

Nevertheless, ablation of the posterior LA is attracting growing interest. Elimination of the posterior LA substrate, containing triggers, plexus and re-entrant circuits, due to fibrosis and the variably layered myocardial fiber wall construction, is increasingly considered of added value in the treatment of longstanding persistent AF. Surgical PV isolation with a box-lesion isolating the LA posterior wall resulted in a success rate > 90 %.⁹² Endocardial posterior LA ablation (isolation and/or debulking) in addition to PVAI did not substantially improve clinical outcome yet. However, clinical outcome was usually assessed after a single ablation procedure, whereas esophageal injury was avoided by decreasing energy delivery at the posterior LA and passing over posterior LA regions in close proximity to the esophagus.⁹³⁻⁹⁶

In summary, in view of the projected increase of AF prevalence in an aging population, and obvious arguments for improvement of clinical success, safety (minimizing complication rate due to multiple procedures) and cost-efficiency, durable PVAI accomplished safely and at once is of the utmost importance (**this thesis**).

Because electroporation ablation enables the creation of deep (transmural) myocardial lesions without insurmountable harmful side-effects on the

surrounding tissues, durable PVAI at once might be easier to achieve. The same could apply to sufficient CFAE ablation. In addition, as myocardial lesions lack vital zones of undamaged myocardium around blood vessels due to the absence of the heat sink effect, adjuvant linear LA lesion ablation can be performed adequately (without gaps in the lesions) and improve clinical success (**this thesis**). When electroporation ablation lacks a harmful impact on the esophagus, electroporation ablation of the posterior LA may be safely incorporated into the armamentarium of ablation techniques in patients with longstanding persistent AF and improve clinical outcome (**not published yet**).

B. Epicardial ablation of ventricular tachycardia (VT) and atrial fibrillation (AF)

Epicardial electroporation ablation can be used for the treatment of both atrial and ventricular arrhythmias. Although epicardial VT ablation can be repeated after a failure, it is still associated with a complication risk of 5% per procedure.⁴⁴ Electroporation applications of 200 J are proven sufficiently powerful to create continuous and transmural ventricular lesions, without adverse effects on coronary arteries (**this thesis**). Therefore, homogenization of scar tissue, elimination of deep intramural foci and ablation on or near coronary arteries may become a real possibility in VT ablation.

The epicardial electroporation ablation technique can also be developed into a safe and effective single-shot device for ablation of AF via video-assisted thoracoscopy. Lower energy settings, between 30 and 100 J, would probably be sufficient to create transmural LA lesions. When applied during concomitant cardiac surgery, epicardial electroporation ablation may reduce the cross-clamp time significantly.

7. Limitations of electroporation ablation in this thesis

1. Although we might expect similar outcomes, we are not informed about the size and depth of lesions created in the atrium and by endocardial electroporation ablation.
2. The dose-response relationship between the magnitude of an electroporation application and lesion depth was hampered by significant shrinkage of the transmural lesions due to scar contracture. Studies with lower energy settings, for example between 30 and 100 Joule, could refine this relationship.
3. Skeletal muscle contraction due to electroporation ablation, may disrupt 3-D electro-anatomical mapping and discomfort after the procedure. Therefore, general anesthesia with the use of muscle relaxants is required.

4. In epicardial electroporation ablation the potential negative influence of (the amount of) epicardial fat or preexisting myocardial fibrosis on lesion size was not investigated. In RF ablation the negative impact of epicardial fat on the creation of myocardial lesions is well-known. The use of irrigation allows more energy delivery creating deeper lesions (up to 5 mm in scar). However, irrigated RF ablation generally cannot produce epicardial lesions in the presence of a fat layer > 3.5 mm.⁹⁷
5. The occurrence of pro-arrhythmic effects due to electroporation ablation can not be ruled out. After intensive treatment with amiodarone, evidence of malignant arrhythmias and/or sudden death was not noticed in our porcine electroporation studies.
6. Irregular lesion margins due to extensions of connective tissue in the surrounding undamaged myocardium have been observed (**Chapter 10**). Whether these extensions represent pre-existing strands of connective tissue or are the result of the electroporation ablation because more frequently found at the borderzone than in undamaged myocardium, is unclear. In pursuing creation of transmural lesions this finding might be of limited interest.
7. With respect to mechanical adverse effects we do not have information about the impact of multiple electroporation ablations delivered at exactly the same site. One might imagine that additional ablation in a newly ablated area would be able to achieve mechanical damage. However, no significant impact was found in the PVs subjected to 10 overlapping 200 J electroporation ablations.

8. Future research on electroporation ablation

1. injury to the phrenic nerve (PN)

Preservation of the architecture of nerves incorporated in IRE-lesions has been demonstrated in both previous IRE-studies as our own electroporation ablation studies. However, transient decrease of nerve functionality after IRE has been described whereas proliferation of Schwann cells enables recovery of the nerve function via axonal regeneration.

In our study both immediately after electroporation ablation as well as during follow-up the PN remained functionally intact. However, PN injury could still have occurred: a partial damage of the PN, close to the electrode site of the circular electroporation catheter, that not affects PN functionality in its entirety, can not be ruled out. Therefore additional studies have to investigate whether or not epicardial electroporation ablation affects the PN function and integrity.

2. injury to the peri-esophageal nerves and esophagus

In contrast to the PN, peri-esophageal nerves are mainly unmyelinated. Myelin is postulated to operate as a layer of electrical isolation preventing nerve damage from electrical energy. Unmyelinated nerves are not allowed to regenerate. Potential injury to peri-esophageal nerves was not investigated in this thesis.

Injury to peri-esophageal nerves may cause pyloric spasm, gastric hypomotility and prolonged gastric emptying time, leading to abdominal bloating and discomfort for weeks till months. Moreover, by dissolving the endoluminal lesions the acid reflux as result of injury to peri-esophageal nerves may enforce development of a left-atrio-esophageal fistula. Therefore, a transient deficit of the peri-esophageal nerves may exert deleterious effects on the esophagus too.

The impact of electroporation ablation on the esophagus in a worst case scenario has been studied in a porcine model (but not published yet). Preliminary data demonstrate significant lesions in the muscularis propria after 200 J applications directly delivered esophagus. After two days only transient mucosal (luminal) abnormalities were observed by gross inspection. One might assume that the esophageal lesions due to endocardial electroporation ablation at the adjoining LA side will be smaller. However, we have no comprehensive data on this subject yet.

3. cerebral infarction

Transient ischemia or cerebral infarction in the brain is one of the most serious complications in current thermal AF ablation, caused by char formation at the tip of the ablation catheter or the ablation site (particularly RF ablation), development of thrombi on the ablation catheter or within sheaths, or disruption of pre-existing thrombus by catheter manipulation or restored atrial contraction. Because of the non-thermal nature of IRE, char embolism is avoided. However, we do not have data on brain infarction due to thrombus formation as the porcine vascular anatomy protects the cerebral circulation.

In addition, during electroporation ablation hyperechoic clouds can be seen with echocardiography. They are most likely caused by formation of microbubbles due to the electrolysis of water. The amount of gas is unknown, and so is its potential risk on embolic events in heart and brain.

4. proper electrode-tissue contact

Lesion size created by electroporation ablation grossly depends on the amount of energy delivery (peak voltage, peak current). Proper electrode-tissue contact is thought to be elementary for sufficient energy transmission into the tissue. Consequently, real-time assessment of individual electrical electrode-tissue contact

before electroporation ablation is pivotal. The final catheter design that complies with proper electrode-tissue contact remains a major challenge and needs further investigation. Considering the prerequisite of proper electrode-tissue contact and the ability of electroporation to create deep and wide myocardial lesions, the ideal position of the circulator catheter for prospective human PV isolation is anticipated between PV ostium and antrum, or even inside the PV. In our studies an area proximal to the PV ostium was demonstrably affected after a circular 200 J electroporation ablation in the PV (**Chapter 2**). Due to the anatomical variation in PV course and diameter, ablation hoops with different diameters might be needed. The electrode size, inter-electrode spacing and total applied energy should be scaled proportional to maintain the same lesion depth and safety margin.

9. References

1. Lerman BB, Weiss JL, Bulkley BH, Becker LC, Weisfeldt ML. Myocardial injury and induction of arrhythmia by direct current shock delivered via endocardial catheters in dogs. *Circulation*. 1984;69:1006-1012
2. Brodman R, Fisher JD. Evaluation of a catheter technique for ablation of accessory pathways near the coronary sinus using a canine model. *Circulation*. 1983;67:923-929
3. Gonzalez R, Scheinman M, Margaretten W, Rubinstein M. Closed-chest electrode-catheter technique for his bundle ablation in dogs. *The American journal of physiology*. 1981;241:H283-287
4. Bardy GH, Ideker RE, Kasell J, Worley SJ, Smith WM, German LD, Gallagher JJ. Transvenous ablation of the atrioventricular conduction system in dogs: Electrophysiologic and histologic observations. *The American journal of cardiology*. 1983;51:1775-1782
5. Lemery R, Leung TK, Lavallee E, Girard A, Talajic M, Roy D, Montpetit M. In vitro and in vivo effects within the coronary sinus of nonarcing and arcing shocks using a new system of low-energy dc ablation. *Circulation*. 1991;83:279-293
6. Lavee J, Onik G, Mikus P, Rubinsky B. A novel nonthermal energy source for surgical epicardial atrial ablation: Irreversible electroporation. *The heart surgery forum*. 2007;10:E162-167
7. Hong J, Stewart MT, Cheek DS, Francischelli DE, Kirchhof N. Cardiac ablation via electroporation. *Conference proceedings: ... Annual International Conference of the IEEE Engineering in Medicine and Biology Society. IEEE Engineering in Medicine and Biology Society. Annual Conference*. 2009;2009:3381-3384
8. Cunningham D, Ahsan AJ, Rowland E, Rickards AF. Impedance changes during catheter ablation and their relationship to electrical arcing and clinical efficacy. *Pacing and clinical electrophysiology: PACE*. 1989;12:144-149
9. Bardy GH, Coltorti F, Stewart RB, Greene HL, Ivey TD. Catheter-mediated electrical ablation: The relation between current and pulse width on voltage breakdown and shock-wave generation. *Pacing and clinical electrophysiology: PACE*. 1986;9:1381-1383
10. Arentz T, Jander N, von Rosenthal J, Blum T, Furmaier R, Gornandt L, Josef Neumann F, Kalusche D. Incidence of pulmonary vein stenosis 2 years after radiofrequency catheter ablation of refractory atrial fibrillation. *European heart journal*. 2003;24:963-969
11. Saad EB, Rossillo A, Saad CP, Martin DO, Bhargava M, Erciyes D, Bash D, Williams-Andrews M, Beheiry S, Marrouche NF, Adams J, Pisano E, Fanelli R, Potenza D, Raviele A, Bonso A, Themistoclakis S, Brachmann J, Saliba WJ, Schweikert RA, Natale A. Pulmonary vein stenosis after radiofrequency ablation of atrial fibrillation: Functional characterization, evolution, and influence of the ablation strategy. *Circulation*. 2003;108:3102-3107
12. Purerfellner H, Cihal R, Aichinger J, Martinek M, Nesser HJ. Pulmonary vein stenosis by ostial irrigated-tip ablation: Incidence, time course, and prediction. *Journal of cardiovascular electrophysiology*. 2003;14:158-164
13. Haissaguerre M, Jais P, Shah DC, Garrigue S, Takahashi A, Lavergne T, Hocini M, Peng JT, Roudaut R, Clementy J. Electrophysiological end point for catheter ablation of atrial fibrillation initiated from multiple pulmonary venous foci. *Circulation*. 2000;101:1409-1417
14. Gupta A, Perera T, Ganesan A, Sullivan T, Lau DH, Roberts-Thomson KC, Brooks AG, Sanders P. Complications of catheter ablation of atrial fibrillation: A systematic review. *Circulation. Arrhythmia and electrophysiology*. 2013;6:1082-1088
15. Cappato R, Calkins H, Chen SA, Davies W, Lesaka Y, Kalman J, Kim YH, Klein G, Natale A, Packer D, Skanes A, Ambrogi F, Biganzoli E. Updated worldwide survey on the methods, efficacy, and safety of catheter ablation for human atrial fibrillation. *Circulation. Arrhythmia and electrophysiology*. 2010;3:32-38
16. Cappato R, Calkins H, Chen SA, Davies W, Lesaka Y, Kalman J, Kim YH, Klein G, Packer D, Skanes A. Worldwide survey on the methods, efficacy, and safety of catheter ablation for human atrial fibrillation. *Circulation*. 2005;111:1100-1105
17. Taylor GW, Kay GN, Zheng X, Bishop S, Ideker RE. Pathological effects of extensive radiofrequency energy applications in the pulmonary veins in dogs. *Circulation*. 2000;101:1736-1742
18. Qureshi AM, Prieto LR, Latson LA, Lane GK, Mesia CI, Radvansky P, White RD, Marrouche NF, Saad EB, Bash DL, Natale A, Rhodes JF. Transcatheter angioplasty for acquired pulmonary vein stenosis after radiofrequency ablation. *Circulation*. 2003;108:1336-1342

19. De Potter TJ, Schmidt B, Chun KR, Schneider C, Malisius R, Nuyens D, Ouyang F, Kuck KH. Drug-eluting stents for the treatment of pulmonary vein stenosis after atrial fibrillation ablation. *Europace: European pacing, arrhythmias, and cardiac electrophysiology: journal of the working groups on cardiac pacing, arrhythmias, and cardiac cellular electrophysiology of the European Society of Cardiology*. 2011;13:57-61
20. Tse HF, Reek S, Timmermans C, Lee KL, Geller JC, Rodriguez LM, Ghaye B, Ayers GM, Crijns HJ, Klein HU, Lau CP. Pulmonary vein isolation using transvenous catheter cryoablation for treatment of atrial fibrillation without risk of pulmonary vein stenosis. *Journal of the American College of Cardiology*. 2003;42:752-758
21. Chun KR, Schmidt B, Metzner A, Tilz R, Zerm T, Koster I, Furnkranz A, Koektuerk B, Konstantinidou M, Antz M, Ouyang F, Kuck KH. The 'single big cryoballoon' technique for acute pulmonary vein isolation in patients with paroxysmal atrial fibrillation: A prospective observational single centre study. *European heart journal*. 2009;30:699-709
22. Packer DL, Kowal RC, Wheelan KR, Irwin JM, Champagne J, Guerra PG, Dubuc M, Reddy V, Nelson L, Holcomb RG, Lehmann JW, Ruskin JN, Investigators SAC. Cryoballoon ablation of pulmonary veins for paroxysmal atrial fibrillation: First results of the north american arctic front (stop af) pivotal trial. *Journal of the American College of Cardiology*. 2013;61:1713-1723
23. Ho SY, Cabrera JA, Sanchez-Quintana D. Left atrial anatomy revisited. *Circulation. Arrhythmia and electrophysiology*. 2012;5:220-228
24. Sanchez-Quintana D, Cabrera JA, Climent V, Farre J, Weiglein A, Ho SY. How close are the phrenic nerves to cardiac structures? Implications for cardiac interventionalists. *Journal of cardiovascular electrophysiology*. 2005;16:309-313
25. Sacher F, Monahan KH, Thomas SP, Davidson N, Adragao P, Sanders P, Hocini M, Takahashi Y, Rotter M, Rostock T, Hsu LF, Clementy J, Haissaguerre M, Ross DL, Packer DL, Jais P. Phrenic nerve injury after atrial fibrillation catheter ablation: Characterization and outcome in a multicenter study. *Journal of the American College of Cardiology*. 2006;47:2498-2503
26. Swallow EB, Dayer MJ, Oldfield WL, Moxham J, Polkey MI. Right hemi-diaphragm paralysis following cardiac radiofrequency ablation. *Respiratory medicine*. 2006;100:1657-1659
27. Doppalapudi H, Yamada T, Kay GN. Complications during catheter ablation of atrial fibrillation: Identification and prevention. *Heart rhythm: the official journal of the Heart Rhythm Society*. 2009;6:S18-25
28. Durante-Mangoni E, Del Vecchio D, Ruggiero G. Right diaphragm paralysis following cardiac radiofrequency catheter ablation for inappropriate sinus tachycardia. *Pacing and clinical electrophysiology: PACE*. 2003;26:783-784
29. Sacher F, Jais P, Stephenson K, O'Neill MD, Hocini M, Clementy J, Stevenson WG, Haissaguerre M. Phrenic nerve injury after catheter ablation of atrial fibrillation. *Indian pacing and electrophysiology journal*. 2007;7:1-6
30. Lee BK, Choi KJ, Kim J, Rhee KS, Nam GB, Kim YH. Right phrenic nerve injury following electrical disconnection of the right superior pulmonary vein. *Pacing and clinical electrophysiology: PACE*. 2004;27:1444-1446
31. Rumbak MJ, Chokshi SK, Abel N, Abel W, Kittusamy PK, McCormack J, Patel MM, Fontanet H. Left phrenic nerve paresis complicating catheter radiofrequency ablation for wolff-parkinson-white syndrome. *American heart journal*. 1996;132:1281-1285
32. Bunch TJ, Bruce GK, Mahapatra S, Johnson SB, Miller DV, Sarabanda AV, Milton MA, Packer DL. Mechanisms of phrenic nerve injury during radiofrequency ablation at the pulmonary vein orifice. *Journal of cardiovascular electrophysiology*. 2005;16:1318-1325
33. Bai R, Patel D, Di Biase L, Fahmy TS, Kozeluhova M, Prasad S, Schweikert R, Cummings J, Saliba W, Andrews-Williams M, Themistoclakis S, Bonso A, Rossillo A, Raviele A, Schmitt C, Karch M, Uriarte JA, Tchou P, Arruda M, Natale A. Phrenic nerve injury after catheter ablation: Should we worry about this complication? *Journal of cardiovascular electrophysiology*. 2006;17:944-948
34. Pai RK, Boyle NG, Child JS, Shivkumar K. Transient left recurrent laryngeal nerve palsy following catheter ablation of atrial fibrillation. *Heart rhythm: the official journal of the Heart Rhythm Society*. 2005;2:182-184
35. Tsong TY, Su ZD. Biological effects of electric shock and heat denaturation and oxidation of molecules, membranes, and cellular functions. *Annals of the New York Academy of Sciences*. 1999;888:211-232

36. Shah AJ, Pascale P, Miyazaki S, Liu X, Roten L, Derval N, Jadidi AS, Scherr D, Wilton SB, Pedersen M, Knecht S, Sacher F, Jais P, Haissaguerre M, Hocini M. Prevalence and types of pitfall in the assessment of mitral isthmus linear conduction block. *Circulation. Arrhythmia and electrophysiology*. 2012;5:957-967
37. Neven K, Fernandez-Armenta J, Andreu D, Berruezo A. Epicardial ablation: Prevention of phrenic nerve damage by pericardial injection of saline and the use of a steerable sheath. *Indian pacing and electrophysiology journal*. 2014;14:87-93
38. Onik G, Mikus P, Rubinsky B. Irreversible electroporation: Implications for prostate ablation. *Technology in cancer research & treatment*. 2007;6:295-300
39. Pech M, Janitzky A, Wendler JJ, Strang C, Blaschke S, Dudeck O, Ricke J, Liehr UB. Irreversible electroporation of renal cell carcinoma: A first-in-man phase i clinical study. *Cardiovascular and interventional radiology*. 2011;34:132-138
40. Maor E, Ivorra A, Leor J, Rubinsky B. The effect of irreversible electroporation on blood vessels. *Technology in cancer research & treatment*. 2007;6:307-312
41. Schoellnast H, Monette S, Ezell PC, Maybody M, Erinjeri JP, Stubblefield MD, Single G, Solomon SB. The delayed effects of irreversible electroporation ablation on nerves. *European radiology*. 2013;23:375-380
42. Li W, Fan Q, Ji Z, Qiu X, Li Z. The effects of irreversible electroporation (ire) on nerves. *PLoS one*. 2011;6:e18831
43. Schoellnast H, Monette S, Ezell PC, Deodhar A, Maybody M, Erinjeri JP, Stubblefield MD, Single GW, Jr., Hamilton WC, Jr., Solomon SB. Acute and subacute effects of irreversible electroporation on nerves: Experimental study in a pig model. *Radiology*. 2011;260:421-427
44. Sacher F, Roberts-Thomson K, Maury P, Tedrow U, Nault I, Steven D, Hocini M, Koplan B, Leroux L, Derval N, Seiler J, Wright MJ, Epstein L, Haissaguerre M, Jais P, Stevenson WG. Epicardial ventricular tachycardia ablation a multicenter safety study. *Journal of the American College of Cardiology*. 2010;55:2366-2372
45. Paul T, Bokenkamp R, Mahner B, Trappe HJ. Coronary artery involvement early and late after radiofrequency current application in young pigs. *American heart journal*. 1997;133:436-440
46. Roberts-Thomson KC, Steven D, Seiler J, Inada K, Koplan BA, Tedrow UB, Epstein LM, Stevenson WG. Coronary artery injury due to catheter ablation in adults: Presentations and outcomes. *Circulation*. 2009;120:1465-1473
47. Aoyama H, Nakagawa H, Pitha JV, Khammar GS, Chandrasekaran K, Matsudaira K, Yagi T, Yokoyama K, Lazzara R, Jackman WM. Comparison of cryothermia and radiofrequency current in safety and efficacy of catheter ablation within the canine coronary sinus close to the left circumflex coronary artery. *Journal of cardiovascular electrophysiology*. 2005;16:1218-1226
48. Hartzler GO, Giorgi LV, Diehl AM, Hamaker WR. Right coronary spasm complicating electrode catheter ablation of a right lateral accessory pathway. *Journal of the American College of Cardiology*. 1985;6:250-253
49. D'Avila A, Gutierrez P, Scanavacca M, Reddy V, Lustgarten DL, Sosa E, Ramires JA. Effects of radiofrequency pulses delivered in the vicinity of the coronary arteries: Implications for nonsurgical transthoracic epicardial catheter ablation to treat ventricular tachycardia. *Pacing and clinical electrophysiology: PACE*. 2002;25:1488-1495
50. Sosa E, Scanavacca M. Epicardial mapping and ablation techniques to control ventricular tachycardia. *Journal of cardiovascular electrophysiology*. 2005;16:449-452
51. Stavrakis S, Jackman WM, Nakagawa H, Sun Y, Xu Q, Beckman KJ, Lockwood D, Scherlag BJ, Lazzara R, Po SS. Risk of coronary artery injury with radiofrequency ablation and cryoablation of epicardial posteroseptal accessory pathways within the coronary venous system. *Circulation. Arrhythmia and electrophysiology*. 2014;7:113-119
52. Takahashi Y, Jais P, Hocini M, Sanders P, Rotter M, Rostock T, Sacher F, Jais C, Clementy J, Haissaguerre M. Acute occlusion of the left circumflex coronary artery during mitral isthmus linear ablation. *Journal of cardiovascular electrophysiology*. 2005;16:1104-1107
53. Della Bella P, Brugada J, Zeppenfeld K, Merino J, Neuzil P, Maury P, Maccabelli G, Vergara P, Baratto F, Berruezo A, Wijnmaalen AP. Epicardial ablation for ventricular tachycardia: A european multicenter study. *Circulation. Arrhythmia and electrophysiology*. 2011;4:653-659

54. Aliot EM, Stevenson WG, Almendral-Garrote JM, Bogun F, Calkins CH, Delacretaz E, Della Bella P, Hindricks G, Jais P, Josephson ME, Kautzner J, Kay GN, Kuck KH, Lerman BB, Marchlinski F, Reddy V, Schali J, Schilling R, Soejima K, Wilber D, European Heart Rhythm A, Registered Branch of the European Society of C, Heart Rhythm S, American College of C, American Heart A. Ehra/hrs expert consensus on catheter ablation of ventricular arrhythmias: Developed in a partnership with the european heart rhythm association (ehra), a registered branch of the european society of cardiology (esc), and the heart rhythm society (hrs); in collaboration with the american college of cardiology (acc) and the american heart association (aha). *Heart rhythm : the official journal of the Heart Rhythm Society*. 2009;6:886-933
55. Kriebel T, Hermann HP, Schneider H, Kroll M, Selle J, Overwaul A, Sigler M, Paul T. Cryoablation at growing myocardium: No evidence of coronary artery obstruction or intimal plaque formation early and late after energy application. *Pacing and clinical electrophysiology : PACE*. 2009;32:1197-1202
56. Skanes AC, Jones DL, Teefy P, Guiraudon C, Yee R, Krahn AD, Klein GJ. Safety and feasibility of cryothermal ablation within the mid- and distal coronary sinus. *Journal of cardiovascular electrophysiology*. 2004;15:1319-1323
57. Lustgarten DL, Bell S, Hardin N, Calame J, Spector PS. Safety and efficacy of epicardial cryoablation in a canine model. *Heart rhythm : the official journal of the Heart Rhythm Society*. 2005;2:82-90
58. Maor E, Ivorra A, Rubinsky B. Intravascular irreversible electroporation: Theoretical and experimental feasibility study. *Conference proceedings : ... Annual International Conference of the IEEE Engineering in Medicine and Biology Society. IEEE Engineering in Medicine and Biology Society. Annual Conference*. 2008;2008:2051-2054
59. Maor E, Ivorra A, Rubinsky B. Non thermal irreversible electroporation: Novel technology for vascular smooth muscle cells ablation. *PLoS one*. 2009;4:e4757
60. Maor E, Ivorra A, Leor J, Rubinsky B. Irreversible electroporation attenuates neointimal formation after angioplasty. *IEEE transactions on bio-medical engineering*. 2008;55:2268-2274
61. Calkins H, Kuck KH, Cappato R, Brugada J, Camm AJ, Chen SA, Crijns HJ, Damiano RJ, Jr, Davies DW, DiMarco J, Edgerton J, Ellenbogen K, Ezekowitz MD, Haines DE, Haissaguerre M, Hindricks G, Ilesaka Y, Jackman W, Jalife J, Jais P, Kalman J, Keane D, Kim YH, Kirchhof P, Klein G, Kottkamp H, Kumagai K, Lindsay BD, Mansour M, Marchlinski FE, McCarthy PM, Mont JL, Morady F, Nademanee K, Nakagawa H, Natale A, Nattel S, Packer DL, Pappone C, Prystowsky E, Raviele A, Reddy V, Ruskin JN, Shemin RJ, Tsao HM, Wilber D, Heart Rhythm Society Task Force on C, Surgical Ablation of Atrial F. 2012 hrs/ehra/ecas expert consensus statement on catheter and surgical ablation of atrial fibrillation: Recommendations for patient selection, procedural techniques, patient management and follow-up, definitions, endpoints, and research trial design: A report of the heart rhythm society (hrs) task force on catheter and surgical ablation of atrial fibrillation. Developed in partnership with the european heart rhythm association (ehra), a registered branch of the european society of cardiology (esc) and the european cardiac arrhythmia society (ecas); and in collaboration with the american college of cardiology (acc), american heart association (aha), the asia pacific heart rhythm society (aphrs), and the society of thoracic surgeons (sts). Endorsed by the governing bodies of the american college of cardiology foundation, the american heart association, the european cardiac arrhythmia society, the european heart rhythm association, the society of thoracic surgeons, the asia pacific heart rhythm society, and the heart rhythm society. *Heart rhythm : the official journal of the Heart Rhythm Society*. 2012;9:632-696 e621
62. Brooks AG, Stiles MK, Laborderie J, Lau DH, Kuklik P, Shipp NJ, Hsu LF, Sanders P. Outcomes of long-standing persistent atrial fibrillation ablation: A systematic review. *Heart rhythm : the official journal of the Heart Rhythm Society*. 2010;7:835-846
63. Gerstenfeld EP, Callans DJ, Dixit S, Zado E, Marchlinski FE. Incidence and location of focal atrial fibrillation triggers in patients undergoing repeat pulmonary vein isolation: Implications for ablation strategies. *Journal of cardiovascular electrophysiology*. 2003;14:685-690
64. Callans DJ, Gerstenfeld EP, Dixit S, Zado E, Vanderhoff M, Ren JF, Marchlinski FE. Efficacy of repeat pulmonary vein isolation procedures in patients with recurrent atrial fibrillation. *Journal of cardiovascular electrophysiology*. 2004;15:1050-1055
65. Seow SC, Lim TW, Koay CH, Ross DL, Thomas SP. Efficacy and late recurrences with wide electrical pulmonary vein isolation for persistent and permanent atrial fibrillation. *Europace : European pacing, arrhythmias, and cardiac electrophysiology : journal of the working groups on cardiac pacing, arrhythmias, and cardiac cellular electrophysiology of the European Society of Cardiology*. 2007;9:1129-1133

66. Chen SA, Tai CT. Catheter ablation of atrial fibrillation originating from the non-pulmonary vein foci. *Journal of cardiovascular electrophysiology*. 2005;16:229-232
67. Lin WS, Tai CT, Hsieh MH, Tsai CF, Lin YK, Tsao HM, Huang JL, Yu WC, Yang SP, Ding YA, Chang MS, Chen SA. Catheter ablation of paroxysmal atrial fibrillation initiated by non-pulmonary vein ectopy. *Circulation*. 2003;107:3176-3183
68. Ouyang F, Antz M, Ernst S, Hachiya H, Mavrakis H, Deger FT, Schaumann A, Chun J, Falk P, Hennig D, Liu X, Bansch D, Kuck KH. Recovered pulmonary vein conduction as a dominant factor for recurrent atrial tachyarrhythmias after complete circular isolation of the pulmonary veins: Lessons from double lasso technique. *Circulation*. 2005;111:127-135
69. Chun KR, Bansch D, Ernst S, Ujeyl A, Huang H, Chu H, Satomi K, Schmidt B, Antz M, Kuck KH, Ouyang F. Pulmonary vein conduction is the major finding in patients with atrial tachyarrhythmias after intraoperative maze ablation. *Journal of cardiovascular electrophysiology*. 2007;18:358-363
70. Bhargava M, Di Biase L, Mohanty P, Prasad S, Martin DO, Williams-Andrews M, Wazni OM, Burkhardt JD, Cummings JE, Khaykin Y, Verma A, Hao S, Beheiry S, Hongo R, Rossillo A, Raviele A, Bonso A, Themistoclakis S, Stewart K, Saliba WJ, Schweikert RA, Natale A. Impact of type of atrial fibrillation and repeat catheter ablation on long-term freedom from atrial fibrillation: Results from a multicenter study. *Heart rhythm : the official journal of the Heart Rhythm Society*. 2009;6:1403-1412
71. Verma A, Kilicaslan F, Pisano E, Marrouche NF, Fanelli R, Brachmann J, Geunther J, Potenza D, Martin DO, Cummings J, Burkhardt JD, Saliba W, Schweikert RA, Natale A. Response of atrial fibrillation to pulmonary vein antrum isolation is directly related to resumption and delay of pulmonary vein conduction. *Circulation*. 2005;112:627-635
72. Cappato R, Negroni S, Pecora D, Bentivegna S, Lupo PP, Carolei A, Esposito C, Furlanello F, De Ambroggi L. Prospective assessment of late conduction recurrence across radiofrequency lesions producing electrical disconnection at the pulmonary vein ostium in patients with atrial fibrillation. *Circulation*. 2003;108:1599-1604
73. Fassini G, Riva S, Chiodelli R, Trevisi N, Berti M, Carbucicchio C, Maccabelli G, Giraldi F, Bella PD. Left mitral isthmus ablation associated with pv isolation: Long-term results of a prospective randomized study. *Journal of cardiovascular electrophysiology*. 2005;16:1150-1156
74. Jais P, Hocini M, Hsu LF, Sanders P, Scavee C, Weerasooriya R, Macle L, Raybaud F, Garrigue S, Shah DC, Le Metayer P, Clementy J, Haissaguerre M. Technique and results of linear ablation at the mitral isthmus. *Circulation*. 2004;110:2996-3002
75. Nademanee K, McKenzie J, Kosar E, Schwab M, Sunsaneewitayakul B, Vasavakul T, Khunnawat C, Ngarmukos T. A new approach for catheter ablation of atrial fibrillation: Mapping of the electrophysiologic substrate. *Journal of the American College of Cardiology*. 2004;43:2044-2053
76. Yokokawa M, Sundaram B, Oral H, Morady F, Chugh A. The course of the sinus node artery and its impact on achieving linear block at the left atrial roof in patients with persistent atrial fibrillation. *Heart rhythm : the official journal of the Heart Rhythm Society*. 2012;9:1395-1402
77. Zhang ZJ, Chen K, Tang RB, Sang CH, Lao EP, Yan Q, He XN, Du X, Long DY, Yu RH, Dong JZ, Ma CS. Impact of the origin of sinus node artery on recurrence after pulmonary vein isolation in patients with paroxysmal atrial fibrillation. *Chinese medical journal*. 2013;126:1624-1629
78. Sanders P, Jais P, Hocini M, Hsu LF, Scavee C, Sacher F, Rotter M, Takahashi Y, Pasquie JL, Shah DC, Garrigue S, Clementy J, Haissaguerre M. Electrophysiologic and clinical consequences of linear catheter ablation to transect the anterior left atrium in patients with atrial fibrillation. *Heart rhythm : the official journal of the Heart Rhythm Society*. 2004;1:176-184
79. Ernst S, Ouyang F, Lober F, Antz M, Kuck KH. Catheter-induced linear lesions in the left atrium in patients with atrial fibrillation: An electroanatomic study. *Journal of the American College of Cardiology*. 2003;42:1271-1282
80. Sawhney N, Anousheh R, Chen W, Feld GK. Circumferential pulmonary vein ablation with additional linear ablation results in an increased incidence of left atrial flutter compared with segmental pulmonary vein isolation as an initial approach to ablation of paroxysmal atrial fibrillation. *Circulation. Arrhythmia and electrophysiology*. 2010;3:243-248
81. Willems S, Klemm H, Rostock T, Brandstrup B, Ventura R, Steven D, Risius T, Lutomsky B, Meinertz T. Substrate modification combined with pulmonary vein isolation improves outcome of catheter ablation in patients with persistent atrial fibrillation: A prospective randomized comparison. *European heart journal*. 2006;27:2871-2878

82. Haissaguerre M, Hocini M, Sanders P, Sacher F, Rotter M, Takahashi Y, Rostock T, Hsu LF, Bordachar P, Reuter S, Roudaut R, Clementy J, Jais P. Catheter ablation of long-lasting persistent atrial fibrillation: Clinical outcome and mechanisms of subsequent arrhythmias. *Journal of cardiovascular electrophysiology*. 2005;16:1138-1147
83. Vasamreddy CR, Dalal D, Eldadah Z, Dickfeld T, Jayam VK, Henrickson C, Meininger G, Dong J, Lickfett L, Berger R, Calkins H. Safety and efficacy of circumferential pulmonary vein catheter ablation of atrial fibrillation. *Heart rhythm : the official journal of the Heart Rhythm Society*. 2005;2:42-48
84. Chen J, Lin Y, Chen L, Yu J, Du Z, Li S, Yang Z, Zeng C, Lai X, Lu Q, Tian B, Zhou J, Xu J, Zhang A, Li Z. A decade of complex fractionated electrograms catheter-based ablation for atrial fibrillation: Literature analysis, meta-analysis and systematic review. *IJC Heart & Vessels*. 2014
85. Konings KT, Smeets JL, Penn OC, Wellens HJ, Allessie MA. Configuration of unipolar atrial electrograms during electrically induced atrial fibrillation in humans. *Circulation*. 1997;95:1231-1241
86. Yamabe H, Morihisa K, Tanaka Y, Uemura T, Enomoto K, Kawano H, Ogawa H. Mechanisms of the maintenance of atrial fibrillation: Role of the complex fractionated atrial electrogram assessed by noncontact mapping. *Heart rhythm : the official journal of the Heart Rhythm Society*. 2009;6:1120-1128
87. Lin J, Scherlag BJ, Zhou J, Lu Z, Patterson E, Jackman WM, Lazzara R, Po SS. Autonomic mechanism to explain complex fractionated atrial electrograms (cfae). *Journal of cardiovascular electrophysiology*. 2007;18:1197-1205
88. Elayi CS, Verma A, Di Biase L, Ching CK, Patel D, Barrett C, Martin D, Rong B, Fahmy TS, Khaykin Y, Hongo R, Hao S, Pelargonio G, Dello Russo A, Casella M, Santarelli P, Potenza D, Fanelli R, Massaro R, Arruda M, Schweikert RA, Natale A. Ablation for longstanding permanent atrial fibrillation: Results from a randomized study comparing three different strategies. *Heart rhythm : the official journal of the Heart Rhythm Society*. 2008;5:1658-1664
89. Lin YJ, Tai CT, Chang SL, Lo LW, Tuan TC, Wongcharoen W, Udyavar AR, Hu YF, Chang CJ, Tsai WC, Kao T, Higa S, Chen SA. Efficacy of additional ablation of complex fractionated atrial electrograms for catheter ablation of nonparoxysmal atrial fibrillation. *Journal of cardiovascular electrophysiology*. 2009;20:607-615
90. Verma A, Sanders P, Macle L, Deisenhofer I, Morillo CA, Chen J, Jiang CY, Ernst S, Mantovan R. Substrate and trigger ablation for reduction of atrial fibrillation trial-part ii (star af ii): Design and rationale. *American heart journal*. 2012;164:1-6 e6
91. Verma A, Jiang CY, Betts TR, Chen J, Deisenhofer I, Mantovan R, Macle L, Morillo CA, Haverkamp W, Weerasooriya R, Albenque JP, Nardi S, Menardi E, Novak P, Sanders P, Investigators SAI. Approaches to catheter ablation for persistent atrial fibrillation. *The New England journal of medicine*. 2015;372:1812-1822
92. Sirak JH, Schwartzman D. Interim results of the 5-box thoracoscopic maze procedure. *The Annals of thoracic surgery*. 2012;94:1880-1884
93. Sanders P, Hocini M, Jais P, Sacher F, Hsu LF, Takahashi Y, Rotter M, Rostock T, Nalliah CJ, Clementy J, Haissaguerre M. Complete isolation of the pulmonary veins and posterior left atrium in chronic atrial fibrillation. Long-term clinical outcome. *European heart journal*. 2007;28:1862-1871
94. Chen J, Off MK, Solheim E, Schuster P, Hoff PI, Ohm OJ. Treatment of atrial fibrillation by silencing electrical activity in the posterior inter-pulmonary-vein atrium. *Europace : European pacing, arrhythmias, and cardiac electrophysiology : journal of the working groups on cardiac pacing, arrhythmias, and cardiac cellular electrophysiology of the European Society of Cardiology*. 2008;10:265-272
95. Kumagai K, Nakashima H. Noncontact mapping-guided catheter ablation of atrial fibrillation. *Circulation journal : official journal of the Japanese Circulation Society*. 2009;73:233-241
96. Tamborero D, Mont L, Berruezo A, Matiello M, Benito B, Sitges M, Vidal B, de Caralt TM, Perea RJ, Vatasescu R, Brugada J. Left atrial posterior wall isolation does not improve the outcome of circumferential pulmonary vein ablation for atrial fibrillation: A prospective randomized study. *Circulation. Arrhythmia and electrophysiology*. 2009;2:35-40
97. d'Avila A, Houghtaling C, Gutierrez P, Vragovic O, Ruskin JN, Josephson ME, Reddy VY. Catheter ablation of ventricular epicardial tissue: A comparison of standard and cooled-tip radiofrequency energy. *Circulation*. 2004;109:2363-2369
98. Halm U, Gaspar T, Zachaus M, Sack S, Arya A, Piorkowski C, Knigge I, Hindricks G, Husser D. Thermal esophageal lesions after radiofrequency catheter ablation of left atrial arrhythmias. *The American journal of gastroenterology*. 2010;105:551-556

99. Di Biase L, Saenz LC, Burkhardt DJ, Vacca M, Elayi CS, Barrett CD, Horton R, Bai R, Siu A, Fahmy TS, Patel D, Armaganijan L, Wu CT, Kai S, Ching CK, Phillips K, Schweikert RA, Cummings JE, Arruda M, Saliba WI, Dodig M, Natale A. Esophageal capsule endoscopy after radiofrequency catheter ablation for atrial fibrillation: Documented higher risk of luminal esophageal damage with general anesthesia as compared with conscious sedation. *Circulation. Arrhythmia and electrophysiology*. 2009;2:108-112
100. Tilz RR, Chun KR, Metzner A, Burchard A, Wissner E, Koektuerk B, Konstantinidou M, Nuyens D, De Potter T, Neven K, Furnkranz A, Ouyang F, Schmidt B. Unexpected high incidence of esophageal injury following pulmonary vein isolation using robotic navigation. *Journal of cardiovascular electrophysiology*. 2010;21:853-858
101. Carroll BJ, Contreras-Valdes FM, Heist EK, Barrett CD, Danik SB, Ruskin JN, Mansour M. Multi-sensor esophageal temperature probe used during radiofrequency ablation for atrial fibrillation is associated with increased intraluminal temperature detection and increased risk of esophageal injury compared to single-sensor probe. *Journal of cardiovascular electrophysiology*. 2013;24:958-964
102. Badger TJ, Adjei-Poku YA, Burgon NS, Kalvaitis S, Shaaban A, Sommers DN, Blauer JJ, Fish EN, Akoum N, Haslem TS, Kholmovski EG, MacLeod RS, Adler DG, Marrouche NF. Initial experience of assessing esophageal tissue injury and recovery using delayed-enhancement mri after atrial fibrillation ablation. *Circulation. Arrhythmia and electrophysiology*. 2009;2:620-625
103. Schmidt M, Nolker G, Marschang H, Gutleben KJ, Schibgilla V, Rittger H, Sinha AM, Ritscher G, Mayer D, Brachmann J, Marrouche NF. Incidence of oesophageal wall injury post-pulmonary vein antrum isolation for treatment of patients with atrial fibrillation. *Europace : European pacing, arrhythmias, and cardiac electrophysiology : journal of the working groups on cardiac pacing, arrhythmias, and cardiac cellular electrophysiology of the European Society of Cardiology*. 2008;10:205-209
104. Yokoyama K, Nakagawa H, Seres KA, Jung E, Merino J, Zou Y, Ikeda A, Pitha JV, Lazzara R, Jackman WM. Canine model of esophageal injury and atrial-esophageal fistula after applications of forward-firing high-intensity focused ultrasound and side-firing unfocused ultrasound in the left atrium and inside the pulmonary vein. *Circulation. Arrhythmia and electrophysiology*. 2009;2:41-49
105. Martinek M, Bencsik G, Aichinger J, Hassanein S, Schoefl R, Kuchinka P, Nesser HJ, Purerfellner H. Esophageal damage during radiofrequency ablation of atrial fibrillation: Impact of energy settings, lesion sets, and esophageal visualization. *Journal of cardiovascular electrophysiology*. 2009;20:726-733
106. Cummings JE, Barrett CD, Litwak KN, L DIB, Chowdhury P, Oh S, Ching CK, Saliba WI, Schweikert RA, Burkhardt JD, S DEM, Armaganijan L, Natale A. Esophageal luminal temperature measurement underestimates esophageal tissue temperature during radiofrequency ablation within the canine left atrium: Comparison between 8 mm tip and open irrigation catheters. *Journal of cardiovascular electrophysiology*. 2008;19:641-644
107. Neven K, Schmidt B, Metzner A, Otomo K, Nuyens D, De Potter T, Chun KR, Ouyang F, Kuck KH. Fatal end of a safety algorithm for pulmonary vein isolation with use of high-intensity focused ultrasound. *Circulation. Arrhythmia and electrophysiology*. 2010;3:260-265
108. Ahmed H, Neuzil P, d'Avila A, Cha YM, Laragy M, Mares K, Brugge WR, Forcione DG, Ruskin JN, Packer DL, Reddy VY. The esophageal effects of cryoenergy during cryoablation for atrial fibrillation. *Heart rhythm: the official journal of the Heart Rhythm Society*. 2009;6:962-969
109. Ripley KL, Gage AA, Olsen DB, Van Vleet JF, Lau CP, Tse HF. Time course of esophageal lesions after catheter ablation with cryothermal and radiofrequency ablation: Implication for atrio-esophageal fistula formation after catheter ablation for atrial fibrillation. *Journal of cardiovascular electrophysiology*. 2007;18:642-646
110. Furnkranz A, Bordignon S, Schmidt B, Gunawardene M, Schulte-Hahn B, Urban V, Bode F, Nowak B, Chun JK. Improved procedural efficacy of pulmonary vein isolation using the novel second-generation cryoballoon. *Journal of cardiovascular electrophysiology*. 2013;24:492-497



CHAPTER 12

Summary

Summary

limitation of current techniques

At the very end of the Direct Current (DC) era, low-energy DC ablation was demonstrated to cause myocardial lesions by non-thermal irreversible electroporation (permanent formation of pores in the cell membrane, leading to cell death), without arcing and/or barotrauma. DC ablation was rendered obsolete by a much more refined radiofrequency (RF) ablation technique. RF ablation was not intended to create large lesions but to eliminate rather small cardiac targets, as required for catheter-ablation of the atrio-ventricular junction and accessory pathways. However, patients with atrial fibrillation (AF) and ventricular tachycardia (VT) related to structural heart diseases, require transmural and large myocardial lesions, accomplished safely and single-shot. Ideally, the optimal lesion resulting from catheter-ablation should be discrete, circumscribed and confined to target tissue. In catheter-ablation with RF energy, the myocardial lesion is created by heating. Lesion size is determined by tissue properties (fibrosis, thickness), local blood flow (heat sink effect), the amount of energy supply and electrode-tissue contact.

At present, AF ablation with RF energy is time consuming, requires significant operator skills and is beset by a high AF recurrence rate, for both pathophysiological reasons and technical imperfections of current thermal catheter techniques. By all means, recurrence of AF is strongly related to pulmonary vein (PV) re-conduction and ablation of remaining PV-connections improves clinical outcome.

In RF ablation for AF, there is a thin line between insufficient and excessive energy delivery when aiming the creation of transmural lesions at the PV antrum. Insufficient energy supply will result in non-transmural lesions. On the other hand, excessive energy, while create transmural lesions will cause collateral damage outside the heart. Unfortunately, important nerves are located in close proximity to the left atrium (LA) as well as the esophagus, and both intestinal as nerve tissue are very susceptible to RF energy. This thesis is entirely focused on improvement of the technical results of catheter-ablation with a new ablation technique, both in terms of effectiveness and safety. Moreover, we expect that improvement of technical results will contribute to a better understanding of the pathophysiology of AF, such as the value of additional non-PV LA-ablations in patients with longstanding persistent AF.

In 10-20% an epicardial catheter-ablation approach is required for VTs related to structural (scar) heart diseases. However, myocardial tissue in close proximity to a coronary artery is not suitable for catheter-ablation with thermal energy, for both reasons of safety (risk on coronary artery injury) and effectivity (heat sink). Ablation of border areas between scar and myocardium, deep intramural foci and larger areas of scar tissue (homogenization) on or near coronary arteries in a safe and effective manner, may improve the clinical outcome of epicardial VT ablation significantly.

Electroporation for cardiac ablation

The last decade, irreversible electroporation (IRE) has been increasingly used as a new, emerging *non-thermal* ablation modality in the medical field for elimination of specific areas of undesired tissue without destroying surrounding tissues. When incorporated in electroporation lesions, bile ducts, large blood vessels and the urethra are preserved. These promising results rekindled our interest in the DC ablation technique of the 1980s. Use of this energy source may resolve shortcomings of current thermal ablation methods and better meet the requirements of current electrophysiological practice.

In the old DC technique a single catheter electrode was used, in which current density in target tissue decreases with the *square root* of distance from the center of the electrode. Consequently, control over lesion size and depth was poor. The major challenge was application of low-energy DC shocks (without arcing and/or barotrauma) while still allowing for sufficient (deep) and controlled myocardial lesion formation. We hypothesized that by applying a special catheter design using a circular arrangement of 8-10 connected electrodes, a torus-shaped electric field could be created in which voltage and current density decrease more *linearly* from the center of the electrodes. Anticipating prospective use in humans for cardiac arrhythmias, this thesis explores and re-examines the use of low-energy DC ablation in a modified form (circular arrangement) in a porcine model.

This thesis

Chapter 2 describes a pilot safety study to determine the arcing threshold. Relocating the indifferent patch electrode to the lower back increased total impedance and thereby prevented arcing. Secondly, we investigated whether circular electroporation ablation at a low energy level might be a feasible and safe method for PV ostial lesion creation. A number of difficulties was encountered:

positioning of the custom built circular ablation catheter in the PV tubulus was impeded by its non-deflectibility size in conjunction with the small porcine LA cavity and both PV entrances contiguous to the interatrial septum. However, the first results were promising: PV electrogram amplitude decreased and stimulation threshold increased significantly. PV stenosis was not observed after 3 weeks follow-up. Up to 3.5-mm-deep lesions were found.

However, due to the thin atrial wall and the uncertainty where ablations had been performed exactly, lesion size, depth, and continuity could not properly be analyzed in this model. Therefore, subsequent studies were carried out in an epicardial model to investigate more precisely the dose-response relationship between applied energy and lesion size (**Chapters 3-7**). Various custom made devices and energy levels were used. Lesion depth, width and continuity and voltage and current waveforms during electroporation were studied. Also potential hazardous side-effects of electroporation ablation on coronary arteries and reversibly the impact of blood flow in coronary arteries on both lesion size and myocardial lesion formation adjacent to coronary arteries was investigated.

Simulating an endocardial approach, an open-chest tissue-blood environment was used. After sternotomy the pericardial cradle was filled with blood. For the prospective purpose of an effective ablation modality for (video-assisted) thoracoscopic treatment of arrhythmias, a closed-chest model was used. All voltage and current waveforms were smooth, demonstrating the absence of arcing and barotrauma. Lesion depth increases linearly with the magnitude of the current density. In spite of the fact that the electrodes are separated continuous circular lesions could be created with a single 200 J circular application. Lesions depth did not differ significantly between lesions containing arteries and those without arteries. The coronary blood flow did not impact on lesion size. Unaffected myocardial tissue was never found right near a coronary artery that was completely embedded in lesion. Coronary arteries did not develop a significant stenosis within 3 weeks or 3 months after epicardial electroporation ablation.

In **Chapter 8** the response of PV tissue to an excessive number of circular 200-J electroporation applications (worse case scenario) was studied. PV stenosis did not occur as result of multiple non-arcing 200 J applications inside the PV 3 months after ablation.

To assess the risk of PN damage (**Chapter 9**), the porcine right phrenic nerve (PN) was targeted with a single 200-J circular electroporation application delivered in the superior caval vein (SCV). The PN courses along the outside of the fairly thin

SCV, hence within 2-3 mm distance from the electrodes inside the SCV. The PN function was preserved, both immediately after electroporation ablation as during 3 months follow-up.

In **Chapter 10** we studied lesion development after a single 200 J electroporation application. Acute lesions were mainly characterized by contraction band formation and interstitial edema and did not evolve histologically over the course of 1 hour. Except for a more intensive formation of connective tissue, only minimal histological development was noticed in the period between 3 weeks and 3 months. Hemorrhage and inflammatory cell infiltration were almost entirely absent.



CHAPTER 13

Samenvatting

Samenvatting

Beperkingen van de huidige thermale technieken

Aan het einde van het tijdperk van catheter-ablatie d.m.v. gelijkstroom (Direct Current, DC), was het reeds duidelijk dat ook laag-energetische DC-ablatie, zonder vonken of barotrauma, aanzienlijke myocardiale lesies kan veroorzaken, wat tot stand komt door irreversibele elektroporatie (permanente vorming van poriën in de celmembraan, waarna celdood). DC-ablatie werd echter voor zijn uitontwikkeling verlaten en vervangen door de verfijndere radiofrequente (RF) ablatietechniek. In die tijd werden voornamelijk de atrio-ventriculaire knoop en accessoire verbindingen geableerd, hiervoor is RF uitermate geschikt omdat het kleine lesies geeft. Ablatieprocedures voor atriumfibrilleren (AF) en ventriculaire tachycardieën (VT) t.g.v. structurele hartziekten, vereisen daarentegen grote en/of transmurale lesies, veilig en bij voorkeur in één keer aangebracht. Idealiter is de optimale myocardiale lesie scherp begrensd en beperkt tot het beoogde weefsel dat uitgeschakeld moet worden.

Met RF-energie komt de lesie tot stand door verhitting. De lesiegrootte wordt bepaald o.a. door de eigenschappen van het weefsel (fibrose, dikte), doorbloeding (koelend effect op weefselverhitting), de hoeveelheid toegediende energie en het contact tussen ablatie-elektrode en weefsel. Catheter-ablatie met RF-energie ter curatie van AF is tijdrovend, vereist aanzienlijke vaardigheden van de operateur en wordt gekenmerkt door een hoog recidiefpercentage. Behalve pathofysiologische oorzaken (zoals o.a. atriale vergroting en fibrosering) liggen hieraan ook technische gebreken ten grondslag. Immers, een recidief AF is sterk gerelateerd aan herstelde geleiding tussen pulmonaal vene (PV) en het linker atrium (LA); en ablatie van deze resterende verbindingen leidt tot klinische verbetering.

Met betrekking tot het aanbrengen van transmurale lesies t.h.v. het PV antrum is er een marginale grens tussen onvoldoende en een teveel aan energie. Onvoldoende energie in het weefsel leidt tot niet-transmurale lesies, terwijl een overmaat aan energie weliswaar transmurale lesies produceert maar ook schade toebrengt aan de structuren net buiten het hart. Helaas lopen enkele belangrijke zenuwen aan de buitenzijde van het LA, en de slokdarm ligt direct tegen de achterzijde van het LA. Beide zijn gevoelig voor RF-energie.

Ter verbetering van het technische resultaat van catheter-ablaties, richt dit proefschrift zich volledig op bestudering van electroporation ablation als nieuwe

ablatiemethode. Technische verbetering zal m.i. overigens leiden tot beter begrip van de pathofysiologie van AF, zoals bijvoorbeeld de waarde van aanvullende ablaties in het LA bij patiënten met longstanding persistent AF.

In 10-20% is een epicardiale benadering nodig om VT's o.b.v. structureel hartlijden (litteken) te ableren. Echter, hartspierweefsel in de nabijheid van een kransslagader (coronair) is niet benaderbaar voor catheterablatie met thermische energie, zowel vanwege redenen van veiligheid (risico op schade aan coronairen) als redenen van doelmatigheid (koeling door het stromende bloed in de coronairen dat de lesievorming belemmert - heat sink effect). Het bewerkstelligen van catheterablatie op veilige en effectieve wijze in de nabijheid van de coronairen kan de klinische resultaten van epicardiale VT ablatie aanzienlijk verbeteren.

Elektroporatie voor cardiale doeleinden

Sinds een jaar of 10 wordt irreversible electroporation (IRE) als niet-thermische ablatiemodaliteit gebruikt om ongewenst c.q. kwaadaardig weefsel uit te schakelen. Dat vitale structuren die behouden moeten blijven, zoals galwegen, urethra en grote bloedvaten, niet structureel beschadigd zijn in IRE-lesies, biedt ongekende mogelijkheden.

De veelbelovende ontwikkeling van IRE buiten de cardiologie hernieuwde onze belangstelling voor de verlaten DC-ablatietechniek van de jaren '80, die immers ook op IRE gebaseerd is. Wij veronderstelden dat deze energiebron meer tegemoet komt aan de eisen van de huidige ablatiepraktijk (het op veilige wijze creëren van diepe en/of transmurale lesies) mits gevrijwaard van de tekortkomingen van de thermische ablatiemethoden.

Vroeger werd DC-energie via één (distale) catheter-elektrode aan het weefsel geleverd. Ten opzichte van de elektrode neemt de stroomdichtheid in weefsel af met de 2e macht. Controle over lesiegrootte en lesiediepte was daardoor matig. De uitdaging was dan ook om laag-energetische DC-shocks zo af te geven dat diepe en gecontroleerde lesievorming plaatsvindt maar vonken en/of barotrauma niet achterwege bleven. Onze hypothese was dat met een cirkelvormige catheter met 8-10 elektroden een torusvormig (donut) elektrisch veld wordt gecreëerd waardoor afname van de spanning - en stroomdichtheid zich meer lineair tot de afstand van de elektroden verhoudt. Met het oog op humaan gebruik, wordt in deze thesis laag-energetische DC-ablatie opnieuw, maar in een andere toedieningsvorm (cirkelvormig), in een varkensmodel onderzocht.

Dit proefschrift

Hoofdstuk 2 betreft een pilot-studie t.b.v de bepaling van de vonkdrempel. Verplaatsing van de indifferente elektrode naar de onderrug veroorzaakt een toename van de totale lichaamsimpedantie waardoor vonken tijdens de DC-shock kunnen worden voorkomen. In de tweede plaats exploreerden we de haalbaarheid van circulaire elektroporation ablation als veilige en effectieve methode voor PV-ablatie. De studie verliep verre van perfect door de ontoegankelijke anatomie van het varkenshart. Het relatief kleine LA met de beide PV-ingangen grenzend aan het septum, belemmerde de stuurbaarheid van de zelfontworpen niet-flexibele ablatie-catheter in de PVs. De resultaten waren niettemin wel veelbelovend: De amplitude van het PV-elektrogram was na ablatie significant verlaagd en de stimulatiedrempel was significant toegenomen. PV-stenoserig werd niet waargenomen na 3 weken follow-up. Lesies reikten tot 3,5 mm diep.

Omdat de atriale wand relatief dun is en de exacte lokatie van de elektrische puls niet goed te herleiden bij histologisch onderzoek, werd dit (endocardiale) model uiteindelijk niet geschikt bevonden om de diepte en continuïteit van de lesies goed te onderzoeken. Om nauwkeurig de dosis-respons relatie tussen de afgegeven energie en lesiegrootte te bestuderen, werd in het vervolg een epicardiaal model gehanteerd (**hoofdstukken 3-7**). Diepte, breedte en continuïteit van de lesies, en de curven van het beloop van spanning en stroom tijdens energie-afgifte werden uitgebreid bestudeerd. Verschillende circulaire catheters en energienivo's werden gebruikt. Ook de eventueel schadelijke effecten op coronairen, en andersom, de invloed van de bloedstroom in de coronairen op lesievorming i.h.a. en lesievorming t.h.v. het grensgebied tussen myocard en kransslagaders werd nader onderzocht. Bij enkele studies werd een endocardiale benadering gesimuleerd: Na sternotomie werd de pericardiale ruimte gevuld met bloed, waarin epicardiale ablaties plaatsvonden. Met als doel de toekomstige ontwikkeling van een thoraco-chirurgische ablatieinstrument, vonden in andere studies epicardiale ablaties plaats volgens de gebruikelijke niet bloedige epicardiale benadering (via punctie). Alle energie-afgiften verliepen ongestoord zonder vonken of barotrauma. De lesiediepte nam lineair toe met de maximale stroomsterkte tijdens de elektrische puls. Ondanks het feit dat de elektroden op de circulaire catheter van elkaar gescheiden zijn, kan vanaf 200 J met één shock een continue cirkelvormige lesie verkregen worden. De lesiediepte van lesies die coronairen bevatten verschilt niet van die van lesies zonder coronairen. De bloedstroom in de coronairen heeft geen invloed op de lesiegrootte. Bij een coronair in een lesie werd nimmer een spoor

vitaal myocardweefsel gevonden op het grensgebied tussen de coronair en het aangrenzend myocard. Na een elektrische puls ontwikkelden coronairen binnen de termijn van 3 weken of 3 maanden nauwelijks intima-hyperplasie en geen significante stenose.

In **hoofdstuk 8** werden de longaders blootgesteld aan een groot aantal circulaire shocks van 200 J, waarmee een “worse case scenario” werd gesimuleerd. Ondanks vele energieontladingen vond geen stenosering plaats in de 3 maanden na ablatie. Om het risico op beschadiging van de nervus phrenicus (NP) (**hoofdstuk 9**) in te schatten, werd een circulaire shock van 200 J afgeleverd in de vena cava superior (VCS). De NP loopt tegen de de buitenzijde van de dunwandige en elastische VCS, dus binnen 2-3 mm afstand van de elektroden van de circulaire catheter in de VCS. De NP-functie bleef behouden, zowel onmiddellijk na de ablatie als na 3 maanden follow-up.

In **hoofdstuk 10** onderzochten we de ontwikkeling van de lesie na een 200 J shock. Direct na ontstaan worden lesies gekenmerkt door contractiebanden en interstitiële oedeem. Het eerste uur na de ablatie is er geen noemenswaardige histologische ontwikkeling. Behalve een meer uitgesproken bindweefselvorming, vond geen wezenlijke histologische verandering plaats tussen 3 weken en 3 maanden na ablatie. Bloedingen en ontstekingsinfiltraten waren nagenoeg geheel afwezig.



CHAPTER 14

Curriculum Vitae

Curriculum Vitae

The author Vincent Jean Hendrik Michel van Driel was born on August 28th 1967 in Middelburg, the Netherlands. At the age of 8 his family moved to Assen, where he attended the Christelijke Scholengemeenschap Assen and graduated (Atheneum β) in 1985. Vincent studied medicine at the Utrecht University and qualified as a medical doctor in 1993. Then he was drafted for military service as medical officer. From 2001-2003 Vincent was trained as a clinical electrophysiologist at the University Medical Center in Utrecht (UMCU), supervised by professor Hauer. Formal Cardiology residency started at the University Hospital in Nijmegen and was completed at the UMCU followed by appointment as a staff clinical electrophysiologist. In 2007 Vincent joined the inventors of cardiac electroporation ablation (F. Wittkampf and H. van Wessel) and started the ACDC-project. In 2010 Vincent together with old friends and colleagues H. Ramanna and H. van Wessel founded the new department of Electrophysiology at the Haga Teaching Hospital the Hague, where he continues to work. Vincent lives happily together with Lieke Hilligehekken, their children Anne en Auke, and also the teckels Pebbels and Bambam.



CHAPTER 15

Dankwoord

Dankwoord

Dit proefschrift is tot stand gekomen tijdens mijn werkend leven als cardioloog en kent een lange ontstaansgeschiedenis. Ik ben aan velen dank en erkenning verschuldigd.

Professor Doevendans, promotor, beste Pieter, jouw hulp en steun die ik gedurende de jaren onverminderd heb mogen ervaren, was onontbeerlijk voor de totstandkoming van dit proefschrift. Ik was je al erkentelijk voor de stafplaats Cardiologie die je me in 2006 aanbood, dat heeft mijn loopbaan namelijk precies de juiste draai gegeven. Maar nog meer waardeer ik je steun na mijn vertrek naar den Haag, dat is niet vanzelfsprekend. Je zonnige en optimistische inslag ("Komt goed" staat niet voor niets als tegelspreuk aan de muur), zonder de kritische geest te verliezen strekt mij tot voorbeeld. Het is bewonderenswaardig dat je regelmatig je overvolle agenda blokkeerde om de onvoldragen teksten minutieus met mij door te nemen (en te corrigeren).

Dr. Wittkampf, mijn copromotor, beste Fred, jij hebt, samen met enkele anderen uit de goede oude tijd, aan de wieg gestaan van mijn elektrofysiologische loopbaan. Je technische vernuft was altijd van grote waarde bij een elektrofysiologische procedure en met verve vervulde je de rol van joker, als wij het niet meer wisten. Desnoods ontwierp je nog de nodige apparatuur, die, als de omstandigheden dat vroegen, nog gedurende de procedure geupgrade werd tot een nieuwe versie. Je scherpe visie die het evenwicht houdt tussen analytisch en praktisch, is van grote waarde bij mijn ontwikkeling als wetenschapper. Ik ben je bovendien dankbaar voor al je natuurkundige lectures, je tomeloze inzet als nota bene "oudere jongere" in dit project en je kritische beoordeling van de artikelen.

Dr. Hassink, mijn copromotor, beste Rutger, de laatste lootjes wogen ook bij mij het zwaarst. Ik was blij dat je me verder wilde begeleiden bij het schrijfproces, de deadlines bewaakte en ging participeren in het ACDC-project. Daarnaast hebben we in onze overleggen en passant de wereldgeschiedenis verklaard tot de Romeinen. Je bent van vele markten thuis.

Ing. H. van Wessel, paranimf, beste Harry, jij bent met Fred de grondlegger van dit project. Ik was verheugd toen jullie mij benaderden om samen dit project te

starten. Alle begin is moeilijk: catheters en kabels gaven na eenmalig gebruik de geest, en zelf coupes snijden is een gevorderde oefening in geduld. Toch, van begin af aan hadden we het idee dat de juiste weg was ingeslagen en die opvatting heeft ons nooit verlaten. Fijn dat je al die jaren zo betrokken bent geweest bij dit onderzoeksproject. Wij zijn bovendien allen schatplichtig aan die technische knobbel van je. Van onschatbare waarde zijn voor mij de eindeloze discussies in jouw buitenbad van waaruit we de laatste veerdienst over de nachtelijke Nederrijn gadesloegen met een glas in de hand. Inmiddels ben je voor het team in den Haag onze steun en toeverlaat.

Dr. H. Ramanna, paranimf, beste Hemanth. Van jou heb ik in het AZU destijds de elektrofysiologische catheterisatiekunsten geleerd, inclusief stunt-ablaties. Een band voor het leven werd gesmeed. Toen jij me vroeg of ik met jou de "EP" in den Haag wilde opzetten, wist ik dat dit de ware bestemming zou zijn in mijn leven en dat is ook uitgekomen. En dan laat ik al jouw levenslessen, getuigend van een zeer sterk ontwikkeld realiteitsbesef, nog onvermeld! Me beperkend tot je rol bij deze promotie: Ik ben je dankbaar voor alle beschouwingen over het onderwerp en je correcties van de manuscripten. Mijn engels behoefde wel eens "enige aanpassing", zoals jij dat dan voorzichtig door de telefoon vermeldde om me niet al te zeer te kwetsen. Ik heb er alle vertrouwen in dat de humane toepassing van electroporation ablation op korte termijn ook in ons centrum van start gaat.

Dr. K.G.E.J. Neven, beste Kars, collega-onderzoeker. Halverwege het project heb jij het team versterkt. Kort en krachtig is je devies. Een van je vele sterke punten is het omzetten van een idee in een praktische oplossing of aanpak, en daarmee heb je het project in een ware stroomversnelling gebracht. In het dankwoord van jouw proefschrift hoopte je dat ik in de nabije toekomst mijn promotie zou afronden. Welnu, het heeft nog twee jaar gekost, maar het is zo ver! Omdat je me zo vaak geholpen hebt, vervult het me van blijdschap en trots je dit – almost at the end - te mogen zeggen.

Dr. A. Vink, beste Aryan, onze patholoog en mede-auteur. Dank voor al je tijd en energie die je van begin af aan besteedde aan dit project. Je eerlijkheid stond als een huis: "Als ik het niet zie, dan zie ik het niet."

Drs. B.C. du Pré, beste Bastiaan, volleerd onderzoeker en cardioloog in spé, dank voor de vele beoordelingen van de oneindige hoeveelheid coupes, die ik te pas en te onpas onder je microscoop legde en die altijd in een mum van tijd verwerkt werden.

Drs. R. van Es, beste René, je hebt je ontwikkeld tot een enthousiast en talentvol onderzoeker, met onnavolgbare trekjes. Dank voor al je steun. Gelukkig is ook voor jou de promotie snel in zicht!

Dr. P. Gründemann, beste Paul, voor de opstart van dit project heb je ons met raad en daad terzijde gestaan. Jij woonde immers in het GDL, ik wist niet eens waar de letters voor stonden. Dank voor je lessen anatomie en de inking in jouw unieke ideeën-encyclopedie.

Laboranten GDL, beste Cees, Evelyn, Joyce, Merlijn, Grace en Martijn, zonder jullie was geen enkele procedure tot stand gekomen, en over de planning zal ik maar helemaal zwijgen. Fantastisch dat jullie er altijd waren en niets te veel was om eens bij te springen of iets te regelen.

Leden van de leescommissie. Graag wil ik alle leden van de leescommissie, te weten Professor de Bakker, Professor Crijns, Professor Hauer, Professor Smeets, Professor Vos, bedanken voor de beoordeling van mijn proefschrift.

Professor Hauer, beste Richard, ik ben je altijd nog zo dankbaar dat je mij aannam als fellow toen ik op zekere dag als nitwit vanuit Nijmegen aanklopte in Utrecht. Mijn bagage bestond uit niet veel meer dan een vaag vermoeden van de elektrofysiologie en een aanbeveling van een bevriend professor te mijner gunste, betrekking hebbende op mijn persoon en niet mijn kunde. Vele maandagavonden heb jij met mij besteed aan het doorgronden van de registraties voor de dinsdagochtendbespreking. Je wist ontzettend veel en je kon het fantastisch uitleggen, maar vooral: Je deed het allemaal maar! De eerste maanden reed ik tegen middernacht ontluisterd naar huis om de dag erna in alle vroegte te vertrekken en alle registraties in een desolate HCK tot in den treure opnieuw uit te draaien. Menigeen zal zich in dit procedé herkennen. Zelf ben je ooit begonnen met DC-ablatie in Utrecht. Het is een voorrecht dat jij als oude leermeester in mijn beoordelingscommissie zitting hebt.

Professor Smeets, beste Joep, samen hebben we de eerste catheter-ablaties in Nijmegen verricht. Zelden iemand ontmoet die zoveel over het vak kon vertellen en dat dan ook deed. De opleidingstijd is mede daarom zo plezierig verlopen. Ik ben blij dat je in mijn beoordelingscommissie plaats hebt genomen.

Vakgroep Cardiologie UMCU. Beste Maarten-Jan, Corinne, Nicolaas, Henrik, Hans, Pieter, Siyrous, Rienk, Peter, Matthias, Jeroen, Anton, Steven, Gertjan en Michiel. De afgelopen jaren moest ik ontelbare keren de vraag in de wandelgang of er “al” uitzicht was op promotie tot mijn spijt ontkennend beantwoorden. Ik kan nu eindelijk zeggen dat het wel zo is. Dank voor jullie belangstelling al die jaren.

De oude Elektrofysiologie-club UMCU. Ik heb een voortreffelijke tijd met jullie gehad. Dierbaar zijn de herinneringen aan die tijd met jullie.

Peter, ik heb veel van je mogen leren, waaronder ook enkele lessen geduld. Nog steeds stuur ik je in het volste vertrouwen de moeilijkste patiënten voor verdere behandeling. **Matti**, Papnase, aan al je voortreffelijke kwaliteiten t.a.v. devices ga ik nu voorbij, die zijn algemeen bekend. Ik herinner me in de eerste plaats de lol die we al die jaren dagelijks als kamergenoten hebben gehad, waardoor we de dag eigenlijk altijd vrolijk afsloten. Jij bent het levende bewijs dat er wel degelijk humor in zo’n Duitse bast schuilt. **Jeroen**, zoals ik je vader op je afstudeerfeest beloofde, het zou zeker met jou goed komen in de elektrofysiologie. Zelden zo’n risicoloze belofte hoeven doen want ik wist dat je daar zelf voor zou zorgen. Inmiddels zit je, opgeleid in de traditie van de Utrechtse School, stevig als elektrofysioloog in het zadel en moet ik soms bij jou te rade. **Gio**, jij was mijn eerste fellow die ik mee heb opgeleid. Degelijk, kundig en vooral zonder poespas, maar bovenal lid van een inmens grote familie: elke dag was er wel een tante, nicht of achterneef jarig, en dus iets te vieren, en dus iets te eten. **Tuin**, ik roem je immer genuanceerde en integere overwegingen, zeker voor het patiëntenbelang. Ik zat bij jou in de kamer nooit om een goed gesprek verlegen. **Wil**, ontpopt als elektrofysiologie-beest pur sang achter de registraties. Heerlijke tijden waren het op de HCK! **Linda en Cornelia**, planningen maken met jullie was voor mij steeds weer een gezellige onderdeel van de dag. En op donderdag versie ?? Geen probleem, heb je al koffie?

Vakgroep Cardiologie Hagaziekenhuis. Beste Carl, Gabe, Samir, Hemanth, Ramon, Marco, Joris, Wilco, Mattijs, Arnout en Ivo, dank dat ik de ruimte kreeg om het onderzoek door te zetten. Ik heb me altijd door jullie aangemoedigd gevoeld

om het karwij af te maken. Inmiddels zijn we een vakgroep en geen maatschap meer, maar onze cohesie is er niet minder om: *Een voor allen, allen voor een!*

Yvonne en Hettie, de “EP” in den Haag floreert mede door jullie trouwe inzet. En ook voor (wijze?) Haagse levenslessen ben ik bij jullie altijd aan het juiste adres.

Ook de **verpleegkundigen van de afdeling en HCK** wil ik hier niet onvermeld laten, met wie de elektrofysiologie in den Haag zo goed opgebouwd is kunnen worden.

Beste Mike. Een vreselijke voorval heeft jou geveld waardoor je er niet bij kan zijn vandaag. Als geliefd lid van ons EP-team ben je onmisbaar, dat behoefde eigenlijk geen verduidelijking. Ik mis onze wekelijkse ontmoetingen, en ook het slap geouwehoer waarin onze discussies naadloos overgingen, natuurlijk altijd vergezeld van die brede grijns waarvan de snor onmiskenbaar deel uitmaakt. Ik weet, vroeg of laat ben je er weer.

Lieve **ouders**. Dit is het promotieboekje dan. Mijn wetenschappelijke besognes konden altijd op jullie warme belangstelling rekenen. Onvoorwaardelijke steun en vertrouwen van ouders bleek nog steeds onontbeerlijk en actueel. Dankbaar ben ik voor wat jullie me hebben meegegeven waardoor dit tot stand is kunnen komen.

Lieve **schoonouders**, ook jullie leefden erg mee met mijn wetenschappelijke vorderingen. Omdat die te traag verliepen, besloten jullie vorig jaar, ter aanmoediging, het cadeau al te kopen, en later zelfs te geven. Inmiddels heeft het cadeau zijn bestemming gevonden. Doe dat vaker.

Lieve **Anne en Auke**. Jullie vonden mij vaak opgesloten in de studeerkamer. Jullie fundamentele opvatting dat in een uur tijd al wat belangrijk is wel gedaan kan worden, althans zo verstond ik de opmerkingen, is juist en deel ik. Ik slaagde er om een of andere reden niet goed in dit te praktiseren, dat was mijn zwakte. Maar vanaf nu zal ik ook cakes bakken, meegaan op fietstochten en Pebbels en Bambam uitlaten.

Lieve **Lieke**. Jij hebt er alles aan gedaan dat ik avonden, weekeinden en vakanties aan mijn promotie kon werken. Jij redigeerde alle gezinsactiviteiten als ik weer eens verstek moest laten gaan. Zonder knorrig te worden, wat een hele prestatie is, te meer omdat ik wel af en toe knorrig was. Mijn enige magere tegenprestatie was dat ik me er bewust van was. Lieve schat, ik dank je voor de ruimte die je me altijd geeft.



CHAPTER 16

List of publications

List of publications

van Driel, V, Verheugt FWA. De medicamenteuze behandeling van chronisch hartfalen. *Cordiaal* 1999;20:108-112.

van Driel, V, van Langen H, Skotnicki SH, Werf van der T, Verheugt FWA. Niet-invasieve meetmethoden van de vaatfunctie bij chronisch hartfalen. *Cardiologie* 1999;6:375-380.

van Driel, V, van Langen H, Skotnicki SH, Werf van der T, Verheugt FWA. Veranderingen van de vaatfunctie bij chronisch hartfalen. *Cardiologie* 1999;6:381-386.

van Langen H, **van Driel V**, Skotnicki SH, Verheugt FWA. Alterations in the peripheral circulation in patients with mild heart failure. *Eur J of Ultrasound* 2001 Apr;13(1):7-15.

Noë P, **van Driel V**, Wittkamp F, Sreeram N. Rapid recovery of cardiac function after catheter ablation of persistent junctional reciprocating. *Pacing Clin Electrophysiol.* 2002 Feb;25(2):191-4.

Van Driel V, Gehlmann HR. Diagnose in beeld: een man met snelle, onregelmatige hartkloppingen. *Ned Tijdschr geneeskd* 2004;148 276.

Camaro C, **van Driel V**. een patiënte met hartkloppingen en kortademigheid; wat ziet u op het electrocardiogram? *Cordiaal* 2004;1:8,28.7.

Camaro C, **van Driel V**. Een patiënte met pijn op de borst en kortademigheid; wat ziet u op het electrocardiogram? *Cordiaal* 2004; 2:11,28.

Gerritsen KG, Meulenbelt J, Spiering W, Kema IP, Demir A, **van Driel V**. An unusual cause of ventricular fibrillation. *The Lancet*, Volume 373, Issue 9669, Page 1144, March 2009

Hof IE, Velthuis BK, **van Driel V**, Wittkampf FH, Hauer RN, Loh P. Left atrial volume and function assessment by magnetic resonance imaging. *J Cardiovasc Electrophysiol*. 2010 Nov;21(11):1247-50.

Chaldoupi SM, Wittkampf FH, **van Driel V**, Loh P. Measure twice, cut once: pitfalls in the diagnosis of supraventricular tachycardia. *Neth Heart J*. 2010 Feb;18(2):78-84.

Hof IE, Velthuis BK, Chaldoupi SM, Wittkampf FH, **van Driel V**, van der Heijden JF, Cramer MJ, Meine M, Hauer RN, Loh P. Pulmonary vein antrum isolation leads to a significant decrease of left atrial size. *Europace*. 2011 Mar;13(3):371-5.

van Driel V, Wittkampf FH, van Wessel H, Vink A, Hof IE, Gründeman PF, Hauer RN, Loh P. Feasibility of Electroporation for the Creation of Pulmonary Vein Ostial Lesions, *Journal of Cardiovascular Electrophysiology* 2011;22(3):302-309.

Hof IE, Wildbergh TX, **van Driel V**, Wittkampf FH, Cramer MJ, Meine M, Hauer RN, Loh P. Atrial fibrillation with a giant left atrial appendage can be successfully treated with pulmonary vein antrum isolation. *Neth Heart J*. 2012 Apr;20(4):179-81.

Wittkampf FH, **van Driel V**, van Wessel H, Neven KG, Gründeman PF, Vink A, Loh P, Doevendans PA. Myocardial Lesion Depth with Circular Electroporation Ablation *Circulation: Arrhythmia & Electrophysiology* 2012;5(3):581-586.

du Pré BC, **van Driel V**, van Wessel H, Loh P, Doevendans PA, Goldschmeding R, Wittkampf FH, Vink A. Minimal Coronary Artery Damage by Myocardial Electroporation Ablation *Europace* 2013;15(1):144-149.

van der Graaf AW, Bhagirath P, Ramanna H, **van Driel V**, de Hooge J, de Groot NM, Götte MJ. Noninvasive imaging of cardiac excitation: current status and future perspective. *Ann Noninvasive Electrocardiol*. 2014 Mar;19(2):105-113.

Bhagirath P, van der Graaf AW, Karim R, **van Driel V**, Ramanna H, Rhode KS, de Groot NM, Götte MJ. Multimodality imaging for patient evaluation and guidance of catheter ablation for atrial fibrillation - current status and future perspective. *Int J Cardiol*. 2014 Aug 20;175(3):400-408.

van Driel V, Neven K, van Wessel H, van Es R, Doevendans PA, Wittkamp F. Epicardial Linear Electroporation Ablation and Lesion Size Heart Rhythm 2014;11(8):1465-1470.

van Driel V, Neven KG, van Wessel H, du Pré BC, Vink A, Doevendans PA, Wittkamp FH. Pulmonary Vein Stenosis after Catheter Ablation: Electroporation versus Radiofrequency. Circulation: Arrhythmia & Electrophysiology 2014;7(4):734-738.

Neven K, **van Driel V**, van Wessel H, van Es R, Doevendans PA, Wittkamp F. Myocardial Lesion Size after Epicardial Electroporation Catheter Ablation after Subxiphoid Puncture Circulation: Arrhythmia & Electrophysiology 2014;7(4):728-733.

Bhagirath P, van der Graaf M, van Dongen E, de Hooge J, **van Driel V**, Ramanna H, de Groot N, Götte MJ. Feasibility and Accuracy of Cardiac Magnetic Resonance Imaging-Based Whole-Heart Inverse Potential Mapping of Sinus Rhythm and Idiopathic Ventricular Foci. J Am Heart Assoc. 2015 Oct 14;4(10):e002222. doi: 10.1161/JAHA.115.002222.

Neven K, **van Driel V**, van Wessel H, van Es R, du Pré B, Doevendans PA, Wittkamp F. Safety and Feasibility of Closed Chest Epicardial Catheter Ablation using Electroporation Circulation: Arrhythmia & Electrophysiology 2014;7(5):913-919.

van der Graaf AW, Bhagirath P, **van Driel V**, Ramanna H, de Hooge J, de Groot NM, Götte MJ. Computing volume potentials for noninvasive imaging of cardiac excitation. Ann Noninvasive Electrocardiol. 2015 Mar;20(2):132-139.

van Driel V, Neven K, van Wessel H, Vink A, Doevendans PA, Wittkamp FH. Low Vulnerability of the Right Phrenic Nerve for Electroporation Ablation Heart Rhythm 2015;12(8):1838-1844.

van der Graaf AW, Bhagirath P, de Hooge J, Ramanna H, **van Driel V**, de Groot NM, Götte MJ. Non-invasive focus localization, right ventricular epicardial potential mapping in patients with an MRI-conditional pacemaker system - a pilot study. J Interv Card Electrophysiol. 2015 Dec;44(3):227-34.

van Driel V, Neven K, du Pré BC, Aryan V, van Wessel H, Hassink RJ, Doevendans PA, Wittkamp FHM. Time course of myocardial electroporation lesion development. *submitted*

Neven K, van Es R, **van Driel V**, van Wessel H, Fidder H, Vink A, Hassink RJ, Doevendans PA, Wittkamp FHM. Acute and long-term effects of full-power electroporation ablation directly onto the esophagus. *submitted*